eman ta zabal zazu

Universidad del País Vasco
Euskal Herriko Unibertsitatea

DEPARTMENT OF PHARMACOLOGY / FARMAKOLOGIA SAILA

BIOCHEMICAL AND FUNCTIONAL CHARACTERIZATION OF THE CB1 CANNABINOID RECEPTOR COUPLING TO Gαi/o PROTEINS IN SYNAPTOSOMAL MEMBRANES FROM HIPPOCAMPUS AND FRONTAL CORTEX OF CELL-TYPE-SPECIFIC MUTANT MOUSE RESCUE MODEL

CB1 HARTZAILEAREN ETA Gαi/o PROTEINEN ARTEKO AKOPLAMENDUA: HURBILKETA BIOKIMIKO ETA FUNTZIONALA ZELULA ESPEZIFIKOETAN CB1 HARTZAILEAREN ERRESKATE SELEKTIBOA DUTEN SAGU TRANSGENIKOEN HIPOKANPO ETA KORTEX FRONTALETIK ERATORRITAKO SINAPTOSOMA MINTZETAN

PhD Thesis / Tesi doktorala

Miquel Saumell Esnaola

Supervisors / Zuzendariak: Prof. Dr. Joan Salles Alvira and Prof. Dr. Sergio Barrondo Lacarra

Vitoria-Gasteiz, 2021

AURKIBIDEA / INDEX

Abbreviations /

ANOVA: Analysis of variance

ATP: Adenosine triphosphate

BCA: Bicinchoninic Acid Assay

BSA: Bovine serum albumin

CB1: Cannabinoid receptor 1

CNS: Central nervous system

CRIP1a: Cannabinoid receptor associated protein 1a

DAGLα: Diacylglycerol Lipase α

DiIC16: (1,1'-Dihexadecyl-3,3,3',3'-Tetramethylindocarbocyanine Perchlorate)

DMSO: Dimethyl sulfoxide

DSE: Depolarization-Induced Suppression of Excitation

DSI: Depolarization-Induced Suppression of Inhibition

DTT: DL-Dithiothreitol

ECS: Endocannabinoid system

eCB: Endocannabinoid

EDTA: Ethylenediaminetetraacetic acid

EGTA: Ethylene glycol-bis (β-aminoethyl ether)-N,N,N',N'-tetraacetic acid

GABA: Gammaaminobutiric Acid

GAPDH: Glyceraldehyde 3-phosphate dehydrogenase

GDP: Guanosine diphosphate

GFAP: Glial fibrillary acidic protein

GPCR: G-protein-coupled receptor

GTP: Guanosine triphosphate

GTPγS: Guanosine 5′-[γ-thio]triphosphate

HRP: Horseradish peroxidase

H3: acetyl-Histone H3

KO: Knockout

LC-MS: Liquid Chromatography–Mass Spectrometry

MAGL: Monoacylglicerol lipase

MAP2: Microtubule-associated protein 2

MUNC-18/STXB1: Syntaxin-binding protein 1

MβCD: methyl-β-cyclodextrin

NMDA: N-methyl-D-aspartate receptor

NR1: N-methyl-D-aspartate receptor subunit NR1

PLCβ1: Phospholipase β1

PB: Phosphate buffer

PBS: Phosphate buffered saline

PMSF: Phenylmethylsulfonyl Fluoride

PPD: p-phenylenediamine

PSD95: Post synaptic Density Protein 95

PVDF: Polyvinylidene fluoride

Rpm: Revolutions per minute

S.E.M: Standard error of the mean

SDS: Sodium dodecyl sulfate

SNAP-25: Synaptosomal-asociated protein 25

Rab11b: Ras-related protein Rab-11B

TEMED: Tetramethylethylenediamine

THL: Tetrahidrolipstatine

Thy1: Thy-1 membrane glycoprotein

RT: Room temperature

SHANK3: SH3 and multiple ankyrin repeat domains protein 3

TX-100: Triton X-100

WH: Whole homogenate

WT: Wild type

2-AG: 2-arachidonoylglycerol

7TM: Seven-transmembrane receptor

[^{35}S]GTPγS: [^{35}S] Guanosine 5`-(γ-thio)triphosphate

I. SARRERA

Sistema endokannabinoidearen aurkikuntza: Proteinen identifikazioa eta karakterizazioa

Nahiz eta Kannabis Sativa landarea eta honen prestakin ezberdinak modu terapeutikoan eta errekreazionalean mendeetan zehar erabili izan ziren teraputikan eta modu errekreaziolean, kannabisaren alorreko lehen ikerketa zientifikoak ez ziren XIX. mende amaiera arte burutzen hasi. Hala ere, hamarkada batzuk pasatu behar izan ziren Kannabisaren printzio aktibo nagusiak isolatu eta hauen estruktura kimikoak identifikatzeko (Pertwee, 2006; Mechoulam et al., 2014). Adibidez, Δ9-tetrahidrokannabinola (Δ9THC), Kannabisaren printzipio aktiboa eta efektu psikotropikoen erantzule nagusia 1964. urtean isolatu eta identifikatu zen (Mechoulam and Gaoni, 1964). Aurkikuntza honek kannabinoideen alorreko ikerketen gorakada nabarmena ekarri zuen, farmakologiaren disziplinan besteak beste. Hala ere, urteak pasatu behar izan ziren Δ9THC eta beste konposatu kannabinoideen ekintza mekanismoa ezagutzeko. Hasiera batean, kannabinoideek efektu psikotropikoak modu inespezifikoan eragiten zituztela uste zen, mintz plasmatikoaren konposatu lipidikoak desantolatuz eta mintz plasmatikoaren propietate fisikoak aldatuz hain zuzen ere, anestesiko orokorren ekintza mekanismoa ederutzat hartuz (Lawrence and Gill, 1975). 80. harmarkadako erdi aldera hasi ziren hartzaile kannabinoideen existentziaren ebidentzia argiak azaltzen, in vitro experimentuak garatzean hain zuzen ere. Alde batetik, kannabinoide konposatu ezberdinek zelula neuronaletan adenilato ziklasa (AZ) entzima inhibitzen zutela frogatu zen. Gainera, AZ-ren inhibizioa toxina pertusisaren menpekoa zela frogatu zen, Gαi/o proteinari akoplatzen zen hartzaile kannabinoidearen existentzia agerian jarriz (Howlett, 1984, 1985; Howlett and Fleming, 1984; Howlett, Qualy and Khachatrian, 1986). Segidan, saturazio-lotura tekniken garapenak arratoiaren garun kortexetik eratorritako frakzio plasmatikoan lotura-gune espezifikoen existentzia ebidentziatu zuen eta honek kannabinoide ezberdinen karakterizazio farmakologikoa ahalbidetu zuen (Devane et al., 1988). Autoerradiografia teknikaren bitartez, lotura-gune espezifiko hauen garuneko distribuzioa kannabinoide psikotropikoek sortzen zuten efektuekin bat zetorrela ikusi zen (Herkenham et al., 1990, 1991). Azkenik, hartzailearen klonazio eta identifikazioak berretsi zuen lehen hartzaile kannabinoidearen existentzia garunean (CB1) (Matsuda et al., 1990). Urte gutxi pasa behar izan ziren bigarren hartzaile kannabinoideoa (CB2) klonatu eta identifikatzeko (Munro, Thomas and Abu-Shaar, 1993). CB1 hartzailea da sistema endokannabinoideak modulatzen dituen prozesu fisiologikoen erantzule nagusia

nerbio sistema zentralean (NSZ) (Kano et al., 2009). Izan ere, hartzaile honen espresioa eta banaketa handia eta zabala da garunean (Herkenham et al., 1990, 1991; Kano et al., 2009). Gainera, CB1 hartzailea ezabatua duten sagu transgenikoetan edota CB1 hartzailea farmakologikoki inhibitzean Δ9THC-ak nerbio sistema zentralean sorrarazten dituen efektu nagusiak ezabatzen dira (Zimmer et al., 1999; Huestis et al., 2001). Bestetik, aski ezaguna da CB2 hartzailea immunitate sistemako zeluletan expresatzen dela batik bat (Munro, Thomas and Abu-Shaar, 1993). Haatik, ikerketa ezberdinek iradokitzen dute CB2 hartzailearen presentzia NSZan, mikroglian nagusiki. Hala ere, CB2 hartzailearen presentzia CB1 hartzailearena baino askoz ere baxuagoa da (Lu and MacKie, 2016; Komorowska-Müller and Schmöle, 2021).

Hartzaile kannabinoideak identifikatzeak hauen ligando endogenoen bilaketa bultzatu zuen eta segidan identifikatu ziren hartzaile kannabinoideen agonista endogeno nagusiak: N-arakidoniletanolamida (Anandamida) (Devane et al., 1992) eta 2-arakidonilglicerola (2-AG) (Mechoulam et al., 1995; Sugiura et al., 1995) azido arakidonikoaren deribatu lipidikoak. Bi konposatu hauek dira gaurko egunerarte arreta handiena jaso duten eta hobekien karakterizatu diren endokannabinoideak eta hartzaile kannabinoideen ligando nagusitzat hartzen dira (Kano et al., 2009). Bi endokannabinoide nagusien sintesian parte hartzen duten entzimei dagokionez, anandamidaren sintesiaren erantzule nagusia fosfolipasa D (NAPE-PLD) entzima da eta N-arakidonoil fosfatidiletalonamida (NAPE) erabiltzen du sustratu bezala. Bestetik, diazilglizerol lipasa (DAGL) entzimak diazilglizerola (DAG) substratutik eratzen du 2-AG. Hala ere, bi endokannabinoide hauen sintesien urrats limitagarriak NAPE-ren eta DAG-ren produkzioak dira eta bi konposatu hauek N-aziltransferasa (NAT) eta fosfolipasa C (PLC) entzimen bidez sortzen dira, fosfatidiletanolamida eta fosfoinositido (fosfatidilinositol 4,5- bifosfatoa) sustratuak katalizatuz hurrenez hurren (Schmid et al., 1983; Stella, Schweitzer and Plomelli, 1997; Bisogno et al., 2003). Anandamidaren degradazioaren erantzule nagusia gantz azidoen amida hidrolasa (FAAH) entzima da (Cravatt et al., 1996) eta 2-AG ren degradazio nagusia monoazilglizerol lipasa (MAGL) entzima hidrolitikoa da, nahiz eta α/β hidrolasa domeinudun proteina 6-ak (ABHD6) eta α/β hidrolasa domeinudun proteina 12-ak (ABHD12) ere parte hartzen duten (Blankman, Simon and Cravatt, 2007). MAGL ak garuneko 2-AG ren hidrolisian duen kontribuzioa %85koa dela estimatu da eta ABHD12 eta ABHD6 entzimen kontribuzioa %15 koa (Blankman, Simon and Cravatt, 2007). COX-2-ak ere 2-AG-a degradatzeko gaitasuna duela proposatu da (Murataeva, Straiker

and MacKie, 2014). Anandamida eta 2-AG-az aratago, beste hainbat konposatu endogeno ere deskribatu dira ligando endokannabinoide gisa. Adibidez: noladin eterra, virodamina eta N-arakidonoildopamina agonista ortosterikak besteak beste. Bestetik, esfingosina eta hemopresina konposatuak CB1 hartzailearen antagonista konpetitibo bezala identifikatu dira eta modulatzaile alosteriko ezberdinen ebidentziak ere plazaratu dira, adibidez, pregnenolona eta pepcan-12 alosteriko negatiboak eta lipoxin A4 modulatzaile alosteriko positiboak (Pertwee, 2015).

Aipatutako hartzaile kannabinoideek, hauen ligandoak diren endokannabinoideek eta azken hauen sintesian eta degradazioan parte hartzen duten entzima ezberdinek osatzen dute sistema endokannabinoidea (Piomelli, 2003).

Sistema endokannabinoidearen funtzio nagusiak nerbio sistema zentralean

Sistema endokannabinoidearen funtzioak zerrendatzea ez da lan erraza, izan ere, gorputzeko prozesu fisiologiko askotan hartzen du parte (Maccarrone et al., 2015; Piazza, Cota and Marsicano, 2017). Adibidez NSZ-an ezaguna da sistema endokannabinoideak kognizioan, estresa, ikara eta antsietatea bezalako emoziotan, ikasketa eta memoria prozesuetan, janari kontsumoarekin erlazionatutako portaeretan, funtzio motorean edota nozizepzioan duen garrantzia (Busquets-Garcia et al., 2015a; Lutz et al., 2015; Maldonado, Cabañero and Martín-García, 2020). Sistema endokannabinoideak sari sistemarekin eta menpekotasunarekin erlazionaturiko portaerak modulatzen dituela ere ongi ikertua dago (Manzanares et al., 2018) eta zenbait egoera patologikoetan (gaixotasun neurodegeneratiboak, neuroinflamazioa, garun infartoan etabar) garuneko ehun eta neuronen biziraupenerako babes sistema gisa funtzionatzen duela ere ebidentziatu da (Fernández-Ruiz, Romero and Ramos, 2015).

Aipaturiko prozesu hauetan sistema endokannabinoideak duen garrantzia agerian jartzen da seinaleztapen endokannabinoidea osatzen duten elementu ezberdinen espresioa edota aktibitatea asaldatzen badira (Pertwee et al., 2010). Gainera, kannabinoideen kontsumoak sorrarazten dituen efektuak prozesu neurobiologiko hauetan sistema honek duen parte hartzearen isladapena da. Adibidez, aski ezaguna da kannabinoide exogenoek efektu antsiolitikoak edo efektu antsiogenikoak sorrarazten dituztela dosiaren arabera (Moreira, Grieb and Lutz, 2009; Lutz et al., 2015) eta kannabisaren kontsumoaren efektu nagusietako bat jateko gogoa bultzatzea dela (Mattes et al., 1994; Kirkham, 2009).

Honekin lotuta, aipatzekoa da Rimonabant farmakoaren kasua ere, obesitatearekin erlazionaturiko sindrome metabolikoak tratatzeko merkaturatu zena 2006. urtean Sanofi industria farmazeutikoaren eskutik (Scheen et al., 2006). CB1 hartzailearen antagonista honekin tratatutako pazienteek antsietate sintomak eta buruaz beste egiteko arrisku handiagoa zutela frogatu zen (Christensen et al., 2007) eta 2008. urtean farmako hau merkatutik erretiratu zen. Kognizio arazoak eta ikasketa eta memoria galerak ere kannabisaren kontsumo akutu eta kronikoak sorrarazten dituen efektuak dira (Broyd et al., 2016). NSZ-an sistema kannabinoidearen beste eginkizun garrantzitsu batzuk funtzio motorraren, gorputz tenperaturaren eta min sentzazioaren erregulazioak dira. Horrela, aski ezaguna da kannabinoide exogenoek sortzen dituzten eta tetrada efektuen parte diren katalepsia, hipotermia, hipoaktibitatea eta analgesia (Martin, 1986).

Aipatu den moduan, nerbio sistema zentraleko prozesu fisiologiko garrantzitsuenetan hartzen du parte sistema endokannabinoideak. Beraz, ez da arritzekoa izan sistema endokannabinoidearen elementuen alterazioak ebidentziatu izana zenbait prozesu patologikoetan, adibidez gaixotasun mental eta neurodegeneratiboetan, drogen adikzioan edota obesitatean besteak beste. Hori dela eta, palologia hauen aurkako diana terapeutiko erakargarria bihurtu da sistema endokannabinoidea (Cristino, Bisogno and Di Marzo, 2020; Fernández-Ruiz et al., 2020).

Sistema endokannabinoidearen rola transmisio sinaptikoan

Plastizitate sinaptikoa NSZ-an sinapsiaren indarra erregulatzeko epe motz eta epe luzean ematen diren aldaketa biokimiko eta estrukturalen multzoa da. Endokannabinoideen bidezko atzera-seinaleztapen sinaptikoa da plastikotasun sinaptikoa erregulatzeko NSZ-ak duen mekanismo homeostatiko garrantzitsuenetarikoa (Kano et al., 2009; Alger and Kim, 2011; Castillo et al., 2012; Katona and Freund, 2012). Beraz, sistema endokannabinoidearen elementuen kokapena mota honetarako seinaleztapenean oinarritzen da. Horrela, sintesirako makineria alde postsinaptikoan kokatzen da eta CB1 hartzailea, aldiz, terminal presinaptikoan (Katona and Freund, 2012) (ikusi 1. Irudia) Endokannabinoideak neurona postsinaptikotik askatzen dira neurona presinaptikoaren terminaleko mintzean aurkitzen diren CB1 hartzaileekin interakzionatuz neurotransmisoreen askapena inhibitzeko, azkenik transmisio sinaptikoaren eraginkortasunean aldaketak eraginez epe laburrean zein epe luzean. Zehazki, plastizitate

fenomeno hauei epe laburrerako depresioa (short-term depresion, STD) eta epe luzerako depresioa (long-term depression, LTD) deritze (Kano et al., 2009; Castillo et al., 2012; Ohno-Shosaku et al., 2012). CB1 hartzailea terminal glutamatergiko eta GABAergikoetan expresatzen denez nagusiki (Mailleux and Vanderhaeghen, 1992; Katona et al., 1999, 2006; Marsicano and Lutz, 1999), fenomeno sinaptiko hauek garuneko aktibitate eszitatzaile-inhibitzailearen arteko oreka erregulatzen dute, azkenik aipaturiko eta sistema endokannabinoidearen modulazioaren parte diren NSZ-ko oinarrizko prozesu fisiologikoak erregulatuz (Mechoulam and Parker, 2013; Busquets-Garcia et al., 2015b; Lutz et al., 2015).

Nahiz eta endokannabinoide bakoitzak duen papera transmisio sinaptikoaren modulazioan guztiz ezaguna ez izan, 2-AG-a proposatzen da atzera-seinaleztapen sinaptikoaren erantzule nagusia (Kano et al., 2009; Alger and Kim, 2011). Anandamidaren bitartekaritza, berriz, egoera zehatz batzuetara mugatzen da (Pan et al., 2009; Straiker and Mackie, 2009; Alger and Kim, 2011). Izan ere, DAGLα-ren ezabaketa genetikoak edota farmakologikoak CB1 hartzailearen menpeko plastikotasun sinaptiko fenomeno gehienak galarazten ditu (Sugiura et al., 1999; Gao et al., 2010; Tanimura et al., 2010; Yoshino et al., 2011). Neurotransmisore klasikoak ez bezala, endokannabinoideak ez dira ez bixikuletan metatzen ezta exozitosi bidez askatzen. Endokannabinoideak, mintz plasmatikoko fosfolipidoen degradazioaren bidez beharrezkoak direnean ekoizten eta askatzen dira neurona postsinaptikoaren aktibitateari erantzunez. Neurona postsinaptikoaren despolarizarioak boltai menpeko kaltzio erretenen irekiera, NMDA hartzaile ionotropikoaen irekiera edota organuluetako kaltzio intrazelularraren mobilizazioa eragiten du, zelula barneko kaltzio intrazelularraren kontzentrazioa igoaz. Kaltzio intrazelularraren igoera honek 2-AG-a eratzea dakar, alde batetik guztiz ezaguna ez den mekanismo molekular baten bitartez DAGLα-ren aktibitate entzimatikoa induzituz. Bestetik, Gαq/11 proteinari akoplatzen diren hartzaile metabotropikoen aktibazioak PLCβ entzimak fosfatidilinositol 4,5- bifosfatoa (PIP2) hidrolizatzea eragiten du DAG-a eratzeko. Ondoren DAGLα-ak DAG-a sustratu moduan erabiltzen du 2-AG-a eratzeko (Chevaleyre, Kanji A Takahashi and Castillo, 2006; Ohno-Shosaku et al., 2012). Hala ere aipatzekoa da bi mekanismo independete hauek sinergian funtzionatu dezaketela, PLCβ-ak kointzidentzia detektagailu gisa funtzionatzen duelako 2-AG-a produzitzen duten bi seinale postsinaptikoak integratuz. Izan ere, PLCβ-ren aktibazio entzimatikoa kaltzio menpekorra da. Horrela, nahiz eta independenteki ez

lukete 2-AG-a produzitzeko gaitasuna izango, intentsidadeko baxuko depolarizazioak eta hartzaile metabotropikoaren aktibazio baxuak 2-AG ren sintesia eta askapena induzitzen du (Hashimotodani et al., 2005; Maejima et al., 2005). Eredu honek dirudi fisiologikoki esangura izango lukeena endokannabinoideen produkzioaren eta askapenaren prozesuan (Chevaleyre, Kanji A Takahashi and Castillo, 2006; Ohno-Shosaku et al., 2012).

Sintetizatu ondoren, endokannabinoideak neurona postsinaptikoetatik tarte sinaptikora askatzen dira. Endokannabinoideak konposatu hidrofobikoak direnez, oraindik ez dago guztiz argi nola zeharkatzen duten tarte sinaptikoa alde presinaptikoan aurkitzen diren CB1 hartzaileekin interakzionatzeko, ezta nola hedatzen diren alboko sinapsiak modulatzeko (Alger and Kim, 2011). Adibidez, anandamida, mikrogliak medio estrazelularrera askatzen dituen ektosoma eta exosomen mintzean aurkitu da, zein neuronetako CB1 hartzailea aktibatzeko gai dela frogatu da (Gabrielli et al., 2015). Litekeena da 2-AG-a ere neurona postsinaptikotik besikuletan askatzea, izan ere, besikula hauek aproposak dira molekula hidrofobikoak garraiatzeko. Besterik, lipokalina eta albumina bezalako gantzen garraiatzaileak ere proposatu dira endokannabinoideen garraiatzaile potentzialak (Piomelli, 2003).

Esan bezala, terminal presinaptikoan aurkitzen den CB1 hartzaileari interakzionatuz endokannabinoideek neurotransmisorearen askapena inhibitzen dute, aipatu den moduan epe laburreko eta epe luzerako depresio fenomeno plastikoak induzituz. Bi fenomeno plastiko hauen atzean dagoen mekanismoa ezberdina da eta CB1 hartzailea aktibatzen den denbora tartea funtsezkoa da horretarako (Chevaleyre, Kanji A Takahashi and Castillo, 2006; Kano, 2014). Epe laburreko depresioan, CB1 hartzailen aktibazioa laburrak (segunduak) kaltzio erretenak inhibitzen ditu eta neurotransmisioaren askapena segundu gutxi batzuetan inhibitzen da. Bestetik, CB1 hartzailearen aktibazioa minutu batzukoa izan behar da epe luzerako depresio fenomenoa induzitzeko. Kasu honetan, neurotransmisioaren askapena denbora tarte luzeetan inhibitzen da eta horretarako beharrezkoa da proteinen espresioan aldaketak izatea, terminal presinaptikoan aldaketa estrukturalak emateko kano (Chevaleyre, Kanji A Takahashi and Castillo, 2006; Kano, 2014).

MAGL-a terminal presinaptikoetan kokatzen da CB1 hartzailea kokatzen den inguruan. Gainera, MAGL espresio maila handienak CB1 hartzailea aurkitzen den garun zonaldetan aurkitzen dira (Gulyas et al., 2004; Ludányi et al., 2011). Kokapen hau atzerapen bidezko seinaleztapen endokannabinoidea kontrolpean mantentzeko aproposa da, CB1

hartzailearen estimulazioa erregulatzea ahalbidetzen du eta. Horrela, MAGL-ren genea ezabatuta duten saguetan eginiko ikerketek edota entzimaren inhibizio farmakologikoak erakutsi dute MAGL-ak 2-AG-ren menpekoak diren plastizitate sinaptikoen iraupena eta tamaina kontrolatzen duela (Szabo et al., 2006; Hashimotodani, Ohno-Shosaku and Kano, 2007; Straiker and Mackie, 2009; Schlosburg et al., 2010; Pan et al., 2011).

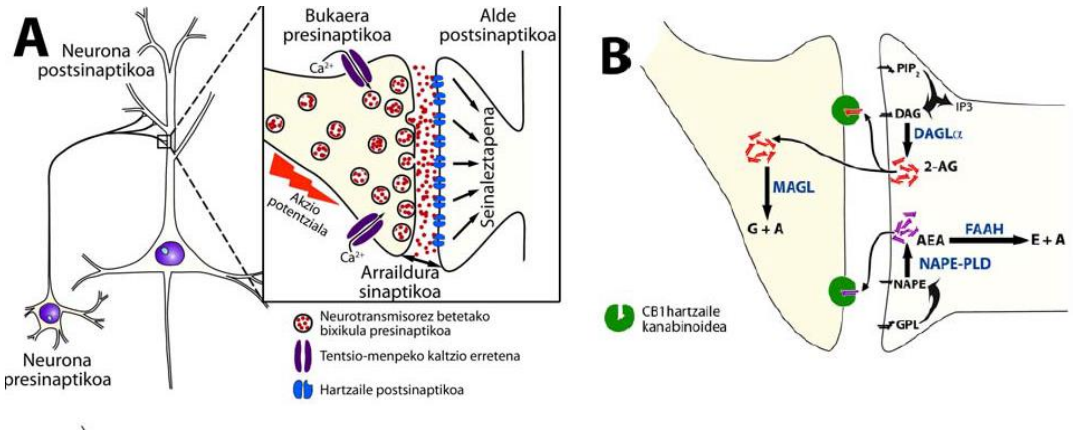

1. irudia. Neurotransmisioaren ezaugarriak sinapsi klasikoan eta sistema kannabinoide endogenoan. **A.** Neuronen arteko sinapsi klasikoa **B** endokannabinoideak «*on-demand*» sintetizatzen atzera-mezulari moduan jokatzeko. CB1 hartzaile presinaptikoak kitzikatzen dituzte. Seinaleztapena 2-AG MAGL entzima degradatzen du.

CB1 hartzaile kannabinoidea: CB1 hartzailearen estruktura molekularra

CB1 hartzailea arratoian klonatu zen lehendabiziz 1990. urtean (Matsuda et al., 1990) eta gizakian urte bat geroago isolatu eta identifikatu zen (Gerard et al., 1991). CB1 hartzailea espezie ornodunen artean ongi kontserbatua aurkitzen da (Elphick and Egertova, 2001; Murphy et al., 2001; Mcpartland and Glass, 2003). Adibidez, gizakiaren eta arratoiaren arteko azido nukleikoen eta aminoazidoen homologia maila %93 eta %97-koa da, hurrenez hurren. Gizakiaren eta saguaren kasuan aldiz, %90 eta %97-koa da. Saguaren eta arratoiaren arteko azido nukleikoen eta aminoazidoen homologia maila berriz, %95 eta %100-koa da, hurrenez hurren. (Matsuda et al., 1990; Gerard et al., 1991; Chakrabarti, Onaivi and Chaudhuri, 1995; Abood et al., 1997). CB1 hartzailea 7 mintz-zeharreko domeinu (7TM) dituen hartzaile bat da. Horregatik, mintz-zeharreko familia bereko hartzaileekin ezaugarri estrukturalak partekatzen ditu. Hala, CB1 hartzailea mintz

plasmatikoa 7 aldiz zeharkatzen duen proteina kate bakar batez dago osatua, arratoiean eta saguan 473 aminoazidoez osaturik dagoena eta 472 aminoazidoez gizakian, amino terminaleko domeinu estrazelularrean aminoazido bat gutxiago duelako. Kate proteiko hau, amino terminaleko domeinu estrazelularraz, 3 bihurgune estrazelularrez eta zelula barneko hiru bihurgunez elkarturik aurkitzen diren 7 mintz-zeharreko α helizez eta zelula barneko karboxi terminalaz osatzen da (Howlett et al., 2002) (ikusi 2. Irudia)

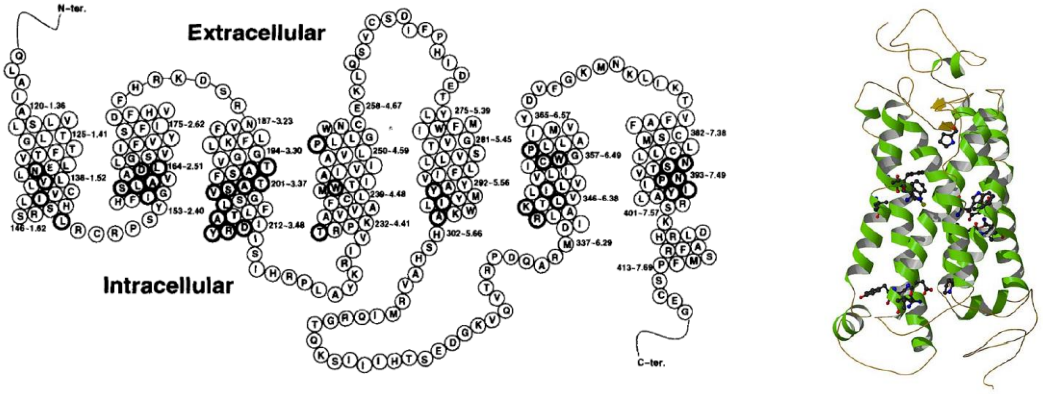

2. irudia. Ezkerraldean, CB1 hartailearekin errepresentazio bidimentsionala (Bramblett et al., 1995-tik eraldatua). Eskuinaldean, CB1 hartzailearen errepresentazio tridimentsionala (Montero et al., 2005-tik eraldatua).

CB1 hartzailearen bi splicing aldaera deskribatu dira gizakian eta saguan, hCB1a eta hCB1b eta mCB1a eta mCB1b isoformak hain zuzen ere (Shire et al., 1995; Ryberg et al., 2005; González-mariscal et al., 2016; Ruehle et al., 2017). Isoforma hauek, euren amino terminalaren luzeeran desberdintzen dira. Zehazki, hCB1a isoformaren amino terminalak hCB1 hartzailearen lehen 89. aminoazidoak 28 aminoazidoez osaturiko sekuentzia berri batengatik ditu ordezkaturik (Shire et al., 1995) eta hCB1b isoformak aldiz, hCB1 hartzailearen amino terminaleko 22 eta 52. aminoazidoen arteko 33 aminoazidoak ditu ezabatuak (Ryberg et al., 2005). Bestetik, mCB1a hartzaileak amino terminaleko 35. aminoazidoaren ondorengo 39 aminoazidoen trunkazio bat du eta mCB1b hartzaileak berriz, amino terminaleko 28. aminoazidoaren ondorengo 62 aminoazidoak ditu ezabatuak (Ruehle et al., 2017). Hala ere, isoforma hauen produktu proteikoak ez dira detektatuak izan oraindik, beraz, hauen garrantzi funtzionala aztertzeke dago.

CB1 hartzaile kannabinoidea: CB1 hartzailea osatzen duten domeinu estrukturalen garrantzi funtzionala

CB1 hartzailearen sekuentzian, 7 mintz-zeharreko domeinuen aurrean dauden aminoazidoek mutur amino terminala osatzen dute alde estrazelularrerantz orientaturik aurkitzen dena. Amino terminal domeinu honek duen garrantzi funtzionala ez da oso ezaguna. Hala ere, beste 7 mintz-zeharreko hartzaileetan deskribatu den moduan, CB1 hartzailearen amino terminala hartzailearen biosintesi prozesua erregulatzeko entitate garrantzitsua da, mintz plamatikora bideratzen den hartzailearen kantitate maila erregulatzen duelako (Andersson et al., 2003). Bestetik, nahiz eta amino terminalak CB1 hartzailearen funtzionalitatearen erregulazioan duen parte-hartzea ez den zuzenean aztetu, aipatu diren isoformek ezaugarri farmakologiko ezberdinak erakusten dituzte CB1 hartzaile kanonikoarekin alderatuta (Shire et al., 1995; Xiao et al., 2008; Straiker et al., 2012; Ruehle et al., 2017). Bestetik, CB1 hartzailearen amino terminalean N-glikosilazioa jasateko bi sekuentzia kontsentsu aurkitzen dira (Matsuda et al., 1990; Ruehle et al., 2017). Nahiz eta CB1 hartzailea glikosilatua aurkitzen den (Song and Howlett, 1995; Onaivi, Chakrabarti and Chaudhuri, 1996; De Jesús et al., 2006; Esteban et al., 2020), glikosilazioak duen garrantzi estrukturala edo funtzionala ez da ezagutzen.

Bikapa lipidikoa zeharkatzen duten α helize hidrofobikoak ingurugiro apolarrean murgildurik aurkitzen dira eta mintz-zeharreko domeinu hauek, medio estrazelularreko eta zelula barneko bihurguneek interkonektatzen dituzte. Mintz-zeharreko α helizeetan eta bihurgune estrazelularretan aurkitzen dira konposatu kannabinoideen interakzio guneak. Azken urte hauetan burutu diren CB1 hartzailearen mutazio, molekula dinamiken simulazio eta egitura kristalinoen analisiek zehaztazunez identifikatu dituzte konposatu kannabinoide endogeno eta exogenoen lotura gune ortosteriko eta alosteriko hauek (McAllister et al., 2004; Durdagi et al., 2010; Shim, Ahn and Kendall, 2013; Scott et al., 2013; Shao et al., 2016, 2019; Hua et al., 2016, 2017, 2020; Sabatucci et al., 2018; Al-Zoubi, Morales and Reggio, 2019; Díaz, Dalton and Giraldo, 2019; Krishna Kumar et al., 2019). Gainera, ikerketa hauek ligando kannabinoideen eta CB1 hartzailearen arteko interakzioen xehetasun molekularrak eta CB1 hartzailearen aktibazioan gertatzen diren aldaketa estrukturalak zehaztasunez ezagutzea ekarri dituzte. Horrela, beste 7 mintz-zeharreko hartzaileetan deskribatu den moduan, CB1 hartzailearen egoera inaktiboa mintz-zeharreko helizeetan ongi kontserbatutako sekuentzia domeinuetan gertatzen diren interakzio hidrofobikoek eta gatz zubiek mantentzen dituzte. Gainera, mintz-zeharreko

domeinuek zelula barneko bihurguneekin eta karboxi terminalarekin mantentzen dituzten interakzioek CB1 hartzailea egoera inaktiboan egonkortzen laguntzen dute. Hartzailearen egoera inaktiboak alde zitoplasmatikoruntz orientatuta aurkitzen diren seinaleztapen proteinen interakzio domeinuak estaltzen ditu. Hartzailearen aktibazioak aldaketa konformazional txikiak (mikro-mugimenduak) induzitzen ditu kontserbatutako sekuentzia gune hauetan eta aldaketa konformazio guzti hauek azkenik alde zitoplasmatikoan seinaleztapen proteinen lotura guneak agerian geratzea induzitzen dituzte (Gurevich and Gurevich, 2017, 2019). Aipatu den moduan, CB1 hartzailea Gαi/o proteinekin akoplatzen den hartzaile bat da. Gαi/o proteina heterotrimerikoekin interakzionatzen duten CB1 hartzailearen gune estrukturalak zelula barneko hirugarren bihurgunean eta karboxi terminalaren alde proximalean aurkitzen dira. Adibidez, hartzailearen hirugarren bihurgune intrazelularrean aurkitzen dira Gαi1 eta Gαi2 proteinekin akoplatzeko lotura guneak eta Gαi3 eta Gαo proteinekin interakzionatzeko lotura guneak aldiz, karboxi terminalaren alde proximalean aurkitzen dira (Mukhopadhyay et al., 1999, 2000, 2002; Mukhopadhyay and Howlett, 2001).

Karboxi terminala CB1 hartzailearen funtzionalitatea erregulatzeko domeinu garrantzitsu bat da ere. Izan ere, CB1 hartzailearen trafikoa, mintzeko lokalizazioa eta seinaleztapenaren anplitudea eta zinetika modulatzen duten domeinu estrukturalak karboxi terminalean aurkitzen dira (Stadel, Ahn and Kendall, 2011). Domeinu hauetariko batzuk prozesu hauek erregulatzen dituzten zenbait asoziazio proteinen interakzio guneak dira (Howlett, Blume and Dalton, 2010) eta karboxi terminalean ematen diren aldaketa postransdukzionalek erregulatzen dituzte proteina modulatzaile hauek duten afinitatea karboxi terminalarekiko. Adibidez, CB1 hartzailearen karboxi terminala fosforilazioa jasan dezaketen serina eta treonina aminoazidoetan dago aberastua eta aminoazido hauen fosforilazio defosforilazio dinamikek hartzailearen funtzionalitatea erregulatzen duten asoziazio proteinen interakzioak modulatzen dituzte. Adibidez, β-arrestinak, fosforilatutako hartzailearekin interakzionatzen du desensibilazio eta internalizazio prozesuak abian jartzeko. Alde batetik, G protein-coupled receptor kinase (GRK) kinasek karboxi terminalaren zonalde zentraleko S426 eta S429 aminoazidoak fosforilatzean (Bakshi, Mercier and Pavlopoulos, 2007; Daigle, Kwok and Mackie, 2008) β-arrestinak CB1 hartzailea Gαi/o proteinekin akoplatzea inhibitzen du (desensibilizazioa), β-arrestinak G proteinarekin esterikoki lehatzen duelako CB1 hartzailearekin interakzionatzeko (Farrens et al., 1996; Szczepek et al., 2014; Kang et al., 2015; Gurevich

and Gurevich, 2017, 2019), Bestetik, karboxi muturrean aurkitzen diren sei serina treonina residuoen fosforilazioak β-arrestina karboxi terminalaren domeinu honekin interakzionatzea induzitzen du, ondoren klatrina eta AP2 bezalako endozitosiko makinaria erreklutatzeko (Hsieh et al., 1999; Jin et al., 1999; Bakshi, Mercier and Pavlopoulos, 2007; Daigle, Kwok and Mackie, 2008).

Cannabinoid interacting protein 1a (CRIP1a) proteina karboxi terminalera lotzen den eta CB1 hartzailearen seinaleztapena eta trafikoa erregulatzen duen beste asoziazio proteina bat da. Batetik, CRIP1a proteinak karboxi terminal muturraren azken 9 aminoazidoekin interakzionatzen du (Niehaus et al., 2007). Hori dela eta, CRIP1a proteinak β-arrestinarekin domeinu honetan esterikoki lehiatzen du eta ondorioz β-arrestinaren menpekoa den CB1 hartzailearen internalizazioa negatiboki erregulatzen du. CB1 hartzailearen fosforilazio mailak determinatzen du β-arrestinen edo CRIP1a proteinaren asoziazio gaitasuna, izan ere CB1 hartzailearen karboxi terminalaren forma ez fosforilatuak CRIP1a-ren asoaziazioa induzitzen du eta karboxi terminalaren fosforilazioak aldiz, β-arrestinen lotura induzitzen du (Ahmed et al., 2014; Blume et al., 2017; Singh et al., 2019). Bestetik, CRIP1a-ak CB1 hartzaileak Gαo eta Gαi3 proteinekin akoplatzea inhibitzen du ere. Bestetik, karboxi terminaleko zisteina residuoaren palmitoilazioa CB1 hartzailearen lokalizazio eta seinaleztapena modulatzeko ematen den beste aldaketa postransdukzional bat da. Izan ere, palmitoilazioak, mintz plasmatikoan CB1 hartzailea egonkortzeaz gain, lipid-raft deritzen mintz plasmatikoko mikrodomeinu espezifikoetara bideratzen du (Oddi et al., 2012, 2017, 2018). Kolesterolean eta esfingosinan aberastutako lipid-raft mikrodomeinu hauek CB1 hartzailearen seinaleztapena modulatzeko plataforma efizienteak kontsideratzen dira (Bari, Battista, et al., 2005; Dainese et al., 2007).

CB1 hartzaile kannabinoidea: CB1 hartzailearen distribuzio zelularra eta azpizelularra

CB1 hartzaileak NSZ-an duen distribuzioaren eta espresioaren lehen ikerketak 90. harmarkadan burutu ziren. Lehenik, erradioaktibitateaz markatutako kannabinoideak erabiliz lotura-teknikak garatu ziren, autoerradiografia eta saturazio lotura-teknikak hain zuzen ere (Devane et al., 1988; Herkenham et al., 1990, 1991; Mailleux and Vanderhaeghen, 1992; Glass, Dragunow and Faull, 1997). CB1 hartzailearen klonazioak, CB1 hartzailearen RNA mezulariaren distribuzioa ikasteko aukera eman zuen in situ hibridazio teknikaren bitartez (Mailleux and Vanderhaeghen, 1992; Matsuda, Bonner and Lolait, 1993; Marsicano and Lutz, 1999) eta urte gutxietara garatu ziren CB1 hartzailearen aurkako lehen antigorputzak immunohistokimia eta mikroskopio elektroniko tekniketan erabiltzeko (Pettit et al., 1998; Tsou et al., 1998, 1999; Katona et al., 1999; Egertová and Elphick, 2000) (ikusi 3. Irudia). Gaur egunera arte, NSZ-an CB1 hartzailearen distribuzioa eta espresioa aztertu duten ikerketak ugariak dira (McPartland, Glass and Pertwee, 2007). Orokorrean, CB1 hartzailearen maila altuak gongoil basaletan, hipokanpoan, isokortexean, zerebeloan eta usaimen erraboilean aurkitzen dira. CB1 hartzailearen neurrizko espresioa berriz, septumean, amigdalan, hipotalamoan eta bizkar muineko alde dortsalean aurkitzen da. Talamoko eta bizkar muineko alde bentralak aldiz, hartzailearen maila baxuak espresatzen dituzte (Herkenham et al., 1990, 1991; Mailleux and Vanderhaeghen, 1992; Matsuda, Bonner and Lolait, 1993; Marsicano and Lutz, 1999; Mackie, 2005). CB1 hartzailearen distribuzioa hau zuzenki erlazionaturik dago sistema endokannabinoideak parte hartzen duen prozesu fisiologikoen modulazioan, adibidez funtzio motorraren, emozioen, prozesu kognitiboen eta memoriaren erregulazioan. Orokorrean, CB1 hartzailearen distribuzioa ugaztunetan kontserbatzen da (Herkenham et al., 1990, 1991) nahiz eta ezpezien artean zenbait ezberdintasun aurkitu daitezkeen: Adibidez, gizakietan funtzio kognitiboarekin erlazionaturiko zonaldeetan, adibidez kortex frontalean eta hipokanpoan, CB1 hartzailearen dentsitate handiagoak aurkitzen dira. CB1 hartzailearen espresioa handiagoa da arratoi eta saguetan mugimenduarekin erlazionaturiko zonaldeetan, adibidez zerebeloan eta caudato-putamenean, (McPartland, Glass and Pertwee, 2007).

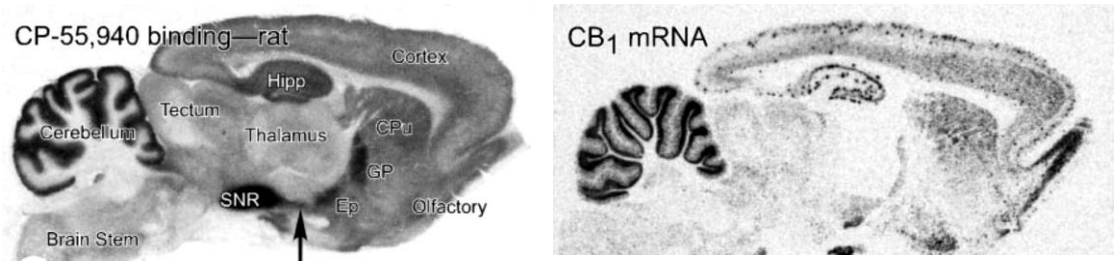

3. irudia. CB1 hartzailearen distribuzioa arratoiaren garun mozketa sagitaletan. Ezkerrean, autoerradiografia irudia [H^3]-CP 55,940 ligandoarekin burutua. Eskuinaldean, CB1 hartzailearentzat espezifikoa den oligonukleikoarekin markatutako CB1 hartzailearen mRNA (Freund, Katona and Piomelli, 2003-tik eraldatua)

Aipatu den moduan, CB1 hartzailearen espresioa handia eta zabala da NSZ-an. Hala ere, hartzailearen espresioaren bi markaketa pofril aurkitu daitezke garunean, espresio markaketa uniformea eta espresio markaketa ez-uniformea duten garun zonaldeak. Alde batetik, area ez kortikal gehienetan, neurona populazio haundi batek espresatzen du CB1 hartzailea. Neurona hauetan, CB1 hartzailearen espresio maila ertaina edo baxua da (Mailleux and Vanderhaeghen, 1992; Matsuda, Bonner and Lolait, 1993; Marsicano and Lutz, 1999; Tsou et al., 1999). Bestetik, zonalde kortikaletan CB1 hartzailearen espresio maila altua interneurona gutxi batzuetara mugatzen da. Neurona glutamatergiko kopuru nabarmen batek, aldiz, CB1 hartzailearen dentsitate maila baxua espresatzen du (Mailleux and Vanderhaeghen, 1992; Matsuda, Bonner and Lolait, 1993; Katona et al., 1999, 2006; Marsicano and Lutz, 1999; Tsou et al., 1999; Egertová and Elphick, 2000; Kawamura et al., 2006). Adibidez, neokortexean CB1 hartzailea neurona glutamatergikoen %50-an espresatzen dela proposatu da (Hill et al., 2007). Beraz, NSZ-an CB1 hartzailea neurona glutamatergikoetan eta neurona gabaergikoetan aurkitzen da nagusiki, orokorrean espresio maila neurona kiltzikatzaileetan neurona inhibitzaileetan baino nabarmen baxuagoa izanik. Adibidez, zerebeloko eta hipokanpoko neuronen terminal sinaptikoetan CB1 hartzailearen espresio maila 5-6 eta 10-20 aldiz baxuagoa dela egiaztatu da, hurrenez hurren (Kawamura et al., 2006). Nahiz eta CB1 hartzailea nagusiki aipaturiko bi neurona mota hauetan aurkitu, ikerketa ezberdinek iradokitzen dute hartzaile honen presentzia beste neurona mota batzuetan, adibidez neurona serotonergikoetan (Häring et al., 2007, 2015), neurona noradrenergikoetan (Oropeza, Mackie and Van Bockstaele, 2007; Scavone, Mackie and Van Bockstaele, 2010) edota neurona kolinergikoetan (Gábor Nyíri et al., 2005). Gainera, nahiz eta neuronetan baino maila baxuagoan espresatu, zelula glialetan ere aurkitzen da CB1 hartzailea, astrozitoetan adibidez (Rodríguez, Mackie and

Pickel, 2001; Salio et al., 2002; Han et al., 2012), non zenbait funtzio fisiologiko garrantzitsu modulatzen dituen, adibidez memoria eta ikaskuntza prozesuak (Navarrete, Díez and Araque, 2014; Metna-Laurent and Marsicano, 2015). Ama zelulek (Aguado et al., 2005, 2006; Zimmermann et al., 2018) eta endotelio baskularreko zelulek ere CB1 hatzailea espresatzen dutela frogatu da (Golech et al., 2004).

Mikroskopia elektronikoko teknikek ahalbidetu zuten CB1 hartzailearen lokalizazio azpizelularra karakterizatzea. Horrela, CB1 hartzailea neuronen axoien segmentu preterminaleko eta terminal presinaptikoko mintzean kokatzen da nagusiki (Katona et al., 1999, 2006; Bodor et al., 2005; G. Nyíri et al., 2005; Kawamura et al., 2006; Lafourcade et al., 2007; Thibault et al., 2013). CB1 hartzailearen kokapen estrategiko honek berresten du CB1 hartzailearen funtzio nagusia neurotransmisoreen askapena erregulatzea dela (Freund, Katona and Piomelli, 2003; Kano et al., 2009). CB1 hartzailearen lokalizazio sinaptiko zehatz honek ere arrazoitzen du hartzailearen markaketa patroiean ezberdintasunak aurkitzea immunohistokimia eta autoerradiografia eta in situ hibridazio tekniken artean. Izan ere, in situ hibridazio teknikak nagusiki neuronen sometan aurkitzen den mRNA markatzen du eta immunohistokimia eta autoerradiografia teknikek, aldiz, CB1 hartzailearen proteina markatzen dute. Adibidez, gongoil basaletan CB1 hartzailearen mRNA estriatuko proiekzio neuronen soman detektatzen den bitartean, CB1 hartzailea globo palido, sustantzia negra pars erretikulata edota nukleo entopedunkularrean detektatu daiteke, estriatuko proiekzio neuronen terminal axonikoak bertan aurkitzen direlako (Freund, Katona and Piomelli, 2003; Kano et al., 2009).

Neuronen terminal presinaptikoan, CB1 hartzailearen dentsitate altuena zonalde perisinaptikoan detektatzen da, zonalde estrasinaptikoan dentsitate maila baxuagoa den bitartean. Zonalde aktiboan, CB1 hartzailea nekez detektatzen da. Hala ere, nahiz eta dentsitate altuena zonalde perisinaptikoan aurkitu, CB1 hartzaile kopuru gehiena zonalde estrasinaptikoan aurkitzen da, CB1 hartzailearen %90-a inguru hain zuzen ere. Izan ere, terminal sinaptikoaren mintz plasmatikoa nagusiki mintz estrasinaptikoz osatzen da, zonalde aktiboko eta perisinapsiko mintzaren kontribuzioa oso baxua den bitartean (G. Nyíri et al., 2005). Neurotransmisoaren askapena inhibitzeko gaitasuna zonalde perisinaptikoan aurkitzen den CB1 hartzaileari egotzi zaio. Izan ere, populazio zehatz hau egongo liteke egoki kokatua zonalde aktiboan aurkitzen diren boltai menpeko kaltzio erretenak inhibitzeko (G. Nyíri et al., 2005; Dudok et al., 2015). Bestetik, mintz estrasinaptikoan aurkitzen diren hartzaileek ez lukete boltai menpeko kaltzio kanalak

inhibitzeko gaitasuna izango, izan ere, hauek distantzia urrunegian aurkituko lirateke CB1 hartzailearekin interakzionatzeko. Mintz estrasinaptikoan kokatzen diren CB1 hartzaileei proposatu zaizkien funtzioak AZ-ren inhibizioa, potasio erretenen aktibazioa edota erreserba populazio bat izatea dira (G. Nyíri et al., 2005; Dudok et al., 2015).

CB1 hartzailea nagusiki terminal presinaptikoan kokatzen den arren, zelularen beste konpartimentu batzuetan funtzionalki espresatzen dela frogatu da. Adibidez, CB1 hartzailea neuronen eta zelula glialen mitokondrien mintzean aurkitzen da, non mitokondrietan ematen den arnasketa zelularra eta metabolismo energetikoa erregulatzen duen (Bénard et al., 2012; Hebert-Chatelain et al., 2014, 2016). (Bonilla-Del Río et al., 2019; Gutiérrez-Rodríguez et al., 2018). CB1 hartzailearen espresioa mintz somatodendritikoan eztabaidagarriagoa da. Izan ere, inmunohistokimia eta mikroskopia elektroniko entseguetan detektatzen den CB1 hartzailearen seinale somatodendritikoa sintesian eta degradazioan parte hartzen duten organulu intrazelularretik (gorputz multibesikularrak, Golgi eta erretikulo endoplasmatikoa, endosomak, lisosomak) datorrela onartua dago. Hala ere, badira zenbait ikerketa anatomiko eta biokimiko CB1 hartzailearen espresioa detektatu dutenak mintz somatodendritikoan (Ong and MacKie, 1999; Rodríguez, Mackie and Pickel, 2001; Pickel et al., 2004; Köfalvi et al., 2005; Thibault et al., 2013), nahiz eta beste ikerkuntza talde batzuek ez diren emaitza eta ondorio berdinetara iritsi (Katona et al., 1999; Irving et al., 2000; Coutts et al., 2001; Freund, Katona and Piomelli, 2003; Bodor et al., 2005). Entsegu funtzionalek ere iradokitzen dute CB1 hartzailearen kokapen postsinaptikoa (Bacci, Huguenard and Prince, 2004; Marinelli et al., 2009; Maroso et al., 2016). Adibidez, kortex somatosensorialeko neurona piramidal eta interneurona populazio mugatuek 2-AG-ren eta CB1 hartzailearen menpeko mekanismo autokrino baten bitartez, euren aktibitatea inhibitzeko gaitasuna dutela ebidentziatu da. Akzio potentzial iraunkorrek 2-AG-a ekoiztea induzitzen dute eta CB1 hartzailearen aktibazioak potasio erretenen aktibazioa eta irekiera induzitzen du, neuronaren hiperpolarizazioa induzituz (Bacci, Huguenard and Prince, 2004; Marinelli et al., 2009). Bestetik, hipokanpoan CB1 hartzaile postsinaptikoaren menpeko zelula barneko mekanismo konplexu baten bitartez, neurona postsinaptikoa dendriteri datorkien imput kiltzikagarrien integrazioa eta eszibilitatea gutxitu dezake (Maroso et al., 2016). Dagoeneko aipatu bezala, CB1 hartzailearen proportzio haundi bat sintesi, birziklapen eta degradazio bideen parte diren organulu ezberdinetan ere aurkitzen da, adibidez endosometan eta lisosometan besteak beste. Bi

konpartimentu hauetan aurkitzen den CB1 hartzailearen frakzio bat mintz plamatikoko hartzailearen endozitozitik datorren arren (Leterrier et al., 2004), hartzailearen proportzio bat zuzenean konpartimentu biosintetikotik bideratzen da konpartimentu intrazelular hauetara. Endosometan eta lisosometan aurkitzen den CB1 hartzaile populazio hau funtzionala dela ebidentziatu da (Rozenfeld and Devi, 2008; Grimsey et al., 2010; Brailoiu et al., 2011) (Ikusi 4. Irudia).

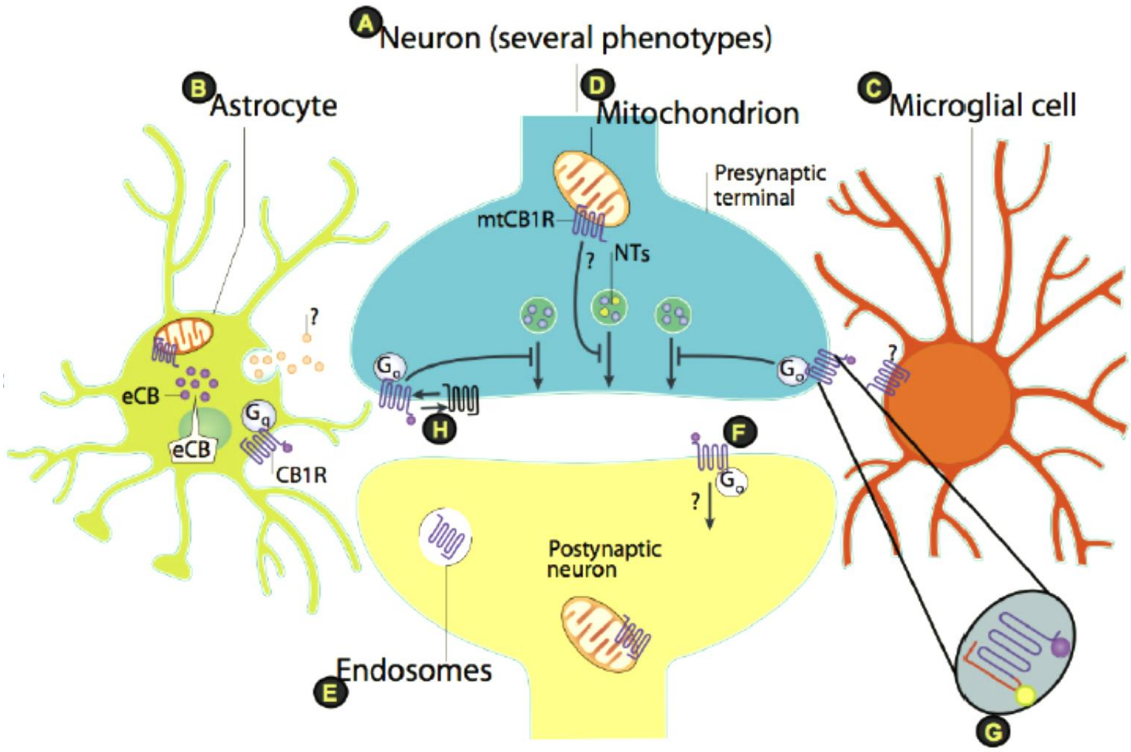

4.. irudia. CB1 hartzailearen espresio funtzionala nerbio sistema zentraleko zelula eta zelula hauen konpartimentu ezberdinetan.A) Neuronak B) astrozitoa, C) Mikroglia, D) Mitokondria, E) Endosoma F) Mintz somatodendritikoa. (Busquets et al., 2016-tik eraldatua).

CB1 hartzaile kannabinoidea: CB1 hartzailearen farmakologia

Aipatu den bezala, CB1 hartzailea mintz-zeharreko 7 domeinu dituen hartzaileen familiako proteina bat da. Hartzaile hauek zelularen mintz plasmatikoan kokatzen dira eta kanpo estimulu edo seinale estrazelularrak zelularen barnera transduzitzen dituzte zelularen erantzun fisiologikoak erregulatzeko (Kenakin, 2002). CB1 hartzailearen kasuan, kanpo estimulu hauek kannabinoide endogenoak, fitokannabinoideak eta kannabinoide sintetikoak dira (Pertwee et al., 2010; Pertwee, 2015). CB1 hartzailearen agonista kannabinoideak estruktura molekularraren arabera lau multzo nagusitan sailkatzen dira. Kannabinoide klasikoak dibenzopiranoen deribatuak dira eta multzo honetan aurkitzen dira kannabisaren printzipio aktiboa den Δ9THC fitokannabinoidea eta HU-210-a, Δ8THC-ren analogo sintetikoa. Kannabinoide ez klasikoen multzoa, Δ9THC-ren analogo bizikliko eta triziklikoek osatzen dute eta CP 55,940 konposatua da multzo honetako kannabinoide ezagunena. Aminoalkilindol estruktura molekularra duten konposatuek osatzen dute agonista kannabinoideen hirugarren multzoa eta talde honen konposatu prototipikoa WIN 55,212-2 kannabinoide sintetikoa da. Azkenik, Anandamida eta 2-AG endokannabinoideak dira eikosanoideen familiaren konposatu nagusiak. HU-210, CP 55,940, WIN 55,212-2 eta 2-AG kannabinoideek eraginkortasun intrinsiko berdintsua dute, entsegu funtzional gehienetan agonista oso gisa konportatzen direlako kannabinoide hauek. Δ9THC-aren eta anandamidaren eraginkortasun intrintsikoa aldiz, aurretik aipatutakoena baino nabarmen baxuagoa da eta horregatik bi konposatu hauek normalean agonista partzial gisa konportatzen dira entsegu funtzional gehienetan. Aipatutako konposatu kannabinoideek CB1 hartzailearekiko duten afinitatea aldakorra da ere. HU-210 eta CP 55940 kannabinoide sintetikoek afinitate handiena erakusten duten bitartean, 2-AG eta anandamida kannabinoide endogenoek afinitate baxuena erakusten dute. Nahiz eta orokorrean aipaturiko kannabinoide hauek CB1 hartzailearenganako duten afinitatea handia izan, ez dira guztiz espezifikoak, CB2 hartzailearentzako afinitate antzekoa dutelako. CB1 hartzailearentzat selektiboak diren kannabinoideen artean anandamidaren analogo sintetikoak aurkitu ditzazkegu, adibidez, metanandamida konposatua. Metanandamidak, anandamidaren afinitate eta eraginkortasun intrintsiko antzekoa du (Pertwee et al., 2010).

Aipaturiko agonista kannabinoide hauek CB1 hartzailearen lotura gune ortosterikoarekin interakzionatzen dute, hau da, anandamida eta 2-AG endokannabinoideek interakzionatzen duten CB1 hartzailearen domeinuarekin. CB1 hartzaileak lotura gune

alosterikoak dituela ere plazaratu da. Lotura gune alosterikoak, agonista endogenoak lotzen ez diren CB1 hartzailearen interakzio guneak dira eta modulatzaile alosterikoak CB1 hartzailearen aktibitatea modulatzeko lotura gune alosterikoekin interakzionatzen duten ligandoak dira. Hauek ligando ortosterikoen afinitatea eta eraginkortasuna positiboki (PAM alosterikoak) edo negatiboki (NAM alosterikoak) erregulatu dezakete, edota berezko agonismo ezaugarriak izan (Ago-alosterikoak) Azkenik ligando ortosterikoen funtzioa modulatzen ez duten modulatzaile alosterikoak aurkitzen dira (NAL). CB1 hartzailearen zenbait ligando alosteriko identifikatu eta karakterizatu dira azken urte hauetan. Hauetariko batzuk aipatu diren konposatu endogenoak dira, adibidez pregnenolona eta pepkano-12 modulatzaile alosteriko negatiboak eta lipoxina A4 modulatzaile alosteriko positiboa. Beste batzuk konposatu sintetikoak dira, adibidez GAT211 modulatzaile alosteriko positiboa eta ORG27569 eta PSNCBAM modulatzaileak. Azken bi modulatzaile alosteriko hauek propietate farmakologiko bereziak dituzte, CP 55,940 agonista kannabinoidearen loturaren modulatzaile positiboak diren bitartean, Gαi/o proteinen akoplamenduaren modulatzaile negatiboak direlako. Kannabidiola, Δ9THC-kin batera kannabisaren printzipio aktibo nagusiena dena, CB1 hartzailearen modulatzaile alosteriko negatibo bezala identifikatu da (Pertwee et al., 2010; Pertwee, 2015; Khurana et al., 2017).

Agonista kannabinoideek CB1 hartzailearekin interakzionatzean honen konformazio aktiboa estabilizatzen dute, zelularen barneko transdukzio proteinekin interakzionatzea induzituz. CB1 hartzailea Gαi/o proteina heterotrimerikoekin akoplatzen da, nahiz eta Gαs eta Gαq/11 proteinetara ere akoplatzeko gaitasuna duela ebidentziatu den (Howlett et al., 2002; Turu and Hunyady, 2010). Agonista, hartzaile eta Gi/o proteinaren arteko interakzioak Gαi/o proteina heterotrimerikoaren α subunitateari lotuta dagoen GDP nukleotidoa askatzea eta GTP nukleotidoa lotzea eragiten du. GDP-GTP trukeak proteina heterotrimeroa osatzen duten subunitateen eta CB1 hartzailearen arteko disoziazioa eragiten du. Egoera honetan, Gα eta Gβy subunitateek efektore ezberdinekin interakzionatzen dute agonisten estimuloa zelula barnera transduzitzeko. Subunitate hauen seinaleztapena amaitzeko eta prozesu hau ziklikoki emateko, Gαi/o proteina bere forma heterotrimerikoan osatu behar da. Horretarako, Gα subunitatearen GTPasa aktibitateak GTP nukleotidoa GDPan hidrolizatzen du, Gα subunitatea eta Gβy dimeroaren elkarketa ahalbidetuz. (Gilman, 1987).

Aipatu den moduan, Gα eta Gβy subunitateek efektore ezberdinekin interakzionatzen dute zelula barneko seinaleztapen bideak aktibatzeko. Adibidez, Gαi/o proteinaren Gα subunitateak adenilato ziklasaren aktibitate entzimatikoa inhibitzen du bigarren mezularia den AMP ziklikoaren ekoizpena gutxituz. Honek AMP ziklikoak estimulatzen duen proteina kinasa A-ren (PKA) aktibazioaren gutxitzea eta honen sustratoak diren proteina ezberdinen fosforilazio maila gutxitzea dakar, azkenik beste zenbait efektoreen aktibitatea erregulatuz, adibidez boltai menpeko A motako K+ erretenen aktibazioa, oxido nitriko sintasaren inhibizioa edo zenbait transkripzio faktoreren aktibitatearen erregulazioa besteak beste. Bestetik, Gβy subunitateak boltai menpeko N eta P/Q kaltzio erretenak itxitzen eta G protein-coupled inwardly-rectifying potassium (GIRK) eta A potasio erretenak irekitzen dituela aski ezaguna da. Gainera, Gβy subunitateak ere adenilato ziklasaren isoforma espezifikoak aktibatu ditzakela ikusi da eta PLCβ entzima aktibatu dezakenaren ebidentziak ere badaude. Mitogenoek aktibaturiko proteina kinasaren (MAPK) aktibazioa (ERK1/2, JNK edota p38MAPK kinasak) Gi/o proteinek martxan jartzen duten beste seinaleztapen bide bat da. CB1 hartzaileak, MAPK kinasak aktibatzeko bide ugari erabili ditzakela deskribatu da: cAMP/PKA seinaleztapen bidearen inhibizioaren eta honen ondoriozko c-fas kinasaren fosforilazio gutxipena, fosfatidilnositol 3 kinasa/proteina kinasa B seinaleztapen bidearen aktibazioa edota src edo fyn-en fosforilazioa batzuk aipatzearren. Adierazi den moduan, CB1 hartzaileak Gαs eta Gαq/11 proteinetara ere akoplatzeko gaitasuna duela ebidentziatu da. Kasu honetan, Gαs proteinaren aktibazioak adenilato ziklasaren aktibate entzimatikoa estimulatzen du AMP ziklikoa bigarren mezularia produzitzeko, nukleotiko zikliko honen menpeko erreten ionikoak eta PKA kinasa aktibatuz. CB1 hartzaileak Gαq/11 proteinari akoplatuz, berriz, PLCβ entzima estimulatzen du inositol trifosfatoa (IP3) eta DAG-a bigarren mezulariak produzituz. IP3-ak erretikulu endoplasmatikoan IP3 hartzaileari lotzean, kaltzio biltegietatik kaltzioa zitoplasmara askatzea induzitzen da eta DAG-ak proteina kinasa C (PKC) entzima aktibatzea eragiten du, azken honek beste entzima batzuen aktibitatea erregulatzeko. (Howlett et al., 2002; Turu and Hunyady, 2010) (ikusi 5. Irudia). Azken urte hauetan, CB1 hartzaileak G proteinekiko independenteak diren efektoreak aktibatu ditzakela deskribatu da. Adibidez, β-arrestinen rola CB1 hartzailea eta Gαi/o proteinen arteko interakzioa erregulatzeaz haratago doa eta seinaleztapen proteinak erreklutatu eta aktibatzen dituela ebidentziatu da (Pierce and Lefkowitz, 2001; Luttrell and Lefkowitz, 2002). Hala, β-arrestinak CB1 hartzailearen aktibazioak sortzen dituen epe luzerako efektuetan inplikatu dira, adibidez geneen transkripzioaren eta

proteinen sintesiaren erregulazioan. Izan ere, CB1 hartzailearen aktibazioak β-arrestinen menpekoa den ERK1/2, src, MEK1/2, JNK1/2/3, CREB eta P38α proteinen fosforilazioa induzitzen du.(Ahn, Mahmoud and Kendall, 2012; Ahn et al., 2013; Bagher et al., 2013; Baillie et al., 2013; Flores-Otero et al., 2014; Laprairie et al., 2014; Mahavadi et al., 2014; Delgado-Peraza et al., 2016). Esfingomielinaren hidrolisia eta zeraminaren produkzioa ere CB1 hartzailen aktibazioak bultzatu dezakeen beste prozesu bat da, esfomielinasa neutroarekin asoziatutako faktorearekin (FAN) interakzionatzen duelako CB1 hartzaileak (Guzmán, Galve-Roperh and Sánchez, 2001; Sánchez et al., 2001).

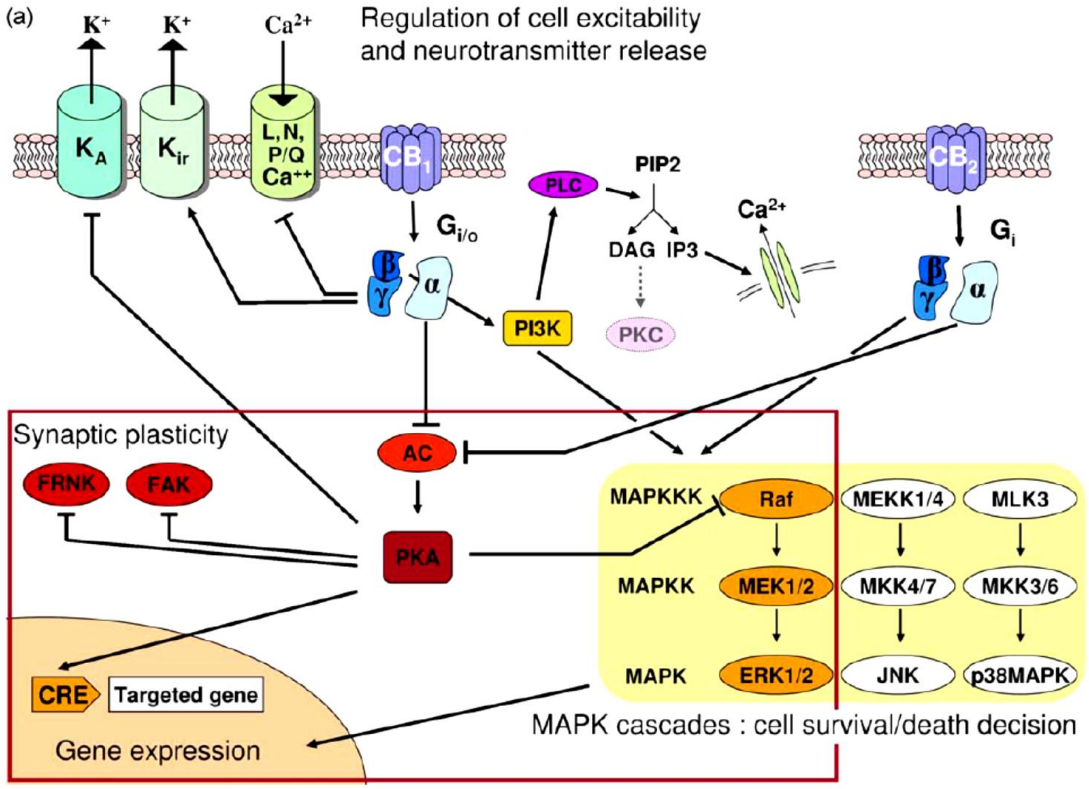

5. irudia. CB1 hartzailearen seinaleztapen bide nagusiak. Gαi/o proteinen akoplazioa eta Gα-GTP eta Gβγ subunitateen bitartez zelula barneko efektore ezberdinen aktibazioa, adibidez adenilato ziklasaren inhibizioa, kaltzio eta potasio erretenen erregulazioa eta MAP bideen aktibazioa besteak beste (Bosier et al., 2010-tik eraldatua).

CB1 hartzaileak aktibatzen dituen sinaleztapen bideak in vitro entseguetan karakterizatu dira, zelula mota ezberdinak erabiliz. Horregatik, kontu handiz interpretatu behar dira sistema heterologoetan lortzen diren emaitzak, CB1 hartzaileak aktibatzen dituen seinaleztapen bideak testuinguru zelularraren menpekoak direlako. Hau da, hartzailearen, transdukzio proteinen eta proteina osagarrien espresio mailak eragin zuzena du hartzaileak proteina efektore hauekin akoplatzeko duen gaitasunean, eta proteina hauen

espresioa aldakorra da zelulen artean (Busquets-Garcia, Bains and Marsicano, 2018). Horregatik, CB1 hartzaileak aktibatutako seinaleztapen bide ezberdinak in vivo duten esangura edo hauen funtzio biologikoa zein den aztertu behar da (Nogueras-Ortiz and Yudowski, 2016). Adibidez, terminal presinaptikoetan espresatzen den CB1 hartzaileak Gαi/o proteinari akoplatuz erregulatzen du neurotransmisioaren askapena. Epe laburreko depresioan, Gαi/o proteinaren βy subunitatek boltai menpeko kaltzio erretenak inhibitzen ditu eta neurotransmisorearen askapena segundu batzuetan gutxitzen da.(Chevaleyre, Kanji A. Takahashi and Castillo, 2006; Ohno-Shosaku et al., 2012). GIRK eta A motatako potasio erretenen parte hartzea ere proposatu da, baina hipotesi hau ez dago baieztatua. (Chevaleyre, Kanji A. Takahashi and Castillo, 2006). Epe luzerako depresioan, CB1 hartzaileak martxan jartzen dituen seinaleztapen bideak ere ez dira guztiz ezagunak. Hala ere, ezaguna da CB1 hartzailearen aktibazioa minutu batzukoa izan behar dela epe luzerako depresioa fenomenoa induzitzeko. Aktibazio irakunkor honek adenilato ziklasaren aktibitate entzimatikoa murrizten du Gαi/o proteinaren α subunitatearen bitartez eta honek AMP ziklikoa/PKA seinaleztapenaren aktibazioaren gutxipen bat eragiten du, transkripzio genikoan aldaketak bultzatuz. Horrela, neurotransmisioraren prozesuan garrantzitsuak diren proteinen espresioan aldaketak ematen dira, azkenik terminal presinaptikoan aldaketa estrukturalak emanez (Chevaleyre, Kanji A. Takahashi and Castillo, 2006; Ohno-Shosaku et al., 2012).

Farmakologiaren ikuspuntu klasikotik 7 mintz-zeharreko domeinu dituzten hartzaileak etengailu soilak kontsideratu dira, hartzailea konformazio inaktiboan edo aktiboan aurkitu daitekelarik. Horregatik, agonisten eraginkortasunaren kontzeptu farmakologikoa lineala dela asumitu da, hau da, agonistek hartzailea aktibatzean honekin konektatuta dauden zelularen barneko seinaleztapen bide guztiak martxan jartzen dituela pentsatu izan da. Hala ere, gaur egungo datuek adierazten dute farmakologiaren eraginkortasunaren kontzeptua pluridimentsionala dela, hau da, agonista ezberdinek seinaleztapen bide zelular batzuk aktibatu eta lehenetsi ditzaketela beste bide batzuen aurretik, kalitate eta kantitate ezberdineko erantzun zelularrak sortzeko. Izan ere, agonista bakoitzak hartzailearen egoera aktiboaren konformazio multzo bakarra estabilizatzen du eta hartzailearen konformazio aktibo multzo bakoitzak erantzun intrazelular ezberdinetara akoplatzeko joera ezberdina dute. Selektibitate funtzionalaren fenomeno honek interes handia piztu du terapeutikan, efektu onuragarriak eragiten dituen seinaleztapen bideak hautatzeko eta efektu desiragarrien arduradunak diren bide zelularrak inhibitzeko aukera

ematen duelako. GPCR-en ligando ortosterikoek eta alosterikoek erakutsi dute seinaleztapen bide intrazelularrak hautatzeko edo lehenesteko gaitasuna. Ligando alosterikoen kasuan, hauek selektibitate funtzionala duten agonistak izan daitezke edota agonista ortosterikoen selektibitate funtzionala modulatu dezakete (Kenakin and Christopoulos, 2013; Kenakin, 2015).

CB1 hartzailearen selektibitate funtzionala aztertu duten entsegu ugari publikatu dira azken urte hauetan. Entsegu hauek erakutsi dute CB1 hartzaileak Gαi/o azpi mota bakoitza aktibatzeko duen eraginkortasuna agonista kannabinoidearen menpekoa dela. Adibidez, entsegu hauetan determinatu da WIN 55,212-2 Gαi azpi mota guztien agonista osoa den bitartean, metanandamida Gαi3 agonista osoa eta Gαi1 eta Gαi2 azpi moten alderantzizko agonista dela (Glass and Northup, 1999; Mukhopadhyay and Howlett, 2005). Ikerketa hauen aurkikuntza garrantzisu bat izan da 2-AG-a eta anandamida endokannabinoideek, zenbait ligando kannabinoide sintetikorekin batera, transdukzio bide intrazelularrak estimulatzeko joera desberdina dutela azaltzea. Hala, entsegu hauek erakutsi dute anandamida 2-AG-a baino eraginkorragoa dela AMP ziklikoaren produkzioa inhibitzen 1/2ERK-ren fosforilazioa induzitzen baino (Khajehali et al., 2015). Beste ikerketa batean, adibidez, CB1 hartzaileak Gαi/o, Gαq/11, Gαs, Gβy eta β-arrestinen menpekoak diren seinale intrazelularretara akoplatzeko gaitasuna entseguan erabiltzen den agonista kannabinoidearen (exogeno edota endogeno) araberakoa dela frogatu da (Laprairie et al., 2016). Orokorrean, CB1 hartzailearetatik haratago selektibitate funtzionalaren fenomenoa aztertu duten ikerketa gehienak agonistek G proteinen eta β-arrestinen menpekoak diren bide intrazelularren aktibazioa bereizteko gaitasunean zentratu dira. CB1 hartzailearen kasuan, modulatzaile alosterikoek erakutsi dute bi seinaleztapen bide hauek bereizteko gaitasuna, Org27569 eta PSNCBAM-1 konposatu alosterikoek hain zuzen ere. Zehazki, bi konposatu hauek β-arrestinen menpeko transdukzio bideen modulatzaile alosteriko positiboak eta G-proteinen menpeko sinaleztapen bideen modulatzaile alosteriko negatiboak dira (Ahn, Mahmoud and Kendall, 2012; Ahn et al., 2013).

Orokorrean, mintz plasmatikoko hartzaileen espresioak agonisten hasierako estimulu maila kontrolatzen du eta agonistarekiko erantzuna hartzailearen dentsitate mailarekin proportzionala izaten da. Beraz, ez da arritzekoa hartzaileen mailak zelula eta garun zonalde ezberdinetan zehar aldakorrak izatea, seinaleztapen bideen aktibazioa zehaztasunez erregulatzeko mekanismo aproposa da eta (Kenakin, 2002). Hala ere,

hartzaileak martxan jarri ditzaken zelula barneko seinaleztapen bideen aktibazioa ez da beti ere hartzailearen espresioarekiko proportzianala. Adibidez, CB1 hartzaile maila baxuak aurkitzen diren zonalde batzuetan, CB1 hartzaileak Gαi/o proteinetara akoplatzeko duen gaitasuna CB1 hartzailearen espresio maila altuagoak dituzten zonaldetan baino handiagoa dela ikusi da (Breivogel, Sim and Childers, 1997). Bestetik, garun zonalde berdineko zelula ezberdinetan ere CB1 hartzailearen menpeko Gαi/o proteinen bidezko seinaleztapenaren eraginkortasuna aldakorra izan daiteke. Fenomeno hau adibidez hipokanpoan deskribatu da. Hala, nahiz eta neurona glutamatergikoetan espresatzen den CB1 hartzailearen maila nabarmen baxuagoak izan neurona gabaergikoetan espresatzen direnarekin alderatuta, hauek Gαi/o proteinetara akoplatzeko efizientzia handiagoa erakutsi dute. Zehazki CB1 hartzaileak aktibatzen dituen Gαi/o proteinen %50-a baino gehiago neurona glutamatergikoetan ematen da eta neurona gabaergikoetan espresatzen den CB1 hartzailea, aldiz, Gαi/o proteinen aktibazioaren %20-30-aren erantzulea da (Steindel et al., 2013).

Faktore ugari proposatu dira 7 mintz-zeharreko domeinu ditutzten hartzaileen funtzionalitate kanonikoa baldintzatu dezaketenak, adibidez, G proteina azpi-mota, hartzaile:G proteina estekiometria, proteina osagarrien presentzia edota hartzailea mintz plasmatikoko domeinu espezifikoetan kokatzea besteak beste. Adibidez, agonistak aktibaturiko CB1 hartzailea efizientzia ezberdinarekin akoplatu daiteke Gαi/o subunitate azpi mota bakoitzarekin (Gαi1, Gαi2, Gαi3, Gαo1 eta Gαo2), beraz, hauen espresio mailak ezberdinak badira garun zonalde edota zelula ezberdinetan, CB1 hartzaileak Gαi/o azpi-mota baten aktibazioa lehenetsi dezake besteen aurretik. Gainera, G proteinen espresioa aldakorrak badira garun zonaldeen eta fenotipo zelular ezberdinen artean, CB1:G proteina estekiometria eta akoplamenduaren efizientzia aldakorra izatea eragin dezake (Breivogel, Sim and Childers, 1997). Aipatu bezala, CB1 hartzailearekin interakzionatzen duten zenbait proteina osagarrik hartzailearen funtzionalitatea baldintzatu dezake. Adibidez, CRIP1a, CB1 hartzailearen seinaleztapena erregulatzen duen proteina osagarri bat da. CRIP1a-ak, CB1 hartzailea Gαi/o azpi-motetara akoplatzeko gaitasuna baldintzatzen duela egiaztatu da, Gαi2 eta Gαi3 proteinen akoplamendua lehenetsiz Gαi1 eta Gαo kaltean (Niehaus et al., 2007; Smith, Sim-Selley and Selley, 2010; Blume et al., 2017). Proteina hau neurona piramidaletan eta neurona gabaergikoetan espresatzen dela ikusi da (Guggenhuber et al., 2016). Beraz, CB1 hartzailearen funtzioa bi fenotipo neuronal hauetan erregulatzeko proteina aproposa da

CRIP1a. Bestetik, mintz plasmatikoan aurkitzen diren zenbait lipidoek CB1 hartzailearen funtzioa modulatu dezaketela frogatu da (Bari, Battista, et al., 2005; Bari, Paradisi, et al., 2005; Díaz, Dalton and Giraldo, 2019). Adibidez, kolesterolak CB1 hartzailearen funtzioa negatiboki erregulatzen duela ebidentziatu da. Izan ere, mintzeko kolesterol mailaren gutxipenak CP 55,940 agonista kannabinoidearen eta CB1 hartzailearen lotura eta CB1 hartzailearen eta Gαi/o proteinen arteko akoplazioa handitzen du (Bari, Battista, et al., 2005; Bari, Paradisi, et al., 2005). Kolesterolak modu espezifikoan burutzen ditu efektu hauek, izan ere, CB1 hartzailearen estruktura kristalinoa aztertu duten ikerketek baieztatu dute kolesterolak CB1 hartzailearekin espezifikoki interakzionatzen duela. Hori dela eta, kolesterola CB1 hartzailearen moduladore alosteriko negatiko endogeno gisa identifikatu da (Hua et al., 2017, 2020). Honekin bat dator CB1 hartzailearen aminoazido sekuentzian kolesterolarekin interakzionatzeko gune espezifikoak identifikatu izana, colesterol recognition aminoacid consensus (CRAC) eta cholesterol consensus motif (CCM) domeinuak hain zuzen ere (Oddi et al., 2011; Sabatucci et al., 2018; Hua et al., 2020). Horrenbestez, mintz plasmatikoko lipidoen konposizioa faktore garrantzitsua izan liteke 7 mintz-zeharreko domeinu dituzten hartzaileen aktibitatea modulatzeko. Hala, hartzaile hauek lipid-raft izenez ezagutzen diren eta kolesterola eta esfingosina konposatuetan aberastuta dauden mintz plasmatikoko domeinu espezifikoetan aurkitu daitezke. Domeinu hauek transdukzio seinaleak erregulatzeko plataformak kontsideraten dira, hartzaileen eta hauen seinaleztapen proteinen arteko interakzioak efizienteki burutu daitezen zihurtatzen dituztenak (Hancock, 2006; Pike, 2006). CB1 hartzailea lipid-raft domeinuetan aurkitzen denez (Sarnataro et al., 2005; Dainese et al., 2007; Asimaki et al., 2011) eta mintz plasmatikoko domeinu hauetan kolesterolaren mailak mintzeko ez-raft domeinuetan baino nabarmen handiagoak direnez kolesterolak CB1 hartzailearen funtzioa negatiboki erregulatzeko estruktura aproposak direla proposatu dira lipid-raft-ak (Dainese et al., 2007; Maccarrone et al., 2009)- Izan ere, mintzeko kolesterol maila murrizteko erabiltzen diren estrategiek, adibidez β-metilziklodextrina konposatuaren bitarteko mintzen tratamenduak, kolesterola batez ere lipid-raft domeinuetatik deplezionatzea eragiren du, mintz plasmatikoko domeinu hauek desestrukturatuz (Dainese et al., 2007; Maccarrone et al., 2009).

II. LAN HIPOTESIA ETA HELBURUAK

Nerbio sistema zentralean CB1 hartzailea neurona glutamatergikoetan kantitate baxuan eta neurona GABAergikoetan dentsitate altuan espresatzen da nagusiki (Mailleux and Vanderhaeghen, 1992a; Katona *et al.*, 1999, 2006; Marsicano and Lutz, 1999). Bi terminal presinaptiko mota hauetan aurkitzen den CB1 hartzailearen aktibazio endogenoak plastizitate forma ezberdinak induzitzen ditu neurotransmisio eszitatzaile eta inhibitzailean. (Chevaleyre, Takahashi and Castillo, 2006; Kano *et al.*, 2009; Castillo *et al.*, 2012; Kano, 2014). Horrela, CB1 hartzaileak rol garrantzitsua jokatzen du balantze eszitatzaile-inhibitzailean eta horregatik bere kontribuzioa oso garrantzitsua da portaera ezberdinak erregulatzeko.(Busquets-Garcia *et al.*, 2015; Lutz *et al.*, 2015). Adibidez, neurona glutamatergikoetan aurkitzen den CB1 hartzailea neuroprotekzioan (Monory *et al.*, 2006; Chiarlone *et al.*, 2014), usaimen prozesuetan (Soria-Gómez *et al.*, 2014), estresan eta antsietan (Steiner *et al.*, 2008; Jacob *et al.*, 2009; Kamprath *et al.*, 2009; Dubreucq *et al.*, 2012; Metna-Laurent *et al.*, 2012; Rey *et al.*, 2012) eta jatearen gogoaren erregulazioan (Lafenêtre, Chaouloff and Marsicano, 2007; Bellocchio *et al.*, 2010) parte hartze zuzena du. Bitartean, CB1 hartzaile GABAergikoak ikasketa eta memoria prozesuetan, (Puighermanal *et al.*, 2009; Albayram *et al.*, 2016), droga adikzioan (Talani and Lovinger, 2015; Martín-García *et al.*, 2016) eta neurona glutamatergikoetako CB1 hartzaileak sorrarasten dituen alderantzizko prozesuak erregulatzen ditu (Monory *et al.*, 2006; Dubreucq *et al.*, 2012).

Horregatik, CB1 hartzailearen eta Gαi/o proteinen arteko akoplamentuaren azterketa zehatza beharrezkoa da CB1 hartzailearen agonisten efektuak garunean zehar karakterizatzeko. Adibidez, hipokanpoan, CB1 hartzailearen eta Gαi/o proteinen arteko akoplamendua neurona glutamatergikoetan neurona GABAergikoetan baino eraginkorragoa dela determinatu da (Steindel *et al.*, 2013). Zentzu hortan, agonisten selektibitate funtzionalak GPCR hartzaileen eta farmakoen garapenean paradigma aldaketa ekarri zuen bezala, neurona glutamatergiko eta GABAergikoetako G proteinen menpeko seinaleztapenaren eraginkortasunean ematen diren desberdintasunak antzeko aldaketa eragin behar lukete. Orain dela gutxi, zelula mota espezifikoetan CB1 hartzailea erreskatua duen sagu transgenikoen garapenak, neurona glutamatergiko eta GABAergikoetako CB1 hartzaileak paradigma esperimental honetan sistematikoki aztertzeko aukera ematen du (Ruehle *et al.*, 2013; Remmers *et al.*, 2017). Beraz, hipokanpoko eta kortex frontaleko sinaptosometan CB1 hartzailearen Gαi/o proteinen menpeko seinaleztapen kanonikoa (agonistek-estimulatutako [^{35}S]GTPγS lotura

entseguen bitartez aztertua), hartzailea aurkitzen den neuronaren menpekoa izan liteke, baita mintz plasmatikoaren mikrodominio espezifikoetan aurkitzearen menpekoa ere. Horregatik, CB1 hartzailea eta Gαi/o proteinak konpartimentu azpi-sinaptikoetan (sinaptosometatik eratorritako pre-, post- eta gune estrasinaptikoan) eta lipid-raft deritzen mintz plasmatikoko mikrodomeinu berezietan hauen espresio erlatiboa aztertzea ere garrantzitsua da, aipatu bezaka G proteinen bitarteko seinaleztapena lokalizazio honen menpekoa ere izan daitekelako. Gainera, sagu transgeniko hauetan CB1 hartzailearen erreskatea zelula espezifikoetan era egokian eta endogenoki espresatzen den kantitatetan burutzeak berebiziko garrantzia du.

Bestetik, azken urteetan, mintz plasmatikoa osatzen duten zenbait lipidoek, kolesterolak nagusiki, GPCR hartzaileen lokalizazioa eta funtzioa erregulatzen dutela ikusi da (Gimpl, 2016). Adibidez, metil-β-ciclodextrina (MβCD) konposatua erabiliz mintz plasmatikoko kolesterolaren mailaren gutxipenak CB1 hartzailearen agonisten lotura maximoa (Bmax) eta agonistek estimulatutako [^{35}S]GTPyS loturaren eraginkortasuna handitzen du (Bari, Battista, *et al.*, 2005; Bari, Paradisi, *et al.*, 2005; Oddi *et al.*, 2011). Hala ere, fenomeno honen ingurukoak zelula modelo heterologoetatik lortu da (Hudson, He and Kelly, 2010). Horregatik, MβCD tratamenduaren bitartez, kolesterolak eraginkortasun ezberdineko agonista kannabinoideek estimulatutako CB1 hartzailearen eta Gαi/o proteinen arteko akoplamendua kortexetik isolatutako sinaptosoma mintzetan erregulatzen duen aztertzea garrantzitsua da.

Helburuak

Tesi honen helburu nagusia saguen frontaleko eta hipokanpoko neurona glutamatergiko eta GABAergikoetan aurkitzen den CB1 hartzailearen Gαi/o proteinen bitarteko seinaleztapen kanonikoaren azterketa orokor bat burutzea da, CB1 hartzailearen mintzeko antolamendua eta funtzionalitate kanonikoaren printzipioak ezagutzeko entsegu biokimikoek duten gaitasuna plazaratzearekin batera. Horretarako, biologia molekularreko, biokimikako eta farmakologiako teknika ezberdinak konbinatu ditugu.

Tesi doctoral honetan zehaztutako helburu espezifikoak hurrengoak dira:

1. Sistema endokannabinoidea osatzen duten proteinen espresioa ikastea WT eta CB1 hartzailea zelula espezifikoetan erreskatua duen sagu transgenikoan kortex frontaleko eta hipokanpoko sinaptosometan.

2. CB1 hartzailearen eta Gαi/o proteinen distribuzio azpi-sinaptikoaren deskribapen zehatza burutzea, CB1 hartzailearen erreskatearen estrategiak CB1 hartzailearen maila endogenoak berrezartzen dituela frogatzeko.

3. CB1 hartzailearen Gαi/o proteinen menpeko seinaleztapen kanonikoa karakterizatzea sinaptosoma mintzetan, CB1 hartzailearen seinaleztapen hau neurona glutamatergikoetan edota neurona GABAergikoetan aurkitzearen menpekoa izan daitekeen frogatzearekin batera.

4. Sinaptosoma mintzetan, kolesterola mailaren deplezioak terminal glutamatergikoko eta GABAergikoko CB1 hartzailearen agonisten propietate farmakologikoetan (Eraginkortasuna eta potentzia) izan dezakeen eragina aztertzea.

III. MATERIALA

ANIMALIAK

Sprague-Dawley arraoiak eta C57BL/6j saguak Harlan Iberica (Bartzelona, Espainia) eta Janvier-labs (Le Genest-Saint-Isle, Frantzia) enpresetatik erosi genituen. Animaliak iristean, gehienez ere, binakako edo hirunakako taldetan kaiolatu ziren ingurugiro kontrolatuan (12 orduko argi-iluntasun zikloak, argia goizeko 8:00 tan hasita eta 22 ℃ ± 2 inguru tenperaturan), ad libitum janari eta urarekin hornituta. 8 eta 12 aste bitarteko animaliak, gutxienez astebetez utzi ziren ingurunera egokitzen esperimentuak hasi aurretik. Prozedura esperimental goizeko 10:30 etatik 12:00 tara bitartean burutu ziren. Arratoi eta saguak arreta osoaren manipulatu ziren, mina eta sufrimendua ahalik eta gehien murrizteko, Europar Batasuneko Kontseiluaren 2010eko irailaren 22ko Zuzentarauen (2010/63/EU) eta Espainiako araudiaren (53/2013 Errege Dekretua, 2013-02-08ko BOE) jarraibideen arabera.

CB1 hartzailearen erreskatea duten sagu transgenikoak (Ruehle et al., 2013; Remmers et al., 2017) Beat Lutz doktoreak zuzentzen duen "Molecular Mechanisms of Behavior" ikerkuntza taldeak eskeini zizkigun. CB1 hartzailea ezeztaturiko sagu transgenikoan (Stop-CB1), CB1 hartzailearen espresioa inhibituta aurkitzen da sekuentzia kodifikatzailearen aurrean kasete bat duelako txertaturik (transcriptional stop cassette) CB1 hartzaile endogenoaren sekuentzia kodifikatzailea irakurri ahal ez izateko hain zuzen ere. Kasete hau bi loxP guneen artean aurkitzen da. Horrela, CB1 hartzailearen erreskate partziala edo osoa lortzeko sagu hau NEX-Cre edota Dlx-Cre eta EIIa-Cre sagu transgenikoarekin gurutzatzen da, hurrenez hurren. Zehazki, Glu-CB1-RS saguan CB1 hartzailea telentzefalo dortsaleko neurona glutamatergikeotan erreskatatzen da eta GABA-CB1-RS saguan berriz, aurre garuneko neurona GABAergikoetan berreskuratzen da CB1 hartzailea. WT moduko CB1-RS saguetan, CB1 hartzailearen erreskate osoa lortzen da.

ERREAKTIBO OROKORRAK

- Azetona (Panreac, 211007).
- Azida Sodikoa (Panreac, 122712).
- Azido Klorhidrikoa %37 (Panreac).
- Behi albumina serikoa (Sigma-Aldrich, A3608).
- Behi albumina serikoa, gantz azido gabea (Sigma-Aldrich, 126575).
- BCA proteina kuantifikatzeko Kit-a (Abcam, ab102536).
- Biotool Protein A/G bola magnetikoak ((Cat#: B23201).
- Bradford Erreaktiboa (Bio-Rad, 500-0006) eta γ-Globulina estandarra (Bio-Rad, 500-0208).
- Calbiochem Cholesterol/Cholesteryl Ester-a kuantifikatzeko kit-a (Sigma-Aldrich, 428901).
- CHAPS (Sigma-Aldrich, C9426).
- Kloral hidratoa (Panreac, 141975).
- Dexoxikolato sodikoa (Sigma-Aldrich, D6750).
- Dimetilsulfoxidoa (DMSO) (Sigma-Aldrich, D8418).
- DL-Ditiotreitola (DTT) (Sigma-Aldrich, 43815).
- Dodezil sulfato sodikoa (SDS, Amersham, L3771).
- EDTA (Sigma, ED).
- EGTA (Sigma-Aldrich, E4378).
- Fenilmetanesulfonilo fluoruroa (PMSF, Sigma-Aldrich, P7626).
- Filtro-Papera (Bio-Rad, 165-0962).
- Gelatina (Panreac, 142060).
- Glizerola (Sigma-Aldrich, G8773).
- Glizina (Bio-Rad, 161-0724).
- Igepal CA-630 (Sigma, 18896).
- Isopropanola (Sigma-Aldrich, 278475).
- Isofluranoa (IsoVet –Braun, 469860).
- Iodoazetamida (Sigma-Aldrich, I1149).
- Kaltzio kloruroa (Panreac, 211221.1211).
- Kloroformoa (Sigma, C2432).
- Magnesio Kloruro Hexahidratoa (Panreac, 131396).
- Metanol Absolutua (Sigma-Aldrich, 32213).

- Methil-β-ziklodextrina (Sigma-Aldich, 332615).
- Mowiola (Calbiochem, 17951).
- Octil β-D-glukopiranosidoa (Sigma-Aldich, O8001).
- Paraformaldehidoa (Panreac, 141451).
- PNGase F (New England Biolabs, P0704).
- Potasio Kloruroa (Sigma-Aldrich, P5405).
- PPD (Sigma-Aldrich, P1519).
- Sakarosa (Sigma-Aldrich, S0389).
- Saponina (Sigma-Aldrich, 84510).
- Sodio Fosfato dibasikoa (PO4Na2H, Sigma-Aldrich, S0876).
- Sodio Fosfato monobasikoa (PO4NaH2, Sigma, S0751).
- Sodio Hidroxidoa (Probus, 131687).
- Sodio Kloruroa (Sigma-Aldrich, S7653).
- Tris[Hidroximetil]aminometanoa (Trizma® Base, Sigma-Aldrich, T1503).
- Triton X-100 (Sigma-Aldrich, T8787).
- Tween-20 (Bio-Rad, 170-6531).
- Urea (Sigma-Aldrich, U5378).
- β-merkaptoetanola (Sigma-Aldrich, M7522).
- 5 µm-ko filtroak (Whatman, 10 462 000).
- 96 putzutako EIA/RIA Plakak (Corning, 3590).

ERREAKTIBO ETA MATERIAL ESPEZIFIKOAK

[35S]GTPγS lotura entseguak

- Guanosina 5′-difosfato gatz sodikoa (Sigma-Aldrich, G7127).
- Guanosina 5′-O-(3-tiotrifosfato), gatz tetralitioduna (Sigma-Aldrich, 1022064700).
- Guanosina trifosfatoa, gamma fosfato taldean markaturik 35S-kin - GTPγS, [35S]-1250Ci/mmol, 12.5mCi/ml, 250 µCi (Perkin-Elmer, NEG030H250UC).
- Ultima Gold 2x5L zentelleo likidoa (Perkin-Elmer, 6013329).
- Whatman beirazko mikrozuntzezko iragazkiak GF/C 460 mm x 570 mm (GE Healthcare Life Sciences, 1822-915).
- Pyrex® 12x75 mm kultur hodiak(Corning, 99445-12).

- WIN 55,212-2 mesylate (Tocris BioScience, 1038).
- CP 55,940 (Tocris BioScience, 0949).
- (R)-(+)-Methanandamide (Tocris BioScience, 1782).

Western Blot

- Acrilamida/Bis-acrilamida, %40ko soluzioa (Bio-Rad, 161-0148).
- Amonio persulfatoa (Bio-Rad, 161-0700).
- Esne Gaingabetu Hautsa (Bio-Rad, 170-6404).
- Bromofenol Urdina (Sigma-Aldrich,11439).
- CL-XPosure Film Fotosentikorra (Thermo Scientific, 34089).
- Coomassie Urdina (Bio-Rad, 161-0400).
- ECL Clarity™ Western Sustratua (Bio-Rad, 170-5060).
- Errebelatzailea (Sigma-Aldrich, 7042).
- Filme fotosentikorren fixatzailea (Sigma-Aldrich, P7167).
- Laemmli Tanpoia (Bio-Rad, 161-0737).
- Precision Plus Protein™ kolore-estandarrak (Bio-Rad, 161-0374).
- PVDF Immuno-Blot® Mintza (Bio-Rad, 162-0177).
- TEMED (Bio-Rad, 161-0800).

Antigorputz eta sueroak inmunofluoreszentzia eta Western blot entseguetarako

Antigorputz primarioak

Antigorputza	**Diluzioa**		**Hostalaria klonalitatea**	**Isotipoa**	**Antigenoa**	**Erreferentzia.**
	IF	**WB**				
CB1 hartzailea		1:1000	Ahuntz poliklonala	Sueroa	Saguaren karboxi-terminalaren azken 31 aa (NM007726)	Frontier Institute CB1-Go-Af450
CB1 hartzailea		1:1250	Untxi poliklonala	Sueroa	Saguaren karboxi-terminalaren azken 31 aa (NM007726)	Frontier Institute CB1-Rb-Af380

CB1 hartzailea		1:5000	Untxi poliklonala	IgG	Segidako inmunozaziok saguaren karboxi-terminalaren azken 31 aa	Immunogenes anti-CB1 polyclonal antibody
DAGLα		1:4000	Untxi poliklonala	Sueroa	Saguaren karboxi-terminalaren azken 42 aminoazidoak (NM198114)	Frontier Institute,DGL-Rb-AF380-1
Crip1a/b		1:500	Untxi poliklonala	IgG	Gizakiaren CRIP1-ren peptido ezezaguna	Sta. Cruz Biotech. Inc sc-137401
Flotilina 1		1:1000	Untxi poliklonala	IgG	Gizakiaren Flotilina 1-ren 1 - 100 aminoazidoen tarteko peptido sintetikoa	Abcam ab41927
Gαq/11		1:1000	Untxi poliklonala	IgG	Saguaren Gα 11-ren peptido ezezaguna.	Sta. Cruz Biotech. Inc sc-392
Gαo		1:5000	Untxi poliklonala	IgG	Arratoiaren Gαo-ren peptido ezezaguna	Sta. Cruz Biotech. Inc sc-387
Gαi-1		1: 2500	Untxi poliklonala	IgG	Arratoiaren Gα1-ren peptido ezezaguna	Sta. Cruz Biotech. Inc sc-391
Gαi-2		1: 1000	Untxi poliklonala	IgG	Arratoiaren Gα2-ren peptido ezezaguna	Sta. Cruz Biotech. Inc sc-7276
Gαi-3		1:75000	Untxi poliklonala	IgG	Arratoiaren Gα3-ren karboxi terminalaren peptidoa	Sta. Cruz Biotech. Inc Sc-262
Gβ		1:10000	Untxi poliklonala	IgG	Arratoiaren Gβ-ren karboxi terminalaren peptidoa	Sta. Cruz Biotech. Inc sc-378
GAPDH		1:2000	Sagu monoklonala	IgG1	Zehaztu gabea	Abcam ab8245
Gefirina		1:1000	Untxi poliklonala	IgG	Saguaren Gefirinaren karboxi terminalaren peptido sintetikoa	Abcam, ab32206
GFAP	1:500	1:1000	Untxi poliklonala	IgG1	Behi bizkarrezur muinetik isolatuta	DAKO Z0334
Azetil-Histona H3		1:1000	Untxi monoklonala	IgG	H3 histonaren Lys9-aminoazidoa inguratzen duen aminoazid sekuentziaren peptido azetilatu sintetikoa	Cell signaling, 9671

MAP2	1:500	-	Sagu monoklonala	IgG_1	Behi MAP2	Sigma-Aldrich M2320
MAGL		1:1000	Ahuntz poliklonala	IgG	Giza MAGL-ren 17-29 aminoazidoen barneko sekuentziari dagokion peptido sintetikoa (C-QDLPHLVNADGQY)	Abcam, ab77398
MUNC-18/STXBP1-IsoA		1: 5000	Ahuntz poliklonala	Sueroa	NP_003156.1 karboxi terminalaren peptidoa (SRVSFEDQAPTME)	Sigma-Aldrich; SAB2500659
Na^+/K^+ ATPase	-	1:450	Sagu monoklonala	IgG_1	Arkume giltzurrunetik purifikatutako Na^+ / K^+ ATPasaren α1 azpiunitatea. Epitopoa 496-506 aminoazidoen tartean	Sigma-Aldrich A277, clone M8-P1-A3
NMDAR1	-	1:2000	Untxi monoklonala	IgG	Arratoiaren NMDA1 hartzailearen azpiunitatearen C-muturrari dagokion peptido sintetikoa (909-938 aminoazidoak)	Millipore AB9864
PLCβ1 (N-ter)	-	1:750	Sagu monoklonala	IgG_1	Arratoiaren PLCβ1-ren 4-159 aminoazidoei dagokien peptido sintetikoa	BD Transduction Laboratories 610924
PSD95		1:5000	Untxi poliklonala	IgG1	Gizakiaren PSD95-ren Gly99 aminoazidoen inguruko peptido sintetikoa	Cell Signaling 3450
Rab11b		1:8000	Sagu monoklonala	IgG2a	Gizakiaren Rab1. 86-207 aminoazidoen tarteko peptidoa	BD Transduction Laboratorie 610656
SHANK3		1:10000	Untxi poliklonala	IgG	Saguaren SHANK3-ren SH3 inguruko peptido sintetikoa	Abcam ab104702
SNAP-25	1:1000	1:4000	Sagu monoklonala	IgG1	Giza post-mortem garuneko prestakin sinaptiko gordina	Abcam ab24732

Sinaptofisina	1:8000	Untxi poliklonala	IgG1	Giza sinaptofisinaren 41-62 aminoazidoei dagokien peptidoa	Abcam ab14692
Sintaxina	1:1000	Sagu monoklonala	IgG1	Arratoiaren sintaxinaren 3-225 aminoazidoen tarteko peptidoa	Abcam ab3265
CD90/Thy1	1:1000	Untxi poliklonala	IgG	Giza CD90/Thy1 proteinaren amino-terminaletik gertu kokatzen den epitopoa	Abcam, ab92574

1. taula. Erabilitako antigorputz primarioak

Antigorputz Sekundarioak eta tintatzaile fluoreszenteak

- Alexa Fluor 488 Goat anti-Rabbit (Invitrogen, A11034).
- DyLight 649 Donkey anti-Mouse (Jackson Immuno Research, 715-496-151).
- DiIC16 (invitrogen, D384)Suero Normalak
- Anti-rabbit IgG HRP conjugate (Amersham, NA934).
- Anti-mouse IgG HRP conjugate (Amersham, NXA931).
- Anti-Goat IgG HRP conjugate (Sigma-Aldrich, A5420).

Suero Normalak

- Ahuntz-suero normala (normal goat serum -NGS-, Vector Laboratories, U0328).
- Asto-suero normala (normal donkey serum -NDS-, Vector Laboratories, U0111).

IV. METODOLOGIA

Ehunaren preparazioa

Arratoi edota saguak “kloral hidrato” edo isoflurano gaindosi batekin anestesiatu ziren dekapitatu aurretik. Garuna erauzteko, garezurra guraizeak erabiliz moztu zen eta burmuina osoa espatula baten laguntzaz atera genuen. Ondoren, burmuina odol-koaguluak eta meningeez garbitu zen garun eskualde desberdinen disekzioa hasi aurretik. Garunaren erdialdean ebaki sagital bat egin zen hemisferioak bereizteko. Lehenik, hipokanpoa isolatu genuen eta ondoren kortexa dientzefalotik eta gongoil basaletatik bereiztu zen. Isolaturiko laginetatik materiazuria ahalik eta gehien kendu ondoren, ehunak - 80 °C-tan gorde ziren erabili arte.

Sinaptosomen preparazioa

Sinaptosometan aberastutako preparazioa aurretiaz “Dodd et al” deskribatutako modu berean prestatu genuen, aldaketa txiki batzuk eginez (Dodd *et al.*, 1981; Garro *et al.*, 2001). - 80 °C-tara biltegiratutako sagu edo arratoien garuneko kortex eta hipokanpo laginak fosfato homogenizazio tanpoi batean (0.32 M sakarosa, 80 mM Na2HPO4, 20 mM NaH2PO4 pH 7.4) proteasa inhibitzaileekin (Iodoacetamida 50µM eta PMSF 1mM). desizoztu arte murgildu genituen. Ehuna, 1:10 (p/b) proportzioan homogenizazio tanpoiarekin homogeneizatu genuen Potter-Evelhem batean, irabiagailu elektriko (RSLAB 13/20) batera akoplatutako teflonezko enbolo baten laguntzaz (10 pase 800 rpm-ko abiaduran, 4 °C-tara hoztuta). Esekidura homogeneoa lortutakoan, zentrifuga hodietan banandu eta hauek 1000 x g-tara, 4 °C-tan 10 minutuz zentrifugatu genituen (Kontron, Centrikon T-42K, A-19C errotorea). Pelleta (P1; hautsi gabeko zelulak, nukleoak eta pisu handiko mintzak) berreseki eta prozedimendua berriz errepikatu genuen. Ondoren, gainjalkinak 15000 x g-tara 4 °C-tan 30 minutuz zentrifugatu genituen (Kontron, Centrikon T-42K, A-18C errotorea) mintz sinaptosomal gordinaren pelleta (P2) lortzeko. Pelletak 16 ml homogenizazio tanpoiean berreseki ostean, 1.2 M sakarosa duen 8 ml fosfato tanpoiarekin batera gradiente ez jarraikor bat osatu genuen. Gradiente hau 180000 x g-tara zentrifugatu zen 30 minutuz 4 °C-tan (Beckam XL-100, 70ti errotorea). Gradientearen interfasean atxikitutako elementuak (sinaptosomak, mielina eta mikrosomak) pasteur pipeta batekin jaso eta 0.32 M sakakosa duen fosfato tanpoiarekin diluitu ziren 16 ml amaierako bolumena izan arte. Azken prozedimendua berriz errepikatu

genuen, kasu honetan gradiente ez jarraikorra 0,8 M sakarosa duen fosfato tanpoiarekin sortuz. Sedimentutako pelletean lortutako sinaptosomak sakarosarik gabeko fosfato tanpoiean berreseki ondoren 1,5 ml-ko ependorfetan alikuotatu ziren eta 40000 x g tan zentrifugatu ziren 30 minutuz 4 °C-tan (Kontron, Centrikon T-42K, A-21C errotorea). Azkenik, gaingalkina xurgatu eta sinaptosomez osatutako pelletak - 80 °C-tan izoztu ziren. Sinaptosoma pelleten proteina kantitatea Bradford metodologiaren bitartez estimatu zen.

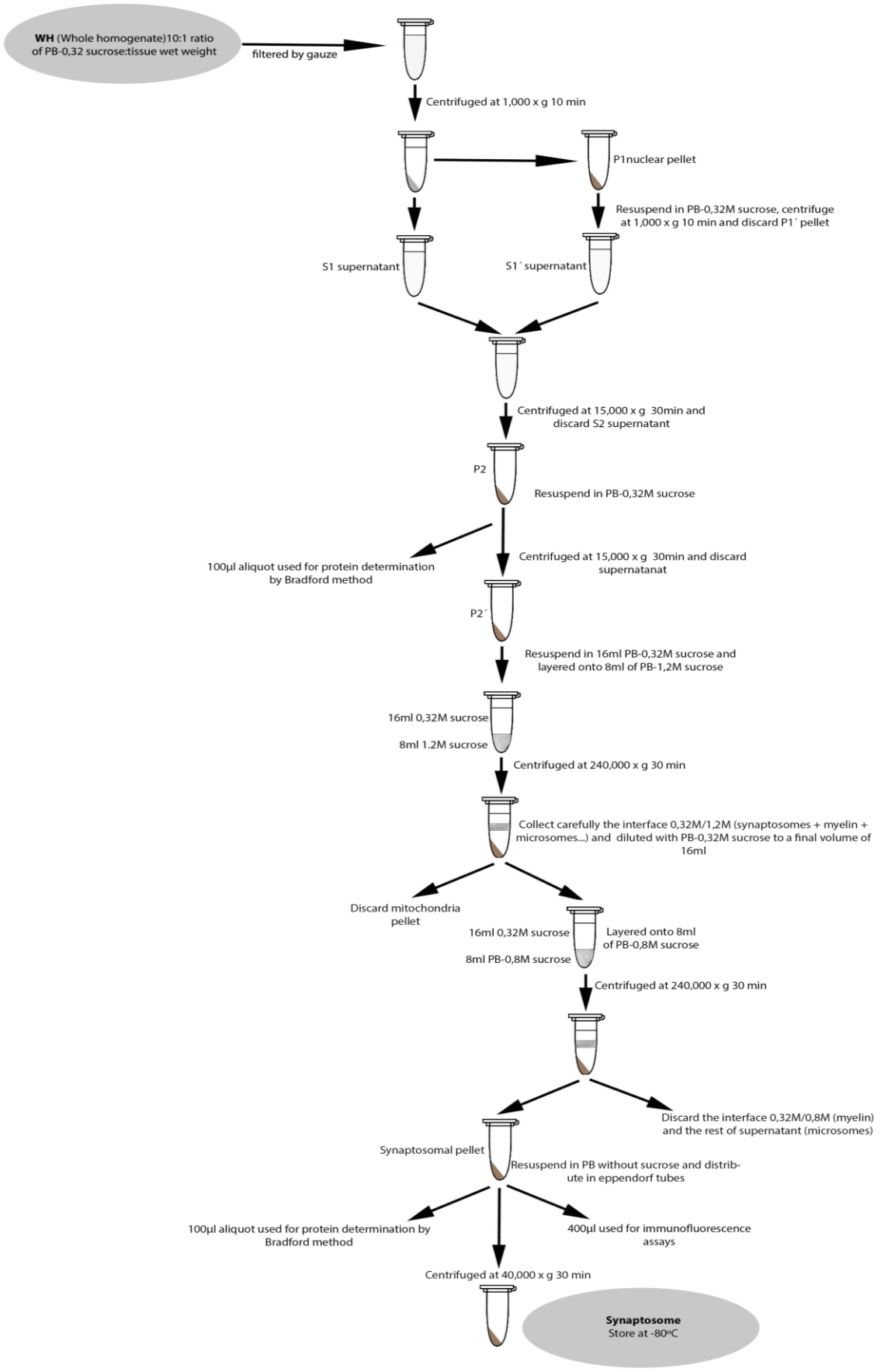

6. irudia. Sinaptosomak lortzeko garun laginen frakzionamendua.

Sinaptosomen frakzionamendu subsinaptikoa

Saguen kortexetik eratorritako sinaptosomak frakzionatzeko Phillips *et al.*, (2001) deskribaturiko metodologia erabili genuen. Horrela, dentsitate postsinaptikoa (PSD), presinapsiko zona aktiboa (PAZ) eta frakzio estrasinaptikoa (EXTRA) isolatu ziren. 4-5 mg proteina sinaptosomal 10 ml-tan disolbatu zen solubilizazio tanpoian (%1 Triton X-100, 20 mM Trisma basea, 0.1 mM $CaCl_2$, pH 6.0) eta 30 minutuz inkubatzen jarri ziren 4 °C-tan. Ondoren, sinaptosomak 40000 x g-tan zentrifugatu ziren 30 minutuz 4 °C-tan. Zentrifugazioan lortutako pelleta PSD eta PAZ-az osaturik dago, gainjalkinean EXTRA frakzioa disolbaturik aurkitzen den bitartean. Alde batetik, gainjalkina azetonarekin nahastu genuen (1:6 b/b gainjalkina/azetona proportzioa) - 20 °C tan eta 4 orduz jalkitzen utzi genuen nahaskina. Azkenik prezipitatutako proteinak 18000 x g-tan 30 minutuz 4 °C tan zentrifugatu genuen (Kontron, Centrikon T-42K, A-21C errotorea) proteina extrasinaptikoan aberatsa den frakzioa sedimentatuz. Bestetik, PSD eta PAZ frakzioek osatzen duten pelleta 10 ml solubilizazio tanpoian (%1 Triton X-100, 20 mM Trisma basea, 0.1 mM $CaCl_2$, pH 8.0) berreseki eta 30 minutuz inkubatzen jarri ziren 4 °C-tan. Ondoren, lagina 40000 x g-tan zentrifugatu zen 30 minutuz 4 °C-tan. Zentrifugazioan lortutako pelleta PSD-an aberatsa den frakzioa da, gainjalkinean PAZ frakzioa aurkitzen den bitartean. Alde batetik, gainjalkina azetonarekin nahastu genuen (1:6 b/b gainjalkina/azetona proportzioa) - 20 °C-tan eta 4 orduz jalkitzen utzi genuen nahaskina. Azkenik PAZ frakzioa jalkitzeko lagina 18000 x g-tan 30 minutuz 4-°C tan zentrifugatu genuen (Kontron, Centrikon T-42K, A-21C errotorea). Azkenik, frakzio azpi-sinaptikoak % 5-ko SDS-an solubilizatu ziren eta frakzio hauen proteina kontzentrazioa BCA metodologiaren bidez determinatu zen.

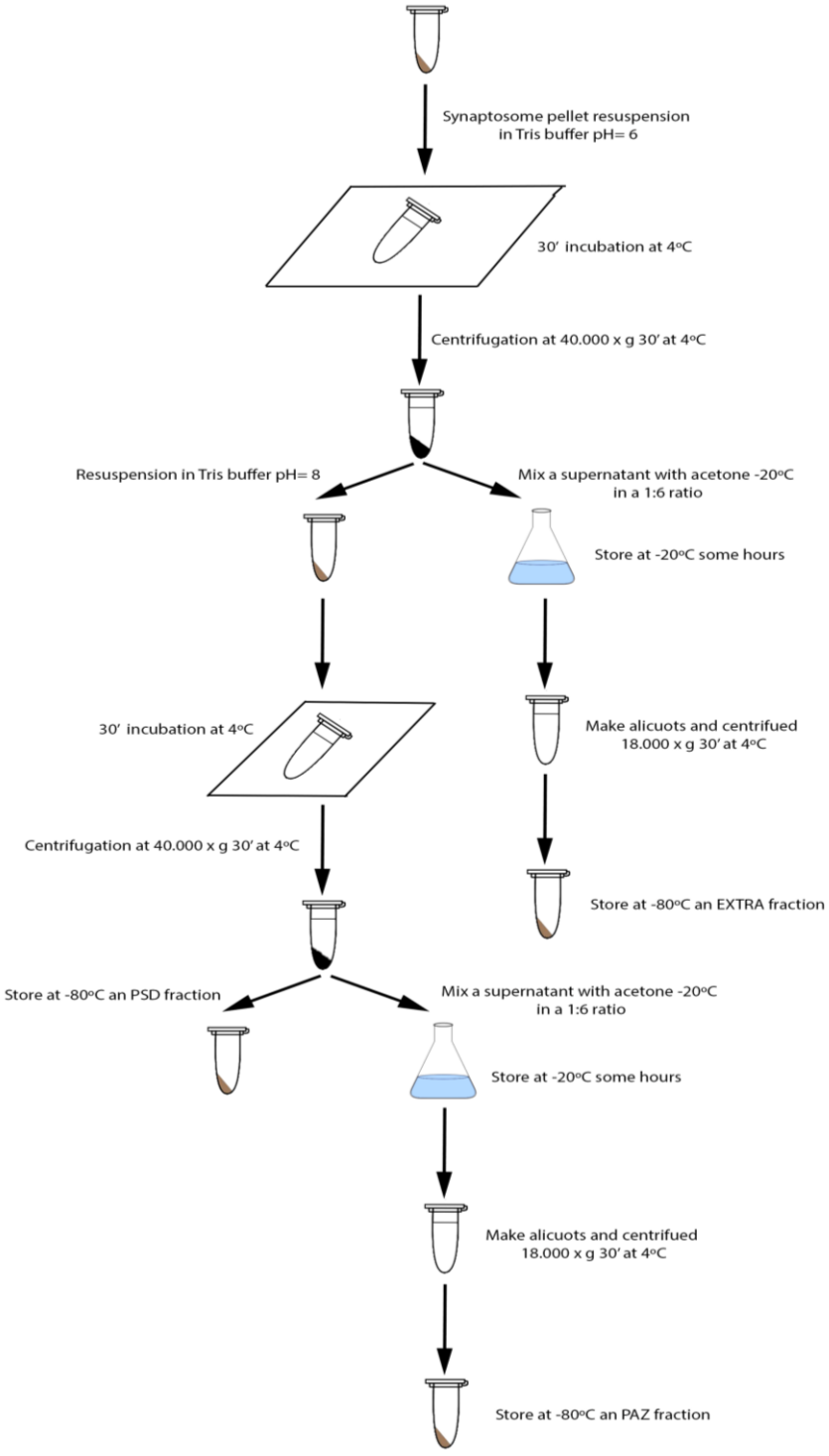

7. irudia Sinaptosomen frakzionamendu azpi sinaptikoaren diagrama

Lipid rafts mikrodomeinuen isolaketa sinaptosometatik abiatuta

6-8 mg sinaptosoma 2 ml % 1 Triton X-100 duen fosfato tanpoiean (80 mM Na2HPO4 eta 20 mM NaH2PO4, pH 7.4) berreseki ziren eta 30 minutuz inkubatu zen 4 ° C-tan. Laginaren 2 ml-ak % 90 sakarosa eta % 1 Triton X-100 duen 2 ml fosfato tanpoiarekin nahastu ziren. Gradiente ez jarraikor bat osatu genuen 4ml % 1 Triton X-100 duen fosfato tanpoia % 35 sakarosa eta % 1 Triton X-100 duen 4ml fosfato tanpoiaren gainean ezarriz eta azken hau % 45-ko sakarosa duen laginaren gainean ezarriz. Horrela, sinaptosomak 140000 x g 4 ° C-tan (Beckman XL-100, SW-40ti errotorea) zentrifugatu ziren 18 orduz. Zentrifugazioa amaitzean, 5 eta %35 sakarosa interfasean lipid-raft materiaren banda argi bat ikusi zitekeen. 1 ml bolumeneko 12 frakzio jaso genituen goitik behera eta frakzio hauen proteina, kolesterol edukia eta fosfatasa alkalinoaren aktibitatea determinatu genituen BCA metodologiarekin (ab102536), kolesterola maila kuantifikatzeko kitaren bidez (428901-1KIT) eta fosfatasa alkalina kuantifikatzeko kitarekin (ab83369), hurrenez hurren.

PNGasa F metodo entzimatikoa sinaptosometako proteinak deglikosilatzeko

N-loturaz elkarturiko oligosakaridoak (manosak, hibridoak eta oligosakarido konplexuak) glikoproteinetatik kentzeko PNGasa F metodo entzimatikoa (New England BioLabs) erabili zen. Fosfato tanpoiean berresekitako sinaptosomen (2,3 µg / µl) 9 zati 10 x glikoproteina desnaturalizazio tanpoiaren (% 5 SDS, 400 mM DTT) zati batekin nahastu zen. Ondoren, glikoproteinak 10 minutuz 60 °C-tan desnaturalizatu ziren. Desnaturalizatutako lagina 1:1 proportzioan nahastu zen 2 x GlycoBuffer 2 eta 2% NP-40 diluitutako H20-kin. Azkenik, desnaturalizatutako 20 µg proteina bakoitzeko 1 µl PNGasa F gehitu zen eta nahasketa 37 ° C-tan inkubatu zen ordubetez. CB1 hartzailearen glikosilazio maila SDS-PAGE eta inmunoblot bidez aztertu zen, deglikosilazio eta glikosilatutako sinaptosoma laginen arteko mugikortasuna alderatuz.

CB1 hartzailearen inmunoprezipitazioa eta masa espektrometria

Garbitutako 25 µL bola magnetiko (Biotool Protein A/G Magnetic Beads) 3 µg Rabbit Immunogenes anti-CB1 antigorputzarekin edo Rabbit Frontier anti-CB1 antigorputzarekin nahastu genituen eta 20 minutuz inkubatu genuen nahaskina 200 µL PBS tanpoieko amaiera bolumenean. Antigorputz-bola magnetikoen konplexua imana erabiliz banandu zen PBS soluziotik eta jarraian bi garbiketa azkar egin zitzaizkion konplexuari PBS-T tanpoia erabiliz. Bitartean, deglikosilatutako 200 µg sinaptosoma (0.4 µg/µL proteina kontzentrazioa) ingurugiro tenperaturan inkubatu ziren 10 minutuz inmunoprezipitazio tanpoian (50 mM PB, 1 mM DTT, 1% NP-40, 2.5 mM CHAPS, 0.5% deoxikolato sodikoa, 0.1% SDS, 60 mM n-octil-D-glukopiranosidoa, pH 7.4 eta 50 µL/mg proteasa inhibitzaileen koktela-Sigma). Ondoren, sinaptosomak 4 °C-tan 15000 x g-tan zentrifugatu ziren 5 minutuz eta gainjalkina antigorputz-bola magnetikoen konplexuarekin nahastu eta inkubatu zen 30 minutuz ingurugiro tenperaturan. Jarraian, bola magnetiko-antigorputz-antigeno konplexua imana erabiliz banandu zen soluziotik eta ondoren hiru garbiketa azkar egin zitzaizkion konplexuari solubilizazio tanpoiarekin. Output-a 2x urea desnaturalizazio tanpoiarekin (40 mM Tris-HCl, pH 8.0. 24% glizerola, 24% Urea, 10% ditiootreitola, 4% sodium dodezil sulfato sodikoa, 0.02% bromofenol urdina) desnaturalizatu zen 60 °C-tan 5 minutuz inkubatuz. Bestetik, antigenoa antigorputz-bola magnetikoen konplexutik eluitzeko, bola magnetiko-antigorputz-antigeno konplexua urea desnaturalizazio tanpoian (20 mM Tris-HCl, pH 8.0, 12% glizerola, 12% Urea, 5% ditiotreitola, 2% dodezil sulfato sodikoa, 0.01% bromofenol urdina) desnaturalizatu zen 5 minutuz 60 °C-tan inkubatuz.

Inmunoprezipitatutako proteinak SDS-PAGE eta inmunoblot metodologiaren bidez aztertu ziren. Masa espektrometria analisiarako, CB1 hartzaileak migratzen duen poliakrilamida gel zonaldeak moztu (∼40 kDa, ∼37kDa eta ∼35 kDa) eta bertako proteinak sekuentziatzera bidali ziren. Horretarako, proteinak tripsinarekin liseritu ziren eta peptidoak kromatografia likidoaz [EASY nLC-1200 (Thermo)] eta masa espektrometriaz [Q Exactive HF-X (Thermo)] analizatu ziren. Lortutako espektro ezberdinak Proteome Discoverer 2.2 (Thermo) softwarea erabiliz aztertu ziren eta proteinak UniProtSwissProt (Mus musculus) (www.uniprot.org) databasea erabiliz identifikatu ziren.

Sinaptosoma mintzen kolesterolaren deplezioa

Sinaptosomen mintz plasmatikotik kolesterola ezabatzeko, sinaptosomen berresekidura (1mg/ml) 5 mM, 10 mM edo 20 mM β-metil ziklodextrina duen 50mM Tris-HCl pH 7.4 tanpoiarekin inkubatu zen 30 minutuz 37 °C-tan. Jarraian, sinaptosomak Tris-HCl tanpoiarekin garbitu ziren eta 15 minutuz 15000 x g-tan zentrifugatu ziren 4 °C-tan (Kontron, Centrikon T-42K, A-18C errotorea). Pelleta berreseki eta garbiketa prozedura errepikatu zen. Sinaptosomak berreseki ondoren 1,5 ml ko ependorfetan alikuotatu ziren eta 15000 x g-tan zentrifugatu ziren 30 minutuz 4 °C-tan (Kontron, Centrikon T-42K, A-21C errotorea). Azkenik, gaingalkina xurgatu eta sinaptosomez osatutako pelletak – 80 °C-tan izoztu ziren. Sinaptosoma pelleten proteina kantitatea Bradford metodologiaren bitartez estimatu zen.

Proteina Kontzentrazioaren Estimazioa: Bradford Metodoa

Laginen proteina kontzentrazioa zehazteko Bradford mikrometodoa erabili genuen. Kontzentrazio ezaguneko (2 mg/ml) γ-globulina proteinaren soluzio komertzialetik 25 µg/ml kontzentrazioa duen ama-soluzio bat lortu genuen. Ondoren ama-soluzio honetatik patroi zuzen bat eraiki genuen. Bestalde, lagin esperimentalaren proteina estimazio bat izanik 25 µg/ml kontzentrazioa lortzeko diluzioa egin genituen eta estandarrarekin egin bezala diluzio seriatuak burutu ziren:

γ-globulina estandarra (25 µg/µL)			**Lagin experimentala (25 µg/µL estimazioa)**	
[γ-globulina] = µg/mL	**γ-globulina estandarraren soluzioa (µL)**	**H_20 (µL)**	**Lagin esperimentalaren soluzioa (µL)**	**H_20 (µL)**
0	0	1000		
2.5	100	900	100	900
5.0	200	800	200	800
7.5	300	700	300	700
10.0	400	600	400	600

2. taula. y-globulin estandarraren eta lagin esperimentalaren diluzio seriatuak

200 µl Bradford erreaktibo gehitu genizkien saiodi bakoitzari eta 10 minutuz ingurune tenperaturan inkubatu genituen erreaktiboa proteinekin erreakzionatu zezan. Ondoren, espektrofotometro batekin saiodien absorbantziak neurtu genituen (595 nm-ko uhin luzeera). Lortutako puntu esperimentalekin absorbantzia vs. kontzentrazioa grafiko bat sortu eta erregresio lineal zuzen bat eraikiz laginaren kontzentrazioa ondoko formularen bitartez kalkulatu genuen:

[Proteina] = m´/m x 80 x 25 µg/ml

Non m´ eta m lagina eta estandarraren erregresio linealaren bidez lortutako zuzenen maldak diren hurrenez hurren, 80 zenbakia laginaren diluzio konstantea da eta 25 µg/ml kontzentrazioa, γ-globulina soluzio komertziala diluitzearen ondorioz lortutako ama-soluzioaren kontzentrazioa da

Proteina Kontzentrazioaren Estimazioa: Azido Bizinkoninikoaren metodoa

Metodo honen bitartez proteina kantitateak determinatu ahal izateko Abcam-en BCA proteina-kuantifikazio kit-a (abcam, ab102536) erabili genuen. Lehenik, kit-ak dakarren 10 mg /ml kontzentrazioa duen BSA soluzio batetik 0,64 mg/ml kontzentrazioa duen "stock soluzioa" eratu genuen. "Stock soluzio" honetatik abiatuta, diluzio seriatuak egin genituen bakoitzean kontzentrazioa erdira diluitzen (ikusi 3. taula). Horrela, BSA patroi-zuzena eraiki genuen. Lagin esperimentalaren proteina estimazio bat izanik, lagina 0,6 mg/ml kontzentrazioa lortzeko behar haina diluitu genuen eta honetatik BSA patroi zuzenaren besteko diluzio seriatuak egin genituen (ikusi 3. taula).

Tutua	BSA soluzioa (1 µg/µl)	Tanpoia (µl)	50 µl =
8	Stock Soluzioa (256)	144	32 µg
7	8. tutua (200)	200	16 µg
6	7. tutua (200)	200	8 µg
5	6. tutua (200)	200	4 µg
4	5. tutua (200)	200	2 µg
3	4. Tutua (200)	200	1 µg
2	3. tutua (200)	200	0.5 µg
1		200	0 µg

3. taula. BSA soluzioaren eta lagin esperimentalaren diluzio seriatuak

ELISA plaka baten putzu bakoitzean, BSA disoluzio estandarraren edo laginaren 50 µl eta kit-ak dakartzan agente kupriko eta BCA (1:50) nahasketa baten 100 µl gehitu genituen. Nahasketa hauek astiro eraginez ordubetez 37 °C-tara inkubatu genituen eta ondoren absorbantziak mikroplaka-neurgailu (Tecan®, Sunrise) batekin neurtu genituen. Lortutako absorbantzien baloreak absorbantzia vs. kontzentrazio grafikoa batean irudikatuz puntuen erregresio linealaren zuzenak kalkulatu genituen. Laginaren hasierako proteina kantitatea horrela kalkulatu genuen:

[Proteina] = m'/m x n x 0,64 mg/ml

Non m' eta m laginaren malda eta estandarraren maldak diren hurrenez hurren, n, hasierako laginaren diluzio konstantea den eta 0,64 mg/ml estandar soluzioaren hasierako kontzentrazioa den.

Sinaptosoma mintzen kolesterol kantitatearen determinazioa

The Calbiochem® Cholesterol/Cholesteryl Ester Quantitation Kit-a (428901-1KIT) erabili genuen mintzen kolesterola maila determinatzeko kolorimetria bidez. Kloroformo:Isopropanol:NP-40 (7:11:0.1) nahastearen 200 µl, sinaptosoma berresikiduraren (1mg/ml) 200 µl-kin nahastu genuen eta 20000 x g-tan 4 °C-tan 10 minutuz zentrifugatu genuen. Fase organikoa jaso ondoren, 30 minutuz 50° C-tan aire lehorraz disolbatzaile organikoa lurruntzea induzitu genuen. Ondoren, lipidoak kolesterol errakzio tanpoiaren 200 µl-tan disolbatu genuen 5 minutuz bortex-eatuz eta laginaren 20 µl 50 µl amaierako bolumenera ajustatu genuen kolesterol entsegu tanpoiarekin. 0.5 µg/µl kolesterol estandarra kolesterol estandarraren 20 µl 180 µl kolesterol erreakzio entseguaren tanpoiarekin nahastuz prestatu genuen. Estandarraren kurba patroia hurrengo eran prestatu genuen:

0.5 µg/ µl kolesterol estandarra	**Kolesterol erreakzio tanpoia**	**Kolesterola putzuko**
0 µl	50 µl	0 µg
4 µl	46 µl	2 µg
8 µl	42 µl	4 µg
12 µl	38 µl	6 µg
16 µl	34 µl	8 µg
20 µl	30 µl	10 µg

4. taula. Kolesterol estandarraren diluzio seriaturak

50 µl erreakzioaren nahaskina (44 µl kolesterol erreakzio tanpoia, 2 µl kolesterol proba, 2 µl entzima and 2 µl kolesterol esterasa) putzu bakoitzari gehitu zitzaion eta nahaskina 1 orduz 37 ° C-tan inkubatu zen. Absorbantzia 570 nm*tan neurtu zen. Kolesterol estandarraren kontzentrazio eta hauen absorbantzia balioekin lortutako kurbaren ekuaziotik laginaren kolesterol kontzentrazioa determinatu zen hurrengo eran:

$$C = A/V \text{ (µg/micro;l)}$$

A = estandarraren kurbatik determinatutako kolesterol kantitatea (in µg).

V = putzura gehitutako laginaren bolumen kantitatea (in µl).

Alkalina fosfatasa aktibitatearen determinazioa

Fosfatasa alkalina kit-a (ab83369) sinaptosometatik isolatutako lipid-raft eta ez-raft frakzioen fosfatasa alkalinoaren aktibitatea neurtzeko erabili genuen. Lehenik, 1 mM pNPP-ren estandarra prestatzeko 5 mM pNPP-ren 40 µL 160 µL entsegu tanpoiarekin nahastu genuen eta estandarraren patroia hurrengo eran prestatu genuen:

Standard	pNPP 1 mM Standard (µL)	Assay Buffer (µL)	Final volume standard in well (µL)	End amount pNPP in well (nmol/well)
1	0	300	120	0
2	10	290	120	4
3	20	280	120	8
4	30	270	120	16
5	40	260	120	32
6	50	250	120	64

5. Taula: pNPPl estandarraren soluzioaren eta lagin esperimentalaren diluzio seriatuak**.**

Lagin esperimentalaren diluzio ezberdinak prestatu genituen (2-80 µL) entsegu tanpoiarekin nahastuz (amaierako bolumena 80 µL/ putzuko), irakurketa estandarren baloreen tartean aurkitzeko. 5 mM pNPP soluzioaren 50 µL gehitu zitzaion lagin experimentalaren eta kontrol laginen putzu bakoitzari. Fosfatasa alkalina entzimaren soluzioaren 10 µL gehitu zitzaion Pnpp estandarraren putzu bakoitzari. Putzuak 25 °C-tan 60 minutuz inkubatu ziren argiataz babesturik pNPP sustratua Nitrofenol konposatuan bihurtzeko. Laginaren eta estandarraren erreakzioa amaitzeko tanpoiaren 20 µL gehitu genuen eta output-a 405 nm-tan irakurri genuen. Estandarraren kurba sortu ondoren, laginaren fosfatasa alkalinaren aktibitatea (µmol/min/mL edo U/mL) hurrengo eran kalkulatu genuen:

$$\text{ALP aktibitatea} = (B\Delta T * V) * D$$

non: B = pNP kantitatea laginaren putzuan estandarraren kurbatik kalkulatua (µmol).

ΔT = erreakzioaren denbora (minutuak).

V = erreakzio putzuan gehitutako hasierako laginaren bolumena (mL).

D = laginaren diluzio faktorea.

Western blot protokoloa

Western blot entseguak aldez aurretik deskribatutako protokoloetan oinarrituz burutu genituen (De Jesús *et al.*, 2006; Montaña *et al.*, 2012). Lagina berresekiduran bazegoen, hau 1:3 proportzioan urea 4x desnaturalizazio tanpoiarekin (80 mM Tris-HCl, pH 8.0. 48% glizerola, 48% urea, 40% ditiootreitola, 8% sodium dodezil sulfato sodikoa, 0.04% bromofenol urdina) nahastuz eta 5 minutuz 60 °C-tan inkubatuz desnaturalizatu genuen. Bestetik, pelletak urea 1x desnaturalizazio tanpoiarekin (20 mM Tris-HCl, pH 8.0, 12% glizerola, 12% Urea, 5% ditiotreitola, 2% dodezil sulfato sodikoa, 0.01% bromofenol urdina) berreseki eta 5 minutuz 60 °C-tan inkubatuz desnaturalizatu genituen. Desnaturalizatutako proteinak, elektroforesi bidez % 10-ko poliakrilamida gel batean zehar migratu genituen, 4 °C-tan 110 V-tara, Mini Protean II (BioRad, Hércules, CA, USA) ekipoa erabiliz. Ondoren, gelean zehar pisu molekularraren arabera banatutako proteinak nitrozeluloza edo metanolean aktibaturiko PVDF (polyvinylidene fluoride, polibinilideno fluoruroa) mintzera transferitu genituen gau osoan zehar 4 °C-tan eta 30 V-tan Mini TransBlot (BioRad, Hércules, CA, USA) ekipoa erabiliz. Hurrengo egunean, ur distilatuarekin garbitu eta guztiz lehortu genituen mintzak. Ondoren mintzak metanolarekin ber-hidratatu eta azido azetiko 7 %-an eta metanola 10 %-an duen ur distilatu disoluzio batean 15 minutuz ingurune tenperaturan inkubatu genituen proteinak mintzean egoki fixatzeko. Blokeo tanpoiarekin (0.2 M PB, pH 7.5; % 0.2 Tween-20, 5 % esne-hauts gaingabetua, % 0.5 BSA) ordu betez ingurune tenperaturan inkubatu ostean, antigorputz primarioak gau osoan zehar 4 °C-tan beharrezko kontzentrazioan inkubatu genituen esne-hautsik gabeko blokeo tanpoian (Ikusi 1. Taula). Hurrengo goizean, mintza PBS-T tanpoiarekin 10 minutuz 3 aldiz garbitu ondoren, 1:10000-an esne-hautsarekin eginiko blokeo tanpoiean diluitutako errefau-peroxidasarekin (HRP) konjokatutako beharrezko antigorputz sekundarioarekin inkubatu genituen 90 minutuz inguruneko tenperaturan Azkenik, PBS-T tanpoiarekin 10 minutuko 3 garbiketa eta PBS tanpoiaren 10 minutuko azken garbiketa bat egin ostean, Clarity Western ECL sistema (BioRad) fabrikatzailearen argibideak jarraituz immunomarkaketaren errebelaketa burutu genuen. Sortutako kemiluminiszentzia seinalea X-izpi filmean zuzenean eskuratu edota ImageQuant 350 (GE Healthcare) sistemaren bitartez eskuratu eta digitalizatu genuen.

X-izpi filmean eskuratutako seinale inmunoerreaktiboak transmitantzi eskanerra erabiliz digitalizatu genuen. Banda inmunoerreaktiboen irudi digitalak dentsitometriaz kuantifikatu ziren irudien analisirako ImageJ sofwarea erabiliz ((ImageJ, NIH, Bethesda,

MD, USA). Laginen arteko proteinen espresioa alderatzeko, analisi semikuantitatibo metodologia bat edo beste aukeratu genuen, eskuragarri genuen lagin kantitateak baldintzatua. Erabili genuen metodorik zehatzena malden arteko konparaketa izan zen. Proteina karga gorakorrak eta proteina karga bakoitzerako lortutako seinale immunorreaktiboen dentsitate optiko integratuaren (OD) balioak marrazteak erregresio linealaren ekuazioa determinatzea ahalbidetu zigun. Aztertzen diren laginen arteko kurben malden arteko erlazioak proteinaren espresio maila erlatiboa determinatzea ahalbidetu zigun. Proteina kopurua mugatua zenean, proteinen espresioaren analisi erdi kuantitatiboa lagin esperimentalen OD balioak kurba estandarraren ekuazioan integratuz burutu genuen, edo proteina kantitate berdinak erresolbitu baziren zuzenean lagin esperimentalen seinale inmunoerreaktiboen OD balioen arteko erlazioa kalkulatuz. Proteina karga, sinaptosometan aberastutako proteinen aurkako antigorputzak erabiliz edo Coomassie Blue Blue gel tindaketaren bidez egiaztatu zen.

Datuak antolatzeko eta esangura estatistikoa aztertzeko GraphPad Prism (5.0 bertsioa, GraphPad Software Inc., San Diego, CA, AEB) softwarea. Emaitzak kurben malden arteko erlazio gisa edo bataz besteko ± errore estandar (SEM) bezala adierazi ziren, gutxienez hiru esperimentu independente eginez. Azterketa estatistikoa irudi bakoitzean zehazten da. Esangura estatistikoa % 95-eko konfiantza mailan ezarri zen.

Inmunofluoreszentzia entsegua

Sinaptosomak % 0.5 DMSO duen 0.1 M PB tanpoiarekin berreseki ziren 50 µg /150 µl-ko proteina kontzentrazioa lortuz. Sinaptosomaz osatutako esekiduraren 2.5 ml 20 µm diametroko filtro batetik eta ondoren 5 µm diametroko filtro batetik pasatu zen. Iragazia 1:1 proportzioan diluitu zen berresekidura tanpoiarekin. Sinaptosomen 150 µL (jatorrian 25 µg proteina sinaptosomalari dagokio) gelatinizaturiko portetan inkubatu ziren 30 minutuz. Ondoren PBS tanpoiarekin 2 garbiketa azkar egin ziren itxatsi ez ziren partikulak ezabatzeko. Gelatinizatutako portetan itxatsitako sinaptosomak 10 minutuz DiIC16 mintz tindatzailearekin inkubatu ziren. Ondoren, zenbait garbiketa azkar burutu ostean, sinaptosomak % 4-an paraformaldehidoa duen fosfato tanpoiarekin fixatu ziren 10 minutuz. PBS tanpoiarekin 3 garbiketa azkar egin ostean sinaptosomak permeabilizatzeko % 0.05-an TX-100-a duen PBS tanpoiarekin tratatu ziren 5 minutuz. Berriz ere PBS tanpoiarekin 3 garbiketa azkar egin eta sinaptosomak % 1 BSA eta % 1-

an suero normala duen non-Perm tanpoiarekin blokeatu ziren 1 orduz. Jarraian sinaptosomak antigorputz primarioarekin (ikusi 1.taula) inkubatu ziren 4 °C-tan gau osoan zehar. Hurrengo egunean PBS tanpoiarekin 10 minutuko 3 garbiketa egin eta non-Perm tanpoiarekin 1 orduz ingurune tenperaturan inkubatu genituen beharrezko antigorputz sekundarioarekin. Azkenik, sinaptosomak berriz ere 3 aldiz garbitu ziren non-Perm tanpoiarekin 10 minutuz eta mikroskopioaren bidez aztertu ahal izateko, mowiol muntai-medioarekin beirazko portetan muntatu genituen estalkiak.

Mikroskopia irudi guztiak Carl Zeiss Axio Observer.Z1 epifluoreszentzia mikroskopioarekin lortu genituen. Aparatua, HXP120C haluro metalikoko lanpara eta erresoluzio handiko AxioCam MRm (1388 X 1040 pixel) kamera monokromatikoarekin hornitua dago, biak Carl Zeiss Microimaging, Inc. (Gottingen, Alemania) enpresarenak. Ohiko epifluoreszentzia-irudiak 20x Plan-Apochromat (NA 0,8) objektiboarekin egin genituen. Erresoluzio handiagokoak aldiz, ApoTome argiztapen estrukturatuko moduluarekin eta XYZ-n motorizatutako plataforma batekin (Carl Zeiss Microimaging, Inc.) 63x Plan- Apocromat (NA 1,4) objektiboarekin egin genituen. Erabili genituen argi-filtroak 49 DAPI (Ex G 365/Em 445/50) Hoechst tindaketarako, 38 He eGFP (Ex 470/40. Em 525/50) Alexa Fluor 488 fluoroforoarentzako eta 43 HE Cy3 estatikoa (Ex 550/25, Em 605/70) Alexa Fluor 568 fluoroforoarentzako izan ziren. Lortutako irudiak digitalizatzeko Zeiss Axiovision 4,8 (Carl Zeiss Microimaging, Inc.) softwarea erabili genuen. Kanal bakoitzari pseudokolore bat egokitu genion eta ebaketa optikoen gainjartzea eta irudiaren baloreen egokitzapena ImageJ softwarearekin (NIH, Bethseda, MD, USA) burutu genuen. Ilustraziorako, irudiak TIFF formatura esportatu eta Adobe Photoshop Cs6 (San José, CA, USA) programarekin etiketatu genituen.

Agonistak estimulaturiko [^{35}S]GTPγS loturaren entsegua

Sinaptosomak desizoztu ostean [35S]GTPγS-inkubazio tanpoiean (0.5 nM [35S]GTPγS, 1 mM EGTA, 3 mM MgCl2, 100 mM NaCl, 0,2 mM DTT, 50 μM GDP, BSA 0,5% and 50 mM Tris-HCl, pH 7.4) inkubatu ziren 2 orduz 30°C tan. Inkubazio tutuan CP55940 edo WIN 2212-2 (10-9 – 3x 10-5 M) CB1 hartzailearen agonista gehituz CB1 hartzaileak estimulatutako [35S]GTPγS lotura determinatu zen eta lotura ez espezifikoa inkubazioan 10 μM GTPγS presentzian. Lotura basala CB1 hartzailearen agonista gabeko lotura espezifikoa bezala definitzen da. Inkubazio erreakzioa hutsa eta filtrazio azkar baten bidez amaitu zen, Whatman GF/B beira-zuntzezko iragazkiak erabiliz eta iragazkian loturik geratutako erradioaktibitatea zentelleo likidoaren espektrofotometriaz neurtu zen.

Datuen analisia burutzeko Agonistaren kontzentrazio-erantzun kurbak lau parametroko Hillen ekuaziora egokitu ziren erregresio ez-linealaren bidez

$$E = \text{Basala} + \text{Emax- Basala}/1+ 10\ (\text{Log EC50-Log [A]})\ nH$$

Non E-k efektua adierazten duen, log [A] agonistaren kontzentrazioaren logaritmoa, nH erdiko puntuaren malda, Log EC50 erdiko puntuaren kokapen-parametroaren logaritmoa, eta Emax eta basala goiko eta beheko asintotak, hurrenez hurren.

Entsegu independente bakoitzean agonistak estimulaturiko [35S]GTPγS loturaren puntu esperimental bakoitza hiru aletan/pro triplicado burutzen zen. Gutxienez 3 entsegu independente egin ziren.

Datu esperimentalak, GraphPad Prism Softwarean (5.0 bertsioan) analizatu ziren aurrez deskribatutako eredu matematikora egokituz. Lagin esperimentalen Emax eta pEC50 balioen arteko diferentzien esangura estatistikoa Studenten t probaren bidez aztertu zen, ondoren Tukey-Kramerren konparazio anizkoitzeko proba burutuz. Esangura estatistikoa % 95eko konfiantza-mailan finkatu zen. Laginen balioak, batez bestekoa ± S.E.M. bezala adierazten dira.

V. RESULTS

BIOCHEMICAL CHARACTERIZATION OF THE CB1 RECEPTOR IN SYNAPTOSOMAL MEMBRANES FROM BRAIN CORTEX OF ADULT MOUSE

The CB1 receptor is preferentially expressed in the presynaptic membrane of neurons, where it plays a pivotal role in the retrograde signalling function assigned to the ECS (Kano *et al.*, 2009). In order to study by biochemical methods the CB1 receptor expressed in synaptic terminals without the interference of CB1signals from other subcellular compartments, a fractionation protocol was implemented to purify synaptosomes from fresh brain tissue.

We purify synaptosomes using a fractionation protocol based on differential centrifugation, which allowed us to separate synaptic terminals from other particles of different subcellular origin according to their density and weight. In summary, mouse brain cortical tissue was homogenized and applied different centrifugation steps to it. First, we centrifuged the homogenate (WH) of the frontal cortex at low speed, obtaining on the one hand a supernatant composed of cytoplasm and plasmatic membranes and on the other hand a pellet composed of nucleus, unleased cells and heavy membranes (P1). Subsequently, we centrifuged the supernatant at a higher speed obtaining a sediment enriched in plasmatic membranes (P2) and a cytosolic supernatant enriched in light intracellular membranes (S1). After ultracentrifuging the P2 fraction in a sucrose gradient, we recovered a pellet composed of mitochondria and a gradient interface enriched in synaptosomes, myelin, and microsomes. Finally, we ultracentrifuged an interface in a new sucrose gradient recovering a pellet enriched in synaptosomes (SYN), while the myelin and the microsomes were distributed in the interface and in the supernatant, respectively.

Validation of fractionation procedure to purify cortical synaptosomes

Western blot and Immunofluorescence techniques were used to validate the fractionation procedure and to assess the suitability of the synaptosomes enriched fraction. For that purpose, we resolved by SDS-PAGE the same amount of protein of different subcellular fractions. Then, the polyacrylamide gel was stained with a Coomassie blue dye as a loading control (Figure 8A). The staining clearly showed that the protein loading was

equal between the analysed fractions. In addition, the staining suggested that the protein composition of the fractions was different, as the distribution profile of protein bands was significantly different between the fractions. To determine the purity of synaptosomes, Western blot assays were carried out using antibodies raised against proteins of specific subcellular compartments. As shown in figure 8B, the immunoreactivity for different synaptic proteins such as synaptophysin, syntaxin 1a, and N-methyl-D-aspartate receptor subunit NR1 (NR1) was enriched in synaptosomes. The immunoreactivity of Ras-related protein 11b (Rab11b), which is found in synaptic endosomes among other cellular compartments, was also preferentially enriched in synaptosomes. This markers were also detected in the nuclear fraction (P1) and in the crude membrane fraction (P2), although their signals were significantly lower than in synaptosomes. On the other hand, the signals for non-synaptic markers were nearly undetectable in synaptosomes, indicative of low contamination of this fraction with non-synaptic membranes. Specifically, the immunoreactivity of the nuclear marker acetyl-Histone H3 (H3) and a glial origin marker glial fibrillary acid protein (GFAP) appeared enriched in the nuclear fraction (P1), whereas the cytosolic marker glyceraldehyde 3-phosphate dehydrogenase (GAPDH) was detected in the cytoplasm fraction (S1).

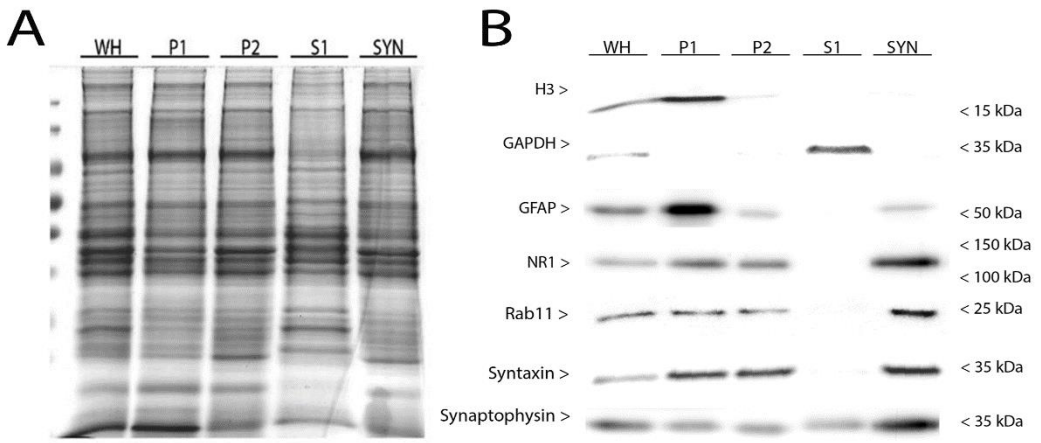

Figure 8A. SDS-PAGE and Coomassie blue staining of sequential fractionation obtained from homogenates of adult mouse brain cortex run in parallel (10µg /line). WH, Whole homogenate; P1, crude nuclei; P2, crude membranes/crude synaptosomes; S1, cytoplasm; SYN, synaptosomes. Figure 8B. Representative images of Western blot performed in same samples using specific markers of different fractions. Immunoblot against H3, GAPDH, GFAP, NR1, Rab11b, syntaxin 1a and synaptophysin. Protein migration was consistent with their theoretical molecular mass (H3, 15.4 kDa; GAPDH, 35.8 kDa; GFAP, 50 kDa; NR1, 130 kDa; Rab11b, 24.5 kDa; Synaptophysin, 34 kDa; Syntaxin 1a, 33 kDa. On the right is indicated the migration of standard molecular weights.

We also examined synaptosomes by double immunofluorescence and high-resolution microscopy, combining the Microtubule-associated protein 2 (MAP2) or Synaptosomal-asociated protein 25 (SNAP-25) protein antibody with the GFAP protein antibody and the plasma membrane dye DiIC16. The DiIC16 dye allowed us to quantify the size and the origin of all particles found in the preparation. Immunofluorescence assays showed that about 80% of particles displayed a size between 0.25-1.5 µm, which is consistent with that described for synaptosomes. On the other hand, 15% and 5% of the particles showed a size less than 0.25 µm and greater than 1.5 µm, respectively. Half the DiIC16 positive particles within 0.25-1.5 µm range size were identified as neuronal origin by MAP2 and SNAP-25 staining, whereas very low astroglial contamination was observed by GFAP-immunostaining. SNAP-25 and MAP2 labelling also revealed that about half of the particles in the synaptosomes enriched fraction were composed of presynaptic or postsynaptic elements. (Figure 9). These results demonstrated the suitability of the efficiency protocol used to purify mouse brain synaptosomes.

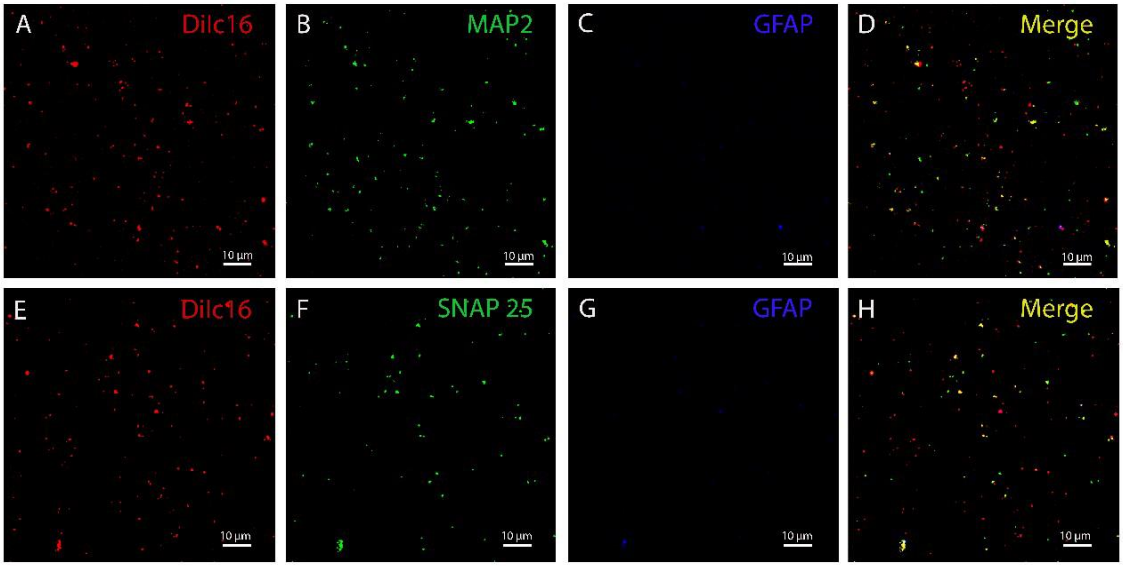

Figure 9. Isolated cortical synaptosomal preparations from mouse brain cortex on poly-L-ornitine coated coverslip. A-D. Double-immunofluorescence MAP2/GFAP and SNAP-25/GFAP combined with the membrane marker DiIC16. Quantification of particles size. 79.65% ± 2.33% between 0.25-1.5 µm; 6.89% ± 3.40% >1.5 µm; 14.47% ± 0.25% < 0.25 µm. Quantification of particles origin. Positive for MAP2: 48.57% ± 4.54%; SNAP-25: 44.75% ± 2.37%; GFAP: 4.64% ± 1.29%; Non-identifiable: 48.69% ± 2.42%. Data values are mean ± SEM. Two independent assays were performed.

Identification of immunoreactive signals detected by anti-CB1 antibodies

To study the endogenous CB1 receptor protein in synaptosomes by Western blot assays, we used three commercially available antibodies (CB1-Immunogenes, CB1-Go-Af450 and CB1-Rb-Af380), all raised against the 31 amino acids of the extreme carboxyl terminus of the mouse CB1 receptor. To test the specificity of these antibodies, synaptosome samples from WT and Stop-CB1 mice were resolved in parallel by SDS-PAGE and assayed by immunoblot. As shown in figure 10, all the three antibodies recognized a specific band at ~50 kDa consistent with the 52 kDa theoretical molecular mass of mouse CB1 receptor, which was absent in synaptosomes from Stop-CB1 mice (Figure 10). Additionally, the CB1-Immunogennes and Go-Af450 antibodies clearly recognized a specific extra band at ~35 kDa. Strikingly, in most experiments with the Rb-Af380 antibody, this lower band was hardly or no detectable.

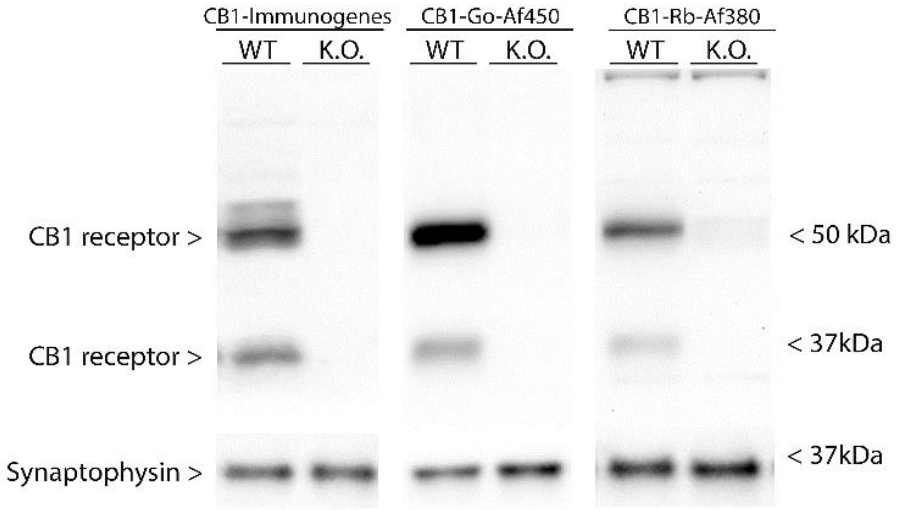

Figure 10. Representative Western blots carried out loading same amount of cortical synaptosomes from WT and Stop-CB1 mice (20 µg/lane). Immunoblot against CB1 receptor protein using CB1-immunogenes, CB1-Go-Af450 and CB1-Rb-Af380. Synaptophysin was used as a protein load control. The molecular weights depicted correspond to the signal of the standard molecular weight markers.

To analyze whether the migration of the observed ~50 and ~35 kDa bands was impacted by protein degradation of the CB1 receptor, we performed Western blot assays on synaptosome samples incubated at 37 ^{o}C in presence or absence of protease inhibitors. The changes observed, if any, did not support that the ~35 kDa results from proteolytic degradation of the ~50 kDa band, as the ratio of ~50 kDa/~35 kDa signals, rather than decrease, slightly decreased over incubation time, irrespectively of the presence or

absence of protease inhibitors (Figure 11). Moreover, no differences were observed when synaptosome-enriched fractions were obtained in the absence or presence of protease inhibitors during the fractionation procedure. These results strongly suggest that proteolytic degradation of the ~50 kDa band protein during the fractionation procedure or handling and processing synaptosomes does not account for the appearance of the ~35 kDa.

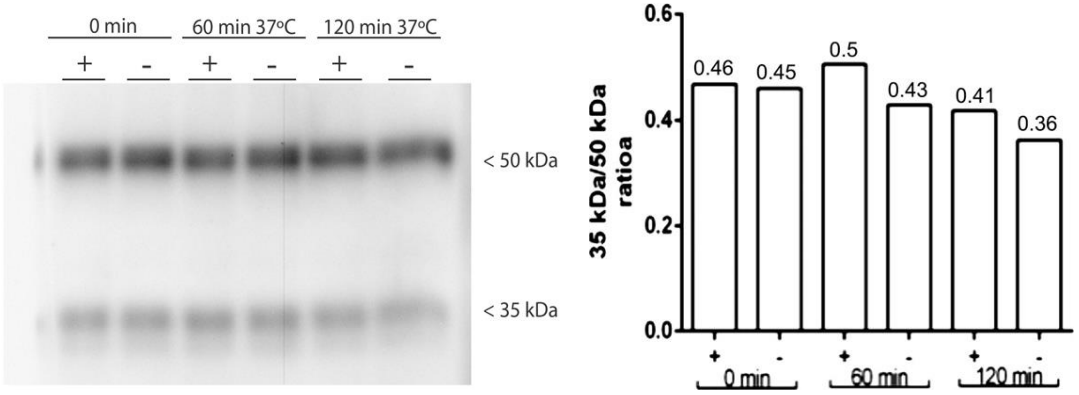

Figure 11. Representative Western blot, using CB1-Immunogenes antibody, performed in parallel on frontal cortical control synaptosomes and synaptosomes incubated at 37 ºC during 1 or 2 hours with or without protease inhibitors (20 µg/lane). The positions of molecular weight standards are shown in the right side of the panel. Bar graph depicts the ratio between the optical densities of the two immunoreactive bands. The values of the ratios are shown in above the corresponding bar.

Because the extracellular N-terminus of the mouse CB1 receptor has two consensus sequences for N-linked glycosylation (Ruehle *et al.*, 2017), we examined whether the two immunoreactive bands detected in Western blot assays could correspond to glycosylated and non-glycosylated forms of the receptor. To this end, synaptosome proteins from mouse brain cortex were subjected to enzymatic deglycosylation before being resolved by SDS–PAGE and analyzed by immunoblot using anti-CB1 antibodies. Thus, synaptosome samples were subjected to enzymatic treatment with Peptide N-glycosidase F (PNGase F) from *Flavobacterium meningosepticum*, an asparagine amidase that releases N-glycans from glycoproteins by cleaving the β-aspartylglucosamine bond between the innermost N-Acetylglucosamine (GlcNAc) of N-linked protein glycans and asparagine residues, which results deaminated to aspartic acid. As expected, no changes were observed in the immunoreactive band patterns between synaptosome samples incubated in deglycosylation buffer (Figure 12) and untreated samples (Figure 10). By

contrast, treatment of synaptosomes with PNGase F enzyme led to a clear shift in the migration profile of the ~50 kDa band, which resulted virtually undetectable with any of the three antibodies used. Instead, two new specific bands migrating at ~40 and ~37 kDa could be detected with all three antibodies, whereas no changes in intensity of the ~35 kDa band were observed when CB1-Immunogenes or CB1-Go-Af450 antibodies were used. Strikingly, the CB1-Rb-Af380 antibody, which hardly detected the ~35 kDa band in untreated samples, recognized a strong ~35 kDa band in PNGase F-treated synaptosome samples (Figure 12).

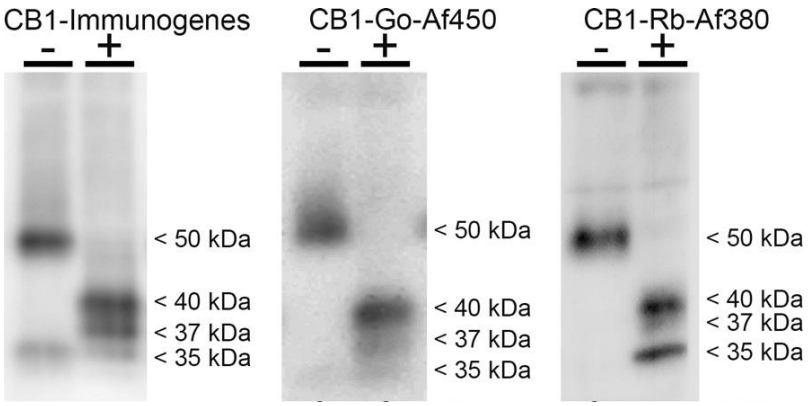

Figure 12. Representative Western blots using CB1-Immunogenes, CB1-Go-Af450 and CB1-Rb-Af380 antibodies in sham-treated (-) and PNGase F-treated (+) mouse cortical synaptosomes. Samples were incubated for one hour at 37 °C in deglycosylation buffer with (+) or without (-) PNGase F (25 U/µg synaptosome protein). The approximate molecular masses of the immunoreactive species detected on the blot are indicated.

To analyze the specificity of immunoreactive bands resulting from deglycosylation, synaptosome samples from WT and Stop-CB1 mice were subjected to PNGase F treatment, resolved by SDS-PAGE and immunoblotted with the CB1-Immunogenes and CB1-Rb-Af380 antibodies. As shown in figure 13, no immunoreactive bands were detected in Stop-CB1 samples when CB1-Immunogenes antibody was used. In contrast, CB1-Rb-Af380 antibody detected a strong band migrating at ~35 kDa in PNGase F-treated synaptosome samples from both WT and Stop-CB1 animals. This results demonstrate the unspecificity of this ~35 kDa immunoreactive band.

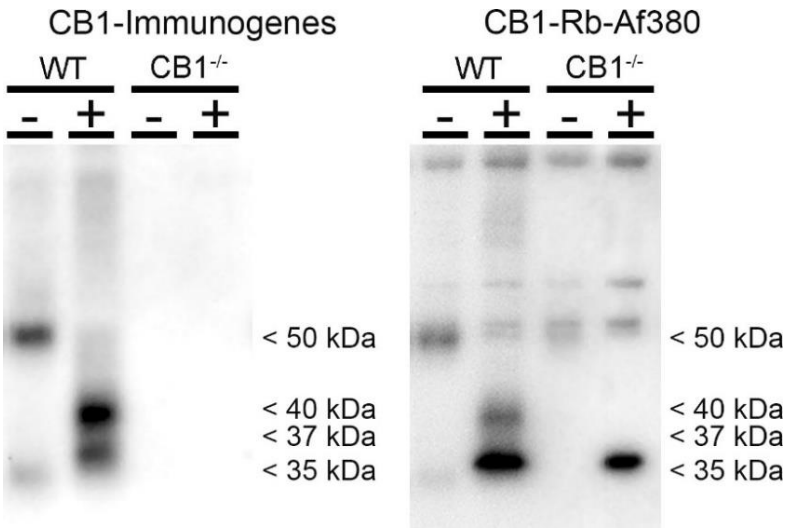

Figure 13. Representative Western blots using CB1-Immunogenes, and CB1-Rb-Af380 antibodies in sham-treated (-) and PNGase F-treated (+) in mouse cortical synaptosomes from WT and Stop-CB1 animals. The approximate molecular masses of the immunoreactive species detected on the blot are indicated.

The possibility that the ~40 and ~37 kDa immunoreactive band appearing after PNGase F-treatment could be products of partial deglycosylation of the CB1 receptor was tested by doubling PNGase amount, incubation time or both during enzymatic digestion. No changes were observed in either of these three conditions compared to the standard procedure carried out according to the manufacturer's instructions. These results are consistent with complete deglycosylation of CB1 receptor after treatment with PNGase F under standard conditions, indicating that the ~40 and ~37 kDa immunoreactive bands are unlikely to result from different deglycosylation levels and actually correspond to distinct CB1 receptor species.

Next, we hypothesized that the different CB1 receptor-specific immunoreactive bands detected in PNGase F-treated synaptosomes could correspond to mouse CB1 receptor variants generated by alternative splicing of the primary Cnr1 gene transcript. Indeed, the recently described (Ruehle *et al.*, 2017) mCB1a and mCB1b mouse splice variants differ from the canonical CB1 receptor protein in that display deletions of 39 and 62 amino acids in their N-terminal extracellular domains, respectively. In addition, N-glycosylation sites are absent in mCB1b variant. In an attempt to check whether any of the three bands detected in PNGase F-treated synaptosomes could correspond to the recently described mouse splice variants mCB1a and mCB1b, which differ with respect to the canonical CB1

receptor protein in their N-terminal extracellular domain (Ruehle *et al.*, 2017), we carried out immunoprecipitation assays of PNGase F-treated synaptosome samples followed by trypsin digestion of the ~40, ~37 and ~35 kDa bands and subsequent mass spectrometry-based identification of variant-specific tryptic peptides. After IPP using CB1-Immunogenes and CB1-Rb-Af380 antibodies, protein from immunoprecipitates were denatured and resolved by SDS-PAGE. A piece of gel loaded with half of each immunoprecipitate was transferred to PVDF and subjected to immunoblot analysis with the same antibodies used for IPP. As shown in figure 14A, a strong immunoreactive band migrating at ~40 kDa and two additional more diffuse bands migrating at ~37 and ~35 kDa were observed both in the PNGase F-treated input and in immunoprecipitates obtained using either CB1-Immunogenes (Figure 14A) or CB1-Rb-Af380 (Figure 14B) antibodies, whereas these immunoreactive bands were largely depleted from outputs (Figures 14A-B). The resulting image of immunoreactive bands was used as a template to excise, from lanes of the other part of the gel (loaded with half of the immunoprecipitate), the fragments expected to contain CB1-immunoreactive species migrating at ~40, ~37 and ~35 kDa.

Thus, a total of 6 gel fragments (3 per antibody) were subjected to liquid chromatography-tandem mass spectrometry (LC-MS/MS) and the peptide spectra analyzed. As a result of this analysis, two peptides corresponding to mouse CB1 receptor (UniProt Accession: P47746; GenBank Accession: NP_031752.1), with sequences ^{317}SIIIHTSEDGK^{327} and ^{328}VQVTRPDQAR^{337}, were identified. These sequences are both located within the third cytoplasmic loop of CB1 receptor and are common to all the three splice variants. Although we did not identify splice-variant peptides of the mouse CB1 receptor, these results do not conclude that ~40, ~37 and ~35 kDa bands cannot actually represent these splice variants.

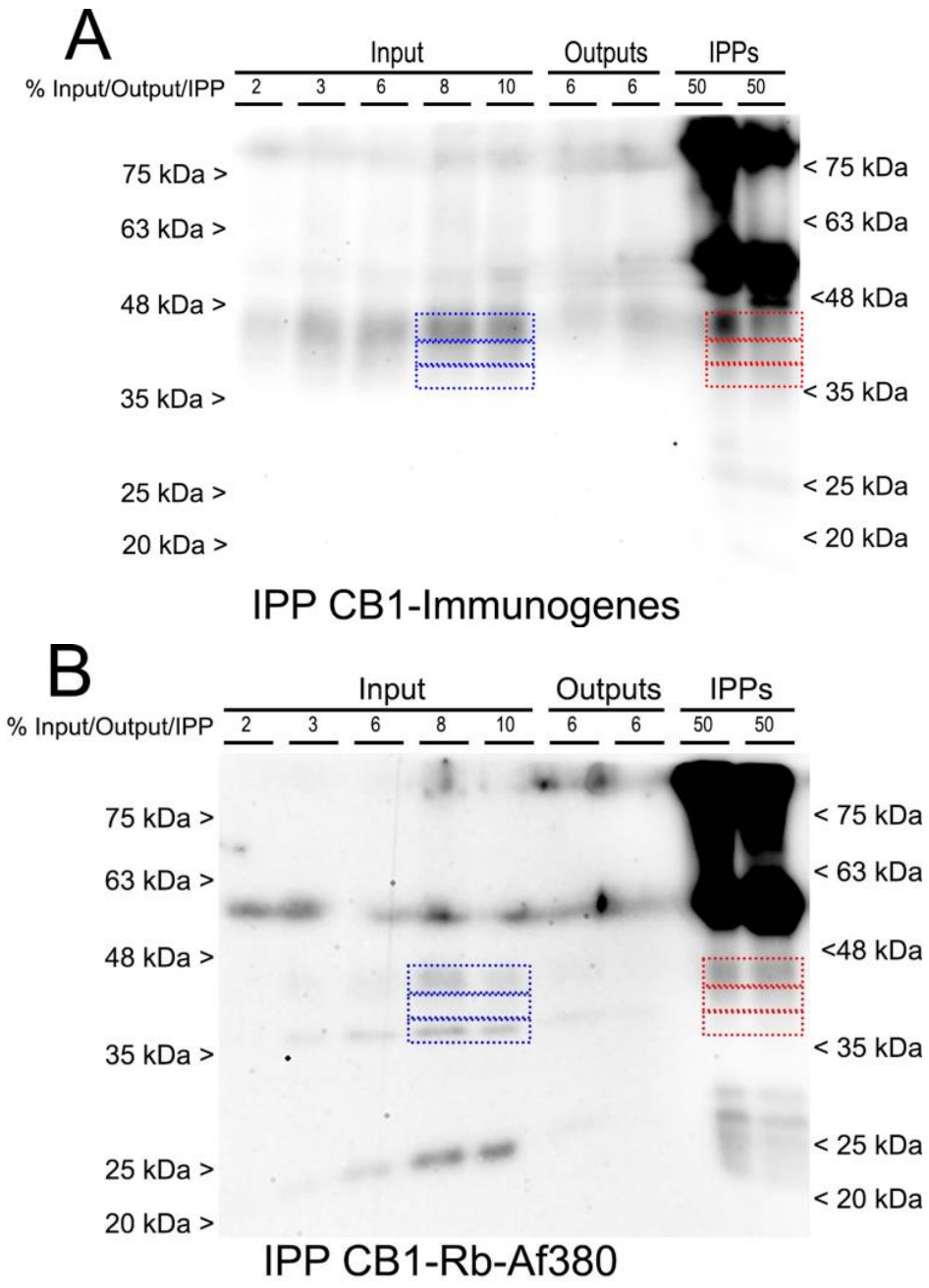

Figure 14. Representative Western blots of PNGase F-treated synaptosome samples and CB1-immunoprecipitates using CB1-immunogenes (A) and CB1-Rb-Af380 antibodies (B). Increasing amounts of PNGase-treated mouse cortical synaptosome samples, equivalent to 2-10% of the input (200 µg), were loaded in lanes 1-5. Lanes 6-7 were loaded with 6% of the outputs from two IPP replicates and lanes 7-8 with half of the immunoprecipitates from the same replicate. The positions of molecular weight standards are depicted at both side of each panel. Blue-lined squares correspond to the positions of the ~40, ~37 and ~35 kDa CB1imunoreactive bands in lanes loaded with PNGase F-treated synaptosome samples. Red-lined squares correspond to the levels from which gel fragments were excised for LC/MS-MS and sequencing.

Subsynaptic compartmentalization of the CB1 receptor and other proteins of the ECS

To fully investigate the synaptic distribution of the CB1 receptor and other proteins of ECS, cortical synaptosomes were fractionated in three major subsynaptic domains: the presynaptic active zone (PAZ), the postsynaptic density (PSD) and the extrasynaptic zone (EXTRA). The EXTRA zone consists on plasma membrane not specialized in synapses and on cytoplasm of synaptic terminal, whereas the presynaptic active zone and the postsynaptic density consist on "particle web" components and protein dense specialization attached to the presynaptic and postsynaptic membrane, respectively.

The protocol for subfractionate synaptosomes is based on differential pH and detergent sensitivity of three major subsynaptic domains. As mentioned in the methodology section, synaptosomes were incubated with a buffer composed of a non-ionic TX-100 adjusted to pH 6 for solubilize the EXTRA zone. After centrifuging the sample, we recovered the EXTRA fraction in the supernatant and the synaptic junctional preparation composed of PAZ and PSD in the sediment. To divide the PAZ and PSD, we incubated it in a buffer composed of non-ionic detergent TX-100 adjusted to pH 8. Under these conditions, we solubilized the PAZ zone and after centrifuging the treated sample, we recovered the PAZ in the supernatant and the PSD in the pellet. We recovered 67%, 12%, and 5% of synaptosome protein in the EXTRA, PSD, and PAZ fractions, respectively. Thus, proteins from the EXTRA region contribute in the largest proportion to synaptosomes fraction, while the contribution of protein for areas specialized in synapses is low.

The efficiency of the subfractionation protocol of synaptosomes was validated by Western blot. Equal amounts of total protein of subsynaptic fractions and increasing amount of total protein of synaptosomes were loaded on the same gel. First, the polyacrylamide gel was stained with a Coomassie blue dye as a loading control. The staining clearly showed that the protein loading was equal between the subsynaptic fractions (Figure 15 left). In addition, the distribution profile of the protein bands was significantly different between fractions, suggesting that the efficiency of the fractionating protocol is high. We used antibodies raised against Post Synaptic Density Protein 95 (PSD95), SH3 and multiple ankyrin repeat domains protein 3 (SHANK3) and gephyrin and Munc-18 and SNAP-25 as markers of PSD and of PAZ and EXTRA subsynaptic domains, respectively. As expected, the immunoreactivity of PSD95,

SHANK3 and gephyrin was only detected in the PSD fraction and it was significantly higher than in the synaptosome fraction, which is in line with the fact that the PSD fraction is purified approximately 8 times with respect to synaptosomes considering the protein yield of each subsynaptic fraction. On the other hand, the presynaptic proteins Munc-18 and SNAP-25 were detected in the PAZ and EXTRA fractions, which were more enriched in the EXTRA fraction than in the PAZ (Figure 15 right). The signalling profile of these two proteins is consistent with what might be expected because they reflect synaptic and non-synaptic populations of proteins found in the synaptic terminal. This results indicated that we are dealing with really efficient protocols for obtaining and subfractionating synaptosomes.

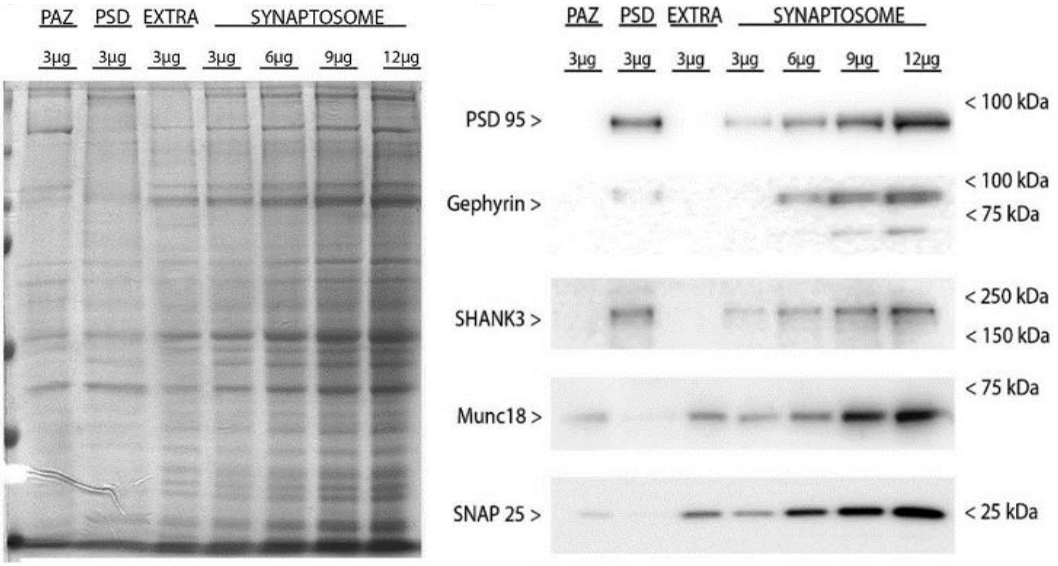

Figure 15. Coomassie blue-stained SDS-PAGE (left) and representative Western blots (right) carried out by immunoblotting increasing amounts of cortical synaptosomes (3, 6, 9 and 12 µg/lane) and different subsynaptic fractions (3 µg/lane). Presynaptic fraction: PAZ, postsynaptic fraction: PSD and extrasynaptic fraction: EXTRA. The efficiency of the subsynaptic separation is assessed by presynaptic markers (Munc-18. SNAP-25), postsynaptic markers (PSD95, Gephyrin, and SHANK3) and extrasynaptic marker (Munc 18 and SNAP-25). Protein migration was consistent with their theoretical molecular mass, except for PSD95 protein, which migrated at a molecular weight of 95 kDa (PSD 95, 80.4 kDa; Gephyrin, 83.2 kDa; SHANK, 185.3 kDa; Munc-18, 66.3 kDa; SNAP-25, 23.3 kDa). The molecular weights depicted correspond to the signal of the standard markers.

Once revealed the efficiency of the subfractionation protocol, we analysed the subsynaptic compartmentalization of the CB1 receptor using CB1-Immunogenes, CB1-Go-Af450 and CB1-Rb-Af380 antibodies. Immunoreactivity was highest in the EXTRA fraction, although a clearly detectable but considerably less intense signal was detected in the PSD fraction (Figure 16 left). In some experiments, a very weak band was detected in the PAZ fraction. The immunoreactive bands were analysed by densitometry. The expression of the CB1 receptor was expressed relative to the total receptor signal detected in the three compartments. Because the immunoreactive signal was hardly detected in the PAZ fraction in the majority of experiments, we did not analysed by densitometry the CB1 receptor expression in this subsynaptic domain. Thereby, 68% and 32% of the immunoreactivity was present in the EXTRA and PSD domain, respectively, with no differences between the results obtained with the three antibodies (Figure 16 left, Table 6), concluding that the density of the CB1 receptor in the extrasynaptic membrane is considerably higher than in the postsynaptic domain. Densitometry analysis of ~35 kDa immunoreactive bands showed similar values in the EXTRA and PSD fractions, indicating that the ~50 kDa and ~35 kDa proteins partition differently (Figure 16 left, Table 1). Although the same protein amount of different fractions was loaded for Western blot analysis, the yield of total synaptosome protein in the EXTRA fraction was almost 5.8-fold higher than in the PSD fraction, revealing that most CB1 receptor are located in the extrasynaptic membrane. Therefore, the immunoreactive signal detected in synaptosomes is mainly derived from the EXTRA fraction and the contribution of the CB1 receptor signal of the PSD is negligible.

Regarding of other proteins of the ECS, three of the subunits of its canonical signalling G inhibitory proteins Gαo, Gαi1 and Gαi3 were exclusively found in the EXTRA fraction (Figure 14 left). Interestingly, Gαi2 was mostly detected in PSD fraction, although a weak signal could be observed in the EXTRA fraction. Similarly to Gαo, Gαi1 and Gαi3 proteins, Cannabinoid receptor interacting protein 1a (CRIP1a) was only detected in the EXTRA fraction. The proteins involved in the synthesis and degradation of the major eCB 2-arachidonylglycerol (2-AG), Gαq/11 subunit, phospholipase C-β1 (PLCβ1) and monoacylglycerol lipase (MAGL) were found in the EXTRA fraction, whereas diacylglycerol lipase-α (DAGLα) was mostly enriched in PSD fraction (Figure 16, right up). Finally, the Gβ subunit signal was highest in the EXTRA fraction, but also clearly detectable in the PAZ and, to a lesser extent, in PSD fractions (Figure 16 left). These

results are consistent with the synaptic retrograde signalling function assigned to brain cannabinoid system.

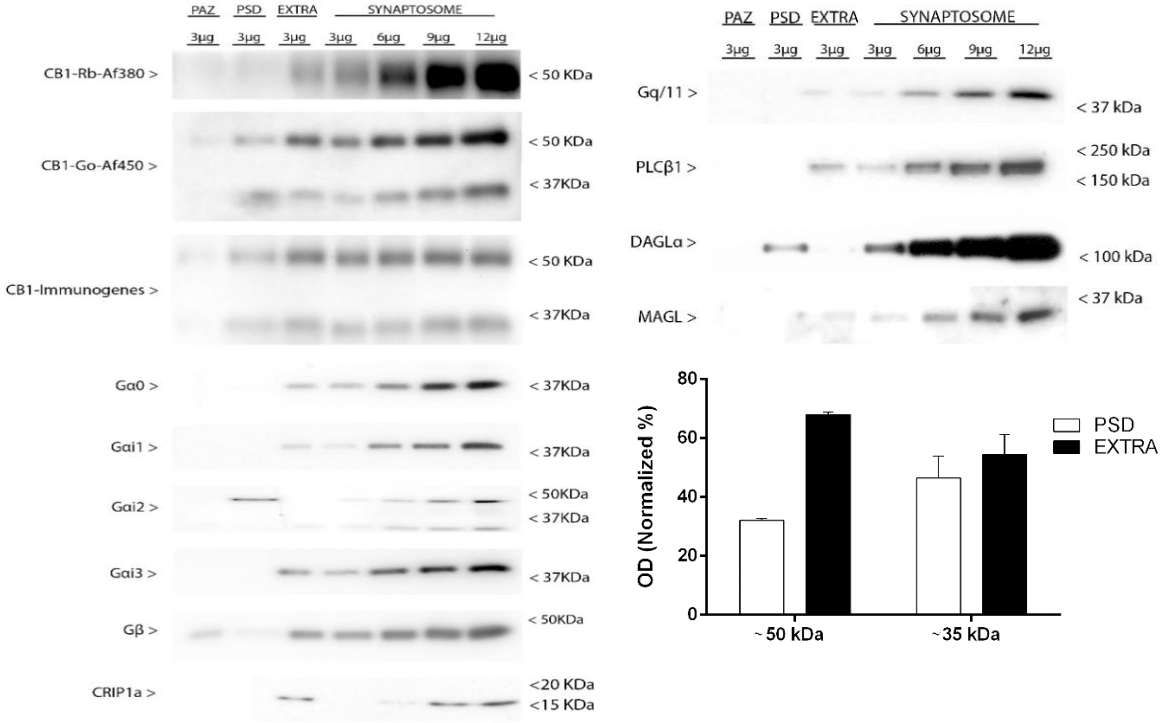

Figure 16. Representative Western blots carried out by immunoblotting increasing amounts of cortical synaptosomes (3, 6, 9 and 12 µg/lane) and different subsynaptic fractions (3 µg/lane). Presynaptic fraction: PAZ, postsynaptic fraction: PSD and extrasynaptic fraction: EXTRA. Protein migration was consistent with their theoretical molecular mass. For CB1 and Gαi2 protein, an extra band migrating at 35kDa and 36 kDa were detected, respectively (CB1, 52.8 kDa; Gα0 40.1 kDa; Gαi1, 40.5 kDa; Gαi2, 40.4 kDa; Gαi3, 40.5 kDa; Gβ1, 37.3 kDa and 36.3 kDa 1 and 2 isoforms; CRIP1a, 18.6 kDa; Gαq/11, 42.0 kDa; PLCβ1, 138.3 kDa and 133.3 kDa 1 and 2 isoforms; DAGLα, 115.3 kDa; MAGL, 33.3 kDa). The molecular weights depicted correspond to the signal of the standard markers.

Frontal cortex	**EXTRA**	**PSD**
~50 kDa	67. 9 ± 0.7	32.0 ± 0.7*
~35 kDa	54.3 ± 6.8	46.5 ± 7.2

Table 6. The subsynaptic distribution of the CB1 immunorreactive signals of ~50 kDa and ~35 kDa. The immunoreactive signal of each subsynaptic fraction is shown normalized to the total signal detected in the three compartments. The values are means ± SEM of three independent assays. Unpaired two tailed t test. (*) = $p < 0.05$

*

Localization of CB1 receptors in lipid raft and non-raft microdomains

Lipid rafts are specific microdomains of plasma membrane rich in cholesterol and sphingolipids, where a large variety of GPCRs and associated signalling proteins reside. Therefore, they are considered as platforms where both receptors and effectors can interact more efficiently, either facilitating or limiting signal transduction. Previous data indicate that in different heterologous cell models the CB1 receptor resides in this microdomains, where its canonical signalling is negatively regulate by cholesterol. To characterize the lipid raft vs non-raft compartmentalization of the CB1 receptor in mouse cortex, these fractions were separated by ultracentrifugation in a sucrose gradient on the basis of the different solubility and different density that these compartments display after treatment of synaptosomes with TX-100 non-ionic detergent. Specifically, lipid raft microdomains are insoluble in non-ionic detergent TX-100 and these domains have a low density, showing a high buoyancy in a sucrose gradient. Both of these features make it possible to separate lipid raft and non-raft domains using an ultracentrifugation protocol.

A total of 12 fractions of increasing density were obtained and biochemically characterized by quantitative analysis of phosphatase alkaline enzymatic activity, determination of the protein concentration and the use of lipid raft and non-raft markers (Figure 17). Low protein content and high alkaline phosphatase activity are characteristic of lipid raft fractions. In Western blot assays, we used antibodies raised against Thy-1 membrane glycoprotein (Thy-1) and flotillin proteins and Na^+/K^+ ATPase protein as a markers of lipid raft and non-raft microdomains, respectively. Alkaline phosphatase activity was highest in fractions 4-5 along with a low protein content (Figure 17 right up and down). We also detected a stronger immunoreactivity for lipid raft markers and lower or absence of immunoreactivity for non-raft markers in this two fractions, suggesting that they were enriched in lipid raft microdomains (Figure 17 left). Specifically, the immunoreactivity of Thy-1 was only detected in 4-5 fractions and the highest intensity signal of flotillin was also detected in this two fractions, with a tendency to weaken in higher density fractions. Furthermore, it should be noted that the protein loading of 4-5 fractions was lower compared to the others because the same volumes of fractions were loaded in these Western blot assays. On the other hand, fractions between 8 and 12 displayed no alkaline phosphatase activity, high protein concentration, and high and low immunoreactivity for Na^+/K^+ATPase and flotillin, respectively. With these results we

concluded that 4-5 fractions were enriched in lipid raft microdomains and 6-12 fractions, on the other hand, were non-raft fractions. Subsequently, the expression of CB1 receptor and Gαi/o subtype proteins was analysed (Figure 17). Unexpectedly, CB1 immunoreactivity distribution profile varied depending on the antibody used. Whereas CB1-Rb-Af380 antibody recognized a single specific band at ~50 kDa molecular weight exclusively in lipid raft fraction, the CB1-Immunogenes antibody recognized ~50 kDa and ~35 kDa specific bands in both lipid raft and non-raft fractions. On the other hand, the CB1-Go-Af450 antibody did not detect any CB1 signal in both fractions. Different Gαi/o proteins were detected in both lipid raft and non-raft fractions, suggesting that CB1 receptor can interact with different Gαi/o subtypes in both compartments.

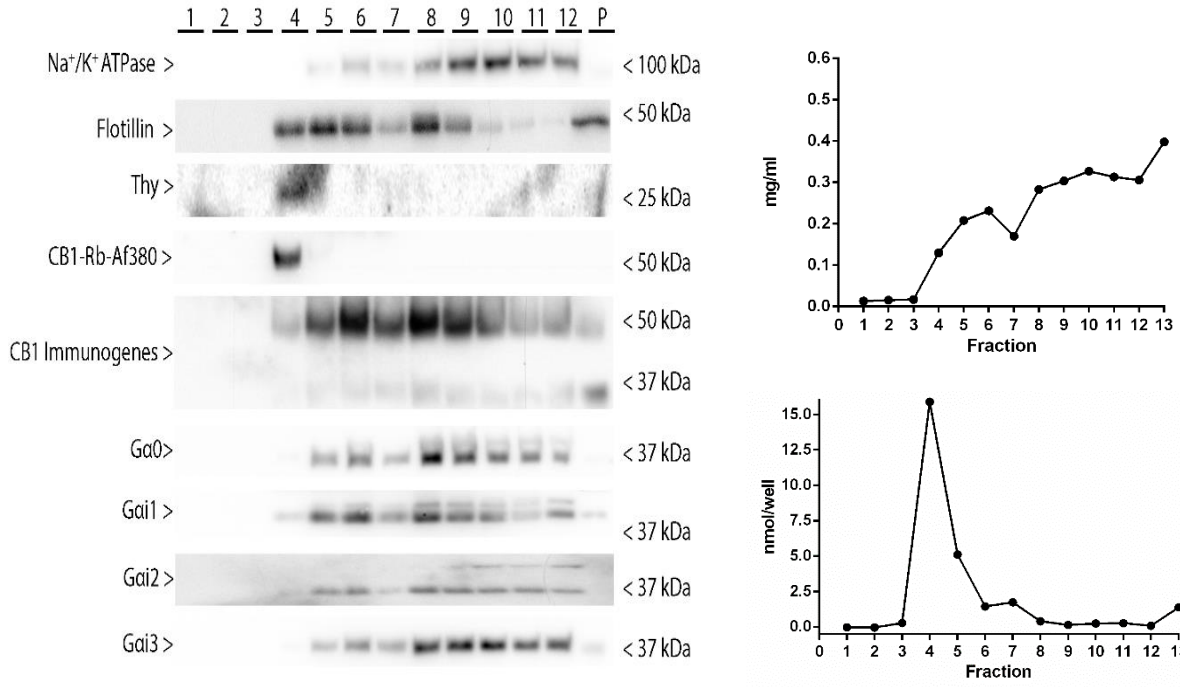

Figure 17. Representative Western blots running in parallel same volume of lipid raft and non-raft fractions derived from frontal cortical synaptosomes (20 µl/lane). Immunoblot against Na^+/K^+ ATPase, Flotillin, Thy-1, CB1 and $G\alpha_{i/o}$ subtypes. Protein migration was consistent with their theoretical molecular mass. For CB1 and Gαi2 protein, an extra band migrating at 35 kDa and 36 kDa were detected (Na^+/K^+ATPase, 112.3 kDa; Flotillin, 47.5 kDa; Thy-1, 18.1 kDa; CB1, 52.8 kDa; Gα0 40.1 kDa; Gαi1, 40.5 kDa; Gαi2, 40.4 kDa; Gαi3, 40.5 kDa). The molecular weights depicted correspond to the signal of the standard markers. **Right up.** Determination of the protein quantity in lipid raft and non-rafts fractions. **Right down.** Determination of alkaline phosphatase activity on lipid raft and non-rafts fractions.

CHARACTERIZATION OF THE CB1 RECEPTOR COUPLING TO Gαi/o PROTEINS IN GLUTAMATERGIC AND GABAERGIC SYNAPTIC TERMINALS FROM BRAIN FRONTAL CORTEX AND HIPPOCAMPUS OF ADULT MOUSE

As mentioned, the CB1 receptor is mainly expressed in glutamatergic and in GABAaergic neurons in the CNS, although the level of expression is variable between this two types of neurons. Generally, the density of the CB1 receptor in glutamatergic neurons is significantly lower than in GABAergic neurons throughout the cerebral cortex (Katona *et al.*, 1999, 2006; Marsicano and Lutz, 1999). However, the activation of Gαi/o proteins is not always proportional to the receptor expression. For example, in the hippocampus the CB1 receptor expressed in glutamatergic neurons has shown greater efficiency to coupling with Gαi/o proteins compared to the CB1 receptor expressed in GABAergic neurons (Steindel *et al.*, 2013), showing the influence that exert the cellular context on the functionality of the CB1 receptor. This phenomenon has been attributed to the CB1 receptor located in synaptic terminals. However, the [^{35}S]GTPγS binding assays were not performed in synaptosomes, but rather in hippocampal tissue homogenates. Therefore, this phenomenon cannot be directly attributed to the CB1 receptor found in synaptic terminals because the interference of signals from CB1 receptors located in other subcellular compartments can bias the results.

To study the impact of the cellular context in the functionality of the CB1 receptor expressed in synaptic terminals, Western blot and [^{35}S]GTPγS binding assays were performed in frontal and hippocampal synaptosomes. Glu-CB1-RS and GABA-CB1-RS transgenic mouse models created by the "Molecular Mechanisms of Behavior" research group led by Professor Beat Lutz were used as a reliable tool to dissect the CB1 receptor belonging to the two major phenotypes of neurons (Ruehle *et al.*, 2013; Remmers *et al.*, 2017). In Glu-CB1-RS mouse model a CB1 receptor is rescued in dorsal telencephalic glutamatergic neurons, whereas in GABA-CB1-RS mouse model a CB1 receptor is rescued specifically in forebrain GABAergic neurons. In WT-like CB1-RS mice, a ubiquitous CB1 receptor rescue is achieved. Stop-CB1 mice display a complete CB1 receptor deficiency, because the expression of the CB1 gene is blocked by a transcriptional stop cassette upstream of the endogenous CB1 coding sequence. First, to verify the functionality of the genetic rescue approach, synaptosomes from CB1-RS mice

were characterized for expression, subsynaptic distribution, lipid raft vs non-raft compartmentalization and functionality of the CB1 receptor, and compared results in synaptosomes obtained from WT mice

Biochemical characterization of CB1-RS: Analysis of CB1 receptor expression in frontal cortical and hippocampal synaptosomes from WT and CB1-RS

Synaptosome samples from WT and CB1-RS mice were resolved in parallel by SDS-PAGE and assayed by immunoblot to study the relative expression of the CB1 receptor in frontal cortex and hippocampus. We used-Immunogenes anti CB1 antibody, because it recognizes the CB1 receptor located in both lipid raft and non-raft compartments (Figure 18). No statistical differences were observed in the immunoreactivity of the ∼50 kDa band between WT and CB1-RS mice both in hippocampal and in frontal cortical synaptosomes (Figure 18 and Table 7). We also did not observe a significant differences in the immurreactive signals of the ∼35 kDa band in frontal cortical synaptosomes. However, in hippocampal sinaptosomes the immunoreactivity of the ∼35 kDa band was significantly lower in CB1-RS mice than in WT mice, 25% less in fact. Therefore, this results showed no significant differences in the amount of CB1 receptor protein between CB1-RS and WT in frontal cortex, although in the hippocampus there is a small difference with respect to the CB1 receptor protein detected as an immunoreactive signal of ∼35 kDa.

We also could analyse the relative expression of the CB1 receptor between this two cortical regions, because frontal cortical and hippocampal synaptosomes samples were resolved in parallel by SDS-PAGE. Densitometry analysis showed that the difference observed between frontal cortex and hippocampus for both ∼50 kDa and ∼35 kDa immunoreactive bands was statistically significant both in WT and CB1-RS mice (Table 7). Indeed, a signal detected in hippocampal synaptosomes double that of the frontal cortex synaptosomes, suggesting a higher density expression of the CB1 receptor in hippocampal membranes than in frontal cortical membranes, which is in agreement with previous anatomical and pharmacological reports (Herkenham *et al.*, 1990; Mailleux and Vanderhaeghen, 1992a; Breivogel, Sim and Childers, 1997; Marsicano and Lutz, 1999).

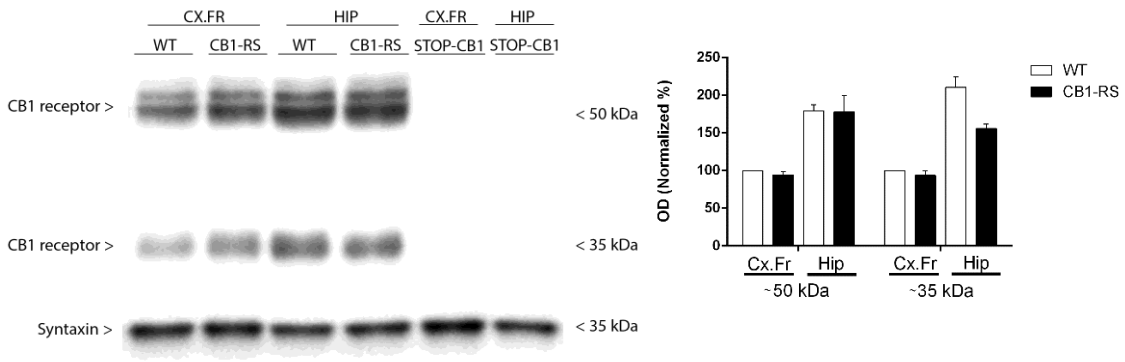

Figure 18. Representative image of Western blots carried out by immunoblotting same amounts of WT, CB1-RS and Stop-CB1 cortical and hippocampal synaptosomes (20 µg/lane). Immunoblot against CB1 receptor and syntaxin proteins. The molecular weights depicted correspond to the signal of the standard markers. Cx.Fr = Frontal cortex; Hip = Hippocampus. The graph shows the relative immunoreactivity values of ~50 kDa and ~35 kDa bands of the CB1, normalized to the signal of frontal cortical synaptosomes of WT mice.

~50 kDa	**WT**	**CB1-RS**
Frontal cortex	1	0.94 ± 0.05
Hippocampus	1.79 ± 0.08*	1.77 ± 0.21*

~35 kDa	**WT**	**CB1-RS**
Frontal cortex	1	0.93 ± 0.06
Hippocampus	2.10 ± 0.14*	1.56 ± 0.06*#

Table 7. Densitometry analysis of immunorreactive signals of ~50 kDa and ~35 kDa bands of the CB1, normalized to the signal of frontal cortical synaptosomes of WT. The values are means ± SEM of at least three independent experiments. Unpaired two tail t test. (*) = Statistically significant differences between regions; (#) = statistically significant differences between WT and CB1-RS. p = < 0.05

Biochemical characterization of CB1-RS: Analysis of compartimentalization of CB1 receptor and other proteins of the ECS in subsynaptic compartments of cerebral cortex

Then, we examined the subsynaptic distribution of the CB1 receptor in frontal cortex of CB1-RS mice and it was compared with the WT mice, to check whether the receptor is properly partition into subsynaptic fractions after his rescue. The subsynaptic marker distribution was qualitatively indistinguishable between the two phenotypes (Figure 15 and 19). Semiquantitative analysis of CB1-immunoreactive bands, showed no statistically significant differences between WT and CB1-RS mice (Figure 16 and 20, Table 6 and 8). In other words, the ~50 kDa and ~35 kDa bands detected by anti-CB1 antibodies were

equally distributed in WT and in CB1-RS mice, concluding that the CB1 receptor is properly partition in the three principal subsynaptic compartments of synaptic terminals after his rescue. We also studied the subsynaptic distribution of proteins of the ECS in CB1-RS mice. The subsynaptic profile of different elements of the ECS and signalling proteins was qualitatively similar between WT and CB1-RS mice (Figure 16 and 20), concluding that the set of genetic modifications which are subjected this transgenic mice do not impact in the subsynaptic distribution of proteins of the ECS.

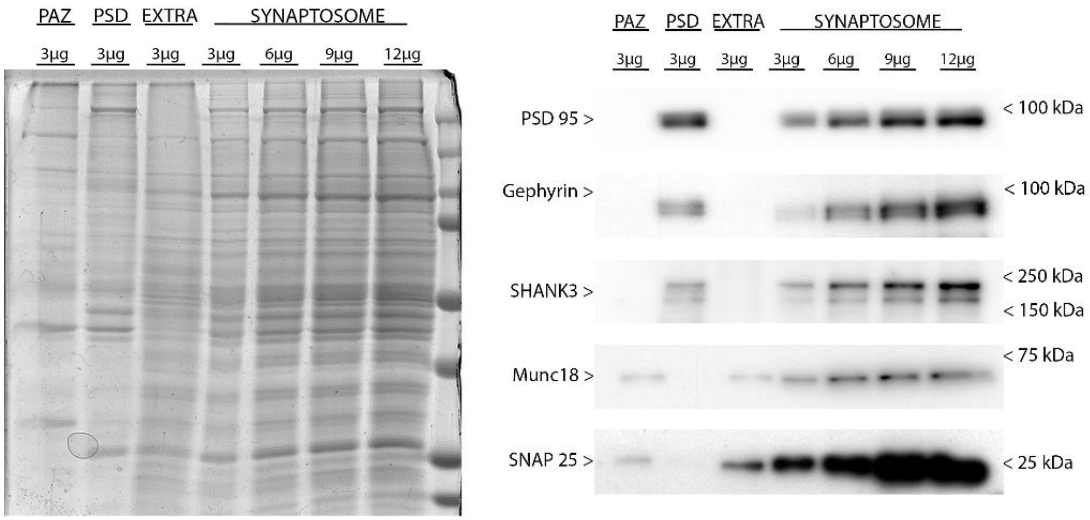

Figure 19. Coomassie blue-stained SDS-PAGE (left) and representative Western blots (right) carried out by immunoblotting increasing amounts of cortical synaptosomes (3, 6, 9 and 12 µg/lane) and different subsynaptic fractions of CB1-RS (3 µg/lane). Presynaptic fraction: PAZ, postsynaptic fraction: PSD and extrasynaptic fraction: EXTRA. The efficiency of the subsynaptic separation is assessed by presynaptic markers (Munc-18. SNAP-25), postsynaptic markers (PSD95, Gephyrin, and SHANK3) and extrasynaptic marker (Munc-18 and SNAP-25). Protein migration was consistent with their theoretical molecular mass, except for PSD95 protein, which migrated at a molecular weight of 95 kDa (PSD95, 80.4 kDa; Gephyrin, 83.2 kDa; SHANK3, 185.3 kDa; Munc-18, 66.3 kDa; SNAP-25, 23.3 kDa). The molecular weights depicted correspond to the signal of the standard markers.

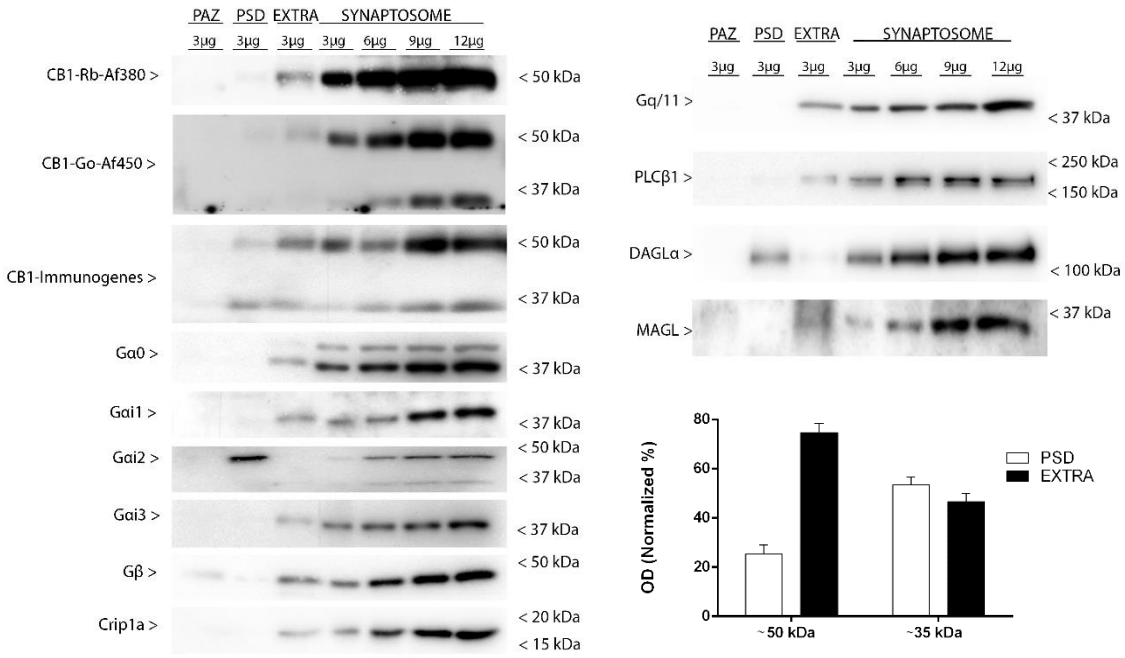

Figure 20. Representative Western blots carried out by immunoblotting increasing amounts of cortical synaptosomes (3, 6, 9 and 12 µg/lane) and different subsynaptic fractions of CB1-RS mice (3 µg/lane). Presynaptic fraction: PAZ, postsynaptic fraction: PSD and extrasynaptic fraction: EXTRA. Protein migration was consistent with their theoretical molecular mass. For CB1 Gαi2 and Gαo protein, an extra band migrating at ~35kDa, ~36 kDa and ~43 kDa were detected, respectively (CB1, 52.8 kDa; Gαo 40,1 kDa; Gαi1, 40.5 kDa; Gαi2, 40.4 kDa; Gαi3, 40.5 kDa; Gβ1, 37.3 kDa and 36.3 kDa 1 and 2 isoforms; CRIP1a, 18.6 kDa; Gαq/11, 42.0 kDa; PLCβ1, 138.3 kDa and 133.3 kDa 1 and 2 isoforms; DAGLα, 115.3 kDa; MAGL, 33.3 kDa). The molecular weights depicted correspond to the signal of the standard markers. The bar graphs show the subsynaptic distribution of the CB1 immunorreactive signals of ~50 kDa and ~35 kDa bands.

Frontal cortex	**EXTRA**	**PSD**
~50 kDa	74.7 ± 3.6	25.3 ± 3.6*
~35 kDa	46.5 ± 3.2	53.4 ± 3.2

Table 8. The subsynaptic distribution of the CB1 immunorreactive signals of ~50 kDa and ~35 kDa. The immunoreactive signal of each subsynaptic fraction is shown normalized to the total signal detected in the three compartments. The values are means ± SEM of three independent assays. Unpaired two tailed t test. (*) = $p < 0.05$

Biochemical characterization of CB1-RS: Localization of CB1 receptors in lipid raft and non-raft microdomains of synaptosomes obtained from frontal cortical brain tissue

We also examined the localization of the CB1 receptor in lipid raft and non-raft microdomains of CB1-RS mice. A total of 12 fractions of increasing density were obtained after subjecting cortical synaptosomes to an ultracentrifugation protocol in a sucrose gradient. As in WT mice, this fractions were biochemically characterized by quantitative analysis of phosphatase alkaline enzymatic activity, determination of the protein concentration and the use of lipid raft and non-raft markers. Briefly, alkaline phosphatase activity was highest in fractions 5-6 along with a stronger immunoreactivity for lipid raft markers and lower or absence of immunoreactivity for non-raft markers, suggesting that this fractions were enriched in lipid raft microdomains (Figure 21). On the other hand, the fractions between 8 and 12 displayed no alkaline phosphatase activity, high protein concentration, and high and low immunoreactivity for non-raft and lipid raft markers, respectively, suggesting that this fractions were non-raft fractions. The lipid raft vs non-raft partitioning of CB1 receptor did not differ qualitatively between WT and CB1-RS mice (Figure 17 and 21), again showing a varied CB1 immunoreactivity distribution profile depending on the antibody used. The partitioning profile of different elements of the eCB signalling proteins analysed was also similar in membrane compartments between WT and CB1-RS mice. Therefore, we can conclude that in CB1-RS mice, the CB1 receptor is properly partition in lipid raft and non-raft microdomains of synaptic terminals after his rescue.

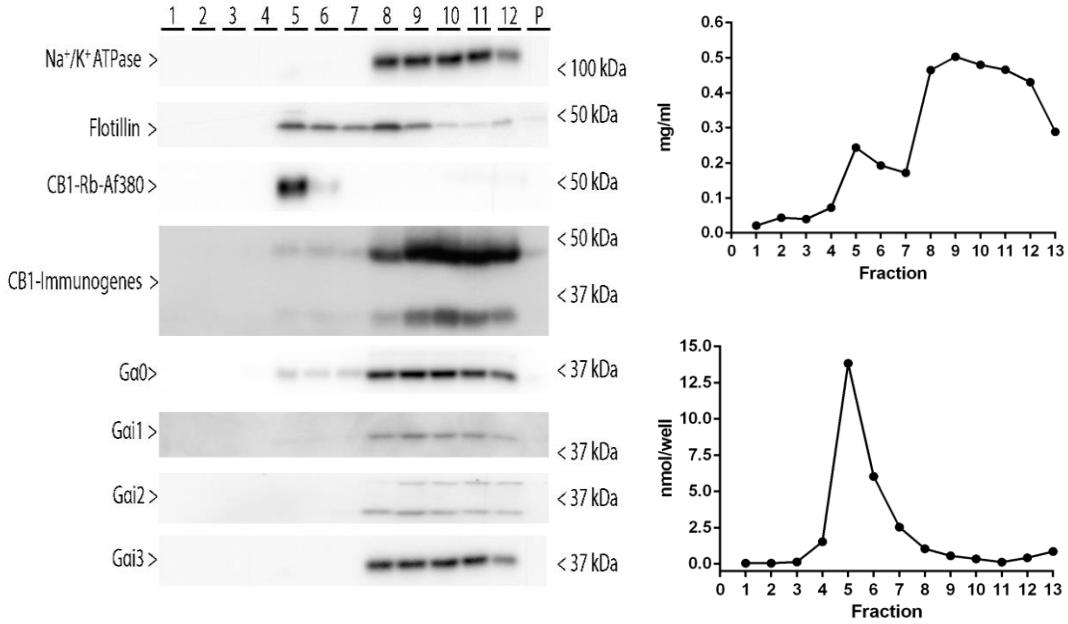

Figure 21. Representative Western blots running in parallel same volume of lipid raft and non-raft fractions derived from frontal cortical synaptosomes of CB1-RS mice (20 µl/lane). Immunoblot against Na^+/K^+ ATPase, Flotillin, CB1 and Gαi/o subtypes. Protein migration was consistent with their theoretical molecular mass. For CB1, an extra band migrating at ~35 kDa and ~36 kDa were detected, respectively. (Na^+/K^+ATPase, 112.3 kDa; Flotilin, 47.5 kDa; CB1, 52.8 kDa; Gαo 40,1 kDa; Gαi1, 40.5 kDa; Gαi2, 40.4 kDa; Gαi3, 40.5 kDa). The molecular weights depicted correspond to the signal of the standard markers. **Right up.** Determination of the protein quantity in lipid raft and non-raft fractions. **Right down**. Determination of alkaline phosphatase activity in lipid raft and non-raft fractions.

Biochemical characterization of CB1-RS: Analysis of the coupling of the CB1 receptor to Gαi/o proteins in synaptosomes obtained from WT and CB1-RS cortical and hippocampal brain tissue

Finally, synaptosomes from CB1-RS mice were characterized for canonical functionality of the CB1 receptor and results were compared with synaptosomes obtained from WT type mice. For this purpose, we performed [^{35}S]GTPyS binding assays stimulated by cannabinoid agonists in synaptosomes purified from frontal cortex and hippocampus. First, some preliminary experiments were conducted to determine the optimal protein load and [^{35}S]GTPyS and GDP concentrations. We determined the maximum response produced by 10 µM of cannabinoid agonist WIN 55,212-2 at 5, 12.5 or 25 µg of protein and 50 or 500 pM of [^{35}S]GTPyS concentration (Figure 22, Table 9). 5 µg of protein and 500 pM of [^{35}S]GTPyS concentration showed the highest maximum response between the analysed conditions, so the following assays were performed under these conditions.

To determine the optimal GDP concentration in the assay, we determined the maximal response produced at 1, 10, 30, 50 and 100 µM of GDP. Therefore, we selected 50 µM of GDP concentration to perform cannabinoid agonist-stimulated [^{35}S]GTPyS binding assays, because it showed the highest value of the maximum response between the conditions that were analysed (Figure 22, Table 9).

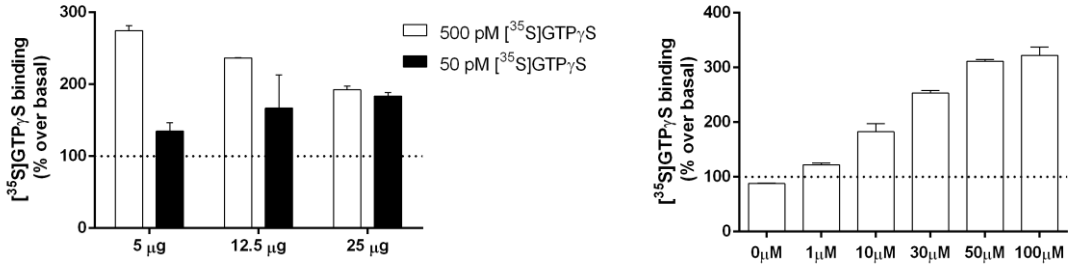

Figure 22. 10 µM WIN 55,212-2-stimulated [^{35}S]GTPγS binding in synaptosomal membranes of frontal cortex. Left graph: [^{35}S]GTPγS maximal binding (expressed as specific [^{35}S]GTPyS bound over basal) at 50 and 500pM [^{35}S]GTPγS concentrations of 5 µg, 12.5 µg and 25 µg of synaptosomes protein. Right graph: [^{35}S]GTPyS maximal binding (expressed as specific [^{35}S]GTPyS bound over basal) at different concentrations of GDP.

	Synaptosomes fraction protein content		
	5 µg	**12.5 µg**	**25 µg**
Emax 50 pM [^{35}S]GTPγS	174.6 ± 6.9	136.7 ± 0.04	92.2 ± 5.3
Emax 500 pM [^{35}S]GTPγS	34.7 ± 11.5	66.7 ± 46.2	83.6 ± 4.8
Basal (cpm) 50 pM [^{35}S]GTPγS	1,265 ± 40	3,463 ± 275	6,906 ± 110
Basal (cpm) 500 pM [^{35}S]GTPγS	15,610 ± 215	40,158 ± 2442	68,518 ± 1860

	GDP concentration					
	0 µM GDP	**1 µM GDP**	**10 µM GDP**	**30 µM GDP**	**50 µM GDP**	**100 µM GDP**
Emax	-12.1 ± 0.6	22.2 ± 2.9	82.3 ± 15.1	153.0 ± 5.2	211.3 ± 3.2	222.3 ± 15.1
Basal (cpm)	81,207 ± 1903	35,454 ± 331	14,212 ± 60	6,946 ± 876	4,459 ± 305	2,827 ± 472

Table 9. Data values are mean ± SEM of two independent experiments.

The analysis of functional coupling of the CB1 receptor by concentration-response curves of [^{35}S]GTPyS binding stimulation by the CB1 receptor agonist CP 55,940, provided same maximal stimulation (Emax) and pEC50 values in frontal cortical and hippocampal synaptosomes from WT and CB1-RS mice (Figure 23 and Table 10), concluding that Gαi/o coupling of CB1 receptors does not differ between WT and CB1-RS mice synaptosomes. Although functional assays were not designed to compare CB1 receptor function between regions, we clearly observed higher Emax values in hippocampal synaptosomes respect to frontal cortical synaptosomes in both WT and CB1-RS, which is in line with a higher CB1 receptor density determined by Western blot (Figure 23 and Table 10).

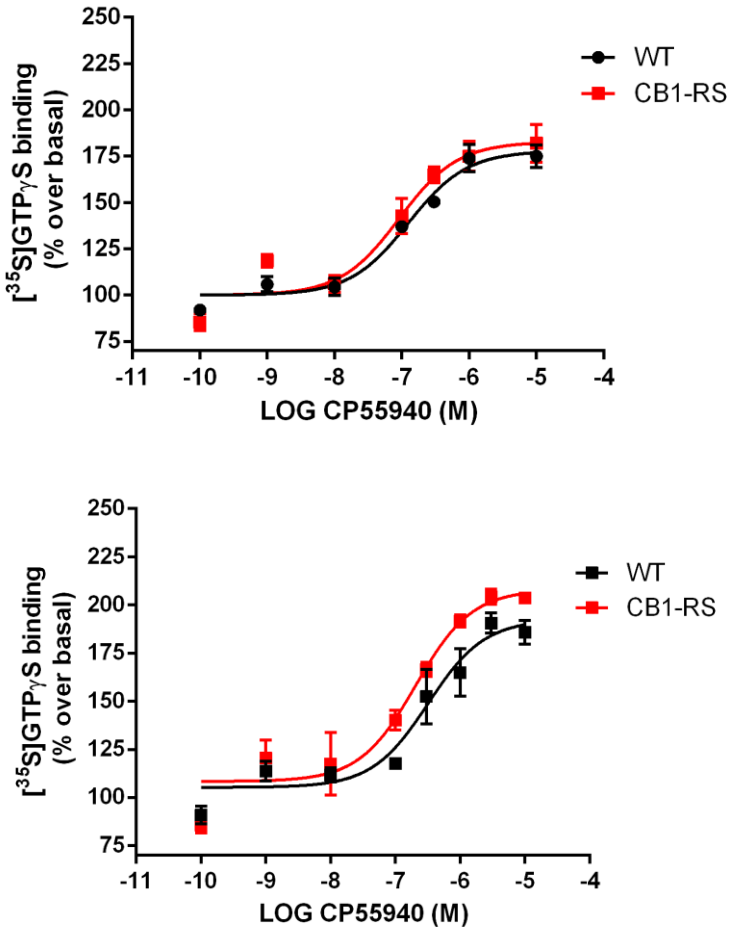

Figure 23. CP 55,940-stimulated [^{35}S]GTPγS binding in frontal cortical (up) and hippocampal (down) synaptosomes of WT and CB1-RS. Concentration response curves were constructed using mean values ± SEM from three independent experiments performed in triplicate (data are expressed as percentage of specific [^{35}S]GTPγS binding over basal).

Frontal cortex	WT	CB1-RS
Emax	90.7 ± 9.8	89.9 ± 3.6
pEC50	6.88 ± 0.17	6.93 ± 0.06
Basal (cpm)	14,548 ± 1788	20,765 ± 2484

Hippocampus	WT	CB1-RS
Emax	123.3 ± 22.85	129.6 ± 15.91
pEC50	6.37 ± 0.25*	6.74 ± 0.04
Basal (cpm)	20,013 ± 487	17,051 ± 409$^{\#}$

Table 10. Data values are mean ± SEM of at least three independent experiments. Unpaired (Emax) or paired (pEC50, Basal) two tailed t test. (*) = statistically significant differences between regions; ($^{\#}$) = statistically significant differences between WT and CB1-RS, $p < 0.05$

In conclusion, this results indicated that CB1-RS mice are indistinguishable from WT mice with respect to the expression level, subsynaptic distribution, lipid raft vs non-raft compartmentalization and Gαi/o coupling of CB1 receptors in synaptosomes. It can be then inferred that analysis of CB1 receptor expression, distribution, lipid raft vs non-raft partitioning and Gαi/o coupling in Glu-CB1-RS and GABA-CB1-RS mice are not biased by the set of genetic modifications that culminate in the rescue of the CB1 receptor, concluding that the selective rescue of the CB1 receptor in glutamatergic and GABAergic neurons are produced satisfactorily.

Analysis of the CB1 receptor expression and coupling to Gαi/o proteins in frontal cortical synaptosomes obtained from Glu-CB1-RS, GABA-CB1-RS and CB1-RS

Once we characterized CB1-RS mice, we analysed expression and functional coupling of CB1 receptor in synaptosomes from Glu-CB1-RS and GABA-CB1-RS mice in Western blot and in [^{35}S]GTPγS binding assays. Increasing amount of total protein of CB1-RS, Glu-CB1-RS and GABA-CB1-RS cortical synaptosomes were resolved by SDS-PAGE and CB1 receptor expression was analysed by immunoblot using CB1-Immunogenes antibody (Figure 24). Anti-syntaxin antibody was used as a protein loading control. A semiquantitative analysis of immunoreactive signals was perform comparing slopes values, which were obtained by regression analysis of curves that were generated plotting OD values for each protein loading. Regression analysis of standard curves revealed a linear relationship (R2 = > 0.98) between the amount of protein and the relative optical density for each sample (Figure 25). The immunoreactivity for the CB1 receptor ~50 kDa

band was similar in synaptosomal fractions from Glu-CB1-RS and GABA-CB1-RS, reaching about 45% of the signal found in CB1-RS in both partial rescue mice, with no statistical differences between Glu-CB1-RS and GABA-CB1-RS (Figure 25, Table 11). The same relative pattern was observed for the ~35 kDa band. Furthermore, the immunoreactivity level in this two neuronal population reached around the 85% of the total signal of the CB1 receptor, indicating that in the frontal cortical synaptic terminals the CB1 receptor is expressed predominately in these two phenotypic neurons although there is an around 15% of CB1 receptor population expressing in other types of synaptic terminals. Although it is known that in cerebral cortex there is a higher density of CB1 receptors in GABAergic than in glutamatergic terminals, the fact that excitatory terminals predominate over the inhibitory ones could explain our observation indicating that both types of terminals contribute equally to the total CB1 receptor signal.

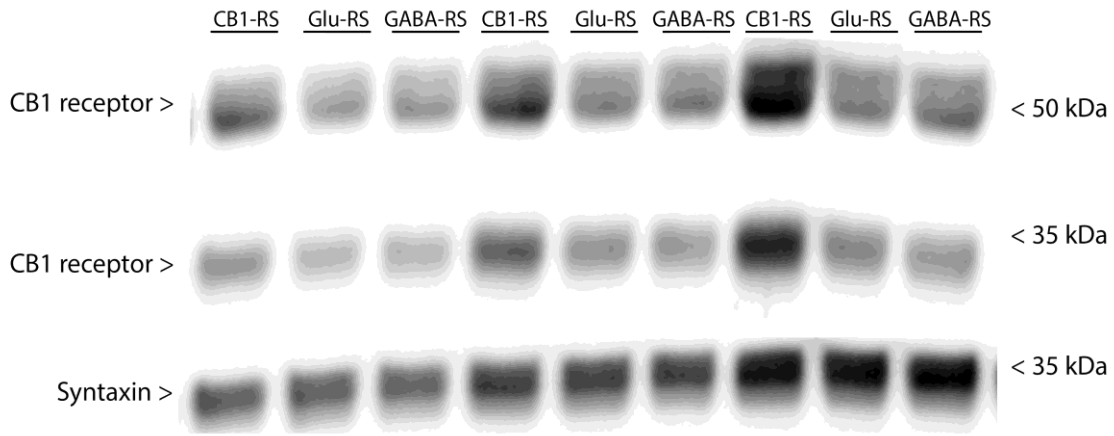

Figure 24. Representative Western blots carried out by immunoblotting increasing amounts of frontal cortical synaptosomal membranes from CB1-RS, Glu-CB1-RS and GABA-CB1-RS mice (6, 9 or 12 µg/line). CB1-Immunogenes antibody was used for detecting CB1 and anti-syntaxin antibody was used as a loading control. The molecular weights depicted correspond to the signal of the standard markers.

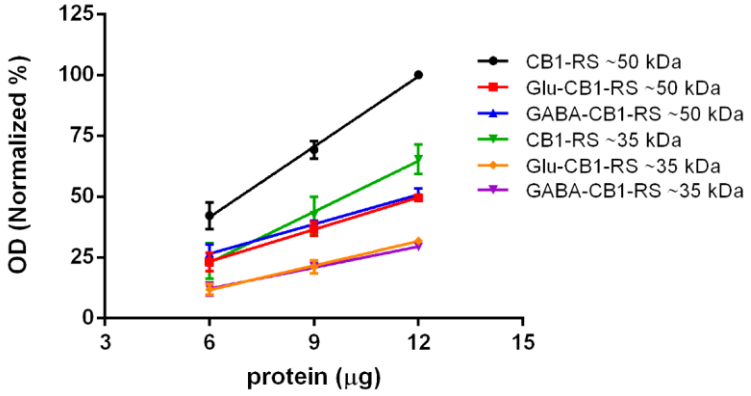

Figure 25. Regression analysis of curves generated by optical density (OD) values of the immunoreactive signals of CB1. **~50 kDa**: CB1-RS: Y = 9.64*x – 16.34; r^2= 0.99. CB1-GLU-RS: Y = 4.39*x – 3.08; r^2= 0.99. GABA-CB1-RS: Y = 4.41*x - 1.81 r^2= 0.99. **~35 kDa**: CB1-RS: Y = 6.79*x – 22.23; r^2= 0.98. Glu-CB1 RS: Y = 3.33*x – 8.41; r^2= 0.99. GABA-CB1-RS: Y = 2.88*x – 5.20; r^2= 0.99.

Slopes ratio	Glu-CB1-RS/CB1-RS	GABA-CB1-RS/CB1-RS	Glu-CB1-RS/ GABA-CB1-RS
~50 kDa	0.44*	0.42*	1.04
~35 kDa	0.49*	0.42*	1.15

Table 11. Analysis of CB1 protein expression by slopes comparison method. Data values are slopes ratio obtained from at least three different experiments. (*) = statistically significant differences between slope values; p= < 0.05

The functional coupling of the CB1 receptor was then assessed in synaptosomes obtained from frontal cortex of CB1-RS, Glu-CB1-RS and GABA-CB1-RS mice by CP 55,940 and WIN 55,212-2-stimulated [^{35}S]GTPγS binding. Similar values of Emax and pEC50 parameters were obtained in GABA-CB1-RS and Glu-CB1-RS mice, with no significant differences between them (Figure 26, Table 12). The Emax value in synaptosomal samples from either partial rescue mice was statistically significantly lower than in CB1-RS samples, whereas no differences were observed in the pEC50. As expected, no cannabinoid agonist-stimulated [^{35}S]GTPγS binding was observed in Stop-CB1 mice. These results demonstrate that the canonical Gαi/o protein-dependent CB1 receptor signalling, as defined by the agonist-stimulated [^{35}S]GTPγS binding assay, is positively co-related with the abundance of CB1 receptors in frontal cortex, irrespectively to the synaptic type (glutamatergic or GABAergic) context.

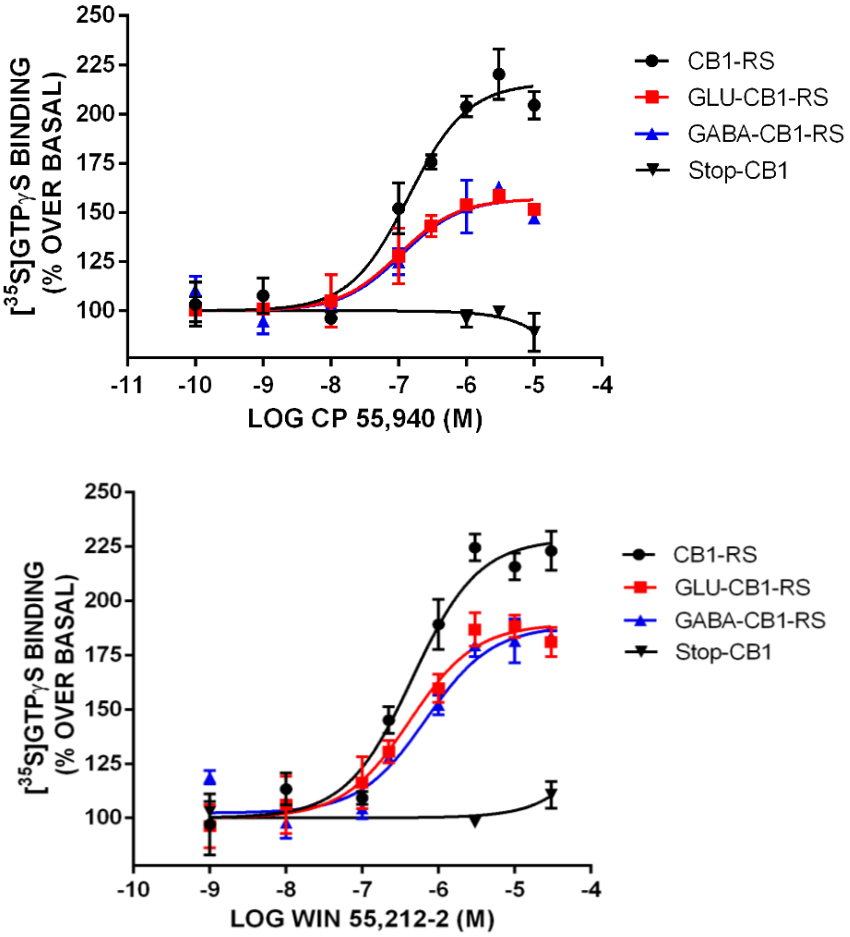

Figure 26. CP 55,940 (up) and WIN 55,212-2 (down) stimulated [^{35}S]GTPγS binding in CB1-RS, Glu-CB1-RS, GABA-CB1-RS and Stop-CB1 frontal cortical synaptosomal membranes. Concentration response curves were constructed using mean values ± SEM from three independent experiments performed in triplicate (data are expressed as percentage of specific [^{35}S]GTPγS binding over basal).

CP 55,940			
	CB1-RS	**Glu-CB1-RS**	**GABA-CB1-RS**
EMAX	111.7 ± 2.37	57.11 ± 1.79*	59.00 ± 1.10*
pEC50	6.85 ± 0.07	6.77 ± 0.12	6.72 ± 0.12
WIN 55,212-2			
	CB1-RS	**Glu-CB1-RS**	**GABA-CB1-RS**
EMAX	148.0 ± 18.74	89.55 ± 12.17*	84.8 ± 6.39*
pEC50	6.22 ± 0.08	6.14 ± 0.12	6.13 ± 0.04
Basal (cpm)	24,688 ± 877	31,062 ± 1823*	28,340 ± 894*

Table 12. Data values are mean ± SEM of at least three independent experiments. Unpaired (Emax) or paired (pEC50, Basal) one-way ANOVA followed by sidak test. (*) = statistically significant over CB1-RS, $p < 0.05$

Analysis of the CB1 receptor expression and coupling to Gαi/o proteins in hippocampal synaptosomes from Glu-CB1-RS, GABA-CB1-RS and CB1-RS

As mentioned, previous data suggest that in the hippocampus the type of synaptic terminal in which/where the CB1 receptor is expressed may condition the efficiency of the receptor coupling to Gαi/o proteins. To confirm this hypothesis, Western blot assays and cannabinoid agonists-stimulated [^{35}S]GTPγS assays were performed in hippocampal synaptosomes of CB1-RS, Glu-CB1-RS and GABA-CB1-RS mice.

The same procedure as in the frontal cortex was followed, that is, increasing amounts of total protein of CB1-RS, Glu-CB1-RS and GABA-CB1-RS hippocampal synaptosomes were resolved by SDS-PAGE and CB1 receptor expression was analysed by immunoblot using CB1-immunogenes antibody (Figure 27). As in the frontal cortex, a semiquantitative analysis of immunoreactive signals was perform comparing slopes values (Figure 28). Anti-syntaxin antibody was used as a protein loading control. The immunoreactivity of the ~50 kDa band differed between synaptosomal fractions from partial rescue mice, reaching a statistical significance (Table 13). About 28% and 70% of the signal found in CB1-RS reached in Glu-CB1-RS and GABA-CB1-RS mice, respectively. As expected, the slope values in synaptosomal samples from either partial rescue mice was significantly lower than in CB1-RS samples. The same relative pattern was observed for the ~35 kDa band. Furthermore, the immunoreactivity level in this two neuronal population reached around the 100% of the total signal of the CB1 receptor, indicating that in the hippocampal synaptic terminals the CB1 receptor is expressed predominantly in these two phenotypic neurons.

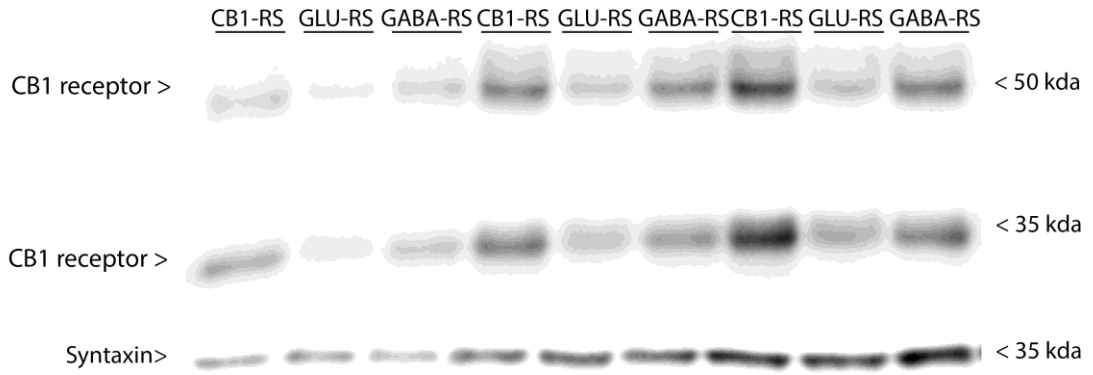

Figure 27. Representative Western blots carried out by immunoblotting increasing amounts of hippocampal synaptosome membranes from CB1-RS, Glu-CB1-RS and GABA-CB1-RS mice (6, 9 or 12 µg/line). CB1-Immunogenes antibody was used for detecting CB1 and anti-syntaxin antibody was used as a loading control. The molecular weights depicted correspond to the signal of the standard markers.

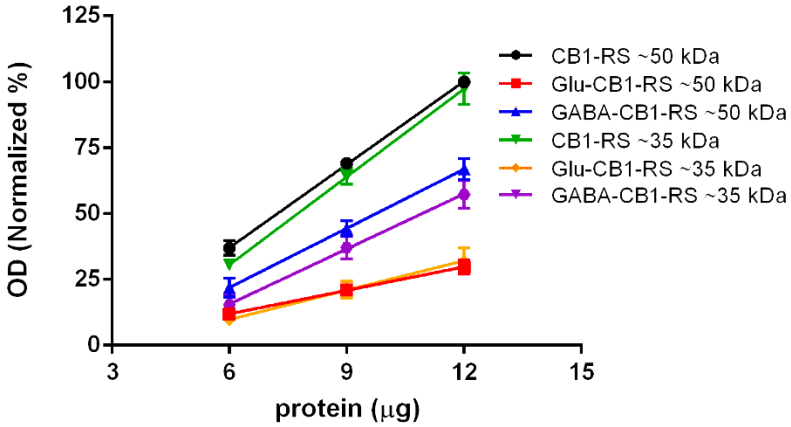

Figure 28. Regression analysis of curves generated by optical density (OD) values of the immunoreactive signals of CB1. Analysis of CB1 expression by slopes comparison method. **~50 kDa**: CB1-RS: Y = 10.52*x – 26.04; r^2= 0.99; Glu-CB1-RS: Y = 2.97*x – 5.87; r^2= 0.99. GABA-CB1-RS: Y = 7.48*x – 22.97 r^2= 0.99. **~35 kDa**: CB1-RS: Y = 11.13*x – 36.19; r^2= 0.99. Glu-CB1- RS: Y = 3.72*x – 12.54; r^2= 0.99. GABA-CB1-RS: Y = 6.97*x – 26.17; r^2= 0.99

Slopes ratio	Glu-CB1-RS /CB1-RS	GABA-CB1-RS/CB1-RS	Glu-CB1-RS/ GABA-CB1-RS
~50 kDa	0.28*	0.71*	0.40*
~35 kDa	0.33*	0.63*	0.53*

Table 13. Analysis of CB1 expression by slopes comparison method. Data values are slopes ratio obtained from at least three different experiments. (*) = statistically significant differences between slope values; p = < 0.05

Then we assess the functional coupling of the CB1 receptor in synaptosomes obtained from hippocampus of Glu-CB1-RS and GABA-CB1-RS mice by CP 55,940 and WIN 55,212-2-stimulated [^{35}S]GTPγS binding. The Emax value in synaptosomal samples from Glu-CB1-RS rescue mice was statistically significantly lower than in CB1-RS synaptosomes, whereas no differences were observed between GABA-CB1-RS and CB1-RS synaptosomes. The Emax value differ between synaptosomal fractions from partial rescue mice, reaching a statistical significance when CP 55,940 agonist was used in the assay. In contrast, no significant difference (Figure 29, Table 14) was obtained between partial rescue mice Emax with WIN 55,212-2, although the value of the Glu-CB1-RS mouse was 40% lower than of GABA-CB1-RS. Similar values of pEC50 parameters were obtained in all three phenotypes, with no significant differences. Again, no cannabinoid agonist-stimulated [^{35}S]GTPγS binding was observed in synaptosomes of Stop-CB1 mice.

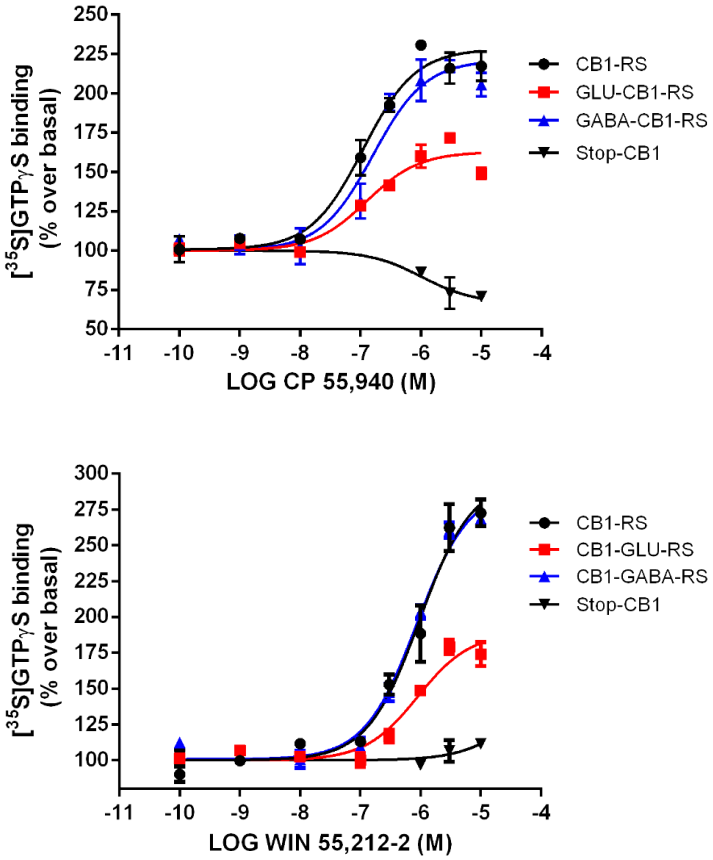

Figure 29. CP 55,940 (up) and WIN 55,212-2 (down) stimulated [^{35}S]GTPγS binding in CB1-RS, Glu-CB1-RS, GABA-CB1-RS and Stop-CB1 hippocampal synaptosomal membranes. Concentration response curves were constructed using mean values ± SEM from triplicate data points (expressed as specific [^{35}S]GTPγS bound over basal) performing at least three independent experiments.

CP 55,940			
	CB1-RS	**Glu-CB1-RS**	**GABA-CB1-RS**
Emax	148.60 ± 16.36	83.43 ± 14.4*	140.60 ± 10.67$^{\#}$
pEC50	6.75 ± 0.11	6.59 ± 0.16	6.61 ± 0.09
WIN 55,212-2			
	CB1-RS	**Glu-CB1-RS**	**GABA-CB1-RS**
Emax	170.90 ± 9.68	95.85 ± 5.44*	158.1 ± 12.70
pEC50	6.11 ± 0.12	5.93 ± 0.13	6.02 ± 0.12
Basal (cpm)	28,040 ± 2102	23,344 ± 1767*	23,559 ± 1725*

Table 14. Data values are mean ± SEM of at least three different experiments performed in triplicate. Unpaired (Emax) or paired (pEC50, Basal) one-way ANOVA followed by sidak test. (*) = statistically significant over CB1-RS; (#) = statistically significant over CB1-GLU-RS, $p < 0.05$

In summary, these results demonstrated that the canonical Gαi/o protein-dependent CB1 receptor signalling, as defined by the agonist-stimulated [^{35}S]GTPγS binding assay, is positively co-related with the abundance of CB1 receptor both in frontal cortex and in hippocampal synaptic membranes, irrespectively to the synaptic type (glutamatergic or GABAergic) context. Or data also demonstrate that the membrane number of CB1 receptors controls the canonical Gαi/o proteins activation, lower receptor densities producing less maximal response than higher densities and vice versa, concluding that receptor density on the cell surface is one means by which the cell control the responses to agonist.

ANALYSIS OF THE IMPACT OF CHOLESTEROL IN THE CB1 RECEPTOR COUPLING TO Gαi/o PROTEINS IN RAT BRAIN CORTICAL SYNAPTOSOMES

It has been shown that cholesterol negatively regulates the functionality of canonical signalling of the CB1 receptor, because cholesterol depletion procedures increases both CB1 receptor agonist maximal binding (Bmax) and agonist-stimulated [^{35}S]GTPγS binding efficacy (Bari, Battista, *et al.*, 2005; Bari, Paradisi, *et al.*, 2005). It has been proposed that lipid rafts are suitable structures for the negative regulation of the CB1 receptor function by cholesterol, because in these microdomains the presence of cholesterol is considerably higher than in non-raft plasma membrane. Indeed, strategies used to reduce membrane cholesterol levels, such as membrane treatment with the MβCD compound, mostly depletes cholesterol from lipid rafts, supporting this hypothesis (our unpublished results). However, most of the information that we have about this phenomenon has been obtained in heterologous cellular models. Therefore, we studied whether cholesterol negatively regulates the functionality of the CB1 receptor in native systems, specifically in synaptosomes of rat brain cortex. To assess this, rat cortical synaptosomes were treated with 20 mM of MβCD, which induced a depletion of 30% of total cholesterol from synaptosomes. This concentration of MβCD which is necessary to deplete membrane cholesterol was established in preliminar optimization assays performed in our lab prior to this thesis (unpublished data).

Effect of cholesterol depletion on the localization of CB1 receptors in lipid raft and non-raft microdomains

First, we purified lipid raft and non-raft fractions from control and cholesterol-depleted (MβCD treated) rat cortical synaptosomes and then we characterize lipid raft vs non-raft compartmentalization of the CB1 receptor. These fractions were biochemically characterized by quantitative analysis of phosphatase alkaline enzymatic activity, determination of the protein concentration and the use of lipid raft and non-raft markers. As in mouse cortical samples, characterization of lipid raft vs non-raft distribution of the CB1 receptor using different antibodies demonstrated the presence of CB1 receptors in both lipid raft and non-raft fractions of cortical synaptosomes, suggesting that lipid rafts

may regulate the functionality of the CB1 receptor located in these microdomains in native tissue (Figure 17 and 30). Contrary to what we expected, cholesterol depletion did not induce a destructuring of lipid rafts and we were able to observe the CB1 receptor and its canonical signalling Gαi/o proteins both in fractions enriched in lipid rafts and in non-raft fractions, an image qualitatively similar to that of the control condition (Figure 31).

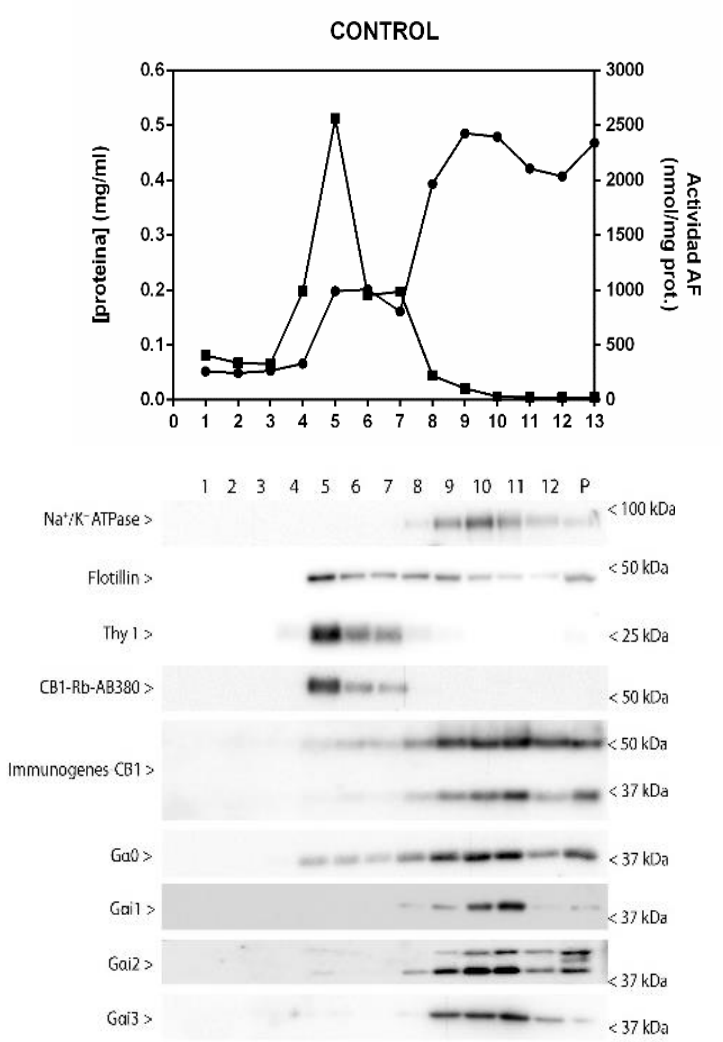

Figure 30. Representative Western blots running in parallel same volume of lipid raft and non-raft fractions derived from control rat cortical synaptosomes (20 µl/lane). Immunoblot against Na^+/K^+ ATPase, Flotillin, Thy-1, CB1 and Gαi/o subtypes. Protein migration was consistent with their theoretical molecular mass (Na^+/K^+ATPase, 112.3 kDa; Flotillin, 47.5 kDa; Thy-1, 18.1 kDa; CB1, 52.8 kDa; Gα0 40.1 kDa; Gαi1, 40.5 kDa; Gαi2, 40.4 kDa; Gαi3, 40.5 kDa). The molecular weights depicted correspond to the signal of the standard markers. Up graph. Determination of the protein quantity and of alkaline phosphatase activity in lipid raft and non-raft fractions.

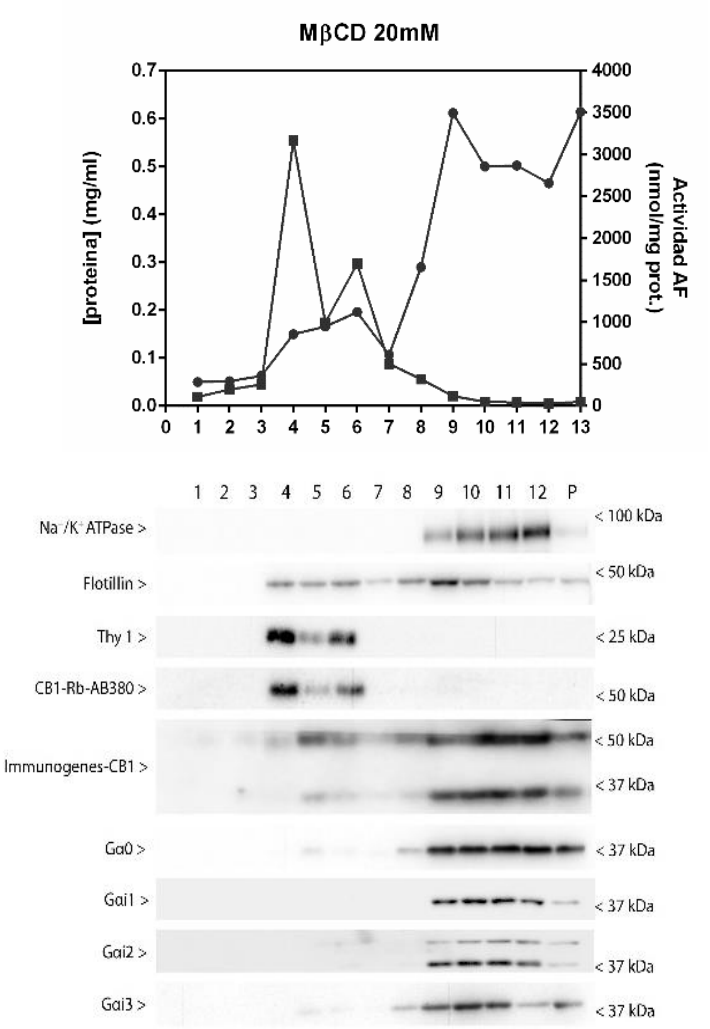

Figure 31. Representative Western blots running in parallel same volume of lipid raft and non-raft fractions derived from 20 mM MβCD treated rat cortical synaptosomes (20 µl/lane). Immunoblot against $Na^{+/}K^{+}$ ATPase, Flotillin, Thy-1, CB1 and Gαi/o subtypes. Protein migration was consistent with their theoretical molecular mass (Na+/K+ATPase, 112.3 kDa; Flotilin, 47.5 kDa; Thy-1, 18.1 kDa; CB1, 52.8 kDa; Gα0 40.1 kDa; Gαi1, 40.5 kDa; Gαi2, 40.4 kDa; Gαi3, 40.5 kDa). The molecular weights depicted correspond to the signal of the standard markers. Up graph. Determination of the protein quantity and of alkaline phosphatase activity in raft and non-raft fractions.

Effect of cholesterol depletion on the CB1 receptor coupling to Gαi/o proteins

To assess whether agonist-stimulated Gαi/o coupling is affected by cholesterol depletion, we generated concentration-response curves of CP 55,940, WIN 55,212-2 and methanandamide-stimulated [^{35}S]GTPγS binding in control and cholesterol-depleted (MβCD compound-treated) cortical synaposomes The stimulation of specific binding of [^{35}S]GTPγS by cannabinoid agonists showed that cholesterol depletion of the plasma membrane produces an increase in the efficacy of three agonists, in addition to produce an increase in the potency of CP 55,940 and methanandamide, concluding that cholesterol negatively regulates the functionality of the canonical CB1 receptor signalling pathway (Figure 32, Table 15).

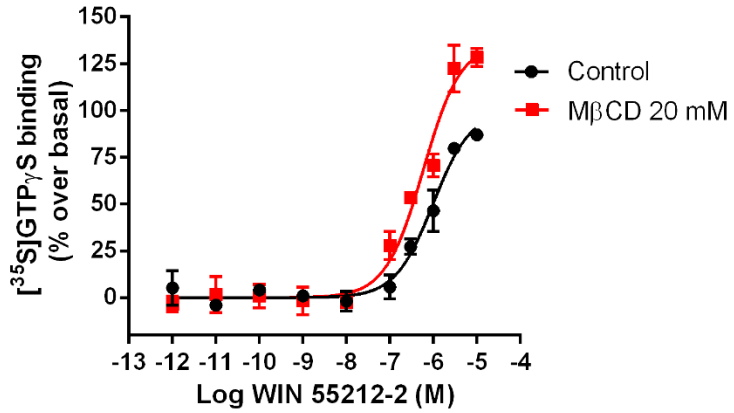

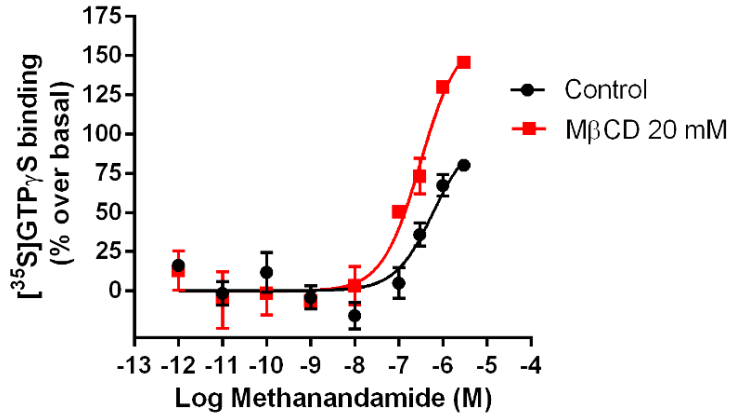

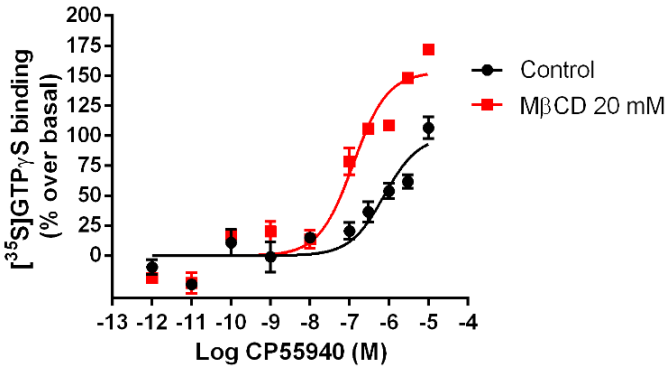

Figure 32. WIN 55,212-2, methanandamide and CP 55,940-stimulated [^{35}S]GTPγS binding in control and 20 mM MβCD treated rat cortical synaptosomes. Concentration response curves were constructed using mean values ± SEM from three independent experiments performed in triplicate (data are expressed as percentage of specific [^{35}S]GTPγS binding over basal).

	WIN 55,212-2		**Methanandamide**		**CP 55,940**	
	Control	**MβCD**	**Control**	**MβCD**	**Control**	**MβCD**
Emax	64.42 ± 1.87	86.87 ± 5.04*	37.44 ± 3.80	65.70 ± 3.88*	48.59 ± 2.33	69.00 ± 3.15*
pEC50	6.24 ± 0.14	6.23 ± 0.09	6.24 ± 0.08	6.51 ± 0.09*	6.49 ± 0.18	6.83 ± 0.13*

	Control	**MβCD**
Basal (cpm)	35597 cpm ± 982 cpm	28959 cpm ± 1232 cpm*

Table 15. Data values are mean ± SEM of at least three independent experiments performed in triplicate. Basal values were obtained pooling data from all independent experiments. Unpaired (Emax) or paired (pEC50, Basal) two tailed t test. (*) = statistically significant over control, $p < 0.05$

The [^{35}S]GTPγS binding assays also showed that cholesterol depletion of the plasma membrane produces a greater increase in the efficacy of the agonist methanandamide, followed by CP 55,940 and WIN 55,212-2. Thus, we analysed the pharmacological profile of these three agonists in each experimental condition. In a control situation, the ligand WIN 55,212-2 behaves as a total agonist because it produced the maximum response of the system, while CP 55,940 is a partial agonist with respect to WIN 55,212-2. On the other hand, it was observed that methanandamide behaves as a partial agonist, its efficacy being markedly lower than that of the CP 55,940 and WIN 55,212-2 ligands (Figure 33, Table 16). However, in cholesterol-depleted synaptosomes, although WIN

55,212-2 continues showing the maximal efficacy among the three agonists, methanandamide and CP 55,940 behave as partial agonists without significant differences between their efficacies (Figure 33, Table 16). These results indicate the impact of cholesterol on CB1 receptor functionality depends on the intrinsic activity of the agonist studied.

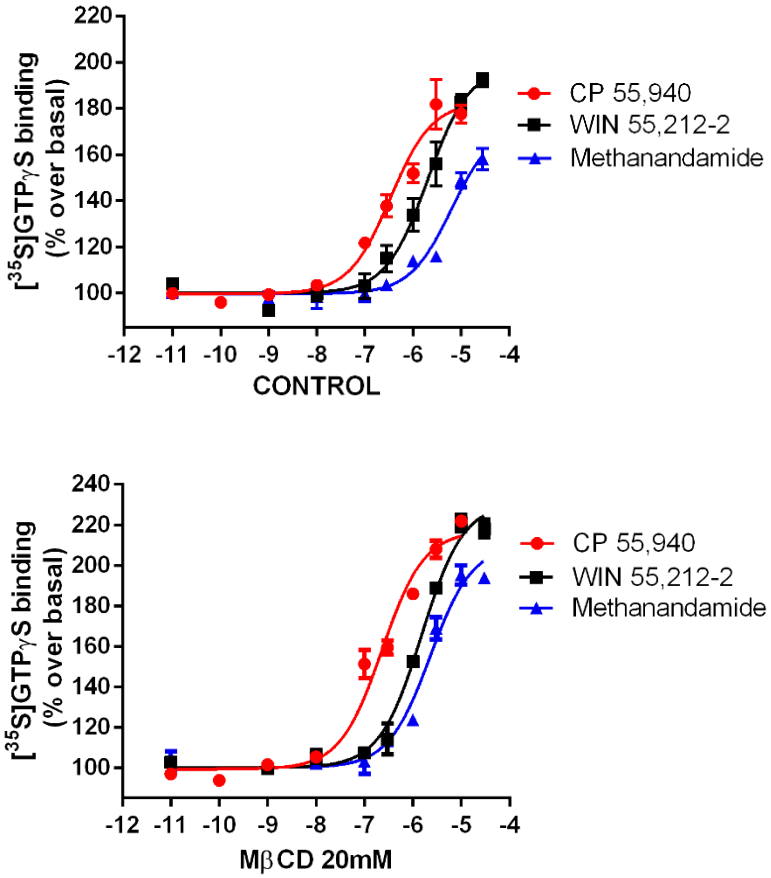

Figure 33. WIN 55,212-2, methanandamide and CP 55,940-stimulated [^{35}S]GTPγS binding in control and 20 mM MβCD treated rat cortical synaptosomes. Concentration response curves were constructed using mean values ± SEM from three independent experiments performed in triplicate (data are expressed as percentage of specific [^{35}S]GTPγS binding over basal).

Control	WIN 55,212-2	Methanandamide	CP 55,940
Emax	86.52 ± 9.73	58.37 ± 9.95*#	73.77 ± 7.60*
pEC50	5.73 ± 0.07	5.74 ± 0.29	6.12 ± 0.19
Basal (cpm)	37,039 ± 5311	37,236 ± 5145	36,199 ± 4063

MβCD	WIN 55,212-2	Methanandamide	CP 55,940
Emax	100.60 ± 4.58	77.35 ± 7.60*	84.26 ± 4.73*
pEC50	5.74 ± 0.05	5.68 ± 0.15	6.26 ± 0.17
Basal (cpm)	30,387 ± 5287	29,752 ± 5569	30,247 ± 5153

Table 16. Data values are mean ± SEM of at least three independent experiments performed in triplicate. Paired one-way ANOVA followed by tukey test. (*) = statistically significant over WIN 55,212-2; (#) = statistically significant over CP 55,940, $p < 0.05$

Effect of cholesterol depletion on the CB1 receptor protein expression

Finally, western blot assays were performed in control and in synaptosome samples subjected to incubation with MβCD to ensure that cholesterol depletion procedure could not increase CB1 receptor agonist efficacy by increasing the amount of receptors present on synaptic membranes. Increasing amount of total protein of cortical synaptosomes were resolved by SDS-PAGE and CB1 receptor expression was analysed by immunoblot using CB1-Immunogenes and CB1-Rb-Af380 antibodies (Figure 34 and 36). Anti-synaptophysin antibody was used as a protein loading control. A semiquantitative analysis of immunoreactive signals was perform comparing slopes values, which were obtained by regression analysis of curves that were generated plotting OD values for each protein loading. Regression analysis of standard curves revealed a linear relationship (R2 = > 0.98) between the amount of protein and the relative optical density for each sample (Figure 35 and 37). We did not detect any significant change in the immunorreactivity of CB1 signals between cholesterol-depleted and control synaptosomes regardless of the antibody used in the assay (Table 17 and 18). These results demonstrated that membrane levels of CB1 receptor were identical in control and cholesterol depleted synaptosomes, concluding that MβCD treatment does not alter the expression of CB1 receptor in synaptic plasma membrane and supporting the idea that cholesterol regulates the functionality of the CB1 receptor through an allosteric modulation mechanism.

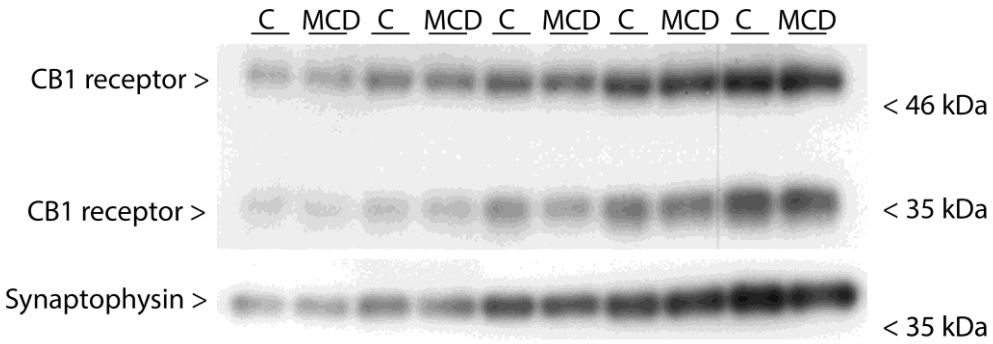

Figure 34. Representative Western blots carried out by immunoblotting increasing amounts of rat cortical synaptosomes. CB1-Immunogenes was used for detecting CB1 and anti-synaptophysin antibody was used as a loading control. The molecular weights depicted correspond to the signal of the standard markers.

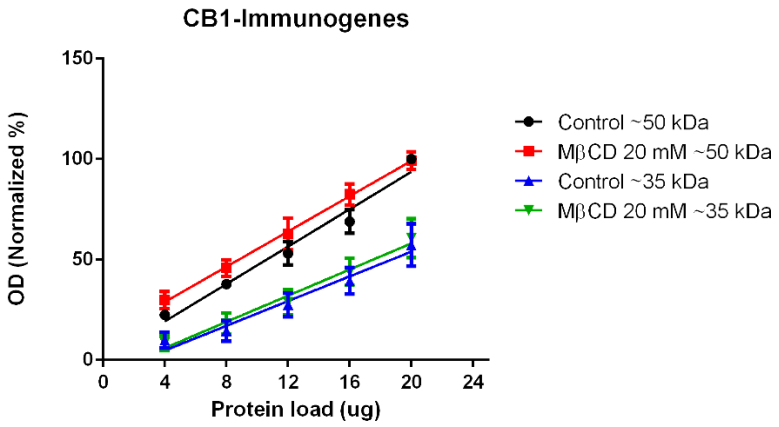

Figure 35. Regression analysis of curves generated by optical density (OD) values of the immunoreactive signals of CB1 detected by CB1-Immunogenes antibody. Control ~50 kDa: Y = 4.65*x + 0.60; MβCD ~50 kDa: Y = 4.39*x + 11.31; Control ~35 kDa: Y = 3.07*x – 7.56; MβCD ~35 kDa: Y = 3.25*x – 7.00.

Slopes ratio	**~50 kDa**	**~35 kDa**
Control/ MβCD	1.05	0.94

Table 17. Analysis of CB1 expression by slopes comparison method. Data values are slopes ratio obtained from at least three different experiments. (*) = statistically significant differences between slope values; p= < 0.05

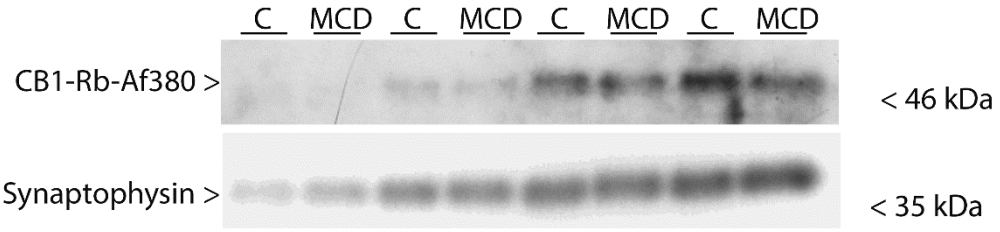

Figure 36. Representative Western blots carried out by immunoblotting increasing amounts of rat cortical synaptosomes. CB1-Rb-Af380 antibodye was used for detecting CB1 protein and anti-synaptophysin antibody was used as a loading control. The molecular weights depicted correspond to the signal of the standard markers.

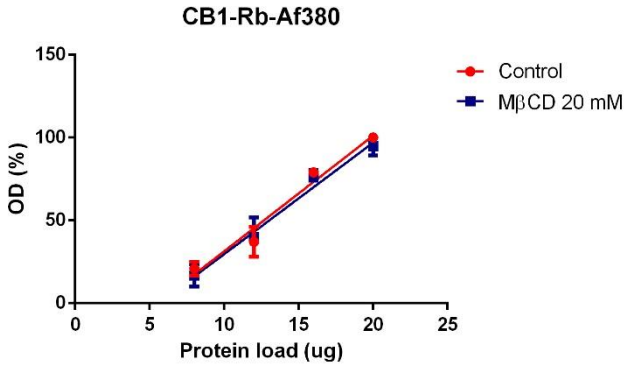

Figure 37. Regression analysis of curves generated by optical density (OD) values of the immunoreactive signals of CB1 detected by CB1-Fr-Af380 antibody. Control: Y= 6.98*x – 38.45; MβCD: Y= 6.73*x -37.66.

Slopes ratio	~50 kDa
Control/ MβCD	1.04

Table 18. Analysis of CB1 expression by slopes comparison method. Data values are slopes ratio obtained from at least three different experiments. (*) = statistically significant differences between slope values; p= < 0.05

Effect of cholesterol depletion on [^{35}S]GTPγS basal binding

As previously shown, synaptosomes incubation with 20 mM MβCD did not modify the CB1 receptor expression level (Figure 33-55 and Table 17 and 18). Also, this treatment did not appear to induce alterations in the expression of Gαi/o proteins (Figure 30 and 31). However, a significant reduction of [^{35}S]GTPγS basal binding (∼ 20%) was observed when agonist-stimulated [^{35}S]GTPγS binding assays were performed (Table 19).

To study the effect of MβCD on [^{35}S]GTPγS binding properties under basal conditions, without agonist stimulation, competition binding assays of unlabelled GTPγS against [^{35}S]GTPγS binding were carried out. These kinds of experiments, where the labelled and unlabelled ligands are chemically identical, represent a useful experimental alternative to saturation binding assays in order to obtain apparent K_D and Bmax values. Competition assays were performed with 0.5 nM [^{35}S]GTPγS, and the binding of the radioligand was measured in the presence of increasing concentrations of unlabelled GTPγS ranging from 0.1 nM to 0.1 mM (11 concentrations). The competition curves were monophasic and data were fitted to a model for fitting homologous competition experiments of GraphPad Prism 5 obtaining apparent K_D and Bmax values for [^{35}S]GTPγS binding in both control and MβCD treated rat brain cortical synaptosomes (Figure 38 and Table 19). Interestingly enough, the treatment of synaptosomes with 20 mM MβCD induced a significant reduction in the apparent Bmax of [^{35}S]GTPγS (∼37%). Additionally, a small but significant increase in [^{35}S]GTPγS affinity was also observed. Overall these results could explain the observed reduction in [^{35}S]GTPγS basal binding in cholesterol depleted synaptosomes.

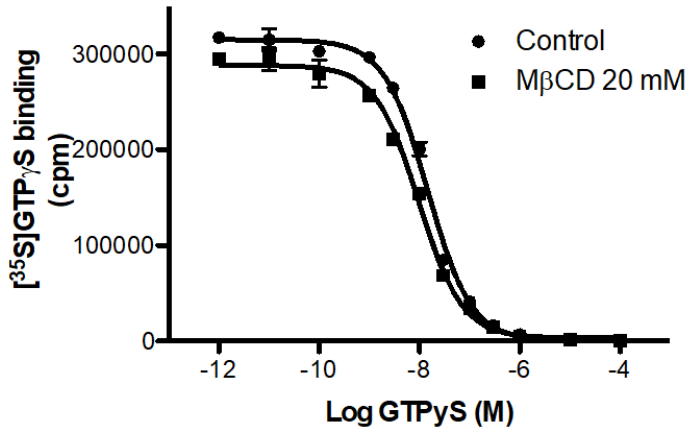

Figure 38. Competitive binding assays of unlabelled GTPγS against [^{35}S]GTPγS in control and 20 mM MβCD treated rat brain cortical synaptosomes. Competition assays were performed with 0.5nM [^{35}S]GTPγS, and the binding of the radioligand was measured in the presence of increasing concentrations of unlabelled GTPγS ranging from 0.1nM to 0.1 mM (11 concentrations). Data are average ± SEM values, determined from two different experiments performed in duplicate.

	CONTROL	20mM MβCD
Bmax (pmol/mg)	141.5 ± 6.2	89.4 ± 0.3 *
pK_D	7.87 ± 0.02	8.03 ± 0.01*

Table 19. Effect of 20mM MβCD treatment on apparent Bmax and KD values of [^{35}S]GTPγS in rat brain cortical synaptosomes Data are average ± SEM values of two different experiments performed in duplicate. (*) = statistically significant over control, $p < 0.05$

Due to the long incubation periods used in [^{35}S]GTPγS assays (2 hours), we also wanted to determine whether the potential accumulation of endogenous cannabinoids during the experimental procedure could contribute to the functional differences observed between control and MβCD treated synaptosomes. To this aim, basal and 10 μM WIN 55,212-2-stimulated [^{35}S]GTPγS binding was measured in the absence or presence of 10 μM tetrahydrolipstatin (THL), a DAGL inhibitor, or 1 mM Phenylmethylsulfonyl fluoride (PMSF), a MAGL and FAAH inhibitor. As shown in figure 39, the presence of THL or PMSF did not modify the [^{35}S]GTPγS basal binding neither in control synaptosomes nor in those treated with MβCD. Furthermore, the presence of 10 μM THL did not induce any change in the increase of efficacy induced by MβCD treatment. However, the presence of 1mM PMSF reduced the efficacy of 10 μM WIN 55,212-2 for stimulating the

[^{35}S]GTPγS binding in both control and MβCD treated synaptosomes, eliminating the ability of MβCD treatment for increasing agonist efficacy.

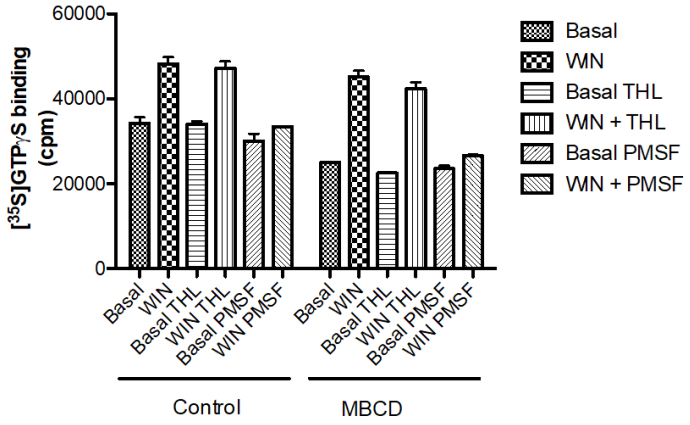

Figure 39. Basal and 10 μM WIN 55,212-2-stimulated [^{35}S]GTPγS binding in the absence or presence of 10 μM THL or 1 mM PMSF. The experiments were performed in control and MβCD treated synaptosomes.

Effect of cholesterol depletion on the modulatory actions of GDP in the agonist-stimulated [^{35}S]GTPγS binding

Due to the functional impact that MβCD treatment has on cannabinoid agonist-stimulated [^{35}S]GTPγS, we tried to evaluate the effect of this treatment on another key step directly implicated in this molecular response. In this context, the GDP modulation of G-protein activation by agonists is especially interesting. Numerous evidences indicate the important role of GDP in agonist-stimulated [^{35}S]GTPγS binding assays. In fact, the inclusion of GDP in these experiments is absolutely necessary for reducing the basal [^{35}S]GTPγS binding in order to detect agonist stimulation. Furthermore, cannabinoid agonists efficacy to stimulate [^{35}S]GTPγS binding appears to be determined by their ability for decreasing the affinity of G-proteins for GDP (Breivogel, Selley and Childers, 1998a).

With these all considerations in mind, competitive binding assays of GDP against [^{35}S]GTPγS in basal and WIN 55,212-2-stimulated conditions were performed in both control and MβCD treated synaptosomes. As shown in figure 40, all the competition curves were best fitted to a two sites model, with a high affinity site for GDP in the nanomolar range, and a low affinity site in the micromolar range (Table 20). In line with

previously published evidences (Breivogel, Selley and Childers, 1998a), the presence of 3 μM WIN 55,212-2 induced a slight, but not significant in our experiments, shift to the right of the low affinity component of GDP. The MβCD treatment did not significantly modify neither the GDP binding properties, nor the ability of WIN 55,212-2 for decreasing the affinity of GDP. As expected, in the absence of GDP no differences in [^{35}S]GTPγS binding were observed between control or WIN 55,212-2-stimulated conditions, demonstrating that the inclusion of high concentrations of GDP is necessary in order to detect agonist stimulation.

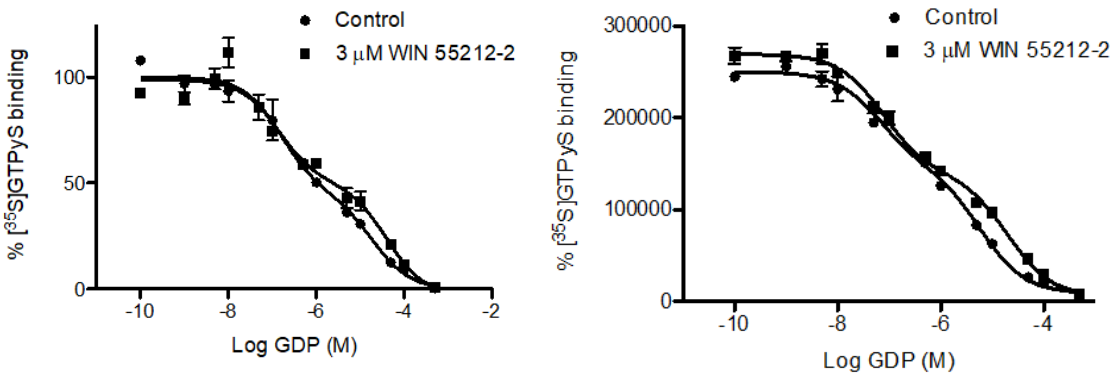

Figure 40. Competitive binding assays of GDP against [^{35}S]GTPγS under basal and WIN 55,212-2

Synaptosomes control		
	Basal	**WIN 55,212-2 (3 μM)**
$IC_{50\,H}$ (nM)	108 ± 52	118 ± 22
$IC_{50\,L}$ (μM)	12.1 ± 5.9	34.6 ±5.6
% High	45 ± 8.5	49 ± 2
20 mM MβCD treated synaptosomes		
	Basal	**WIN 55,212-2 (3 μM)**
$IC_{50\,H}$ (nM)	42 ± 25	52 ± 24
$IC_{50\,L}$ (μM)	4.8 ± 1.1	13.3 ± 6.8
% High	42.5 ± 0.5	40 ± 9

Table 20. IC50 values obtained in competition assays for high affinity [^{35}S]GTPγS binding in control and MβCD treated rat brain cortical synaptosomes stimulated conditions in control (A) and MβCD treated (B) synaptosomes. Competition assays were performed with 0.5 nM [^{35}S]GTPγS, and the binding of the radioligand was measured in the presence of increasing concentrations of GDP ranging from 1nM to 0.5 mM (12 concentrations). Data are average ± SEM values, determined from two different experiments performed in duplicate.

Analysis of the CB1 receptor coupling to Gαi/o proteins in control and cholesterol depleted frontal cortical synaptosomes of Glu-CB1-RS, GABA-CB1-RS and CB1-RS adult mouse

We also assess whether the negative regulation exerted by cholesterol was dependent on the synaptosome type (glutamatergic or GABAergic) where the CB1 receptor is located. For that purpose, we first determined the concentration of MβCD compound necessary to observe an increase in the efficacy of cannabinoid agonists in [^{35}S]GTPγS binding assays. Thus, we analysed the effect of increasing concentrations of MβCD (5 mM, 10 mM, and 20 mM) in CP 55,940 agonist-stimulated [^{35}S]GTPγS binding efficacy, showing an increase in the efficacy with respect to control at 10 mM and 20 mM MβCD (Figure 41, Table 21). Because the maximal increase in efficacy with respect to control was achieved with 10 nM MβCD, this concentration was used for subsequent experiments. CP 55,940 and WIN 55,212-2-stimulated [^{35}S]GTPγS binding assays were performed in control and cholesterol-depleted (MβCD compound-treated) synaposomes from Glu-CB1-RS and GABA-CB1-RS mice. Cholesterol depletion by MβCD increased CP 55,940 and WIN 55,212-2-stimulated [^{35}S]GTPγS binding efficacy, and the magnitude of this effect was not affected by synaptosome type (Figure 42, Table 22).

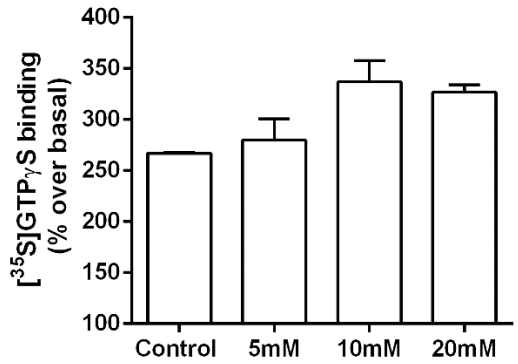

Figure 40. Bar graph of 10 µM CP 55,940-stimulated [^{35}S]GTPγS binding in control and in 5 mM, 10 mM and 20 mM MβCD treated frontal cortical synaptosomes of CB1-RS mice Emax values are expressed a specific [^{35}S]GTPγS bound over basal.

	Control	5 mM MβCD	10 mM MβCD	20 mM MβCD
Emax	167 ± 10	180 ± 21	237 ± 21	227 ± 07
Basal (cpm)	8959 ± 2143	9456 ± 1426	8227 ± 1228	7574 ± 388

Table 21. Data values are mean ± SEM of two independent experiments performed in duplicate.

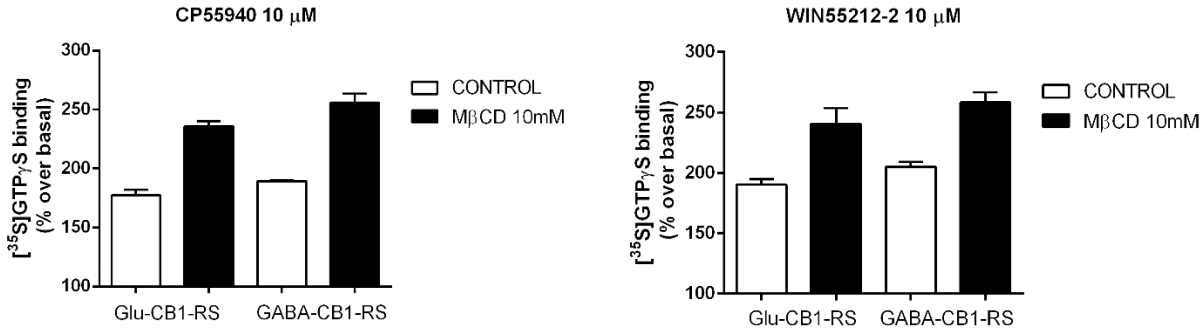

Figure 42. Bar graph of 10 μM CP 55,940 **(left)** and 10 μM WIN 55,212-2 **(right)** stimulated maximal [^{35}S]GTPγS binding in control and 10 mM MβCD treated frontal synaptosomal membranes derived from Glu-CB1-RS and GABA-CB1-RS mice. Emax values are expressed a specific [^{35}S]GTPγS bound over basal.

	Glu-CB1-RS		GABA-CB1-RS	
	Control	**MβCD**	**Control**	**MβCD**
Emax CP 55,940	77.33 ± 4.73	125.87 ± 8.75*	89.2 ± 1.10	155 ± 7.76*
Emax WIN 55,212-2	90.37 ± 4.72	140.50 ± 13.02*	105.20 ± 3.97	158.30 ± 8.42*
Basal (cpm)	22,081 ± 1791	15,397 ± 1578*	22,938 ± 5137	16,384 ± 182

Table 22. Data values are mean ± SEM of at least three independent experiments performed in triplicate. Unpaired (Emax) or paired (Basal) two tailed t test. (*) = statistically significant over control, $p < 0.05$

Next, we generated agonist concentration-response curves of CP 55,940-stimulated [^{35}S]GTPγS binding to determine whether cholesterol depletion impacts on the pEC50 parameter (Figure 43). No statistically significant changes were observed for this parameter between MβCD treated and control synaptosomes in neither Glu-CB1-RS nor GABA-CB1-RS mice (Table 23.). Again, the increase in the efficacy of CP 55,940 agonist induced by MβCD treatment did not differ statistically between excitatory and inhibitory terminals (Table 23) showing that the negative regulation exerted by cholesterol affects CB1 receptor coupling irrespectively of its location in glutamatergic or GABAergic terminals.

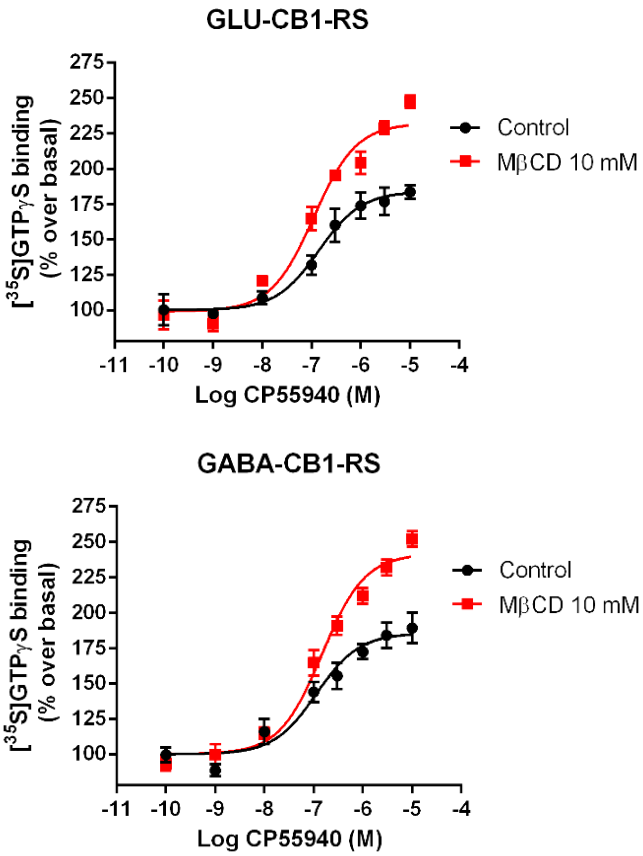

Figure 43. CP 55,940-stimulated [^{35}S]GTPγS binding in control and MβCD 10mM treated prefrontal synaptosomal membranes derived from Glu-CB1-RS and GABA-CB1-RS mice. Concentration response curves were constructed using mean values ± SEM from three independent experiments performed in triplicate (data are expressed as percentage of specific [^{35}S]GTPγS binding over basal).

	Glu-CB1-RS		**GABA-CB1-RS**	
	Control	**MβCD**	**Control**	**MβCD**
Emax CP 55,940	70.95 ± 3.23	125.87 ± 8.75*	67.43 ± 9.17	117 ± 14.20*
pEC50	6.61 ± 0.12	6.78 ± 0.06	7.02 ± 0.08	6.96 ± 0.13
Basal (cpm)	11,175 ± 264	7,443 ± 267*	10,324 ± 457	8,696 ± 95

Table 23. Data values are mean ± SEM of at least three independent experiments performed in triplicate. Unpaired (Emax) or paired (pEC50, Basal) two tailed t test. (*) = statistically significant over control, $p < 0.05$

VI. DISCUSSION

BIOCHEMICAL CHARACTERIZATION OF THE CB1 RECEPTOR LOCATED IN BRAIN CORTICAL SYNAPTIC TERMINALS OF ADULT MOUSE

Subcellular fractionation methods

The use of biochemical and pharmacological techniques allows to characterize the expression and signalling properties of the CB1 receptor in native systems. These experimental approaches are usually performed in unfractionated tissue homogenates or in undefined fractionated preparations. Although the CB1 receptor has been defined as a presynaptic protein, most recent works have demonstrated the presence of functional CB1 receptor also in non-neuronal cells or subcellular compartments such as in astrogia (Rodríguez, Mackie and Pickel, 2001; Han *et al.*, 2012; Ilyasov *et al.*, 2018), in somatodendritic postsynaptic membrane (Ong and MacKie, 1999; Bacci, Huguenard and Prince, 2004; Pickel *et al.*, 2004; Marinelli *et al.*, 2009; Thibault *et al.*, 2013; Maroso *et al.*, 2016) and in intracellular organelles such as in mitochondria (Bénard *et al.*, 2012; Hebert-Chatelain *et al.*, 2014), in endosomes or in lisosomes. Therefore, unfractionated preparations cannot discriminate CB1 receptor signals originating from diverse subcellular organelles, making the interpretation of experimental results complicated and easily biased, especially when a research is focused on a protein located in specific subcellular compartment. This issue can be resolved applying fractionation techniques to separate and purify subcellular particles by centrifugation. This method is based on differences that subsynaptic particles have in a sedimentation rate in a given suspension. Indeed, larger, heavier and denser particles sediment faster than smaller lighter particles. Cellular subfractionation procedures can also improve the sensitivity of assays along with minimising the degree of contamination from other cell types and organelles thereby reducing interferences of signals from undesired fractions. Definitely, these techniques reduce the complexity of an experimental sample and allows the results to be interpreted clearly and precisely.

Subcellular fractionation methods: Synaptosomes preparation as a material for studying the synaptic CB1 receptor

The aim of the present research work has been to characterize the CB1 receptor located in presynaptic membranes applying biochemical and pharmacological methods. Therefore, for that purpose it has been an indispensable requirement to purify synaptosomes (synaptic membranes) from brain tissue applying subcellular fractionation techniques. Synaptosomes are produced when brain tissue is homogenized and the shear forces causes nerve terminals detach from axons and dendrites and reseal into vesicular spherical particles (Whittaker, 1968, 1993; Tai and Jhou, 2017). In general, an isotonic sucrose buffer is used in a homogenization process and it favours the formation of isolated presynaptic terminals and presynaptic terminals with PSD attached to them, in detrimental on the formation of intact bipartite synapsis, presynaptic terminals with membrane-enclosed PSD and isolated postsynaptic terminals (Whittaker, 1993; Tai and Jhou, 2017). Synaptosomes resemble structural features of synaptic terminals found in tissue because they maintain common internal content of synaptic bottoms. For example, electron microscopy studies have shown that synaptosomes commonly contain some intracellular organelles such a mitochondria or synaptic vesicles with neurotransmitters along with a presynaptic active zone with PSD attached to them, a region specialized in neurotransmitter release (Gray and Whitakker, 1962; Dodd *et al.*, 1981; Whittaker, 1993). Synaptosomes have the molecular machinery necessary to uptake, storage and release neurotransmitters and they maintain metabolic activity and membrane potential. Therefore, some functional assays can also be performed in synaptosomal preparations (Whittaker, 1993), in addition to serve as a material for the study of synaptic proteins and their associated functions by biochemical methods.

Preparation of synaptosomes for studying the synaptic CB1 receptor: Validation of fractionation procedure

Many different protocols have been published since Hebb and Whittaker purified synaptosomes for first time in 1958 (Hebb and Whittaker, 1958). New protocols include variations to improve the integrity or the purity of synaptosomal preparation although is not a single optimal protocol as some have advantages and disadvantages can be found in

each of them. The choice depends on the experimental assay to be carried out with the preparation. Synaptic fraction prepared using sucrose are much more enriched in synaptosomes than preparations that use percoll or ficol gradients although the integrity of synaptosomes is worse preserved (Joo and Karnushina, 1975; Dunkley *et al.*, 1986; Tenreiro *et al.*, 2017). The protocol of choice for this work uses sucrose to purify synaptosomes, due to our special interest in obtaining a more purified preparation of synaptosomes. We prepared synaptosomal membranes as previously described by Dodd *et al.* (1981) including some modifications (Garro *et al.*, 2001). The main purpose for including these modifications is to enhance the purity of synaptosomes in detriment of the yield, increasing the washing and centrifugation steps. As mentioned in a methodology section, our procedure to obtain synaptosomes involves a homogenization of cerebral samples in an isotonic phosphate buffer containing 0.32 M sucrose and a combination of differential and sucrose density gradient centrifugations. After homogenizing, a fraction of crude synaptosomes (P2) is obtained by high speed centrifugation of the supernatant (S1) composed of cytoplasm and plasmatic membranes resulting from a first low speed centrifugation in which a P1 pellet containing nuclei, heavy membranes and cell debris is discarded. Subsequently, the crude synaptosome fraction (P2) is subjected to a two ultracentrifugation process in sucrose density gradient to obtain a purified preparation of synaptosomes. In this step contaminants such as myelin, free mitochondria and microsomal membranes are separated from synaptosomes.

Western blot data demonstrated that our protocol for obtaining synaptosomes enriched preparation is suitable and efficient, as synaptic markers (synaptophysin, syntaxin 1a and NR1) were substantially enriched in synaptosomes fraction compared to the total homogenate. Moreover, the enrichment of the rab11b immunoreactivity in synaptosomes is consistent with the expression of this protein in endosomes of synaptic terminals. Furthermore, a signal of synaptic markers was more intense detected in the preparation of synaptosomes than in the fraction of crude synaptosome, which indicates that the ultracentrifugation steps successfully remove different contaminants such as myelin, mitochondria and undefined microsomes to obtain a much more purified fraction of synaptic terminals. A detection of a weak signal of astrocytic, nuclear and cytosolic markers relative to other fractions also indicates that during subcellular fractionation steps gliosomes, nuclei and cytoplasmic proteins are separated from synaptosomes.

Our Western blot results are in line with data obtained from immunofluorescence assays performed in synaptosomal preparations seeded on poly-L-ornitine coated coverslip. SNAP-25 and MAP2 labelling revealed that about half of particles contained presynaptic or postsynaptic elements, indicating that synaptosomes account for the majority of structures in the preparation. We could not perform double immunofluorescence assay combining SNAP-25 and MAP2 labelling because both antibodies are generated in the same species. Combining these two markers would quantify more precisely the nature and the total amount of synaptosomes particles in the preparation, which presumably is greater than we have determined. Even so, these results are in line with previous published data obtained from observations of synaptosomes preparation in electronic microscopy. These studies demonstrated that approximately 50% of the structures are well defined synaptosomes, whereas around 40% of objects do not show clear organelle origin and cannot be unequivocally identified (Gray and Whitakker, 1962; Cotman and Matthews, 1971; Dodd *et al.*, 1981; Hajos, 2003). Many of these unidentifiable elements are presumably non synaptic neuronal and glial contaminants. Indeed, it has been postulated that in synaptosomes fractions up to 40% of particles can be derived from glial tissue, because glial cells constitute a high proportion of brain tissue and can produce fragments (gliosomes) with density properties similar to synaptosomes in the homogenization process (Henn, Anderson and Rustad, 1976). However, the methodological procedure impacts in the portion of glial contamination and Dodd's protocol produces the lowest glial contamination (Dodd *et al.*, 1981). This explains why we observed very low astroglial contamination by GFAP-immunostaining in immunofluorescence assay along with an enrichment and decrease in GFAP signal in P1 and synaptosomes fractions in Western blot assays, respectively.

In summary, our results demonstrated that we are dealing with really efficient protocol for obtaining synaptosomes. Although the process is laborious, this preparation serves as a reliable material for the study of synaptic CB1 receptor at high resolution and with low interference of signals derived from other cell and subcellular organelles, allowing the results to be interpreted accurately and with minimum level of bias.

Characterization of anti-CB1 antibodies to study the endogenous CB1 receptor by Western blot

An available and highly specific anti CB1 antibody is mandatory for identification of the endogenous CB1 receptor by Western blot assay. Although many antibodies designed against distinct antigenic sequences of the CB1 receptor have been developed, until now the identification and the interpretation of detected signals in Western blot assays has been confusing and controversial. Some different apparent molecular weights have been reported for the CB1 receptor and this has led researchers to speculate about what receptor species correspond for each apparent band. A major band migrating at theoretical molecular weight of the CB1 receptor has been suggested to correspond to monomeric CB1 species (Grimsey *et al.*, 2008). In addition, post-translational modifications may account additional bands observed at unexpected molecular weights because this modifications that can alter the migration of proteins in the gel. For example, bands migrating slightly higher than the theoretical weight have been related to N-glycosylation processes of N-terminal tail (Song and Howlett, 1995; Egertová and Elphick, 2000; De Jesús *et al.*, 2006). Bands migrating at high or low molecular weight have been postulated that represent receptor aggregates or oligomer complexes that have not been denatured or partially degraded CB1 species, respectively (Dove Pettit *et al.*, 1998; Egertová and Elphick, 2000; Wager-Miller, Westenbroek and Mackie, 2002; Kearn *et al.*, 2005; Mukhopadhyay and Howlett, 2005). The disparity reported in the molecular weight of CB1 receptor can also be explained by the splice variants of the CB1 receptor that have been identified by genetic techniques (Shire *et al.*, 1995; Ryberg *et al.*, 2005; Bagher *et al.*, 2013; Ruehle *et al.*, 2017). Furthermore, differences on the handling of the sample and on Western blot methodology could also explain some discrepancies and lack of replication between published results. Importantly, it has been shown that some commercially available anti CB1 antibodies are poor specific for the CB1 receptor and they detect multiple bands yielding false positive results (Grimsey *et al.*, 2008; our unpublished data). In fact, in most of published studies no mention is made about the specificity of the antibody or an appropriate negative control is not used, representing a high risk for false data. Hence, the specificity of available antibodies needs to be verified using appropriate negative controls (CB1-KO tissue) before their routine use.

We selected CB1-Rb-Af380, CB1-Go-Af450 and CB1-Immunogenes antibodies, (all raised against the last 30 amino acid of the human carboxyl terminal) validated previously by our research group for the identification of endogenous CB1 receptor in mouse cortical synaptosomes by Western blot assays. All the three antibodies recognized a specific diffuse band at ~50 kDa consistent with the 52 kDa theoretical molecular mass of mouse CB1. Additionally, a specific extra band at ~35 kDa was clearly recognized with CB1-Immunogenes and Go-Af450 antibodies, whereas this band was hardly detectable with the Rb-Af380 antibody in most of experiments. The specificity of the detected signals were validated using CB1-KO cortical sinaptosomes. We were also able to detect nonspecific bands at high exposure times or at high concentrations of the primary dilution, but under usual experimental conditions the signal intensity of these nonspecific bands was negligible.

Identification of specific immunoreactive signals detected by anti-CB1 antibodies in mouse cortical synaptosomes

Different factors could influence the migration profile of proteins in Western blot assays. Here, we performed different experimental approaches to elucidate if proteolysis, expression of isoform and post-translational modifications such as glycosylation could account the observed migration profile of the CB1 receptor in western blot assays.

A detection of unexpected bands at low molecular weight can be indicative of protease degradation. We did not observe changes in the immunoreactivity of ~50 and ~35 kDa in synaptosomes samples incubating at 37 ºC irrespectively of the presence or absence of protease inhibitors, neither when synaptosomes were obtained fractionating cerebral samples in the presence or absence of protease inhibitors. Hence, proteolytic degradation of the ~50 kDa band protein does not account for the appearance of the lower molecular mass band of ~35 kDa, at least during the fractionation procedure or handling and processing synaptosomes. Nevertheless, it cannot be ruled out that this band represents a proteolytic product generated in the tissue prior to sample preparation.

Previous results from our laboratory reported that the CB1 receptor migration can be influenced by its glycosylation status (De Jesús *et al.*, 2006). Indeed, the extracellular N-terminus of the mouse CB1 receptor has two consensus sequences for N-linked

glycosylation (Ruehle *et al.*, 2017). We examined whether the two immunoreactive bands detected in Western blot assays could correspond to glycosylated and non-glycosylated forms of the receptor. An enzymatic treatment with Peptide N-glycosidase F (PNGase F) of mouse cortical synaptosomes resulted in a clear shift in the migration profile of ~50 kDa immunorreactive band, which resulted virtually undetectable with any of the three antibodies used. These observation undoubtedly indicates that the ~50 kDa immunoreactive band represents a glycosylated species of the CB1. Instead, we detected new CB1 specific bands migrating at ~40 and ~37 kDa, in PNGase F treated samples, not observing an enrichment in ~35 kDa signal. In addition, CB1-Rb-380 antibody recognized a new strong signal at ~35 kDa molecular weight which was unspecific for CB1, because it was also detected in CB1-KO animals. This signal very likely corresponds to cross-reactivity of CB1-Rb-Af380 antibody with the 35 kDa PNGase F from Flavobacterium meningosepticum (Plummer and Tarentino, 1991; Tarentino and Plummer, 1994) which is present in deglycosylated synaptosome sample in abundance. ~40 and ~37 kDa immunoreactive bands are unlikely to be products of partial deglycosylation of the receptor and surely reflect non-glycosylated CB1 receptor species, because we doubled PNGase amount, incubation time or both during enzymatic digestion obtaining undistinguished results than standard procedure. Our results also show that all non-glycosylated forms of the CB1 receptor (~40, ~37 and ~35 kDa) migrate faster than expected based on the theoretical molecular weight of the mouse CB1, consistent with previous data (Andersson *et al.*, 2003; De Jesús *et al.*, 2006; Esteban *et al.*, 2020). Tightly packed conformation of proteins in SDS micelles could explain this faster migration (Therien, Grant and Deber, 2001). Therefore, the fact that glycosylated CB1 migrates at its theoretical molecular weight is simply a coincidence.

We also attempted to check if ~40 kDa, ~37 kDa and ~35 kDa immunorreactive bands detected in PNGase F treated synaptosomes reflect the canonical CB1 receptor and mCB1a and mCB1b mouse splice variants generated by alternative splicing of the primary Cnr1 gene transcript that have been identified recently (Ruehle *et al.*, 2017). mCB1a splice variant display a deletion of 39 amino acids in the N terminal tail but the two glycosylation sites of the canonical CB1 receptor are still present. Nevertheless, in a mCB1b splice variant a putative glycosylation sites are removed by deletion of 62 amino acids. If our hypothesis was true, the immunoreactive signal detected at ~50 kDa would reflect the canonical mouse CB1 receptor and mCB1a splice variant whereas ~35 kDa

band would represent a mCB1b splice variant. The glycosylation status of canonical mouse CB1 receptor and mCB1a splice variant would explain the huge difference that exist in the migration of these two species with respect to the mCB1b variant. We carried out immunoprecipitation assays of PNGase F-treated synaptosome samples followed by trypsin digestion of the ~40, ~37 and ~35 kDa bands and subsequent to LC-MS/MS. The fact that ~40 kDa, ~37 and ~35 kDa were observed in immunoprecipitates and that these signals were largely depleted from outputs is indicative of a successful immunoprecipitation procedure using both CB1-Immunogenes and CB1-Rb-Af380 antibodies. Notably, the net band seen at ~35 kDa in PNGase-treated synaptosomes with CB1-Rb-Af380 antibody was undetectably in immunoprecipitates further supporting the notion that the mentioned signal is caused by cross-reactivity of CB1-Rb-Af380 with the ~35 kDa PNGase F used for deglycosylation.

A theoretical analysis of the primary sequence of the CB1 receptor indicated a possibility for obtaining several mouse CB1 splice variant-specific tryptic peptides (Table 23). We detected two specific peptides for the mouse CB1 (UniProt Accession: P47746; GenBank Accession: NP_031752.1), with sequences ^{317}SIIIHTSEDGK^{327} and ^{328}VQVTRPDQAR^{337}. These sequences correspond to regions of the third intracellular loop of the mouse CB1, common to all the three splice variants. Although no peptides spanning the extracellular N-terminal region of the mouse CB1 were detected, these results do not conclude that ~40, ~37 and ~35 kDa bands cannot represent these CB1 species. Therefore, the use of other proteases to digest proteins could be considered for detecting variant specific peptides if detected immunorreactive signals actually represent the aforementioned isoforms. Otherwise, the absence of identified splice-variant peptides is not conclusive that CB1 variants could be actually expressed in mouse synaptosomes. However, the fact that mCB1a and mCB1b display low expression levels in mouse brain tissue makes unlikely the possibility that splice-variant protein products could be detected in mouse cortical synaptosomes. Indeed, quantitative PCR (qPCR) analyses of mRNA from mouse brain have shown that the expression level of mCB1a and mCB1b variants is about 0.02%-0.1% relative to overall CB1 (Ruehle *et al.*, 2017).

Mouse CB1 Splice Variant-Specific Tryptic Peptides

Peptides	Specificity	Specificity
TITTDLLYVGSNDIQYEDIK	mCB1$^{15-34}$; mCB1a$^{15-34}$	CB1 and mCB1a
GDMASK	mCB1$^{35-40}$	mCB1-specific
LGYFPQK	mCB1$^{41-47}$	mCB1-specific
FPLTSFR	mCB1$^{48-54}$	mCB1-specific
GSPFQEK	mCB1$^{55-61}$	mCB1-specific
MTAGDNSPLVPAGDTTD**ITEFY**D**K**	mCB1$^{62-85}$	mCB1-specific
SLSSFK	mCB1$^{86-91}$; mCB1a$^{47-52}$	CB1 and mCB1a
ENEDNIQCGENFMDMECFMILNPSQQLAIAVLSLTLGTFTVLENLLVLCVILHSR	mCB1$^{92-127}$; mCB1a$^{53-107}$	CB1 and mCB1a
GDTTD**ITEFY**D**K**	mCB1a$^{35-46}$	mCB1a-specific
TITTDLLYVGSNDIQENEDNIQCGENFMDMECFMILNPSQQLAIAVLSLTLGTFTVLENLLVLCVILHSR	mCB1b$^{15-84}$	mCB1b-specific

Table 23. Variant-specific peptides resulting from trypsin digestion of the canonical 473 amino acid-mouse CB1 (GenBank Accession: NP_031752.1) and the splice variants 439 and 411 amino acid-splice variants mCB1a and mCB1b identified by Ruehle *et al.* (2017). The aspartic residues resulting from deamination of glycosylated asparagine residues by PNGase F treatment are in bold type. Numbers correspond to the residue positions in the corresponding splice variant.

The emergence of CB1-specific immunoreactive proteins with different apparent molecular masses on SDS-PAGE after deglycosylation could be explained, at least in part, by the formation of a tandem electrophoretic mobility shift (EMS-shift) motif within the sequence of the N-terminus of the CB1 receptor as a consequence of PNGase F-mediated deamination of asparagine residues. Indeed, it has been recently reported that the mobility shift often observed in postraductionally phosphorylated proteins (phosphorylation-dependent electrophoretic mobility shift; PDEMS), rather than by the molecular mass of covalently linked phosphates, is caused by the presence of negatively charged amino acids around the phosphorylation site that generate an electrophoretic mobility shift (EMS)-related motif Θ-X_{1-3}-Θ-X_{1-3}-Θ, where Θ corresponds to an acidic or phosphorylated amino acid and X represents any amino acid) (Lee *et al.*, 2019). As these authors propose, EMS-motifs inhibit the binding of SDS to the peptide bond of proteins by charge-charge repulsion (Figure 44A-B), which results in a decreased ratio of

SDS/peptide stoichiometry causing a mobility shift. It is likely that generation of a tandem EMS-motif in the sequence of the canonical mouse CB1 receptor following PNGase F-catalyzed deamination of Asn78 and Asn84 (Figure 44C) could be sufficient to cause a mobility shift of about 5 kDa, which could also account greater apparent molecular mass of deglycosylated species than the non-glycosylated one (~35 kDa).

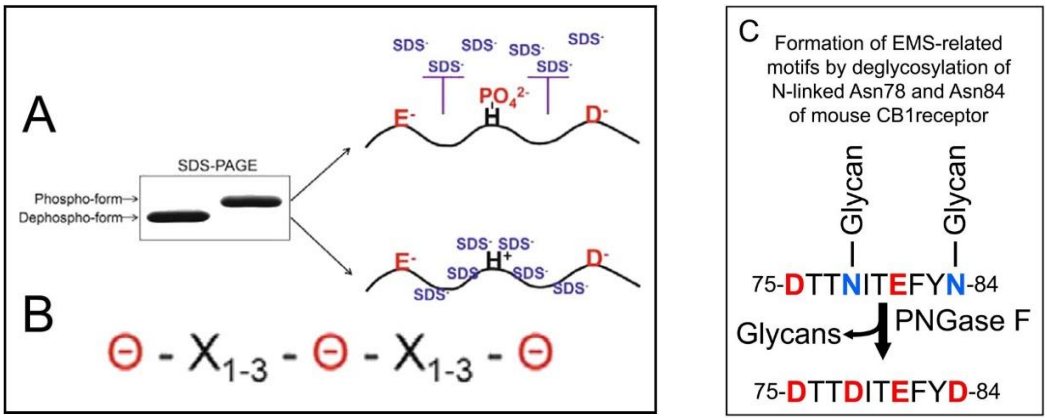

Figure 44. A-B. Model for the phosphorylation-dependent electrophoretic mobility shift (PDEMS) phenomenon and the EMS-related motif. Adapted from figure 4 in Lee *et al*. (2019). A. Molecular model for the PDEMS phenomenon. Protein phosphorylation induces the formation of the electrophoretic mobility shift (EMS) related motif which inhibits the binding of SDS to the peptide bond of proteins by charge-charge repulsion. Consequently, the decreased ratio of bound SDS per protein results in the mobility shift. B. Consensus sequence of the EMS-related motif. Θ symbols corresponds to a negatively charged amino acid (E or D) or phosphorylated amino acid, and X denotes any amino acid. **C**. Appearance of two EMS-related motifs within the extracellular N-terminus of the mouse CB1 as a consequence of deamination of asparagines 78 and 84 following enzymatic deglycosylation using PNGase.

Taking all data together, we concluded that CB1-Immunogenes, CB1-Go-Af350 and CB1-Rb-Af380 are highly specific antibodies for identification of the endogenous CB1 receptor by Western blot. These three antibodies detect the glycosylated form of the CB1 receptor, in addition to an undefined CB1 receptor specie (probably non glycosylated canonical CB1 receptor) that migrates at low apparent molecular weight. Even so, further testing should be performed to elucidate to what post-translational modifications affect the migration profile of the CB1 receptor, which would help in the identification and in the interpretation of CB1 signals detected by Western blot assays.

Subsynaptic compartmentalization of the CB1 receptor and other proteins of the ECS in cerebral cortex of adult mouse

To fully investigate the synaptic distribution of the CB1 receptor, mouse cortical synaptosomes were fractionated in three major subsynaptic domains: the presynaptic active zone (PAZ), the postsynaptic density (PSD) and the extrasynaptic zone (EXTRA). The EXTRA fraction is composed on plasmatic membrane not specialized in synapses and on intracellular components of the presynaptic bottom. PAZ and PSD are presynaptic and postsynaptic membranes specialized in synapsis. An active zone is a specialized region of the presynaptic plasma membrane where the release of neurotransmitter occurs. It is enriched in proteins involved in docking fusion and recycling of synaptic vesicles (Südhof, 2012). On the other hand, the postsynaptic side of the synapse is specialized to receive and transduce the neurotransmitter signal released from the presynaptic terminal. Neurotransmitter receptor and proteins involved in signalling pathways are clustered by macromolecular protein complexes in this specialized region (Sheng and Kim, 2011).

The protocol for subfractionate synaptosomes is based on differential pH and detergent sensitivity of three major subsynaptic domains (Phillips *et al.*, 2001). Because presynaptic and postsynaptic membranes are tightly linkage by fine filaments and synaptic adhesion molecules interacting through a synaptic cleft, the synaptic junction structure is a strongly adhesive complex and resists to a solubilisation of 1% TX-100 at pH 6. This allows the entire non-synaptic plasma membrane of synaptosomes to be solubilized and separate from this synaptic junction by centrifugation. Elevating pH to 8 disrupts the connections between presynaptic and postsynaptic synaptic membranes, solubilize the presynaptic active zone particles and allows purifying this two specialized compartments.

We examined by immunoblotting the synaptosomes fractionation procedure using markers of subsynaptic compartments. Although we did not have any antibody against a protein which is only expressed in extrasynaptic or in presynaptic active zone fractions, the immunoreactivity of SNAP-25 and MUNC-18 proteins (proteins involved in docking and membrane fusion of synaptic vesicles) both in EXTRA and PAZ fractions is agree with the expected and it reflects a synaptic and non-synaptic pools of this two proteins. The immunolabelling of this proteins was significantly higher in the EXTRA fraction than in PAZ fraction, which is consistent with previous results (Phillips *et al.*, 2001). The signals of PSD95, SHANK3 and gephyrin were detected in the insoluble pellet at pH 8

consistent with the postsynaptic membrane nature of this fraction. PSD95 and SHANK3 are postsynaptic scaffolding protein which function as a platforms for the postsynaptic clustering of crucial synaptic proteins at glutamatergic neurons. Meanwhile, Gephyrin is a microtubule-associated protein that anchors and clusters glycine and γ-aminobutyric acid type A receptors at inhibitory synapses. Furthermore, the distribution profile of the protein bands by Coomassie stain clearly showed that three isolated fractions were enriched in different proteins, suggesting that the efficiency of the fractionating protocol is high. The protein yield of each fractions is also consistent with what it is expected. Since the EXTRA fraction is composed of cytoplasm and almost all plasma membrane except synaptic junctions, we recovered the most of the protein content in the EXTRA fraction. In conclusion, this results demonstrate that the protocol for subfractionate synaptosomes in EXTRA PAZ and POST domains is effective, which allowed us to analyse the subsynaptic compartmentalization of the CB1 receptor and different elements of the ECS.

As expected and in agreement with electron microscopy observation reported previously (Nyíri *et al.*, 2005), our data revealed that the CB1 receptor s are primary located in the extrasynaptic membrane of terminals together with Gαi/o proteins involved in its canonical downstream signalling and CRIP1a, a protein that interacts with the CB1 receptor modulating its localization and its canonical function (Niehaus *et al.*, 2007; Guggenhuber *et al.*, 2016; Blume *et al.*, 2017). In some experiments, a very weak signal close to detection limit was detected in the PAZ fraction. This is also consistent with immunogold electron microscopy studies because the CB1 receptor can hardly be found inside the presynaptic active zone (Nyíri *et al.*, 2005). A smaller but clearly detectable pool of receptors was located in the postsynaptic fraction, which is consistent with some previous published data (Rodríguez, Mackie and Pickel, 2001; Köfalvi *et al.*, 2005). This immunorreactive signal could correspond to CB1 receptors located inside the postsynaptic membrane or in the perisynaptic membrane, from where the CB1 receptor would be anchored or connected to this dense postsynaptic region from its internal face by interaction with scaffolding proteins that precisely stablish this specialized region. In fact, there are data suggesting that postsynaptic CB1 receptor activation could regulate negatively N-methyl-D-aspartate receptor (NMDAR) function located at postsynaptic density in situations of excessive NMDAR activation, working with presynaptic CB1 receptor in reducing glutamatergic imput at postsynaptic membrane (Sánchez-Blázquez

et al., 2013; Vicente-Sánchez *et al.*, 2013; Sánchez-Blázquez, Rodríguez-Muñoz and Garzón, 2014). CB1 receptor activation would reduce synaptic membrane expression of NMDAR forming a complex with this ionotropic receptor and internalizing inside the cell. However, the presence and relevance of postsynaptic CB1 receptor is controversial because of the lack of definitive anatomical evidences. As previously suggested by Köfalvi *et al.* (2005), in immunogold electron microscopy studies the sensitivity to detect the CB1 receptor in this specialized region is limited, because the accessibility of antibodies to the corresponding epitopes may be affected by the high concentrate proteinaceous material which is composed this specialized regions. Solubilizing PAZ and PSD fractions would allow antibodies to access to the corresponding epitopes. The yield of total synaptosome protein in the EXTRA fraction was almost 5.8-fold higher than in the PSD fraction revealing that most CB1 receptors are located in the extrasynaptic membrane. Based on this protein yield for each subsynaptic fractions, it is deduced that about 90% of synaptic terminal total CB1 receptor is found in the extrasynaptic fraction. Therefore applying this subsynaptic protocol will allow us to detect subtle changes in the CB1 receptor in these specialized synaptic domains at high resolution level in the future.

Regarding of proteins involved in the synthesis and degradation of the major eCB 2-AG, Gαq/11 subunit, PLCβ1 and MAGL were found in the EXTRA fraction, whereas DAGLα was mostly enriched in postsynaptic density fraction. Although both PLCβ1 and DAGL are located around the postsynaptic dense zone at the edge of glutamatergic synapsis (Katona *et al.*, 2006; Yoshida *et al.*, 2006; Fukaya *et al.*, 2008), DAGL contains binding motifs for interact with synaptic scaffold protein Homer (Jung *et al.*, 2007), which could explain the immunoreactivity of this protein in the PSD fraction rather than in EXTRA fraction. This results indicate that the partition of the CB1 receptor and proteins involved in the synthesis and degradation of the major eCB 2-AG in subsynaptic compartments is in agreement with the retrograde signalling function assigned to the ECS. Furthermore, our study identifies proteins of the ECS as new markers of subsynaptic fractions. Thus, we propose that Gαo, Gαi1, Gαi3, Gαq/11, CRIP1a PLCβ1 and MAGL proteins are pure markers of the EXTRA fraction, while DAGLα is a POST domain marker. Besides, although the immunoreactive labelling of some proteins has been detected in various subsynaptic fractions, such as the case for the CB1 receptor (EXTRA> POST> PAZ), Galphai2 (upper band in POST and down band in EXTRA) and Gβ subunit (EXTRA>

PAZ> POST), detecting a marking profile according to that described in this work would be indicative of a successful fractionation.

Localization of CB1 receptors in lipid raft and non-raft microdomains of synaptosomes obtained from frontal cortical brain tissue of adult mouse

Cellular plasma membranes are laterally heterogeneous and distinct subdomains that differ in their biophysical properties and composition are present there. Lipid raft are transient (short lifetime), dynamic (both in terms of lateral diffusion and formation – dissociation) and relatively small size membrane nanodomains (10–200 nm), which are formed and enriched by preferential association between sterols (cholesterol in particular), glycosylated and saturated lipids (phospholipids and sphingolipids) and lipidated and glycosylated proteins (glycosylphosphatidylinositol-anchored proteins), away from unsaturated lipids and most proteins. Enrichment of these hydrophobic components increase lipid packing and ordering of membrane, and decrease its fluidity, endowing distinct physical properties to these domains in comparison to more fluid and less organized regions (non-raft domains). In addition, lipid rafts can selectively recruit or segregate certain lipids and proteins in order to regulate their interaction with other membrane associated components, functioning as a platform to influence signalling and trafficking of these elements (Hancock, 2006; Pike, 2006; Sezgin *et al.*, 2017; Levental, Levental and Heberle, 2020). In line with this, previous data indicate that lipid rafts are suitable structures to regulate the functionality of the CB1 receptor (Dainese *et al.*, 2007; Maccarrone *et al.*, 2009; Wickert *et al.*, 2018). Indeed, treatment of plasmatic membranes with a lipid raft disruptor MβCD has revealed that the efficacy of CB1 receptor agonists is negatively regulate by this domain (Bari, Battista, *et al.*, 2005; Bari, Paradisi, *et al.*, 2005). However, complete knowledge between lipid raft and CB1 receptor interaction has been obtained in heterologous cellular systems. Therefore, in order to increase the physiological relevance of CB1 receptor lipid raft interaction, we studied the possible localization of the CB1 receptor in lipid raft fraction obtained from mouse cortical synaptosomes.

We applied a protocol described by (Ostrom and Insel, 2006) to separate lipid raft from non-raft membranes. An increase of packing and ordering of components that form lipid

raft makes these membranes resistant to solubilisation by non-ionic detergent, whereas non-raft membranes are soluble. Thus, mouse cortical synaptosomes were incubated with Triton X-100 and then synaptic lipid raft membranes were separated from non-raft membranes by centrifugation in sucrose density gradient. The separation is possible because the high lipid:protein ratio of lipid rafts makes its density less than that of solubilized proteins, showing a high buoyancy in a sucrose gradient. Lipid rafts are also characterized by having low protein content (Cerneus *et al.*, 1993; Hanada *et al.*, 1995) and by the abundant presence of the alkaline phosphatase enzyme. Thus, the resulting fractions were biochemically characterized by quantitative analysis of phosphatase alkaline enzymatic activity, determination of the protein concentration and the use of lipid raft and non-raft markers. The higher level of alkaline phosphatase activity together with the lower protein content allowed us to define fractions 4 and 5 as fractions highly enriched in lipid rafts elements. This conclusion was confirmed studying the immunostaining of these fractions with specific antibodies designed against flotillin and Thy-1, proteins that are mainly located in lipid rafts. Furthermore, the antibody designed to detect the protein Na^+/K^+ATPase, which is located outside of these domains, was not detected in these two fractions. On the other hand, the absence of alkaline phosphatase activity and the presence of high protein concentration and intense immunolabelling for Na^+/K^+ATPase in fractions 8 -12 allowed us define this fractions as non-raft. Although we assumed that 4-5 fractions represent lipid raft enriched fractions, it is unlikely that these preparations reflects a native composition of lipid raft domains because the protein composition of lipid raft preparation varies with the used detergent, with its concentration and with the temperature used in the process (Mayor and Maxfield, 1995). Even so, this preparation provides us reliable information about the propensity of molecules that associate with lipid raft like domains.

We studied the presence of the CB1 receptor and Gαi/o protein subtypes in these subdomains of synaptic plasma membrane by Western blot method. We observed that the CB1 receptor is located both in lipid raft and non-raft compartments, with the possibility of interacting with different effectors of the canonical signalling pathway in both membrane compartments. Therefore, the CB1 receptor that resides in lipid rafts are in a strategic position to be regulated by lipids that constitute this domains, for example by cholesterol (The impact of cholesterol on the CB1 receptor is addressed in the next chapter of the discussion). Unexpectedly, immunoreactivity distribution profile of the

CB1 receptor differed using CB1-Rb-Af380 and CB1-Immunogenes antibodies. Whereas CB1-Rb-Af380 antibody recognized a CB1 receptor exclusively in the lipid raft fractions, the CB1-Immunogenes antibody recognized the receptor preferentially in non-raft fractions, indicating that some (or all) antibodies recognize only a partial pool of the total population of CB1 receptor. In addition, these two polyclonal anti CB1 antibodies are designed against the same last 30 amino acids of the mouse CB1 receptor, thus adding a further degree of complexity to the interpretation of these paradoxical results. Several phosphorylation sites exist at the carboxyl terminal of the CB1 receptor (Daigle, Kwok and Mackie, 2008; Straiker, Wager-Miller and Mackie, 2012) existing the possibility that phosphorylation of these residues could impact in the recognition of epitope by anti CB1 antibodies. This fact additionally with the idea that phosphorylation status of the CB1 receptor could differ between lipid raft and non-raft domains would account our data and would define these antibodies as tools for detecting different states and populations of the CB1 receptor.

ANALYSIS OF THE EXPRESSION AND Gαi/o COUPLING OF THE CB1 RECEPTOR LOCATED IN GLUTAMATERGIC AND GABAERGIC SYNAPTIC TERMINALS OF BRAIN FRONTAL CORTEX AND HIPPOCAMPUS OF ADULT MOUSE

In the cerebral cortex, the CB1 receptor is mainly located in most glutamatergic neurons at low levels and in many GABAergic neurons at high intensity. This implies that the activity balance of the principal excitatory and inhibitory neurons in cortical regions is modulated by the presynaptic CB1 receptor. Using mice lacking the CB1 receptor in forebrain GABAergic (GABA-CB1-KO; Monory *et al.*, 2006), or dorsal telencephalic glutamatergic (Glu-CB1-KO; Monory *et al.*, 2006) neurons and subsecuently trangenic "rescue" mice that express the CB1 receptor exclusively in dorsal telencephalic glutamatergic neurons (Glu-CB1-RS; Ruehle *et al.*, 2013) or in forebrain GABAergic interneurons (GABA-CB1-RS; Remmers *et al.*, 2017) have revealed that the CB1 receptor activities in these two neuronal populations modulate important physiological functions. For example, CB1 receptor on glutamatergic cells plays an important role in the control of neuroprotection (Monory *et al.*, 2006; Chiarlone *et al.*, 2014), olfactory processes (Soria-Gómez *et al.*, 2014), fear memories, stress and anxiety (Steiner *et al.*, 2008; Jacob *et al.*, 2009; Kamprath *et al.*, 2009; Dubreucq *et al.*, 2012; Metna-Laurent *et al.*, 2012; Rey *et al.*, 2012) and feeding behaviour (Lafenêtre, Chaouloff and Marsicano, 2007; Bellocchio *et al.*, 2010). Meanwhile, GABAergic CB1 modulates learning and memory processes (Puighermanal *et al.*, 2009; Albayram *et al.*, 2016), behaviours related with drug addiction (Talani and Lovinger, 2015; Martín-García *et al.*, 2016) and it also controls some behavioural responses in opposite way to glutamatergic CB1 modulation (Monory *et al.*, 2006; Dubreucq *et al.*, 2012). In fact, biphasic effects that produce cannabinoids drugs in food intake, in anxiety or in fear responses are explained by the differential activation of the CB1 receptor in these two neuronal phenotypes. The glutamatergic CB1 activation is responsible of behavioural responses that low doses of agonist produce whereas effect of higher doses of agonist is explained by GABAergic CB1 activation (Hao *et al.*, 2000; Bellocchio *et al.*, 2010; Metna-Laurent *et al.*, 2012; Rey *et al.*, 2012). This led to researches find the mechanistic explanation underlying a differential recruitment of CB1 receptors in this two cell types that account the biphasic effect of cannabinoids, which was given by (Steindel *et al.*, 2013).They evaluated glutamatergic and GABAergic CB1 coupling efficiency to Gαi/o proteins performing

[^{35}S]GTPγS binding assays in hippocampal homogenates of Glu-CB1-KO and GABA-CB1-KO mutant mice. Their data showed that although the level of CB1 receptor expressed in glutamatergic neurons is significantly lower than that expressed in GABAergic neuron, more than 50% of Gαi/o proteins we activated by glutamatergic CB1, while the CB1 receptor expressed in GABAergic neurons was responsible for the activation of 20-30% Gαi/o proteins. These results showed that in glutamatergic cells there is a more effective CB1 dependent Gαi/o protein signalling than in GABAergic cells, which may account why glutamatergic CB1 population responds to low doses of cannabinoids.

Biochemical and pharmacological characterization of CB1-RS

The impact that the cellular context exerts in the functionality of the CB1 receptor has been assumed that takes place in the presynaptic terminal. However, the [^{35}S]GTPγS binding assays were not performed in a preparation enriched in synaptosomes, but rather in hippocampal tissue homogenates. Accordingly, this selective signalling mechanism cannot be directly attributed to the presynaptic CB1 because the interference of signals from CB1 located in other subcellular compartments can affect the results. Therefore, to study the impact that cellular context produce in the presynaptic CB1 signalling, we performed Western blot and [^{35}S]GTPγS binding assays in hippocampal synaptosomes obtained from mice that express the CB1 receptor exclusively in dorsal telencephalic glutamatergic neurons (Glu-CB1-RS; Ruehle *et al.*, 2013) or in forebrain GABAergic neurons (GABA-CB1-RS; Remmers *et al.*, 2017). We also extended the study to the frontal cortex in order to assess whether cell type (glutamatergic vs GABAergic) specific differences in Gαi/o protein coupling occurs globally in the cerebral cortex.

GABA-CB1-RS and Glu-CB1-RS transgenic mouse models have been generated reactivating conditionally (GABA-CB1-RS and Glu-CB1-RS) the endogenous levels of CB1 receptor expression from a complete CB1-KO mice (Stop-CB1). The validity of the genetic approach was evaluated previously comparing CB1-RS mice and WT phenotypes in several biochemical and behavioural procedures, not observing differences between them (Ruehle *et al.*, 2013). For example, CB1-RS mice showed identical CB1 receptor expression in hippocampus and cannabinoid agonist binding in several brain regions by Western blot and receptor autoradiography, respectively. By immunogold electron

microscopy observations, the subcellular distribution of hippocampal CB1 receptors of Glu-CB1–RS GABA-CB1-RS show the usual CB1 receptor distribution and expression in hippocampal cell types (Gutiérrez-Rodríguez *et al.*, 2017). Here, we provided more data that complement the validation of the CB1-RS model, supporting the WT like phenotype of CB1-RS mice and the suitability of the genetic approach. Synaptosomes from CB1-RS mice were characterized for expression, subsynaptic distribution, lipid raft vs non-raft compartmentalization and functionality of the CB1 receptor, and we compared results with synaptosomes obtained from WT mice.

Our results indicated that CB1-RS mice are indistinguishable from the WT mice with respect to the expression level and subsynaptic and lipid raft vs non-raft partition of the CB1 receptor in frontal cortical synaptic terminals, which suggest that presynaptic CB1 receptor is restored at endogenous sites and levels using this genetic rescue methodology. However, in Western blot assays of hippocampal synaptosomes we detected a small difference in the immunoreactivity of the CB1 specie migrating at ~35 kDa between CB1-RS and WT mice, although the principal ~50 kDa band representing the CB1 receptor did not differ. We concluded the characterization of the CB1-RS mice studying the functional coupling of the CB1 receptor to Gαi/o in synaptosomes obtained from frontal cortex and hippocampus samples WT and CB1-RS mice by cannabinoid-stimulated [^{35}S]GTPγS binding assay.

[^{35}S]GTPγS binding assays

An agonist-stimulated binding of radioactive labelled GTP nucleotide analogue ([^{35}S]GTPγS) to Gα proteins measures receptor activation of Gαi/o protein (GDP/GTP turnover) following agonist initial binding. An agonist binding to receptor induces and stabilizes an active state of the CB1 receptor, which translocating in the cell membrane interacts with membrane associated heterotrimeric Gαi/o proteins. A formation of an agonist/receptor/G protein ternary complex induces a dissociation of the GDP nucleotide from α subunit of G protein complex and binding of GTP, producing a dissociation of the heterotrimeric Gαi/o protein in Gα and βy subunits. These subunits interact with effectors until an intrinsic GTPase activity of Gα subunit hydrolyse bound GTP in GDP and re-associates with a Gβy dimer, inactivating both subunits and closing the G protein cycle. Then, the heterotrimeric G protein is able to be activated again (Gilman, 1987). A GTP analogue is resistant to the hydrolysis of the GTPase activity of α subunit of G protein.

Therefore, the lifetime of the [^{35}S]GTPγS bound G protein complex is drastically increased, allowing to determine the agonist stimulation of [^{35}S]GTPγS binding to G protein (Strange, 2010). [^{35}S]GTPγS binding assay can be performed in membranes derived from native tissues for study the CB1 receptor (Dana E Selley *et al.*, 1996; Breivogel, Selley and Childers, 1998a). Membranes are mixed and incubated with [^{35}S]GTPγS and agonist at single time point (2 h in our protocol) and binding is determined detecting a radioactive signal by liquid scintillation counting after filtrating membranes on glass fibre filters to separate bound and free [^{35}S]GTPγS nucleotide.

We conducted some preliminary studies to determine optimal protein amount and [^{35}S]GTPγS and GDP concentrations to maximize the cannabinoid agonist-stimulated [^{35}S]GTPγS binding signal over basal signal. Working with very low amounts of protein allowed us to obtain a very high signal/ basal ratio in addition to a high reproducibility between experimental points. This is mainly due to in synaptosomal membranes the density of the CB1 receptor is high and it improves the sensitivity of assays. The presence of micromolar concentration of GDP and picomolar concentration of [^{35}S]GTPγS is required to detect agonist depending binding, respectively. This micromolar GDP supress basal binding of [^{35}S]GTPγS to non-heterotrimeric G proteins (Dana E. Selley *et al.*, 1996; Strange, 2010) and although GDP also binds to heterotrimeric Gαi/o protein an addition of agonist reduces the affinity of GDP and [^{35}S]GTPγS-G protein binding becomes apparent (Breivogel, Selley and Childers, 1998b).

Agonist concentration responses ([^{35}S]GTPγS-G protein binding) curves can be generated plotting response as a function of the logarithm of concentration of agonist and fitting experimental data by nonlinear regression to the four parameter Hill equation (see methods). Two principal pharmacological parameters can be obtain: the maximal agonist response (Emax) and the potency (EC50). The magnitude of the maximal asymptote is referred as a maximal agonist response (Emax) and reflects the efficacy of the agonist (magnitude of stimulus given to the receptor) and the efficiency of the biological system to convert the receptor stimulus in the observable response. The potency (EC50) is the molar concentration required to produce 50% of the maximal response to the agonist and it reflects the affinity and the efficacy of the agonist and also the efficiency of the amplification machinery necessary to convert the receptor stimulus in the observable response.

Cannabinoid agonist-stimulated [^{35}S]GTPγS binding assay showed us that the WT and CB1-RS mice do not differ in the efficiency of CB1 receptor coupling to Gαi/o proteins both in frontal cortical and in hippocampal synaptosomes. A higher basal [^{35}S]GTPγS binding was observed in CB1-RS than in WT mice in frontal cortex although it was not statistically significant. In some reports it has been suggested that CB1 signalling could contributed to basal [^{35}S]GTPγS binding in native membranes by its constitutive activity and/or by eCB mediated tonic signalling, because it has been shown that micromolar concentrations of SR141716 (inverse agonist of CB1 receptor) inhibits basal Gαi/o proteins signalling (Sim-Selley, Brunk and Selley, 2001; Mato, Pazos and Valdizán, 2002). However, Savinainen *et al.* (2003) elegantly demonstrated that CB1 is not tonically active in [^{35}S]GTPγS binding assays when native membranes are used, because CB1 receptor antagonist inhibit basal G-protein only when tonic adenosine A1 receptor signalling is not eliminated. Consistent with that data, our results show that a major eCB 2-AG tonic signalling does not impact in the basal [^{35}S]GTPγS binding during [^{35}S]GTPγS binding assay procedure, because pretreatment of synaptosomes with a DAGL inhibitor THL or MAGL inhibitor PMSF did not produce changes in basal [^{35}S]GTPγS binding. Therefore, differences observed in WT and CB1-RS basal [^{35}S]GTPγS binding values are not related to CB1 receptor mediated signalling and our results are not biased by this confusing variable.

Thus, besides to restore at endogenous sites and levels, the presynaptic CB1 receptor is fully capable to stimulate the canonical signalling in this rescue model. It can be then inferred that analysis of CB1 receptor expression, distribution, lipid raft vs non-raft partitioning and Gαi/o coupling in Glu-CB1-RS and GABA-CB1-RS mice are not biased by the set of genetic modifications that culminate in the rescue of the CB1 receptor, concluding that the selective rescue of the CB1 receptor in glutamatergic and/or GABAergic neurons are also produced satisfactorily.

Analysis of the CB1 receptor expression and coupling to Gαi/o proteins in frontal cortical and hippocampal synaptosomes obtained from Glu-CB1-RS, GABA-CB1-RS and CB1-RS

We performed Western blot and [^{35}S]GTPγS binding assays in Glu-CB1-RS, GABA-CB1-RS mice synaptosomes and dissected the CB1 receptor expression and canonical functional coupling to Gαi/o proteins in synaptic terminals belonging to the two major phenotypes of neurons. As expected, in both regions the CB1 signal was predominantly detected in glutamatergic and GABAergic phenotypic terminals. In frontal cortical synaptosomes about 45% of the CB1-RS signal was found in both partial rescue mice whereas the CB1 signal in hippocampal synaptosomes of Glu-CB1-RS and GABA-CB1-RS mice was about 28% and 70% of the signal found in CB1-RS, respectively. Thus, in frontal cortical synaptosomes both glutamatergic and GABAergic CB1 populations contribute equally to the total CB1 signal whereas in the hippocampal synaptosomes GABAergic CB1 contributes more than twice to the total CB1 signal compared with glutamatergic CB1s. Nevertheless, anatomical studies have shown that CB1 receptor density in GABAergic terminals is considerably higher than in glutamatergic terminals in almost all cortical areas (Marsicano and Lutz, 1999; Katona *et al.*, 2006; Kawamura *et al.*, 2006; Monory *et al.*, 2006). For example (Kawamura *et al.*, 2006) determined that the density of CB1 receptor in inhibitory terminals in the hippocampus is about 10- 20 higher than in excitatory terminals. Pyramidal cells and GABAergic interneurons are the principal neurons of the cerebral cortex constituting ~80% and ~20% of the total number of neurons, respectively (Kawaguchi and Kubota, 1997; Marín, 2012). Therefore, the fact that excitatory terminals predominate over the inhibitory ones in cerebral cortex and that significant number of glutamatergic neurons and discrete population of GABAergic neurons (Mailleux and Vanderhaeghen, 1992b; Matsuda, Bonner and Lolait, 1993; Marsicano and Lutz, 1999; Tsou *et al.*, 1999; Katona *et al.*, 2006; Uchigashima *et al.*, 2011) express CB1 receptors explains differences observed in the relative expression (glutamatergic vs GABAergic CB1 receptor expression) between our Western blot assay and electron microscopy assays. Several other neurotransmitter systems that innervate both regions such as cholinergic, serotonergic and noradrenergic neurons can also express CB1 receptors (Nyıri et al.2005, Haring et al.2007, scavone et al., 2010). Neverthelles, a very small proportion of the total CB1 is represented by these other cell populations, since the sum of glutamatergic and GABAergic immunoreactivity in frontal cortical and

hippocampal synaptosomes was found to be around the 90% and 100% of the total signal of the CB1 in those areas, respectively.

Cannabinoid agonist-stimulated [^{35}S]GTPγS binding assays in Glu-CB1 and GABA-CB1 rescue mice clearly showed that the maximal response (Emax) correlates with the abundance of CB1 receptors both in frontal cortex and in hippocampus, irrespectively to the synaptic type (glutamatergic or GABAergic) context. In this way, since the contribution of glutamatergic and GABAergic CB1 to the total CB1 population is equal in cortical synaptosomes, we observed that the same level of Gαi/o protein activation was mediated by these two CB1 populations. Meanwhile, in hippocampal synaptosomes where 28% of the signal expressed in CB1-RS was found in Glu-CB1-RS and 70% in GABA-CB1-RS mice, GABAergic CB1 was responsible for considerably more Gαi/o proteins activation. All three phenotypes showed a similar potency for CB1 activation in both regions, with no significant differences between them. A similar correlation between CB1 dependent Gαi/o protein signalling and the expression of the CB1 receptor was also observed when cortical and hippocampal synaptosomes were compared. Thus, the expression of the CB1 receptor and CB1 dependent Gαi/o coupling was systematically higher in hippocampal synaptosomes than in frontal cortical synaptosome samples (both in WT and in rescue mice). Our results are in line with some previous observations in a far removed cell response from the CB1 receptor activation. Ohno-Shosaku *et al.* (2002) reported that in hippocampal slices depolarization induce suppression of excitation (DSE) is less prominent than depolarization induce suppression of inhibition (DSI) and requires longer depolarizations for its induction. Additionally, glutamatergic neurons display less prominent and 30 fold lower potency in cannabinoid induced suppression of inhibitory or excitatory postsynaptic current (IPSC and EPSC) amplitude with respect to GABAergic neurons. This results clearly indicate that cannabinoid sensitivity is lower in glutamatergic neurons than in GABAergic neurons. Taking all the data together, there is enough evidence to state that the receptor density in glutamatergic and in GABAergic terminals is one means by which the neuron controls the magnitude of responses to eCBs.

Our data initially disagree with results reported by Steindel *et al.* (2013), who concluded that more effective CB1 dependent Gαi/o protein signalling occurs in glutamatergic neurons than in GABAergic neurons. Although their Western blot data showed that the level of CB1 receptor expressed in glutamatergic neurons was significantly lower than that expressed in GABAergic neurons, in [^{35}S]GTPγS binding assays more than 50% of

Gαi/o proteins were activated by glutamatergic CB1, while the CB1 receptor expressed in GABAergic neurons was responsible for the activation of 20-30% Gαi/o proteins. This discrepancy could be explained by the fact the [^{35}S]GTPγS binding assays of Glu-CB1-KO and GABA-CB1-KO mutant mice were not performed in synaptosomes, but rather in hippocampal tissue homogenates. As mentioned previously, most recent works have demonstrated the presence of functional CB1 receptor also in other cell types or subcellular compartments such as in in astrogia (Rodríguez, Mackie and Pickel, 2001; Han *et al.*, 2012; Ilyasov *et al.*, 2018), in somatodendritic postsynaptic membrane (Ong and MacKie, 1999; Bacci, Huguenard and Prince, 2004; Pickel *et al.*, 2004; Marinelli *et al.*, 2009; Thibault *et al.*, 2013; Maroso *et al.*, 2016) and in intracellular organelles such as in mitochondria (Bénard *et al.*, 2012; Hebert-Chatelain *et al.*, 2014), in endosomes or in lisosomes. Because tissue homogenates preparations barely discriminate CB1 signals originating from diverse subcellular organelles, these interferences could differentially impact in the glutamatergic and GABAergic maximal response determined in [^{35}S]GTPγS binding, making experimental results to be interpreted differently.

ANALYSIS OF THE IMPACT OF CHOLESTEROL IN THE Gαi/o COUPLING OF THE CB1 RECEPTOR LOCATED IN SYNAPTIC TERMINALS OF BRAIN FRONTAL CORTEX OF ADULT RAT

Recent works have showed that membrane lipids modulate ligand binding and functional properties of 7TM receptors (Bari, Battista, *et al.*, 2005; Bari, Paradisi, *et al.*, 2005; Oates and Watts, 2011). Among different lipids cholesterol is one that receives most attention. It has been reported that cholesterol negatively regulates the CB1 receptor signalling. In fact, reducing cholesterol membrane levels increases the maximal binding and agonist-stimulated [^{35}S]GTPγS binding efficacy of the cannabinoid agonist CP 55,940. (Bari, Battista, *et al.*, 2005; Bari, Paradisi, *et al.*, 2005). Studies examining the crystalline structure of the CB1 receptor have confirmed that cholesterol interacts in the cholesterol consensus motif domain (CCM) of the receptor (Hua *et al.*, 2017, 2020) suggesting a potential allosteric role of this lipid. Additionally, CRAC (cholesterol recognition amino acid consensus) domain is other potential interaction site identified in the amino acid sequence of the CB1 receptor (Oddi *et al.*, 2011; Sabatucci *et al.*, 2018) and the possibility of cholesterol competing with orthosteric ligand cannot rule out (Guixà-González *et al.*, 2017). As mentioned previously, lipid rafts are formed and enriched in particular by cholesterol and saturated phospholipid and sphingolipid compounds. These membrane domains are considered to be transduction signal regulation platforms that ensure that interactions between receptors and their signalling proteins are carried out efficiently (Hancock, 2006; Pike, 2006). Our data indicate that presynaptic CB1 receptor resides in lipid rafts, suggesting that it is located in a strategic position to be regulated by cholesterol. The most common compound that efficiently extracts cholesterol from membranes is MβCD (Mahammad and Parmryd, 2015). As cholesterol is enriched in lipid rafts, MβCD is also considered as a lipid raft-disrupting agent and it is used to study lipid rafts physiological functions (Sezgin *et al.*, 2017).

In our experiments, the incubation of rat brain cortical synapotosomes with 20 mM MβCD did not disrupt lipid-raft microdomains. In fact, the density differences that are used to separate lipid raft and non-raft fractions by ultracentrifugation in sucrose gradient after the treatment of membranes with TX-100 non-ionic detergent remained unaltered. Thus, our results indicate that MβCD treatment extracts the cholesterol from lipid raft fractions without greatly affecting the physicochemical properties that characterize these microdomains. Cholesterol has been proposed as a key element for CB1 receptor

trafficking to the plasma membrane and it´s retention in lipid raft microdomains (Stornaiuolo *et al.*, 2015). However, our results suggest that the functional consequences of cholesterol depletion are not related to alterations in the CB1 receptor location, but rather with allosteric modulations derived from their molecular interaction.

Effect of cholesterol depletion on CB1R expression in rat cortical synaptosomes

To study whether the presynaptic CB1 receptor is under regulatory control of membrane cholesterol, we treated cortical synaptosomes with 20 mM of MβCD and subsequently control and cholesterol depleted membranes were used in cannabinoid agonist-stimulated [^{35}S]GTPγS binding assays. Our results showed that cholesterol depletion from synaptosomal membranes produced an increase in the efficacy of all tested cannabinoids, although this increase was not equal for the three cannabinoids. We observed greater increase in the efficacy of methanandamide, followed by CP 55,940 and WIN 55,212-2. In addition, reduction in the cholesterol content also produced an increase in the potency of CP 55,940 and methanandamide.

Then, we carried out [^{35}S]GTPγS assays binding assays for all three cannabinoids simultaneously to show the change that cholesterol depletion produces in the pharmacological profile of cannabinoid compounds. In a control situation, the ligand WIN 55,212-2 behaves as a total agonist, while CP 55,940 and methanandamide behaves as a high and low efficacy partial agonist with respect to WIN 55,212-2. However, in cholesterol-depleted synaptosomes, although WIN 55,212-2 continues showing a maximal efficacy between the three agonists, methanandamide and CP 55,940 behave as a high partial agonists without significant differences between them. Thus, the ability of cholesterol to impact the CB1 receptor depends on the intrinsic activity of the agonist studied, which is consistent with the allosteric modulation suggested for cholesterol and "probe dependence" properties of allosteric ligands (Kenakin, 2002). Results obtained from western blot assays performed in control and in MβCD treated synaptosomes also ensured that MβCD treatment does not alter the density of CB1 receptor in synaptosomes, supporting that cholesterol regulates the functionality of the CB1 receptor probably through an allosteric mechanism.

Effect of cholesterol depletion on the [^{35}S]GTPγS basal binding

In addition to the increase in cannabinoid agonists efficacy, MβCD treatment induced a significant reduction of basal [^{35}S]GTPγS binding. To study the [^{35}S]GTPγS binding properties, competitive binding assays with unlabelled GTPyS against [^{35}S]GTPγS were performed. Competition assays where the labelled and unlabelled ligands are the same represent an alternative approach to saturation experiments to obtain apparent Bmax and KD values. Anyway, when these experiments are performed in native membranes it cannot be excluded the presence of pre-bound GDP, and all parameters should be considered "apparent", regardless of the presence or absence of added GDP. The results obtained in these experiments revealed that MβCD treatment induced a reduction (37%) in the [^{35}S]GTPγS binding sites together with an small but significant increase in [^{35}S]GTPγS affinity for the remaining sites. The reduction in the apparent Bmax for [^{35}S]GTPγS could explain the reduction in basal [^{35}S]GTPγS binding systematically observed when agonist-stimulated [^{35}S]GTPγS binding curves are performed in MβCD treated synaptosomes. In these experiments the concentration of [^{35}S]GTPγS (0.5 nM) was the same as that used in agonist-stimulated [^{35}S]GTPγS binding assays. When saturation binding assays of [^{35}S]GTPγS have been performed in rat brain membranes biphasic curves have been described, demonstrating the presence of both high and low affinity sites (Breivogel, Selley and Childers, 1998a). Thus, the concentration (0.5 nM) used in our experiments was only able to define the high affinity [^{35}S]GTPγS binding sites. Therefore, our results do not necessarily indicate a reduction in G-protein expression level, but rather a decrease in the population of sites that recognize the [^{35}S]GTPγS with high affinity. Also, taking into account that high affinity sites described for [^{35}S]GTPγS binding represents less than 10% of the total population (Breivogel, Selley and Childers, 1998b), the loss of 37% of sites of such a minority population could be difficult to detect through western blot techniques.

Effect of cholesterol depletion on the modulatory actions of GDP in the agonist-stimulated [^{35}S]GTPγS binding

Attending to the G-protein activation cycle, the activation of a G-protein coupled receptor by an agonist leads to the dissociation of heterotrimeric G- proteins into α subunits and βγ dimers. In this process, the GDP bound to the α subunit (Gα) is released, and a molecule of GTP is bound, leading to the dissociation of the heterotrimer, and activation of different effectors by Gα and βγ subunits. The cycle is completed when the intrinsic GTPase activity of Gα subunits cleaves the bound GTP to GDP, and Gα re-associates with a βγ dimer (Gilman, 1987; Birnbaumer, 1992). After agonist activation GPCRs would act by catalysing the exchange reaction of GDP for GTP in Gα subunits, activating multiple G-proteins. In this context, agonist-stimulated binding of the hydrolysis resistant GTP analog, [^{35}S]GTPγS, represent a useful and widespread technique for GPCR activation studies.

According to these previous considerations, GDP would play a key role in the agonist-stimulated [^{35}S]GTPγS binding assays. The release of GDP from Gα subunits is a key step for [^{35}S]GTPγS binding to occur. In agreement with previously published evidences (Hilf, Gierschik and Jakobs, 1989), under our experimental conditions, which include 3 mM Mg^{2+}, [^{35}S]GTPγS binding was dissociable, as demonstrated by the displacement of [^{35}S]GTPγS binding in the presence of increasing concentrations of GDP. Under these conditions, we decided to carry out competitive binding assays of GDP against [^{35}S]GTPγS in basal and WIN 55,212-2-stimulated conditions, and in both control and MβCD treated synaptosomes. The aim of these experiments was to determine whether the increase in cannabinoid agonist efficacy induced by MβCD treatment was related to modulations in GDP binding properties. In this regard, the efficacy of cannabinoid agonist for stimulating the [^{35}S]GTPγS to rat cerebellar membranes has been correlated to their ability to decrease GDP affinity (Breivogel, Selley and Childers, 1998b).

Our results show that the addition of 3 μM WIN 55,212-2 did not change basal [^{35}S]GTPγS binding in the absence of GDP. This result is in line with previous evidences demonstrating that the use of high concentrations of GDP is necessary to observe agonist effects (Hilf, Gierschik and Jakobs, 1989; Traynor and Nahorski, 1995). Furthermore, the competition curves for GDP were biphasic, indicating that GDP is able to distinguish two different sub-populations of sites within the high affinity population for [^{35}S]GTPγS

binding. Again, in line with previous studies (Breivogel, Selley and Childers, 1998b), the presence of agonist (3 μM WIN 55,212-2) induce a slight shift to the right of the low affinity component for GDP, suggesting that agonist effect could be related to a decrease in GDP affinity. The treatment of synaptosomes with MβCD induced a slight (but no significant) increase in GDP affinity for both high and low components. Although no significant, this slight increase in GDP affinity could contribute to the reduction in basal [^{35}S]GTPγS binding observed in MβCD treated synaptosomes. However, in our experiments no differences in the agonist ability for modulating the GDP binding were observed between control and MβCD treated synaptosomes. Overall our results suggest that the effect of MβCD treatment on agonist efficacy could be more related to the increase in [^{35}S]GTPγS binding affinity than to the decrease of GDP affinity, although the slight increase in GDP affinity contribution to the increase in agonist efficacy by reducing the basal [^{35}S]GTPγS binding cannot be ruled out.

Analysis of the CB1 receptor coupling to Gαi/o proteins in control and cholesterol depleted frontal cortical synaptosomes of Glu-CB1-RS, GABA-CB1-RS and CB1-RS mice

Finally, we used Glu-CB1-RS and GABA-CB1-RS mice to check if the negative regulation exerted by cholesterol is dependent on the synaptosome type (glutamatergic or GABAergic) where the CB1 receptor is located. As expected, cholesterol depletion by MβCD increased CP 55,940 and WIN 55,212-2-stimulated [^{35}S]GTPγS binding efficacy and we did not observe changes in the EC50 parameter. The increase in the efficacy of agonist induced by MβCD treatment was not affected by synaptosome type, showing that the negative regulation exerted by cholesterol affects CB1 receptor coupling irrespectively of its location in glutamatergic or GABAergic terminals.

VII. CONCLUSIONS

The conclusions drawn from the biochemical and pharmacological characterization of the CB1 receptor in the cell-type cell-type-specific mutant mouse rescue model (CB1-RS) are:

1. CB1-Immunogenes, CB1-Go-Af350 and CB1-Rb-Af380 antibodies, all raised against the 31 amino acids of the extreme carboxyl terminus of the mouse CB1 receptor, detect a glycosylated CB1 receptor specific band migrating at ∼50 kDa and additional CB1 specific band migrating at ∼35 kDa in mouse cortical synaptosomes. In our experimental conditions, CB1-Immunogenes displays the highest sensitivity to detect both species together, being the antibody of choice to study the CB1 receptor expression by Western blot.

2. The method of solubilization of subsynaptic fractions from cortical synaptosomes (Phillips *et al.*, 2001) have allowed us to explore the subsynaptic CB1 receptor distribution by western blot analysis with a higher sensitivity that the previously published with the classical immunogold electron microscopy.

3. The total amount of synaptic CB1 receptor immunoreactivity from the initial fraction (cortical synaptosomal membranes) was mostly found in the extrasynaptic fraction (90%) of potential presynaptic and postsynaptic sides. However, we found a nearly 2.5% of the synaptic CB1 receptors in the presynaptic active zone, and nearly 7.5% of them in the postsynaptic density.

4. We also provide biochemical evidences that show for the first time the association of CB1 receptors and Gαi/o proteins with lipid rafts isolated from mouse cortical synaptosomes. Moreover, a qualitative analysis shows that the CB1 receptor partitioning between lipid raft/non-raft membrane microdomains was not disturbed by MβCD, a reagent widely used to selectively extract cholesterol from membranes.

5. From our analysis in cortical synaptosomal membranes, it can be inferred that the subsynaptic distribution (pre-, post- and extrasynaptic), the lipid raft vs non-raft partitioning of the CB1 receptor, and its functional coupling Gαi/o coupling are not biased by the set of genetic modifications that culminate in the total rescue of the CB1 receptor.

6. The canonical Gαi/o protein-dependent CB1 receptor signalling, as defined by the agonist-stimulated [^{35}S]GTPγS binding assay, is positively correlated with the abundance of CB1 receptors both in frontal cortical and hippocampal synaptosomes, irrespectively to the cell type (glutamatergic or GABAergic neurons) context from which it signals.

7. Pretreatment of cortical synaptosomal membranes from Glu-CB1-RS and GABA-CB1-RS with MβCD increase mostly the agonist-stimulated [^{35}S]GTPγS binding efficacy (Emax) of the two full agonists tested, and again the results obtained in Glu-CB1-RS were indistinguishable from the GABA-CB1-RS mice.

8. In rat cortical synaptosomal membranes, where it was possible to determine in parallel the membrane cholesterol depletion, the MβCD treatment increased agonist-stimulated [^{35}S]GTPγS binding efficacy (Emax), being the impact more pronounced on partial than on full efficacy agonists.

9. The reduction in basal [^{35}S]GTPγS binding observed in MβCD treated synaptosomes in agonist-stimulated [^{35}S]GTPγS binding assays could be explained by the reduction in the apparent Bmax for [^{35}S]GTPγS.

10. Altogether, our results enlighten a scenario where cholesterol, as expected for a negative allosteric modulator, impose specific CB1 receptor conformations that show one of the most important features of allostery, the probe dependence. In other words, cholesterol shows a more robust negative effect depending on the orthosteric ligand used as a probe of receptor activity.

VIII. REFERENCES

Abood, M. E. et al. (1997) 'Isolation and expression of a mouse CB1 cannabinoid receptor gene. Comparison of binding properties with those of native CB1 receptors in mouse brain and N18TG2 neuroblastoma cells', Biochemical Pharmacology, 53(2), pp. 207–214. doi: 10.1016/S0006-2952(96)00727-7.

Aguado, T. et al. (2005) 'The endocannabinoid system drives neural progenitor proliferation', The FASEB Journal, 19(12), pp. 1704–1706. doi: 10.1096/fj.05-3995fje.

Aguado, T. et al. (2006) 'The endocannabinoid system promotes astroglial differentiation by acting on neural progenitor cells', Journal of Neuroscience, 26(5), pp. 1551–1561. doi: 10.1523/JNEUROSCI.3101-05.2006.

Ahmed, M. H. et al. (2014) 'Predicting the molecular interactions of CRIP1a-cannabinoid 1 receptor with integrated molecular modeling approaches', Bioorganic and Medicinal Chemistry Letters. Elsevier Ltd, 24(4), pp. 1158–1165. doi: 10.1016/j.bmcl.2013.12.119.

Ahn, K. H. et al. (2013) 'Distinct roles of β-arrestin 1 and β-arrestin 2 in ORG27569-induced biased signaling and internalization of the cannabinoid receptor 1 (CB1)', Journal of Biological Chemistry, 288(14), pp. 9790–9800. doi: 10.1074/jbc.M112.438804.

Ahn, K. H., Mahmoud, M. M. and Kendall, D. A. (2012) 'Allosteric modulator ORG27569 induces CB1 cannabinoid receptor high affinity agonist binding state, receptor internalization, and Gi protein-independent ERK1/2 kinase activation', Journal of Biological Chemistry, 287(15), pp. 12070–12082. doi: 10.1074/jbc.M111.316463.

Al-Zoubi, R., Morales, P. and Reggio, P. H. (2019) 'Structural insights into cb1 receptor biased signaling', International Journal of Molecular Sciences, 20(8). doi: 10.3390/ijms20081837.

Albayram, Ö. et al. (2016) 'Physiological impact of CB1 receptor expression by hippocampal GABAergic interneurons', Pflugers Archiv European Journal of Physiology, 468(4), pp. 727–737. doi: 10.1007/s00424-015-1782-5.

Alger, B. E. and Kim, J. (2011) 'Supply and demand for endocannabinoids', Trends in Neurosciences. Elsevier Ltd, 34(6), pp. 304–315. doi: 10.1016/j.tins.2011.03.003.

Andersson, H. et al. (2003) 'Membrane assembly of the cannabinoid receptor 1: Impact of a long N-terminal tail', Molecular Pharmacology. doi: 10.1124/mol.64.3.570.

Asimaki, O. et al. (2011) 'Cannabinoid 1 receptor-dependent transactivation of fibroblast

growth factor receptor 1 emanates from lipid rafts and amplifies extracellular signal-regulated kinase 1/2 activation in embryonic cortical neurons', Journal of Neurochemistry, 116(5), pp. 866–873. doi: 10.1111/j.1471-4159.2010.07030.x.

Bacci, A., Huguenard, J. R. and Prince, D. A. (2004) 'Long-lasting self-inhibition of neocortical interneurons mediated by endocannabinoids', Nature, 431(7006), pp. 312–316. doi: 10.1038/nature02913.

Bagher, A. M. et al. (2013) 'Co-expression of the human cannabinoid receptor coding region splice variants (hCB1) affects the function of hCB1 receptor complexes', European Journal of Pharmacology, 721(1–3), pp. 341–354. doi: 10.1016/j.ejphar.2013.09.002.

Baillie, G. L. et al. (2013) 'CB1 receptor allosteric modulators display both agonist and signaling pathway specificity', Molecular Pharmacology, 83(2), pp. 322–338. doi: 10.1124/mol.112.080879.

Bakshi, K., Mercier, R. W. and Pavlopoulos, S. (2007) 'Interaction of a fragment of the cannabinoid CB1 receptor C-terminus with arrestin-2', FEBS Letters, 581(25), pp. 5009–5016. doi: 10.1016/j.febslet.2007.09.030.

Bari, M., Paradisi, A., et al. (2005) 'Cholesterol-dependent modulation of type 1 cannabinoid receptors in nerve cells', Journal of Neuroscience Research, 81(2), pp. 275–283. doi: 10.1002/jnr.20546.

Bari, M., Battista, N., et al. (2005) 'Lipid Rafts Control Signaling of Type-1 Cannabinoid Receptors in neuronal Cells', The Journal of Biological Chemistry, 280(13), pp. 12212–12220. doi: 10.1074/jbc.M411642200.

Bellocchio, L. et al. (2010) 'Bimodal control of stimulated food intake by the endocannabinoid system', Nature Neuroscience. Nature Publishing Group, 13(3), pp. 281–283. doi: 10.1038/nn.2494.

Bénard, G. et al. (2012) 'Mitochondrial CB 1 receptors regulate neuronal energy metabolism (Nature Neuroscience', Nature Neuroscience, 15(4), p. 567. doi: 10.1038/nn.3053.

Birnbaumer, L. (1992) 'Receptor-to-effector signaling through G proteins: Roles for βγ dimers as well as α subunits', Cell, 71(7), pp. 1069–1072. doi: 10.1016/S0092-

8674(05)80056-X.

Bisogno, T. et al. (2003) ‘Cloning of the first sn1-DAG lipases points to the spatial and temporal regulation of endocannabinoid signaling in the brain’, Journal of Cell Biology, 163(3), pp. 463–468. doi: 10.1083/jcb.200305129.

Blankman, J. L., Simon, G. M. and Cravatt, B. F. (2007) ‘A Comprehensive Profile of Brain Enzymes that Hydrolyze the Endocannabinoid 2-Arachidonoylglycerol’, Chemistry and Biology, 14(12), pp. 1347–1356. doi: 10.1016/j.chembiol.2007.11.006.

Blume, L. C. et al. (2017) ‘Cannabinoid receptor interacting protein 1a competition with β-arrestin for CB1 receptor binding sites’, Molecular Pharmacology, 91(2), pp. 75–86. doi: 10.1124/mol.116.104638.

Bodor, Á. L. et al. (2005) ‘Endocannabinoid signaling in rat somatosensory cortex: Laminar differences and involvement of specific interneuron types’, Journal of Neuroscience, 25(29), pp. 6845–6856. doi: 10.1523/JNEUROSCI.0442-05.2005.

Brailoiu, G. C. et al. (2011) ‘Intracellular cannabinoid type 1 (CB1) receptors are activated by anandamide’, Journal of Biological Chemistry. Â© 2011 ASBMB. Currently published by Elsevier Inc; originally published by American Society for Biochemistry and Molecular Biology., 286(33), pp. 29166–29174. doi: 10.1074/jbc.M110.217463.

Breivogel, C. S., Selley, D. E. and Childers, S. R. (1998a) ‘Cannabinoid receptor agonist efficacy for stimulating [35S]GTPγS binding to rat cerebellar membranes correlates with agonist-induced decreases in GDP affinity’, Journal of Biological Chemistry. Â© 1998 ASBMB. Currently published by Elsevier Inc; originally published by American Society for Biochemistry and Molecular Biology., 273(27), pp. 16865–16873. doi: 10.1074/jbc.273.27.16865.

Breivogel, C. S., Selley, D. E. and Childers, S. R. (1998b) ‘Cannabinoid receptor agonist efficacy for stimulating [35S]GTPγS binding to rat cerebellar membranes correlates with agonist-induced decreases in GDP affinity’, Journal of Biological Chemistry. doi: 10.1074/jbc.273.27.16865.

Breivogel, C. S., Sim, L. J. and Childers, S. R. (1997) ‘Regional differences in cannabinoid receptor/G-protein coupling in rat brain’, Journal of Pharmacology and Experimental Therapeutics, 282(3), pp. 1632–1642.

Broyd, S. J. et al. (2016) ‘Acute and chronic effects of cannabinoids on human cognition - A systematic review’, Biological Psychiatry. Elsevier, 79(7), pp. 557–567. doi: 10.1016/j.biopsych.2015.12.002.

Busquets-Garcia, A. et al. (2015a) ‘Dissecting the cannabinergic control of behavior: The where matters’, BioEssays, 37(11), pp. 1215–1225. doi: 10.1002/bies.201500046.

Busquets-Garcia, A. et al. (2015b) ‘Dissecting the cannabinergic control of behavior: The where matters’, BioEssays, 37(11), pp. 1215–1225. doi: 10.1002/bies.201500046.

Busquets-Garcia, A., Bains, J. and Marsicano, G. (2018) ‘CB 1 Receptor Signaling in the Brain: Extracting Specificity from Ubiquity’, Neuropsychopharmacology. Nature Publishing Group, 43(1), pp. 4–20. doi: 10.1038/npp.2017.206.

Castillo, P. E. et al. (2012) ‘Endocannabinoid Signaling and Synaptic Function’, Neuron, 76(1), pp. 70–81. doi: 10.1016/j.neuron.2012.09.020.

Cerneus, D. P. et al. (1993) ‘Detergent insolubility of alkaline phosphatase during biosynthetic transport and endocytosis. Role of cholesterol’, Journal of Biological Chemistry. doi: 10.1016/s0021-9258(18)53671-1.

Chakrabarti, A., Onaivi, E. S. and Chaudhuri, G. (1995) ‘Cloning and sequencing of a cDNA encoding the mouse brain-type cannabinoid receptor protein’, Mitochondrial DNA, 5(6), pp. 385–388. doi: 10.3109/10425179509020870.

Chevaleyre, V., Takahashi, Kanji A and Castillo, P. E. (2006) ‘Endocannabinoid-mediated synaptic plasticity in the CNS’, Annual Review of Neuroscience, pp. 37–76. doi: 10.1146/annurev.neuro.29.051605.112834.

Chevaleyre, V., Takahashi, Kanji A. and Castillo, P. E. (2006) ‘Endocannabinoid-mediated synaptic plasticity in the CNS’, Annual Review of Neuroscience, 29, pp. 37–76. doi: 10.1146/annurev.neuro.29.051605.112834.

Chiarlone, A. et al. (2014) ‘A restricted population of CB1 cannabinoid receptors with neuroprotective activity’, Proceedings of the National Academy of Sciences of the United States of America, 111(22), pp. 8257–8262. doi: 10.1073/pnas.1400988111.

Chicca, A. et al. (2017) ‘Chemical probes to potently and selectively inhibit endocannabinoid cellular reuptake’, Proceedings of the National Academy of Sciences of the United States of America, 114(25), pp. E5006–E5015. doi:

10.1073/pnas.1704065114.

Christensen, R. et al. (2007) ‘Efficacy and safety of the weight-loss drug rimonabant: a meta-analysis of randomised trials’, Lancet, 370(9600), pp. 1706–1713. doi: 10.1016/S0140-6736(07)61721-8.

Cotman, C. W. and Matthews, D. A. (1971) ‘Synaptic plasma membranes from rat brain synaptosomes: Isolation and partial characterization’, BBA - Biomembranes, 249(2), pp. 380–394. doi: 10.1016/0005-2736(71)90117-9.

Coutts, A. A. et al. (2001) ‘Agonist-induced internalization and trafficking of cannabinoid CB1 receptors in hippocampal neurons’, Journal of Neuroscience, 21(7), pp. 2425–2433. doi: 10.1523/jneurosci.21-07-02425.2001.

Cravatt, B. F. et al. (1996) ‘Molecular characterization of an enzyme that degrades neuromodulatory fatty-acid amides’, Nature, 384(6604), pp. 83–87. doi: 10.1038/384083a0.

Cristino, L., Bisogno, T. and Di Marzo, V. (2020) ‘Cannabinoids and the expanded endocannabinoid system in neurological disorders’, Nature Reviews Neurology. Springer US, 16(1), pp. 9–29. doi: 10.1038/s41582-019-0284-z.

Daigle, T. L., Kwok, M. L. and Mackie, K. (2008) ‘Regulation of CB1 cannabinoid receptor internalization by a promiscuous phosphorylation-dependent mechanism’, Journal of Neurochemistry. doi: 10.1111/j.1471-4159.2008.05336.x.

Dainese, E. et al. (2007) ‘Modulation of the Endocannabinoid System by Lipid Rafts’, Current Medicinal Chemistry, 14(25), pp. 2702–2715. doi: 10.2174/092986707782023235.

Delgado-Peraza, F. et al. (2016) ‘Erratum: Mechanisms of biased β-arrestin-mediated signaling downstream from the cannabinoid 1 receptor (Molecular Pharmacology (2016) 89 (618-629))’, Molecular Pharmacology, p. 62. doi: 10.1124/mol.115.103176err.

Devane, W. A. et al. (1988) ‘Determination and characterization of a cannabinoid receptor in rat brain’, Molecular Pharmacology, 34(5), pp. 605–613.

Devane, W. A. et al. (1992) ‘Isolation and structure of a brain constituent that binds to the cannabinoid receptor’, Science, 258(5090), pp. 1946–1949.

Díaz, Ó., Dalton, J. A. R. and Giraldo, J. (2019) 'Revealing the Mechanism of Agonist-Mediated Cannabinoid Receptor 1 (CB1) Activation and Phospholipid-Mediated Allosteric Modulation', Journal of Medicinal Chemistry, 62(11), pp. 5638–5654. doi: 10.1021/acs.jmedchem.9b00612.

Dodd, P. R. et al. (1981) 'A rapid method for preparing synaptosomes: Comparison, with alternative procedures', Brain Research, 226(1–2), pp. 107–118. doi: 10.1016/0006-8993(81)91086-6.

Dove Pettit, D. A. et al. (1998) 'Immunohistochemical localization of the neural cannabinoid receptor in rat brain', Journal of Neuroscience Research, 51(3), pp. 391–402. doi: 10.1002/(SICI)1097-4547(19980201)51:3<391::AID-JNR12>3.0.CO;2-A.

Dubreucq, S. et al. (2012) 'Genetic dissection of the role of cannabinoid type-1 receptors in the emotional consequences of repeated social stress in mice', Neuropsychopharmacology, 37(8), pp. 1885–1900. doi: 10.1038/npp.2012.36.

Dudok, B. et al. (2015) 'Cell-specific STORM super-resolution imaging reveals nanoscale organization of cannabinoid signaling', Nature Neuroscience, 18(1), pp. 75–86. doi: 10.1038/nn.3892.

Dunkley, P. R. et al. (1986) 'A rapid method for isolation of synaptosomes on Percoll gradients', Brain Research, 372(1), pp. 115–129. doi: 10.1016/0006-8993(86)91464-2.

Durdagi, S. et al. (2010) 'A computational study on cannabinoid receptors and potent bioactive cannabinoid ligands: Homology modeling, docking, de novo drug design and molecular dynamics analysis', Molecular Diversity, 14(2), pp. 257–276. doi: 10.1007/s11030-009-9166-4.

Egertová, M. and Elphick, M. R. (2000) 'Localisation of cannabinoid receptors in the rat brain using antibodies to the intracellular C-terminal tail of CB1', Journal of Comparative Neurology, 422(2), pp. 159–171. doi: 10.1002/(SICI)1096-9861(20000626)422:2<159::AID-CNE1>3.0.CO;2-1.

Elphick, M. R. and Egertova, M. (2001) 'The neurobiology and evolution of cannabinoid signalling', Philos Trans R Soc Lond B Biol Sc, 356(1407), pp. 381–408. doi: 10.1098/rstb.2000.0787.

Esteban, P. F. et al. (2020) 'Revisiting CB 1 cannabinoid receptor detection and the

exploration of its interacting partners', Journal of Neuroscience Methods. Elsevier, 337(March), p. 108680. doi: 10.1016/j.jneumeth.2020.108680.

Farrens, D. L. et al. (1996) 'Requirement of rigid-body motion of transmembrane helices for light activation of rhodopsin', Science, 274(5288), pp. 768–770. doi: 10.1126/science.274.5288.768.

Fernández-Ruiz, J. et al. (2020) 'Possible therapeutic applications of cannabis in the neuropsychopharmacology field', European Neuropsychopharmacology, 36, pp. 217–234. doi: 10.1016/j.euroneuro.2020.01.013.

Fernández-Ruiz, J., Romero, J. and Ramos, J. A. (2015) Endocannabinoids and neurodegenerative disorders: Parkinson's disease, huntington's chorea, alzheimer's disease, and others, Endocannabinoids. doi: 10.1007/978-3-319-20825-1_8.

Flores-Otero, J. et al. (2014) 'Ligand-specific endocytic dwell times control functional selectivity of the cannabinoid receptor 1', Nature Communications. Nature Publishing Group, 5. doi: 10.1038/ncomms5589.

Freund, T. F., Katona, I. and Piomelli, D. (2003) 'Role of endogenous cannabinoids in synaptic signaling', Physiological Reviews, 83(3), pp. 1017–1066. doi: 10.1152/physrev.00004.2003.

Fukaya, M. et al. (2008) 'Predominant expression of phospholipase Cβ1 in telencephalic principal neurons and cerebellar interneurons, and its close association with related signaling molecules in somatodendritic neuronal elements', European Journal of Neuroscience, 28(9), pp. 1744–1759. doi: 10.1111/j.1460-9568.2008.06495.x.

Gabrielli, M. et al. (2015) 'Active endocannabinoids are secreted on the surface of microglial microvesicles', SpringerPlus, 4(2), pp. 1–32. doi: 10.1186/2193-1801-4-S1-L29.

Gao, Y. et al. (2010) 'Loss of retrograde endocannabinoid signaling and reduced adult neurogenesis in diacylglycerol lipase knock-out mice', Journal of Neuroscience, 30(6), pp. 2017–2024. doi: 10.1523/JNEUROSCI.5693-09.2010.

Garro, M. A. et al. (2001) 'Regulation of phospholipase Cβ activity by muscarinic acetylcholine and 5-HT2 receptors in crude and synaptosomal membranes from human cerebral cortex', Neuropharmacology, 40(5), pp. 686–695. doi: 10.1016/S0028-

3908(00)00206-9.

Gerard, C. M. et al. (1991) ‘Molecular cloning of a human cannabinoid receptor which is also expressed in testis’, Biochemical Journal, 279(1), pp. 129–134. doi: 10.1042/bj2790129.

Gilman, A. (1987) ‘G Proteins: Transducers Of Receptor-Generated Signals’, Annual Review of Biochemistry, 56, pp. 615–649. doi: 10.1146/annurev.biochem.56.1.615.

Glass, M., Dragunow, M. and Faull, R. L. M. (1997) ‘Cannabinoid receptors in the human brain: A detailed anatomical and quantitative autoradiographic study in the fetal, neonatal and adult human brain’, Neuroscience, 77(2), pp. 299–318. doi: 10.1016/S0306-4522(96)00428-9.

Glass, M. and Northup, J. K. (1999) ‘Agonist selective regulation of G proteins by cannabinoid CB1 and CB2 receptors’, Molecular Pharmacology, 56(6), pp. 1362–1369. doi: 10.1124/mol.56.6.1362.

Golech, S. A. et al. (2004) ‘Human brain endothelium: Coexpression and function of vanilloid and endocannabinoid receptors’, Molecular Brain Research, 132(1), pp. 87–92. doi: 10.1016/j.molbrainres.2004.08.025.

González-mariscal, I. et al. (2016) ‘Human CB1 Receptor Isoforms , present in Hepatocytes and β -cells , are Involved in Regulating Metabolism’, Nature Publishing Group. Nature Publishing Group, (June), pp. 1–12. doi: 10.1038/srep33302.

Gray, E. G. and Whitakker, V. P. (1962) ‘The isolation of nerve endings from brain: an electron-microscopic study of cell fragments derived by homogenization and centrifugation.’, Journal of anatomy, 96(1), pp. 79–88. Available at: http://www.ncbi.nlm.nih.gov/pubmed/13901297%0Ahttp://www.pubmedcentral.nih.gov/articlerender.fcgi?artid=PMC1244174.

Grimsey, N. L. et al. (2008) ‘Specific detection of CB1 receptors; cannabinoid CB1 receptor antibodies are not all created equal!’, Journal of Neuroscience Methods, 171(1), pp. 78–86. doi: 10.1016/j.jneumeth.2008.02.014.

Grimsey, N. L. et al. (2010) ‘Cannabinoid Receptor 1 trafficking and the role of the intracellular pool: Implications for therapeutics’, Biochemical Pharmacology. Elsevier Inc., 80(7), pp. 1050–1062. doi: 10.1016/j.bcp.2010.06.007.

Guggenhuber, S. et al. (2016) ‘Cannabinoid receptor-interacting protein Crip1a modulates blCB1 receptor signaling in mouse hippocampus’, Brain Structure and Function. Springer Berlin Heidelberg, 221(4), pp. 2061–2074. doi: 10.1007/s00429-015-1027-6.

Guixà-González, R. et al. (2017) ‘Membrane cholesterol access into a G-protein-coupled receptor’, Nature Communications, 8. doi: 10.1038/ncomms14505.

Gulyas, A. I. et al. (2004) ‘Segregation of two endocannabinoid-hydrolyzing enzymes into pre- and postsynaptic compartments in the rat hippocampus, cerebellum and amygdala’, European Journal of Neuroscience, 20(2), pp. 441–458. doi: 10.1111/j.1460-9568.2004.03428.x.

Gurevich, V. V and Gurevich, E. V (2017) ‘Molecular mechanisms of GPCR signaling: A structural perspective’, International Journal of Molecular Sciences, pp. 1–17. doi: 10.3390/ijms18122519.

Gurevich, V. V and Gurevich, E. V (2019) ‘GPCR signaling regulation: The role of GRKs and arrestins’, Frontiers in Pharmacology, 10(FEB), pp. 1–11. doi: 10.3389/fphar.2019.00125.

Gutiérrez-Rodríguez, A. et al. (2017) ‘Anatomical characterization of the cannabinoid CB1 receptor in cell-type–specific mutant mouse rescue models’, Journal of Comparative Neurology. doi: 10.1002/cne.24066.

Guzmán, M., Galve-Roperh, I. and Sánchez, C. (2001) ‘Ceramide: A new second messenger of cannabinoid action’, Trends in Pharmacological Sciences, 22(1), pp. 19–22. doi: 10.1016/S0165-6147(00)01586-8.

Hajos, F. (2003) ‘An improved method for the preparation of synaptosomal fractions in high purity’, Brain Research, 93(3), pp. 405–489.

Han, J. et al. (2012) ‘Acute cannabinoids impair working memory through astroglial CB 1 receptor modulation of hippocampal LTD’, Cell. Elsevier Inc., 148(5), pp. 1039–1050. doi: 10.1016/j.cell.2012.01.037.

Hanada, K. et al. (1995) ‘Both sphingolipids and cholesterol participate in the detergent insolubility of alkaline phosphatase, a glycosylphosphatidylinositol-anchored protein, in mammalian membranes’, Journal of Biological Chemistry. doi: 10.1074/jbc.270.11.6254.

Hancock, J. F. (2006) ‘Lipid rafts: contentious only from simplistic standpoints’, Nature reviews Molecular Cell Biology, 7(1), pp. 1–7. Available at: papers2://publication/uuid/07D1C2D5-3C89-4F90-8696-17C4D4F6C39B.

Hao, S. et al. (2000) ‘Low dose anandamide affects food intake, cognitive function, neurotransmitter and corticosterone levels in diet-restricted mice’, European Journal of Pharmacology. doi: 10.1016/S0014-2999(00)00059-5.

Häring, M. et al. (2007) ‘Identification of the cannabinoid receptor type 1 in serotonergic cells of raphe nuclei in mice’, Neuroscience, 146(3), pp. 1212–1219. doi: 10.1016/j.neuroscience.2007.02.021.

Häring, M. et al. (2015) ‘Cannabinoid type-1 receptor signaling in central serotonergic neurons regulates anxiety-like behavior and sociability’, Frontiers in Behavioral Neuroscience, 9(september), pp. 1–13. doi: 10.3389/fnbeh.2015.00235.

Hashimotodani, Y. et al. (2005) ‘Phospholipase Cβ serves as a coincidence detector through its Ca 2+ dependency for triggering retrograde endocannabinoid signal’, Neuron, 45(2), pp. 257–268. doi: 10.1016/j.neuron.2005.01.004.

Hashimotodani, Y., Ohno-Shosaku, T. and Kano, M. (2007) ‘Presynaptic monoacylglycerol lipase activity determines basal endocannabinoid tone and terminates retrograde endocannabinoid signaling in the hippocampus’, Journal of Neuroscience, 27(5), pp. 1211–1219. doi: 10.1523/JNEUROSCI.4159-06.2007.

Hebb, B. C. and Whittaker, V. P. (1958) ‘Intracellular distributions of acetylcholine and choline acetylase’, The journal of physiology, 142(1), pp. 187–196.

Hebert-Chatelain, E. et al. (2014) ‘Cannabinoid control of brain bioenergetics: Exploring the subcellular localization of the CB1receptor’, Molecular Metabolism. Elsevier GmbH, 3(4), pp. 495–504. doi: 10.1016/j.molmet.2014.03.007.

Hebert-Chatelain, E. et al. (2016) ‘A cannabinoid link between mitochondria and memory’, Nature. Nature Publishing Group, 539(7630), pp. 555–559. doi: 10.1038/nature20127.

Henn, F. A., Anderson, D. J. and Rustad, D. G. (1976) ‘Glial contamination of synaptosomal fractions’, Brain Research, 101(2), pp. 341–344. doi: 10.1016/0006-8993(76)90274-2.

Herkenham, M. et al. (1990) ‘Cannabinoid receptor localization in brain’, Proceedings of the National Academy of Sciences of the United States of America, 87(5), pp. 1932–1936. doi: 10.1073/pnas.87.5.1932.

Herkenham, M. et al. (1991) ‘Characterization and localization of cannabinoid receptors in rat brain: a quantitative in vitro autoradiographic study’, The Journal of Neuroscience, 11(2), pp. 563 LP – 583. doi: 10.1523/JNEUROSCI.11-02-00563.1991.

Hilf, G., Gierschik, P. and Jakobs, K. H. (1989) ‘Muscarinic acetylcholine receptor-stimulated binding of guanosine 5′-O-(3-thiotriphosphate) to guanine-nucleotide-binding proteins in cardiac membranes’, European Journal of Biochemistry, 186(3), pp. 725–731. doi: 10.1111/j.1432-1033.1989.tb15266.x.

Hill, E. L. et al. (2007) ‘Functional CB1 receptors are broadly expressed in neocortical GABAergic and glutamatergic neurons’, Journal of Neurophysiology, 97(4), pp. 2580–2589. doi: 10.1152/jn.00603.2006.

Howlett, A., Blume, L. and Dalton, G. (2010) ‘CB1 Cannabinoid Receptors and their Associated Proteins’, Current Medicinal Chemistry, 17(14), pp. 1382–1393. doi: 10.2174/092986710790980023.

Howlett, A. C. (1984) ‘Inhibition of neuroblastoma adenylate cyclase by cannabinoid and nantradol compounds’, Life Sciences, 35(17), pp. 1803–1810. doi: 10.1016/0024-3205(84)90278-9.

Howlett, A. C. (1985) ‘Cannabinoid inhibition of adenylate cyclase. Biochemistry of the response in neuroblastoma cell membranes’, Molecular Pharmacology, 26(3), pp. 532–538.

Howlett, A. C. et al. (2002) ‘International Union of Pharmacology. XXVII. Classification of cannabinoid receptors’, Pharmacological Reviews, 54(2), pp. 161–202. doi: 10.1124/pr.54.2.161.

Howlett, A. C. and Fleming, R. M. (1984) ‘Cannabinoid inhibition of adenylate cyclase. Pharmacology of the response in neuroblastoma cell membrane’, Molecular Pharmacology, 26(3), pp. 532–538.

Howlett, A. C., Qualy, J. M. and Khachatrian, L. L. (1986) ‘Involvement of G(i) in the inhibition of adenylate cyclase by cannabimimetic drugs’, Molecular Pharmacology,

29(3), pp. 307–313.

Hsieh, C. et al. (1999) ‘Internalization and recycling of the CB1 cannabinoid receptor’, Journal of Neurochemistry, 73(2), pp. 493–501. doi: 10.1046/j.1471-4159.1999.0730493.x.

Hua, T. et al. (2016) ‘Crystal Structure of the Human Cannabinoid Receptor CB1’, Cell, 167(3), pp. 750-762.e14. doi: 10.1016/j.cell.2016.10.004.

Hua, T. et al. (2017) ‘Crystal structures of agonist-bound human cannabinoid receptor CB 1’, Nature, 547(7664), pp. 468–471. doi: 10.1038/nature23272.

Hua, T. et al. (2020) ‘Activation and Signaling Mechanism Revealed by Cannabinoid Receptor-Gi Complex Structures’, Cell, 180(4), pp. 655–665. doi: 10.1016/j.cell.2020.01.008.

Huestis, M. A. et al. (2001) ‘Blockade of effects of smoked marijuana by the CB1-selective cannabinoid receptor antagonist SR141716’, Archives of General Psychiatry, 58(4), pp. 322–328. doi: 10.1001/archpsyc.58.4.322.

Ilyasov, A. A. et al. (2018) ‘The Endocannabinoid System and Oligodendrocytes in Health and Disease’, Frontiers in Neuroscience, 12(October), pp. 1–10. doi: 10.3389/fnins.2018.00733.

Irving, A. J. et al. (2000) ‘Functional expression of cell surface cannabinoid CB1 receptors on presynaptic inhibitory terminals in cultured rat hippocampal neurons’, Neuroscience, 98(2), pp. 253–262. doi: 10.1016/S0306-4522(00)00120-2.

Jacob, W. et al. (2009) ‘Endocannabinoids render exploratory behaviour largely independent of the test aversiveness: Role of glutamatergic transmission’, Genes, Brain and Behavior, 8(7), pp. 685–698. doi: 10.1111/j.1601-183X.2009.00512.x.

De Jesús, M. L. et al. (2006) ‘Characterization of CB1 cannabinoid receptor immunoreactivity in postmortem human brain homogenates’, Neuroscience, 140(2), pp. 635–643. doi: 10.1016/j.neuroscience.2006.02.024.

Jin, W. et al. (1999) ‘Distinct domains of the CB1 cannabinoid receptor mediate desensitization and internalization’, Journal of Neuroscience, 19(10), pp. 3773–3780. doi: 10.1523/jneurosci.19-10-03773.1999.

Joo, F. and Karnushina, I. (1975) ‘Morphometic assessment of the composition of the synaptosomal fractions obtained by the use of Ficoll gradients’, Journal of n, 4(1), pp. 839–840. doi: 10.14936/ieiej.28.146.

Jung, K. M. et al. (2007) ‘A key role for diacylglycerol lipase-α in metabotropic glutamate receptor-dependent endocannabinoid mobilization’, Molecular Pharmacology, 72(3), pp. 612–621. doi: 10.1124/mol.107.037796.

Kamprath, K. et al. (2009) ‘Endocannabinoids mediate acute fear adaptation via glutamatergic neurons independently of corticotropin-releasing hormone signaling’, Genes, Brain and Behavior, 8(2), pp. 203–211. doi: 10.1111/j.1601-183X.2008.00463.x.

Kang, Y. et al. (2015) ‘Crystal structure of rhodopsin bound to arrestin by femtosecond X-ray laser’, Nature, 523(7562), pp. 561–567. doi: 10.1038/nature14656.

Kano, M. et al. (2009) ‘Endocannabinoid-mediated control of synaptic transmission’, Physiological Reviews, 89(1), pp. 309–380. doi: 10.1152/physrev.00019.2008.

Kano, M. (2014) ‘Control of synaptic function by endocannabinoid-mediated retrograde signaling’, Proceedings of the Japan Academy Series B: Physical and Biological Sciences, pp. 235–250. doi: 10.2183/pjab.90.235.

Katona, I. et al. (1999) ‘Presynaptically Located CB1 Cannabinoid Receptors Regulate GABA Release from Axon Terminals of Specific Hippocampal Interneurons’, The Journal of Neuroscience, 19(11), pp. 4544 LP – 4558. doi: 10.1523/JNEUROSCI.19-11-04544.1999.

Katona, I. et al. (2006) ‘Molecular composition of the endocannabinoid system at glutamatergic synapses’, Journal of Neuroscience, 26(21), pp. 5628–5637. doi: 10.1523/JNEUROSCI.0309-06.2006.

Katona, I. and Freund, T. F. (2012) ‘Multiple functions of endocannabinoid signaling in the brain’, Annual Review of Neuroscience, 35, pp. 529–558. doi: 10.1146/annurev-neuro-062111-150420.

Kawaguchi, Y. and Kubota, Y. (1997) ‘GABAergic cell subtypes and their synaptic connections in rat frontal cortex’, Cerebral Cortex, 7(6), pp. 476–486. doi: 10.1093/cercor/7.6.476.

Kawamura, Y. et al. (2006) ‘The CB1 cannabinoid receptor is the major cannabinoid

receptor at excitatory presynaptic sites in the hippocampus and cerebellum', Journal of Neuroscience, 26(11), pp. 2991–3001. doi: 10.1523/JNEUROSCI.4872-05.2006.

Kearn, C. S. et al. (2005) 'Concurrent stimulation of cannabinoid CB1 and dopamine D2 receptors enhances heterodimer formation: A mechanism for receptor cross-talk?', Molecular Pharmacology, 67(5), pp. 1697–1704. doi: 10.1124/mol.104.006882.

Kenakin, T. (2002) 'Drug efficacy at G protein coupled receptors', Annu. Rev. Pharmacol. Toxicol., 42(2), pp. 349–379.

Kenakin, T. (2015) 'The effective application of biased signaling to new drug discovery', Molecular Pharmacology, 88(6), pp. 1055–1061. doi: 10.1124/mol.115.099770.

Kenakin, T. and Christopoulos, A. (2013) 'Signalling bias in new drug discovery: Detection, quantification and therapeutic impact', Nature Reviews Drug Discovery. Nature Publishing Group, 12(3), pp. 205–216. doi: 10.1038/nrd3954.

Khajehali, E. et al. (2015) 'Biased agonism and biased allosteric modulation at the CB1 cannabinoid receptors', Molecular Pharmacology, 88(2), pp. 368–379. doi: 10.1124/mol.115.099192.

Khurana, L. et al. (2017) 'Modulation of CB1 cannabinoid receptor by allosteric ligands: Pharmacology and therapeutic opportunities', Neuropharmacology, pp. 3–12. doi: 10.1016/j.neuropharm.2017.05.018.

Kirkham, T. C. (2009) 'Cannabinoids and appetite: Food craving and food pleasure', International Review of Psychiatry, 21(2 SPEC. ISS.), pp. 163–171. doi: 10.1080/09540260902782810.

Köfalvi, A. et al. (2005) 'Involvement of cannabinoid receptors in the regulation of neurotransmitter release in the rodent striatum: A combined immunochemical and pharmacological analysis', Journal of Neuroscience, 25(11), pp. 2874–2884. doi: 10.1523/JNEUROSCI.4232-04.2005.

Komorowska-Müller, J. A. and Schmöle, A. C. (2021) 'CB2 receptor in microglia: The guardian of self-control', International Journal of Molecular Sciences, pp. 1–27. doi: 10.3390/ijms22010019.

Krishna Kumar, K. et al. (2019) 'Structure of a Signaling Cannabinoid Receptor 1-G Protein Complex', Cell, 176(3), pp. 448-458.e12. doi: 10.1016/j.cell.2018.11.040.

Lafenêtre, P., Chaouloff, F. and Marsicano, G. (2007) 'The endocannabinoid system in the processing of anxiety and fear and how CB1 receptors may modulate fear extinction', Pharmacological Research, 56(5), pp. 367–381. doi: 10.1016/j.phrs.2007.09.006.

Lafourcade, M. et al. (2007) 'Molecular Components and Functions of the Endocannabinoid System in Mouse Prefrontal Cortex', PLoS ONE, 2(8), pp. 1–11. doi: 10.1371/journal.pone.0000709.

Laprairie, R. B. et al. (2014) 'Type 1 cannabinoid receptor ligands display functional selectivity in a cell culture model of striatal medium spiny projection neurons', Journal of Biological Chemistry, 289(36), pp. 24845–24862. doi: 10.1074/jbc.M114.557025.

Laprairie, R. B. et al. (2016) 'Biased type 1 cannabinoid receptor signaling influences neuronal viability in a cell culture model of huntington diseases', Molecular Pharmacology, 89(3), pp. 364–375. doi: 10.1124/mol.115.101980.

Lawrence, D. K. and Gill, E. W. (1975) 'The effects of Δ1 tetrahydrocannabinol and other cannabinoids on spin labeled liposomes and their relationship to mechanisms of general anesthesia', Molecular Pharmacology, 11(5), pp. 595–602.

Lee, C. et al. (2019) 'Determination of protein phosphorylation by polyacrylamide gel electrophoresis', Journal of Microbiology, 57(2), pp. 93–100. doi: 10.1007/s12275-019-9021-y.

Leterrier, C. et al. (2004) 'Constitutive endocytic cycle of the CB1 cannabinoid receptor', Journal of Biological Chemistry. Â© 2004 ASBMB. Currently published by Elsevier Inc; originally published by American Society for Biochemistry and Molecular Biology., 279(34), pp. 36013–36021. doi: 10.1074/jbc.M403990200.

Levental, I., Levental, K. R. and Heberle, F. A. (2020) 'Lipid Rafts: Controversies Resolved, Mysteries Remain', Trends in Cell Biology. Elsevier Ltd, pp. 341–353. doi: 10.1016/j.tcb.2020.01.009.

Lu, H. C. and MacKie, K. (2016) 'Metabolism of N-acylethanolamine phospholipids by a mammalian phosphodiesterase of the phospholipase D type', Biological Psychiatry, 79(7), pp. 516–525. doi: 10.1016/j.biopsych.2015.07.028.

Ludányi, A. et al. (2011) 'Complementary synaptic distribution of enzymes responsible for synthesis and inactivation of the endocannabinoid 2-arachidonoylglycerol in the

human hippocampus', Neuroscience, 174, pp. 50–63. doi: 10.1016/j.neuroscience.2010.10.062.

Luttrell, L. M. and Lefkowitz, R. J. (2002) 'The role of β-arrestins in the termination and transduction of G-protein-coupled receptor signals', Journal of Cell Science, 115(3), pp. 455–465.

Lutz, B. et al. (2015) 'The endocannabinoid system in guarding against fear, anxiety and stress', Nature Reviews Neuroscience. Nature Publishing Group, 16(12), pp. 705–718. doi: 10.1038/nrn4036.

Maccarrone, M. et al. (2009) 'Lipid rafts regulate 2-arachidonoylglycerol metabolism and physiological activity in the striatum', Journal of Neurochemistry, 109(2), pp. 371–381. doi: 10.1111/j.1471-4159.2009.05948.x.

Maccarrone, M. et al. (2015) 'Endocannabinoid signaling at the periphery: 50 years after THC', Trends in Pharmacological Sciences, 36(5), pp. 277–296. doi: 10.1016/j.tips.2015.02.008.

Mackie, K. (2005) 'Distribution of cannabinoid receptors in the central and peripheral nervous system', Handbook of Experimental Pharmacology, 168, pp. 299–325. doi: 10.1007/3-540-26573-2-10.

Maejima, T. et al. (2005) 'Synaptically driven endocannabinoid release requires Ca2+-assisted metabotropic glutamate receptor subtype 1 to phospholipase C β4 signaling cascade in the cerebellum', Journal of Neuroscience, 25(29), pp. 6826–6835. doi: 10.1523/JNEUROSCI.0945-05.2005.

Mahammad, S. and Parmryd, I. (2015) 'Cholesterol depletion using methyl-β-cyclodextrin', Methods in molecular biology (Clifton, N.J.), 1232, pp. 91–102. doi: 10.1007/978-1-4939-1752-5_8.

Mahavadi, S. et al. (2014) 'Inhibitory signaling by CB1 receptors in smooth muscle mediated by GRK5/β-arrestin activation of ERK1/2 and Src kinase', American Journal of Physiology - Gastrointestinal and Liver Physiology, 306(6), pp. 535–545. doi: 10.1152/ajpgi.00397.2013.

Mailleux, P. and Vanderhaeghen, J. J. (1992a) 'Distribution of neuronal cannabinoid receptor in the adult rat brain: A comparative receptor binding radioautography and in

situ hybridization histochemistry', Neuroscience. Pergamon, 48(3), pp. 655–668. doi: 10.1016/0306-4522(92)90409-U.

Mailleux, P. and Vanderhaeghen, J. J. (1992b) 'Distribution of neuronal cannabinoid receptor in the adult rat brain: A comparative receptor binding radioautography and in situ hybridization histochemistry', Neuroscience, 48(3), pp. 655–668. doi: 10.1016/0306-4522(92)90409-U.

Maldonado, R., Cabañero, D. and Martín-García, E. (2020) 'The endocannabinoid system in modulating fear, anxiety, and stress', Dialogues in Clinical Neuroscience, 22(3), pp. 229–239. doi: 10.31887/DCNS.2020.22.3/RMALDONADO.

Manzanares, J. et al. (2018) 'Role of the endocannabinoid system in drug addiction', Biochemical Pharmacology, 157, pp. 108–121. doi: 10.1016/j.bcp.2018.09.013.

Marín, O. (2012) 'Interneuron dysfunction in psychiatric disorders', Nature Reviews Neuroscience, 13(2), pp. 107–120. doi: 10.1038/nrn3155.

Marinelli, S. et al. (2009) 'Self-modulation of neocortical pyramidal neurons by endocannabinoids', Nature Neuroscience, 12(12), pp. 1488–1490. doi: 10.1038/nn.2430.

Maroso, M. et al. (2016) 'Cannabinoid Control of Learning and Memory through HCN Channels', Neuron. Elsevier Inc., 89(5), pp. 1059–1073. doi: 10.1016/j.neuron.2016.01.023.

Marsicano, G. and Lutz, B. (1999) 'Expression of the cannabinoid receptor CB1 in distinct neuronal subpopulations in the adult mouse forebrain', European Journal of Neuroscience, 11(12), pp. 4213–4225. doi: 10.1046/j.1460-9568.1999.00847.x.

Martín-García, E. et al. (2016) 'Differential control of cocaine self-administration by GABAergic and glutamatergic CB1 cannabinoid receptors', Neuropsychopharmacology, 41(9), pp. 2192–2205. doi: 10.1038/npp.2015.351.

Martin, B. R. (1986) 'Cellular effects of cannabinoids', Pharmacological Reviews, 38(1), pp. 45–74.

Mato, S., Pazos, A. and Valdizán, E. M. (2002) 'Cannabinoid receptor antagonism and inverse agonism in response to SR141716A on cAMP production in human and rat brain', European Journal of Pharmacology, 443(1–3), pp. 43–46. doi: 10.1016/S0014-2999(02)01575-3.

Matsuda, L. A. et al. (1990) ‘Structure of a cannabinoid receptor and functional expression of the cloned cDNA’, Nature, 346(6284), pp. 561–564. doi: 10.1038/346561a0.

Matsuda, L. A., Bonner, T. I. and Lolait, S. J. (1993) ‘Localization of cannabinoid receptor mRNA in rat brain’, Journal of Comparative Neurology, 327(4), pp. 535–550. doi: 10.1002/cne.903270406.

Mattes, R. D. et al. (1994) ‘Cannabinoids and appetite stimulation’, Pharmacology, Biochemistry and Behavior, 49(1), pp. 187–195. doi: 10.1016/0091-3057(94)90475-8.

Mayor, S. and Maxfield, F. R. (1995) ‘Insolubility and redistribution of GPI-anchored proteins at the cell surface after detergent treatment’, Molecular Biology of the Cell. doi: 10.1091/mbc.6.7.929.

McAllister, S. D. et al. (2004) ‘Structural mimicry in class A G protein-coupled receptor rotamer toggle switches: The importance of the F3.36(201)/W6.48(357) interaction in cannabinoid CB1 receptor activation’, Journal of Biological Chemistry. Â© 2004 ASBMB. Currently published by Elsevier Inc; originally published by American Society for Biochemistry and Molecular Biology., 279(46), pp. 48024–48037. doi: 10.1074/jbc.M406648200.

Mcpartland, J. M. and Glass, M. (2003) ‘Functional mapping of cannabinoid receptor homologs in mammals , other vertebrates , and invertebrates’, Gene, 312, pp. 297–303. doi: 10.1016/S0378-1119(03)00638-3.

McPartland, J. M., Glass, M. and Pertwee, R. G. (2007) ‘Meta-analysis of cannabinoid ligand binding affinity and receptor distribution: Interspecies differences’, British Journal of Pharmacology, 152(5), pp. 583–593. doi: 10.1038/sj.bjp.0707399.

Mechoulam, R. et al. (1995) ‘Identification of an endogenous 2-monoglyceride, present in canine gut, that binds to cannabinoid receptors’, Biochemical Pharmacology, 50(1), pp. 83–90. doi: 10.1016/0006-2952(95)00109-D.

Mechoulam, R. et al. (2014) ‘Early phytocannabinoid chemistry to endocannabinoids and beyond’, Nature Reviews Neuroscience, pp. 757–764. doi: 10.1038/nrn3811.

Mechoulam, R. and Gaoni, Y. (1964) ‘Isolation, Structure, and Partial Synthesis of an Active Constituent of Hashish’, Journal of the American Chemical Society, 86(8), pp.

1646–1647.

Mechoulam, R. and Parker, L. A. (2013) ‘The endocannabinoid system and the brain’, Annual Review of Psychology, 64, pp. 21–47. doi: 10.1146/annurev-psych-113011-143739.

Metna-Laurent, M. et al. (2012) ‘Bimodal control of fear-coping strategies by CB 1 cannabinoid receptors’, Journal of Neuroscience, 32(21), pp. 7109–7118. doi: 10.1523/JNEUROSCI.1054-12.2012.

Metna-Laurent, M. and Marsicano, G. (2015) ‘Rising stars: Modulation of brain functions by astroglial type-1 cannabinoid receptors’, Glia, 63(3), pp. 353–364. doi: 10.1002/glia.22773.

Monory, K. et al. (2006) ‘The Endocannabinoid System Controls Key Epileptogenic Circuits in the Hippocampus’, Neuron, 51(4), pp. 455–466. doi: 10.1016/j.neuron.2006.07.006.

Moreira, F. A., Grieb, M. and Lutz, B. (2009) ‘Central side-effects of therapies based on CB1 cannabinoid receptor agonists and antagonists: focus on anxiety and depression’, Best Practice and Research: Clinical Endocrinology and Metabolism, 23(1), pp. 133–144. doi: 10.1016/j.beem.2008.09.003.

Mukhopadhyay, S. et al. (1999) ‘Regulation of G(i) by the CB1 cannabinoid receptor C-terminal juxtamembrane region: Structural requirements determined by peptide analysis’, Biochemistry, 38(11), pp. 3447–3455. doi: 10.1021/bi981767v.

Mukhopadhyay, S. et al. (2000) ‘The CB1 cannabinoid receptor juxtamembrane C-terminal peptide confers activation to specific G proteins in brain’, Molecular Pharmacology, 57(1), pp. 162–170.

Mukhopadhyay, S. et al. (2002) ‘CB1 cannabinoid receptor-G protein association: A possible mechanism for differential signaling’, Chemistry and Physics of Lipids, 121(1–2), pp. 91–109. doi: 10.1016/S0009-3084(02)00153-6.

Mukhopadhyay, S. and Howlett, A. C. (2001) ‘CB1 receptor-G protein association: Subtype selectivity is determined by distinct intracellular domains’, European Journal of Biochemistry, 268(3), pp. 499–505. doi: 10.1046/j.1432-1327.2001.01810.x.

Mukhopadhyay, S. and Howlett, A. C. (2005) ‘Chemically distinct ligands promote

differential CB1 cannabinoid receptor-Gi protein interactions', Molecular Pharmacology, 67(6), pp. 2016–2024. doi: 10.1124/mol.104.003558.

Munro, S., Thomas, K. L. and Abu-Shaar, M. (1993) 'Molecular characterization of a peripheral receptor for cannabinoids', Nature, 365, pp. 61–65. doi: 10.1038/365061a0.

Murataeva, N., Straiker, A. and MacKie, K. (2014) 'Parsing the players: 2-arachidonoylglycerol synthesis and degradation in the CNS', British Journal of Pharmacology, 171(6), pp. 1379–1391. doi: 10.1111/bph.12411.

Murphy, W. J. et al. (2001) 'Molecular phylogenetics and the origins of placental mammals', Nature, 409(6820), pp. 614–618. doi: 10.1038/35054550.

Navarrete, M., Díez, A. and Araque, A. (2014) 'Astrocytes in endocannabinoid signalling', Philosophical Transactions of the Royal Society B: Biological Sciences, 369(1654). doi: 10.1098/rstb.2013.0599.

Niehaus, J. L. et al. (2007) 'CB1 cannabinoid receptor activity is modulated by the cannabinoid receptor interacting protein CRIP 1a', Molecular Pharmacology, 72(6), pp. 1557–1566. doi: 10.1124/mol.107.039263.

Nogueras-Ortiz, C. and Yudowski, G. A. (2016) 'The multiple waves of cannabinoid 1 receptor signaling', Molecular Pharmacology, pp. 620–626. doi: 10.1124/mol.116.104539.

Nyíri, G. et al. (2005) 'CB1 cannabinoid receptors are enriched in the perisynaptic annulus and on preterminal segments of hippocampal GABAergic axons', Neuroscience, 136(3), pp. 811–822. doi: 10.1016/j.neuroscience.2005.01.026.

Nyíri, Gábor et al. (2005) 'GABAB and CB1 cannabinoid receptor expression identifies two types of septal cholinergic neurons', European Journal of Neuroscience, 21(11), pp. 3034–3042. doi: 10.1111/j.1460-9568.2005.04146.x.

Oates, J. and Watts, A. (2011) 'Uncovering the intimate relationship between lipids, cholesterol and GPCR activation', Current Opinion in Structural Biology. Elsevier Ltd, 21(6), pp. 802–807. doi: 10.1016/j.sbi.2011.09.007.

Oddi, S. et al. (2011) 'Functional characterization of putative cholesterol binding sequence (CRAC) in human type-1 cannabinoid receptor', Journal of Neurochemistry, 116(5), pp. 858–865. doi: 10.1111/j.1471-4159.2010.07041.x.

Oddi, S. et al. (2012) ‘Effects of palmitoylation of Cys 415 in helix 8 of the CB 1 cannabinoid receptor on membrane localization and signalling’, British Journal of Pharmacology, 165(8), pp. 2635–2651. doi: 10.1111/j.1476-5381.2011.01658.x.

Oddi, S. et al. (2017) ‘Palmitoylation of cysteine 415 of CB1 receptor affects ligand-stimulated internalization and selective interaction with membrane cholesterol and caveolin 1’, Biochimica et Biophysica Acta - Molecular and Cell Biology of Lipids. Elsevier B.V., 1862(5), pp. 523–532. doi: 10.1016/j.bbalip.2017.02.004.

Oddi, S. et al. (2018) ‘Role of palmitoylation of cysteine 415 in functional coupling CB1 receptor to Gαi2 protein’, Biotechnology and Applied Biochemistry, 65(1), pp. 16–20. doi: 10.1002/bab.1575.

Ohno-Shosaku, T. et al. (2002) ‘Presynaptic Cannabinoid Sensitivity Is a Major Determinant of Depolarization-Induced Retrograde Suppression at Hippocampal Synapses’, Journal of Neuroscience, 22(10), pp. 3864–3872. doi: 10.1523/jneurosci.22-10-03864.2002.

Ohno-Shosaku, T. et al. (2012) ‘Endocannabinoids and retrograde modulation of synaptic transmission’, Neuroscientist, pp. 119–132. doi: 10.1177/1073858410397377.

Onaivi, E. S., Chakrabarti, A. and Chaudhuri, G. (1996) ‘Cannabinoid receptor genes’, Progress in Neurobiology, 48(4–5), pp. 275–283. doi: 10.1016/0301-0082(95)00044-5.

Ong, W. Y. and MacKie, K. (1999) ‘A light and electron microscopic study of the CB1 cannabinoid receptor in primate brain’, Neuroscience, 92(4), pp. 1177–1191. doi: 10.1016/S0306-4522(99)00025-1.

Oropeza, V. C., Mackie, K. and Van Bockstaele, E. J. (2007) ‘Cannabinoid receptors are localized to noradrenergic axon terminals in the rat frontal cortex’, Brain Research, 1127(1), pp. 36–44. doi: 10.1016/j.brainres.2006.09.110.

Ostrom, R. S. and Insel, P. A. (2006) ‘Methods for the study of signaling molecules in membrane lipid rafts and caveolae.’, Methods in molecular biology (Clifton, N.J.), 332, pp. 181–191. doi: 10.1385/1-59745-048-0:181.

Pan, B. et al. (2009) ‘Blockade of 2-arachidonoylglycerol hydrolysis by selective monoacylglycerol lipase inhibitor 4-nitrophenyl 4-(dibenzo[d] [1,3]dioxol-5-yl(hydroxy)methyl) piperidine-1-carboxylate (JZL184) enhances retrograde

endocannabinoid signaling', Journal of Pharmacology and Experimental Therapeutics, 331(2), pp. 591–597. doi: 10.1124/jpet.109.158162.

Pan, B. et al. (2011) 'Alterations of endocannabinoid signaling, synaptic plasticity, learning, and memory in monoacylglycerol lipase knock-out mice', Journal of Neuroscience, 31(38), pp. 13420–13430. doi: 10.1523/JNEUROSCI.2075-11.2011.

Pertwee, R. G. (2006) 'Cannabinoid pharmacology: The first 66 years', British Journal of Pharmacology. doi: 10.1038/sj.bjp.0706406.

Pertwee, R. G. et al. (2010) 'International Union of Basic and Clinical Pharmacology. LXXIX. Cannabinoid receptors and their ligands: Beyond CB1 and CB2', Pharmacological Reviews, pp. 588–631. doi: 10.1124/pr.110.003004.

Pertwee, R. G. (2015) Endocannabinoids and their pharmacological actions, Handbook of Experimental Pharmacology. doi: 10.1007/978-3-319-20825-1_1.

Phillips, G. R. et al. (2001) 'The presynaptic particle web: Ultrastructure, composition, dissolution, and reconstitution', Neuron, 32(1), pp. 63–77. doi: 10.1016/S0896-6273(01)00450-0.

Piazza, P. V., Cota, D. and Marsicano, G. (2017) 'The CB1 Receptor as the Cornerstone of Exostasis', Neuron, pp. 1252–1274. doi: 10.1016/j.neuron.2017.02.002.

Pickel, V. M. et al. (2004) 'Compartment-specific localization of cannabinoid 1 (CB1) and μ-opioid receptors in rat nucleus accumbens', Neuroscience, 127(1), pp. 101–112. doi: 10.1016/j.neuroscience.2004.05.015.

Pierce, K. L. and Lefkowitz, R. J. (2001) 'Classical and new roles of β-arrestins in the regulation of G-PROTEIN-COUPLED receptors', Nature Reviews Neuroscience, 2(10), pp. 727–733. doi: 10.1038/35094577.

Pike, L. J. (2006) 'Rafts defined: A report on the Keystone symposium on lipid rafts and cell function', Journal of Lipid Research. © 2006 ASBMB. Currently published by Elsevier Inc; originally published by American Society for Biochemistry and Molecular Biology., 47(7), pp. 1597–1598. doi: 10.1194/jlr.E600002-JLR200.

Piomelli, D. (2003) 'The molecular logic of endocannabinoid signalling', Nature Reviews Neuroscience, 4(11), pp. 873–884. doi: 10.1038/nrn1247.

Plummer, T. H. and Tarentino, A. L. (1991) 'Purification of the oligosaccharide-cleaving enzymes of Flavobacterium meningosepticum', Glycobiology. doi: 10.1093/glycob/1.3.257.

Puighermanal, E. et al. (2009) 'Cannabinoid modulation of hippocampal long-term memory is mediated by mTOR signaling', Nature Neuroscience, 12(9), pp. 1152–1158. doi: 10.1038/nn.2369.

Remmers, F. et al. (2017) 'Addressing sufficiency of the CB1 receptor for endocannabinoid-mediated functions through conditional genetic rescue in forebrain GABAergic neurons', Brain Structure and Function. Springer Berlin Heidelberg, 222(8), pp. 3431–3452. doi: 10.1007/s00429-017-1411-5.

Rey, A. A. et al. (2012) 'Biphasic effects of cannabinoids in anxiety responses: CB1 and GABA B receptors in the balance of gabaergic and glutamatergic neurotransmission', Neuropsychopharmacology. Nature Publishing Group, 37(12), pp. 2624–2634. doi: 10.1038/npp.2012.123.

Rodríguez, J. J., Mackie, K. and Pickel, V. M. (2001) 'Ultrastructural localization of the CB1 cannabinoid receptor in μ-opioid receptor patches of the rat caudate putamen nucleus', Journal of Neuroscience, 21(3), pp. 823–833. doi: 10.1523/jneurosci.21-03-00823.2001.

Rozenfeld, R. and Devi, L. A. (2008) ' Regulation of CB 1 cannabinoid receptor trafficking by the adaptor protein AP-3 ', The FASEB Journal, 22(7), pp. 2311–2322. doi: 10.1096/fj.07-102731.

Ruehle, S. et al. (2013) 'Cannabinoid CB1 receptor in dorsal telencephalic glutamatergic neurons: Distinctive sufficiency for hippocampus-dependent and amygdala-dependent synaptic and behavioral functions', Journal of Neuroscience, 33(25), pp. 10264–10277. doi: 10.1523/JNEUROSCI.4171-12.2013.

Ruehle, S. et al. (2017) 'Discovery and characterization of two novel CB1 receptor splice variants with modified N-termini in mouse', Journal of Neurochemistry, 142(4), pp. 521–533. doi: 10.1111/jnc.14099.

Ryberg, E. et al. (2005) 'Identification and characterisation of a novel splice variant of the human CB1 receptor', FEBS Letters, 579(1), pp. 259–264. doi: 10.1016/j.febslet.2004.11.085.

Sabatucci, A. et al. (2018) ‘In silico mapping of allosteric ligand binding sites in type-1 cannabinoid receptor’, Biotechnology and Applied Biochemistry, 65(1), pp. 21–28. doi: 10.1002/bab.1589.

Salio, C. et al. (2002) ‘Pre- and postsynaptic localizations of the CB1 cannabinoid receptor in the dorsal horn of the rat spinal cord’, Neuroscience, 110(4), pp. 755–764. doi: 10.1016/S0306-4522(01)00584-X.

Sánchez-Blázquez, P. et al. (2013) ‘Cannabinoid receptors couple to NMDA receptors to reduce the production of NO and the mobilization of zinc induced by glutamate’, Antioxidants and Redox Signaling, 19(15), pp. 1766–1782. doi: 10.1089/ars.2012.5100.

Sánchez-Blázquez, P., Rodríguez-Muñoz, M. and Garzón, J. (2014) ‘The cannabinoid receptor 1 associates with NMDA receptors to produce glutamatergic hypofunction: Implications in psychosis and schizophrenia’, Frontiers in Pharmacology, 4 JAN(January), pp. 1–10. doi: 10.3389/fphar.2013.00169.

Sánchez, C. et al. (2001) ‘The CB1 cannabinoid receptor of astrocytes is coupled to sphingomyelin hydrolysis through the adaptor protein fan’, Molecular Pharmacology, 59(5), pp. 955–959. doi: 10.1124/mol.59.5.955.

Sarnataro, D. et al. (2005) ‘Plasma membrane and lysosomal localization of CB1 cannabinoid receptor are dependent on lipid rafts and regulated by anandamide in human breast cancer cells’, FEBS Letters, 579(28), pp. 6343–6349. doi: 10.1016/j.febslet.2005.10.016.

Savinainen, J. R. et al. (2003) ‘An optimized approach to study endocannabinoid signaling : evidence against constitutive activity of rat brain adenosine A 1 and cannabinoid CB 1 receptors’, British Journal of Pharmacology, 140(8), pp. 1451–1459. doi: 10.1038/sj.bjp.0705577.

Scavone, J. L., Mackie, K. and Van Bockstaele, E. J. (2010) ‘Characterization of cannabinoid-1 receptors in the locus coeruleus: Relationship with mu-opioid receptors’, Brain Research. Elsevier B.V., 1312, pp. 18–31. doi: 10.1016/j.brainres.2009.11.023.

Scheen, A. J. et al. (2006) ‘Efficacy and tolerability of rimonabant in overweight or obese patients with type 2 diabetes: a randomised controlled study’, Lancet, 368(9548), pp. 1660–1672. doi: 10.1016/S0140-6736(06)69571-8.

Schlosburg, J. E. et al. (2010) ‘Chronic monoacylglycerol lipase blockade causes functional antagonism of the endocannabinoid system’, Nature Neuroscience. Nature Publishing Group, 13(9), pp. 1113–1119. doi: 10.1038/nn.2616.

Schmid, P. C. et al. (1983) ‘Metabolism of N-acylethanolamine phospholipids by a mammalian phosphodiesterase of the phospholipase D type.’, Journal of Biological Chemistry, 258(15), pp. 9302–9306. doi: 10.1016/s0021-9258(17)44667-9.

Scott, C. E. et al. (2013) ‘Molecular basis for dramatic changes in cannabinoid CB1 G protein-coupled receptor activation upon single and double point mutations’, Protein Science, 22(1), pp. 101–113. doi: 10.1002/pro.2192.

Seillier, A. and Giuffrida, A. (2018) ‘The cannabinoid transporter inhibitor OMDM-2 reduces social interaction: Further evidence for transporter-mediated endocannabinoid release’, Neuropharmacology. Elsevier Ltd, 130, pp. 1–9. doi: 10.1016/j.neuropharm.2017.11.032.

Selley, Dana E et al. (1996) ‘Cannabinoid r’, Image (Rochester, N.Y.), 59(8).

Selley, Dana E. et al. (1996) ‘Cannabinoid receptor stimulation of guanosine-5’-O-(3-[35S]thio)triphosphate binding in rat brain membranes’, Life Sciences, 59(8), pp. 659–668. doi: 10.1016/0024-3205(96)00347-5.

Sezgin, E. et al. (2017) ‘The mystery of membrane organization: Composition, regulation and roles of lipid rafts’, Nature Reviews Molecular Cell Biology. Nature Publishing Group, pp. 361–374. doi: 10.1038/nrm.2017.16.

Shao, Z. et al. (2016) ‘High-resolution crystal structure of the human CB1 cannabinoid receptor’, Nature. Nature Publishing Group, 540(7634), pp. 602–606. doi: 10.1038/nature20613.

Shao, Z. et al. (2019) ‘Structure of an allosteric modulator bound to the CB1 cannabinoid receptor’, Nature Chemical Biology. Springer US, 15(12), pp. 1199–1205. doi: 10.1038/s41589-019-0387-2.

Sheng, M. and Kim, E. (2011) ‘The postsynaptic organization of synapses’, Cold Spring Harbor Perspectives in Biology, 3(12), pp. 1–21. doi: 10.1101/cshperspect.a005678.

Shim, J. Y., Ahn, K. H. and Kendall, D. A. (2013) ‘Molecular basis of cannabinoid CB1 receptor coupling to the G protein heterotrimer Gαiβγ; Identification of key CB1 contacts

with the C-terminal helix α5 of Gαi', Journal of Biological Chemistry, 288(45), pp. 32449–32465. doi: 10.1074/jbc.M113.489153.

Shire, D. et al. (1995) 'An amino-terminal variant of the central cannabinoid receptor resulting from alternative splicing', Journal of Biological Chemistry, 270(8), pp. 3726–3731. doi: 10.1074/jbc.270.8.3726.

Sim-Selley, L. J., Brunk, L. K. and Selley, D. E. (2001) 'Inhibitory effects of SR141716A on G-protein activation in rat brain', European Journal of Pharmacology, 414(2–3), pp. 135–143. doi: 10.1016/S0014-2999(01)00784-1.

Singh, P. et al. (2019) 'Molecular Interaction between Distal C-Terminal Domain of the CB1 Cannabinoid Receptor and Cannabinoid Receptor Interacting Proteins (CRIP1a/CRIP1b)', Journal of Chemical Information and Modeling, 59(12), pp. 5294–5303. doi: 10.1021/acs.jcim.9b00948.

Smith, T. H., Sim-Selley, L. J. and Selley, D. E. (2010) 'Cannabinoid CB 1 receptor-interacting proteins: Novel targets for central nervous system drug discovery?', British Journal of Pharmacology, pp. 454–466. doi: 10.1111/j.1476-5381.2010.00777.x.

Song, C. and Howlett, A. C. (1995) 'Rat brain cannabinoid receptors are N-linked glycosylated proteins', Life Sciences, 56(23–24), pp. 1983–1989. doi: 10.1016/0024-3205(95)00179-A.

Soria-Gómez, E. et al. (2014) 'The endocannabinoid system controls food intake via olfactory processes', Nature Neuroscience. Nature Publishing Group, 17(3), pp. 407–415. doi: 10.1038/nn.3647.

Stadel, R., Ahn, K. H. and Kendall, D. A. (2011) 'The cannabinoid type-1 receptor carboxyl-terminus, more than just a tail', Journal of Neurochemistry, pp. 1–18. doi: 10.1111/j.1471-4159.2011.07186.x.

Steindel, F. et al. (2013) 'Neuron-type specific cannabinoid-mediated G protein signalling in mouse hippocampus', Journal of Neurochemistry, 124(6), pp. 795–807. doi: 10.1111/jnc.12137.

Steiner, M. A. et al. (2008) 'Conditional cannabinoid receptor type 1 mutants reveal neuron subpopulation-specific effects on behavioral and neuroendocrine stress responses', Psychoneuroendocrinology, 33(8), pp. 1165–1170. doi:

10.1016/j.psyneuen.2008.06.004.

Stella, N., Schweitzer, P. and Plomelli, D. (1997) ‘A second endogenous’ cannabinoid that modulates long-term potentiation’, Nature, 388(6644), pp. 773–778. doi: 10.1038/42015.

Stornaiuolo, M. et al. (2015) ‘Endogenous vs Exogenous Allosteric Modulators in GPCRs: A dispute for shuttling CB1 among different membrane microenvironments’, Scientific Reports. Nature Publishing Group, 5(September), pp. 1–13. doi: 10.1038/srep15453.

Straiker, A. et al. (2012) ‘Differential signalling in human cannabinoid CB 1 receptors and their splice variants in autaptic hippocampal neurones’, British Journal of Pharmacology, 165(8), pp. 2660–2671. doi: 10.1111/j.1476-5381.2011.01744.x.

Straiker, A. and Mackie, K. (2009) ‘Cannabinoid signaling in inhibitory autaptic hippocampal neurons’, Neuroscience, 163(1), pp. 190–201. doi: 10.1016/j.neuroscience.2009.06.004.

Straiker, A., Wager-Miller, J. and Mackie, K. (2012) ‘The CB 1 cannabinoid receptor C-terminus regulates receptor desensitization in autaptic hippocampal neurones’, British Journal of Pharmacology. doi: 10.1111/j.1476-5381.2011.01743.x.

Strange, P. G. (2010) ‘Use of the GTPγS ([35S]GTPγS and Eu-GTPγS) binding assay for analysis of ligand potency and efficacy at G protein-coupled receptors’, British Journal of Pharmacology, pp. 1238–1249. doi: 10.1111/j.1476-5381.2010.00963.x.

Südhof, T. C. (2012) ‘The presynaptic active zone’, Neuron, 75(1), pp. 11–25. doi: 10.1016/j.neuron.2012.06.012.

Sugiura, T. et al. (1995) ‘2-arachidonoylglycerol: A possible endogenous cannabinoid receptor ligand in brain’, Biochemical and Biophysical Research Communications, 215(1), pp. 89–97. doi: 10.1006/bbrc.1995.2437.

Sugiura, T. et al. (1999) ‘Evidence that the cannabinoid CB1 receptor is a 2-arachidonoylglycerol receptor: Structure-activity relationship of 2-arachidonoylglycerol, ether- linked analogues, and related compounds’, Journal of Biological Chemistry. Â© 1999 ASBMB. Currently published by Elsevier Inc; originally published by American Society for Biochemistry and Molecular Biology., 274(5), pp. 2794–2801. doi:

10.1074/jbc.274.5.2794.

Szabo, B. et al. (2006) ‘Depolarization-induced retrograde synaptic inhibition in the mouse cerebellar cortex is mediated by 2-arachidonoylglycerol’, Journal of Physiology, 577(1), pp. 263–280. doi: 10.1113/jphysiol.2006.119362.

Szczepek, M. et al. (2014) ‘Crystal structure of a common GPCR-binding interface for G protein and arrestin’, Nature Communications, 5(May), pp. 1–8. doi: 10.1038/ncomms5801.

Tai, H. and Jhou, J.-F. (2017) ‘The Study of Postmortem Human Synaptosomes for Understanding Alzheimer ’ s Disease and Other Neurological Disorders : A Review’, Neurology and Therapy. Springer Healthcare, 6(s1), pp. 57–68. doi: 10.1007/s40120-017-0070-z.

Talani, G. and Lovinger, D. M. (2015) ‘Interactions between ethanol and the endocannabinoid system at GABAergic synapses on basolateral amygdala principal neurons’, Alcohol. Elsevier Inc, 49(8), pp. 781–794. doi: 10.1016/j.alcohol.2015.08.006.

Tanimura, A. et al. (2010) ‘The Endocannabinoid 2-Arachidonoylglycerol Produced by Diacylglycerol Lipase α Mediates Retrograde Suppression of Synaptic Transmission’, Neuron. Elsevier Ltd, 65(3), pp. 320–327. doi: 10.1016/j.neuron.2010.01.021.

Tarentino, A. L. and Plummer, T. H. (1994) ‘Enzymatic deglycosylation of asparagine-linked glycans: Purification, properties, and specificity of oligosaccharide-cleaving enzymes from Flavobacterium meningosepticum’, Methods in Enzymology. doi: 10.1016/0076-6879(94)30006-2.

Tenreiro, P. et al. (2017) ‘Comparison of simple sucrose and percoll based methodologies for synaptosome enrichment’, Analytical Biochemistry. Elsevier Inc, 517, pp. 1–8. doi: 10.1016/j.ab.2016.10.015.

Therien, A. G., Grant, F. E. M. and Deber, C. M. (2001) ‘Interhelical hydrogen bonds in the CFTR membrane domain’, Nature Structural Biology. doi: 10.1038/89631.

Thibault, K. et al. (2013a) ‘Activation-dependent subcellular distribution patterns of CB1 Cannabinoid Receptors in the Rat Forebrain’, Cerebral Cortex, 23(11), pp. 2581–2591. doi: 10.1093/cercor/bhs240.

Thibault, K. et al. (2013b) ‘Activation-dependent subcellular distribution patterns of CB1

Cannabinoid Receptors in the Rat Forebrain', Cerebral Cortex, 23(11), pp. 2581–2591. doi: 10.1093/cercor/bhs240.

Traynor, J. R. and Nahorski, S. R. (1995) 'Modulation by μ-opioid agonists of guanosine-5'-O-(3- [35S]thio)triphosphate binding to membranes from human neuroblastoma SH-SY5Y cells', Molecular Pharmacology, 47(4), pp. 848–854.

Tsou, K. et al. (1998) 'Immunohistochemical distribution of cannabinoid CB1 receptors in the rat central nervous system', Neuroscience. Pergamon, 83(2), pp. 393–411. doi: 10.1016/S0306-4522(97)00436-3.

Tsou, K. et al. (1999) 'Cannabinoid CB1 receptors are localized primarily on cholecystokinin-containing GABAergic interneurons in the rat hippocampal formation', Neuroscience, 93(3), pp. 969–975. doi: 10.1016/S0306-4522(99)00086-X.

Turu, G. and Hunyady, L. (2010) 'Signal transduction of the CB1 cannabinoid receptor', Journal of Molecular Endocrinology, 44(2), pp. 75–85. doi: 10.1677/JME-08-0190.

Uchigashima, M. et al. (2011) 'Molecular and morphological configuration for 2-Arachidonoylglycerol-mediated retrograde signaling at mossy cell-granule cell synapses in the dentate gyrus', Journal of Neuroscience, 31(21), pp. 7700–7714. doi: 10.1523/JNEUROSCI.5665-10.2011.

Vicente-Sánchez, A. et al. (2013) 'HINT1 protein cooperates with cannabinoid 1 receptor to negatively regulate glutamate NMDA receptor activity', Molecular Brain, 6(1), pp. 1–16. doi: 10.1186/1756-6606-6-42.

Wager-Miller, J., Westenbroek, R. and Mackie, K. (2002) 'Dimerization of G protein-coupled receptors: CB1 cannabinoid receptors as an example', Chemistry and Physics of Lipids, 121(1–2), pp. 83–89. doi: 10.1016/S0009-3084(02)00151-2.

Whittaker, V. P. (1968) 'The morphology of fractions of rat forebrain synaptosomes separated on continuous sucrose density gradients.', The Biochemical journal, 106(2), pp. 412–417. doi: 10.1042/bj1060412.

Whittaker, V. P. (1993) 'Thirty years of synaptosome research', Journal of Neurocytology, 22(9), pp. 735–742. doi: 10.1007/BF01181319.

Wickert, M. et al. (2018) 'The F238L Point Mutation in the Cannabinoid Type 1 Receptor Enhances Basal Endocytosis via Lipid Rafts', Frontiers in Molecular Neuroscience,

11(July), pp. 1–11. doi: 10.3389/fnmol.2018.00230.

Xiao, J. C. et al. (2008) ‘Similar in vitro pharmacology of human cannabinoid CB1 receptor variants expressed in CHO cells’, Brain Research. Elsevier B.V., 1238, pp. 36–43. doi: 10.1016/j.brainres.2008.08.027.

Yoshida, T. et al. (2006) ‘Localization of diacylglycerol lipase-α around postsynaptic spine suggests close proximity between production site of an endocannabinoid, 2-arachidonoyl-glycerol, and presynaptic cannabinoid CB1 receptor’, Journal of Neuroscience, 26(18), pp. 4740–4751. doi: 10.1523/JNEUROSCI.0054-06.2006.

Yoshino, H. et al. (2011) ‘Postsynaptic diacylglycerol lipase α mediates retrograde endocannabinoid suppression of inhibition in mouse prefrontal cortex’, Journal of Physiology, 589(20), pp. 4857–4884. doi: 10.1113/jphysiol.2011.212225.

Zimmer, A. et al. (1999) ‘Increased mortality, hypoactivity, and hypoalgesia in cannabinoid CB1 receptor knockout mice’, Proceedings of the National Academy of Sciences, 96(10), pp. 5780 LP – 5785. doi: 10.1073/pnas.96.10.5780.

Zimmermann, T. et al. (2018) ‘Neural stem cell lineage-specific cannabinoid type-1 receptor regulates neurogenesis and plasticity in the adult mouse hippocampus’, Cerebral Cortex, 28(12), pp. 4454–4471. doi: 10.1093/cercor/bhy258.